

1 Indices spatial distribution and arithmetic differences

1.1 Indices based on fixed thresholds - R10mm, R20mm, CWD, CDD

1.1.1 IMERG DATA

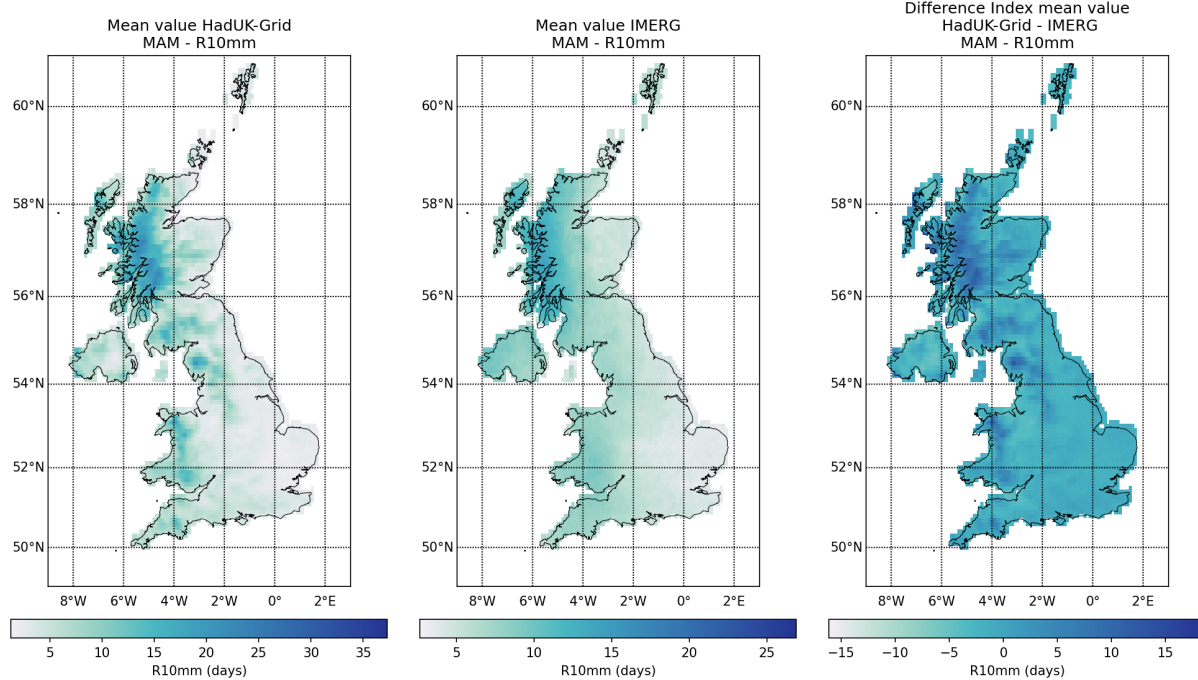


Figure 1: Spatial distribution of R10mm values obtained from HadUK-Grid and IMERG and arithmetic difference between HadUK-Grid and IMERG for spring (MAM) over the 2001–2019 climatological period.

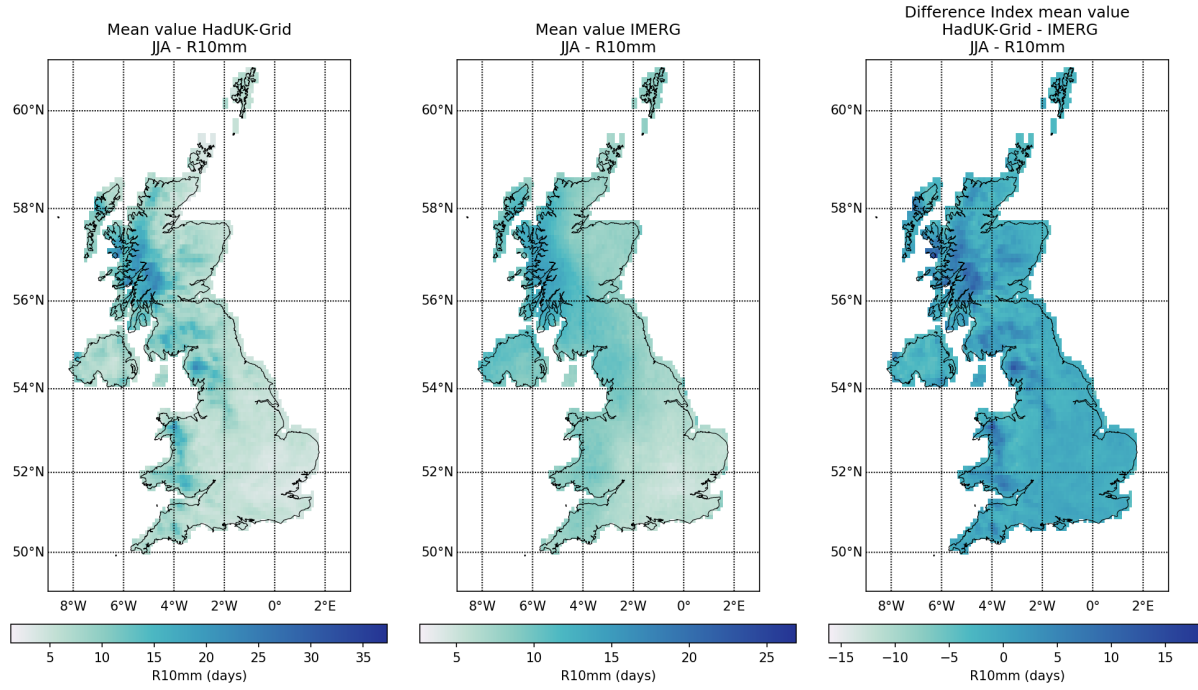


Figure 1: Spatial distribution of R10mm values obtained from HadUK-Grid and IMERG and arithmetic difference between HadUK-Grid and IMERG for summer (JJA) over the 2001–2019 climatological period (cont.).

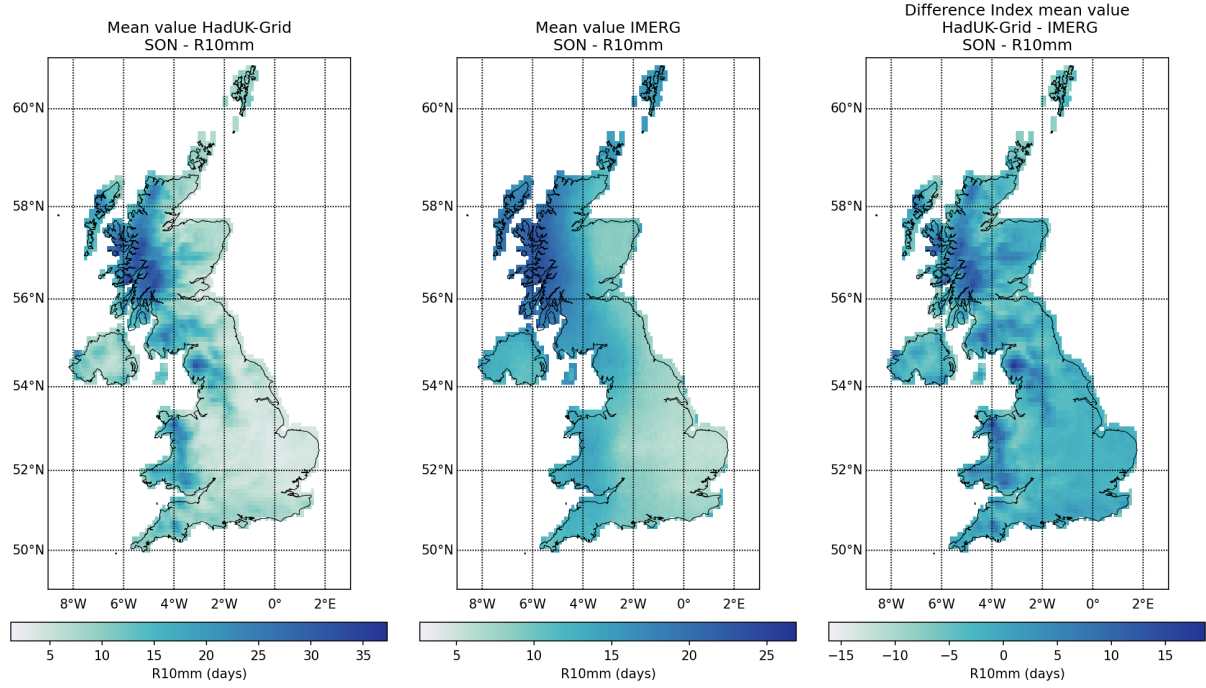


Figure 1: Spatial distribution of R10mm values obtained from HadUK-Grid and IMERG and arithmetic difference between HadUK-Grid and IMERG for autumn (SON) over the 2001–2019 climatological period (cont.).

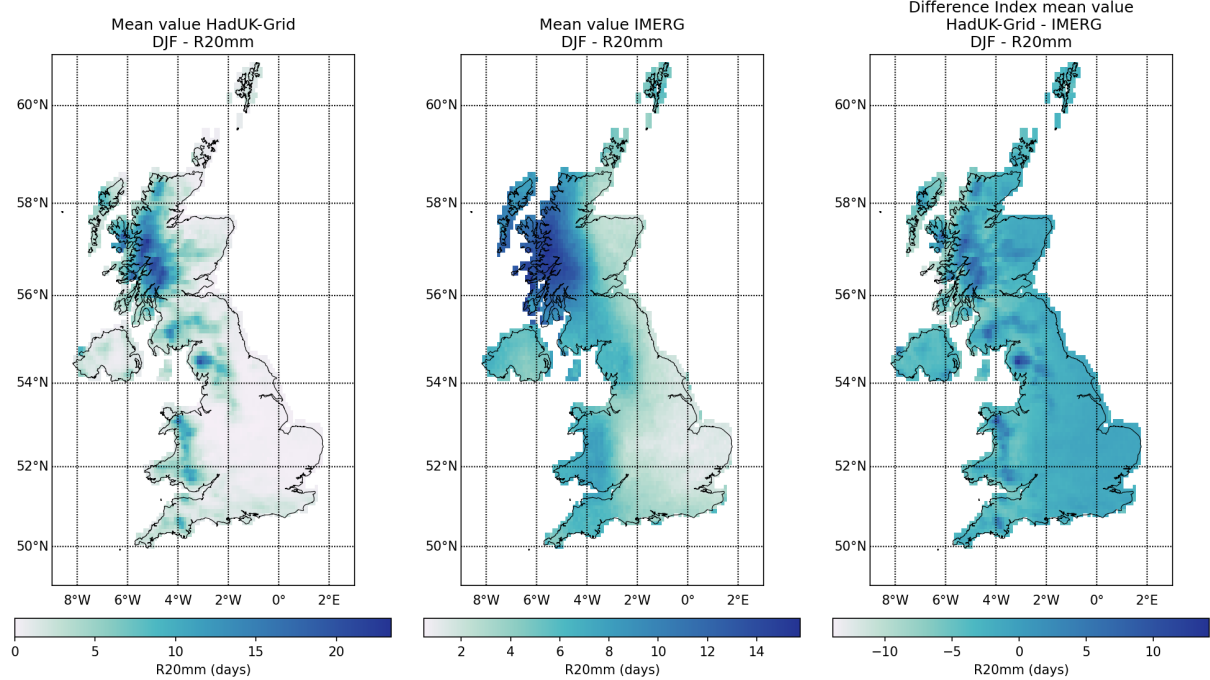


Figure 2: Spatial distribution of R20mm values obtained from HadUK-Grid and IMERG and arithmetic difference between HadUK-Grid and IMERG for winter (DJF) over the 2001–2019 climatological period

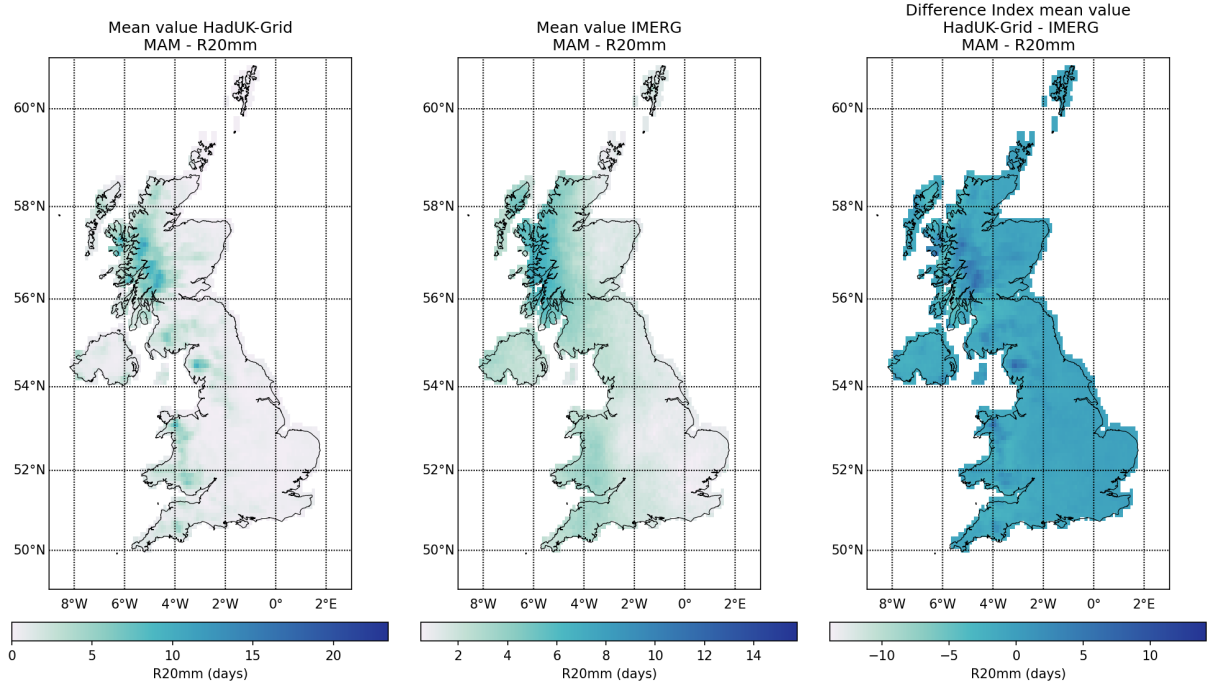


Figure 2: Spatial distribution of R20mm values obtained from HadUK-Grid and IMERG and arithmetic difference between HadUK-Grid and IMERG for spring (MAM) over the 2001–2019 climatological period (cont.).

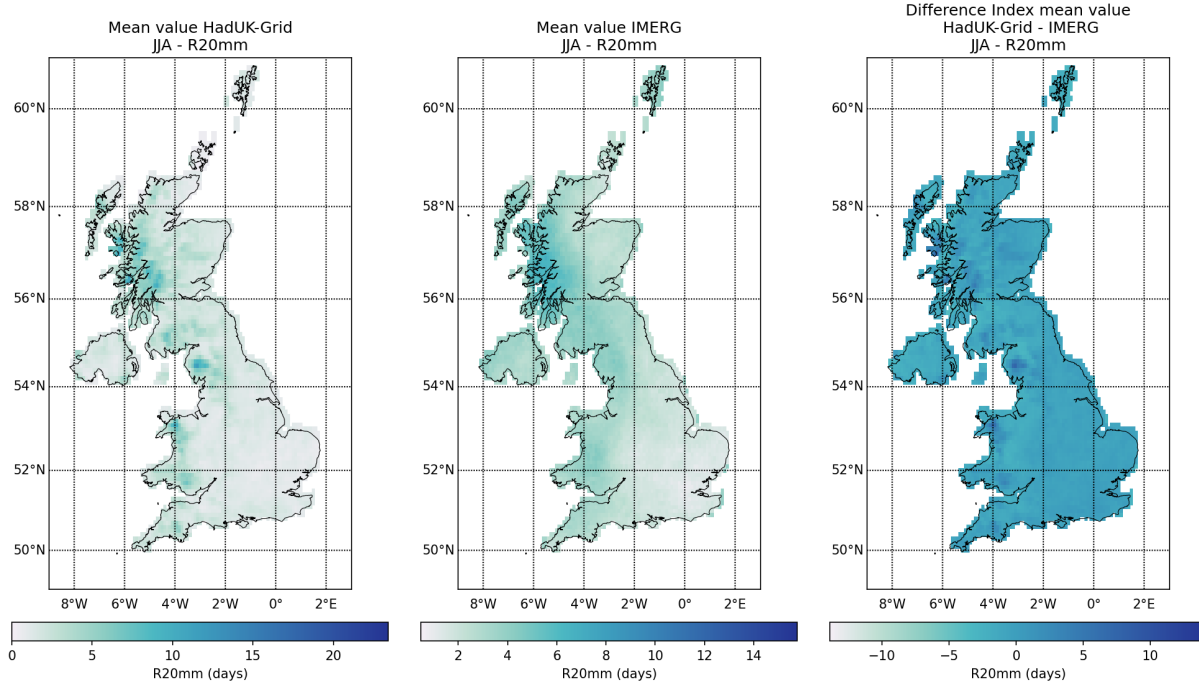


Figure 2: Spatial distribution of R20mm values obtained from HadUK-Grid and IMERG and arithmetic difference between HadUK-Grid and IMERG for summer (JJA) over the 2001–2019 climatological period (cont.).

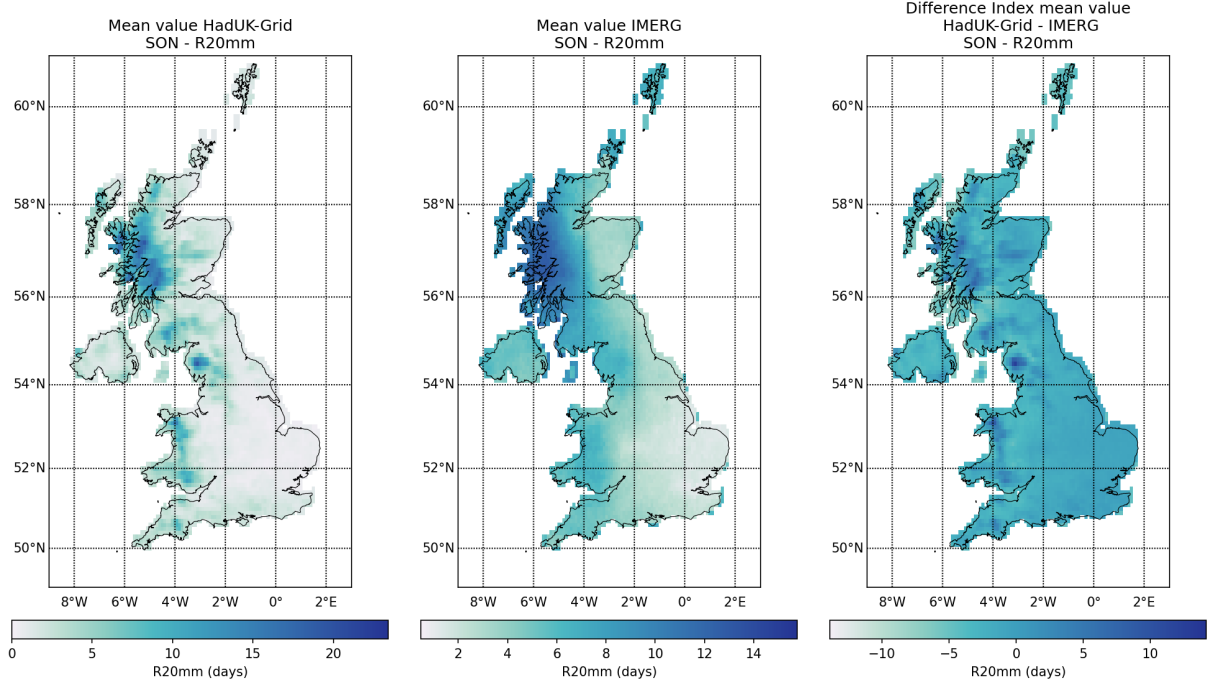


Figure 2: Spatial distribution of R20mm values obtained from HadUK-Grid and IMERG and arithmetic difference between HadUK-Grid and IMERG for autumn (SON) over the 2001–2019 climatological period (cont.).

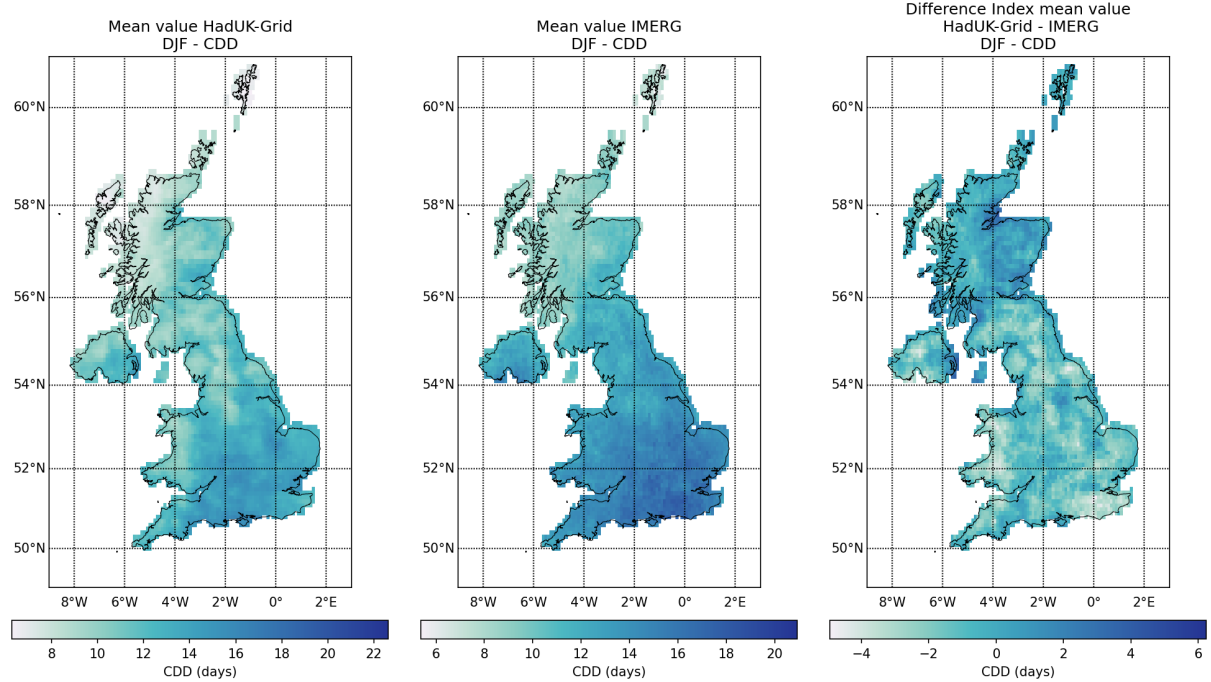


Figure 3: Spatial distribution of CDD values obtained from HadUK-Grid and IMERG and arithmetic difference between HadUK-Grid and IMERG for winter (DJF) over the 2001–2019 climatological period

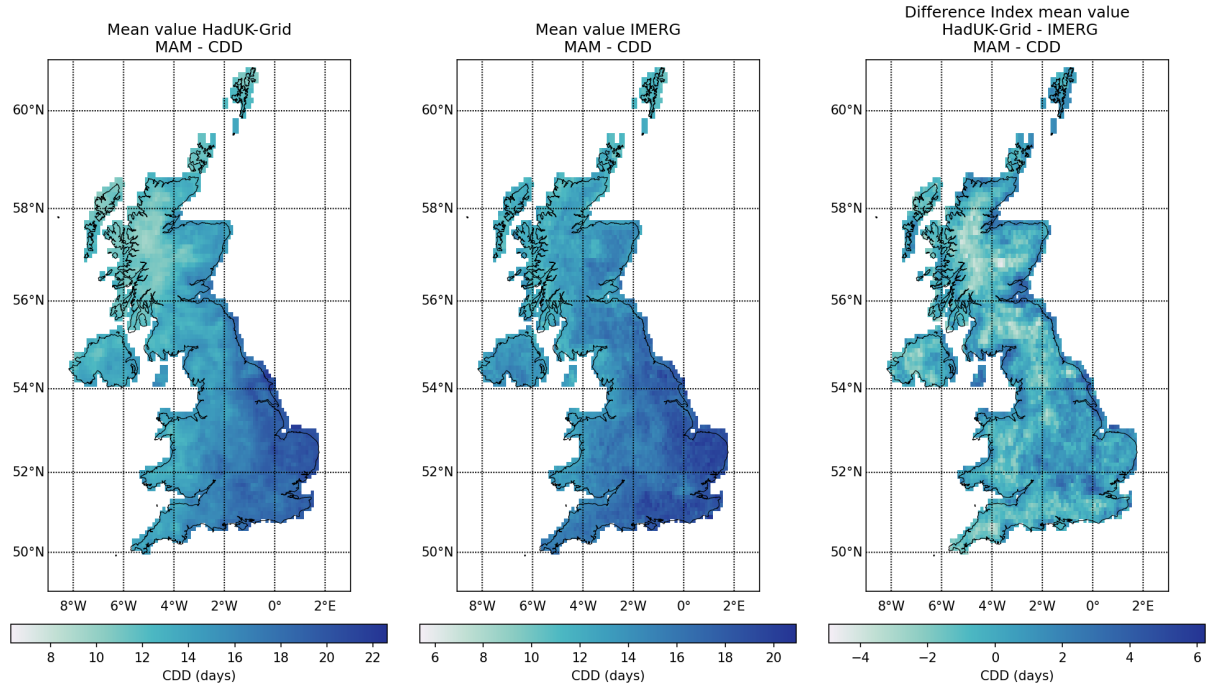


Figure 3: Spatial distribution of CDD values obtained from HadUK-Grid and IMERG and arithmetic difference between HadUK-Grid and IMERG for spring (MAM) over the 2001–2019 climatological period (cont.).

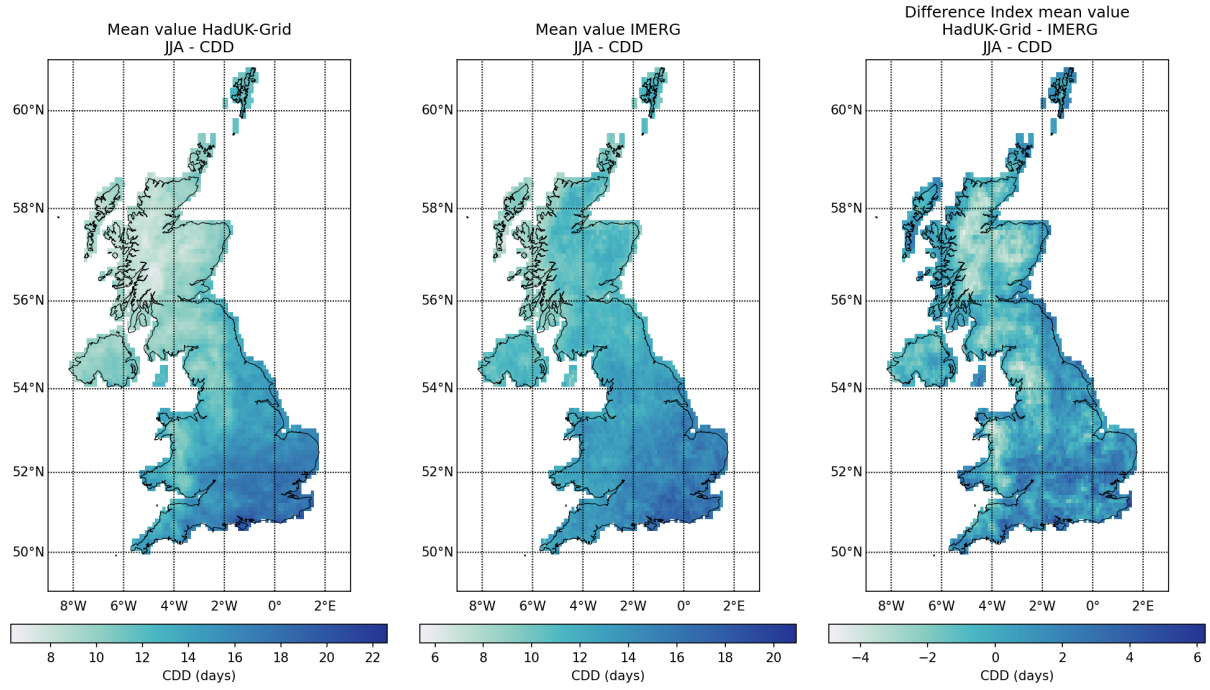


Figure 3: Spatial distribution of CDD values obtained from HadUK-Grid and IMERG and arithmetic difference between HadUK-Grid and IMERG for summer (JJA) over the 2001–2019 climatological period (cont.).

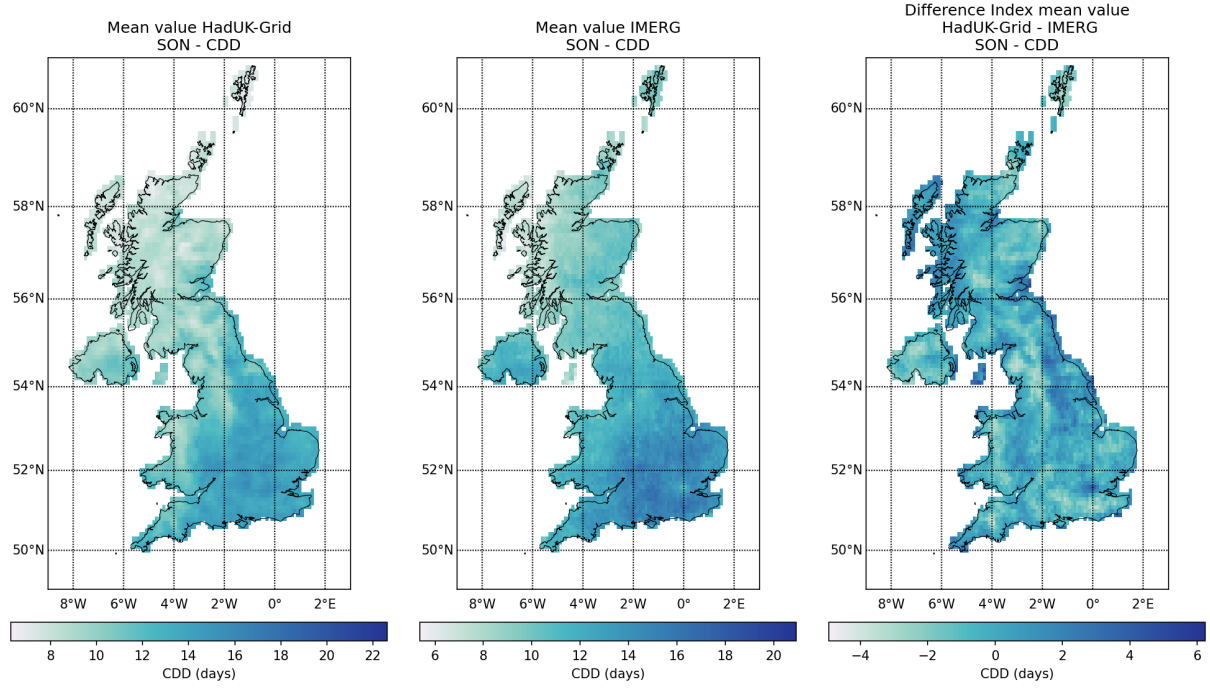


Figure 3: Spatial distribution of CDD values obtained from HadUK-Grid and IMERG and arithmetic difference between HadUK-Grid and IMERG for autumn (SON) over the 2001–2019 climatological period (cont.).

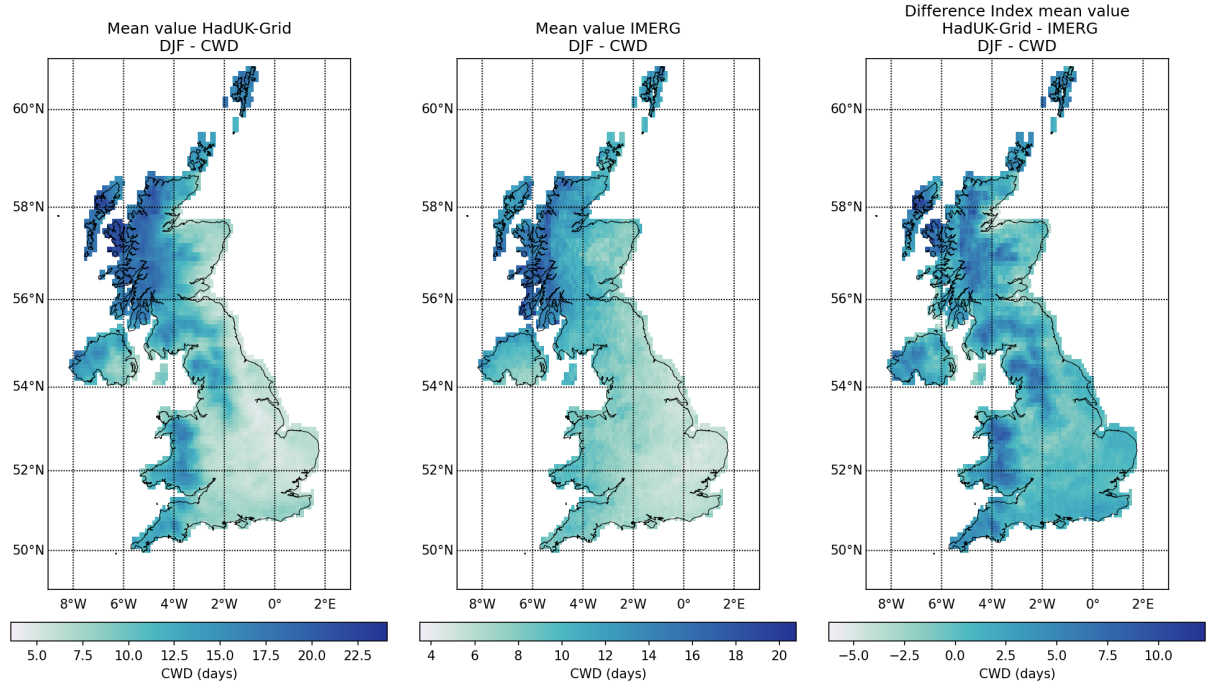


Figure 4: Spatial distribution of CWD values obtained from HadUK-Grid and IMERG and arithmetic difference between HadUK-Grid and IMERG for winter (DJF) over the 2001–2019 climatological period

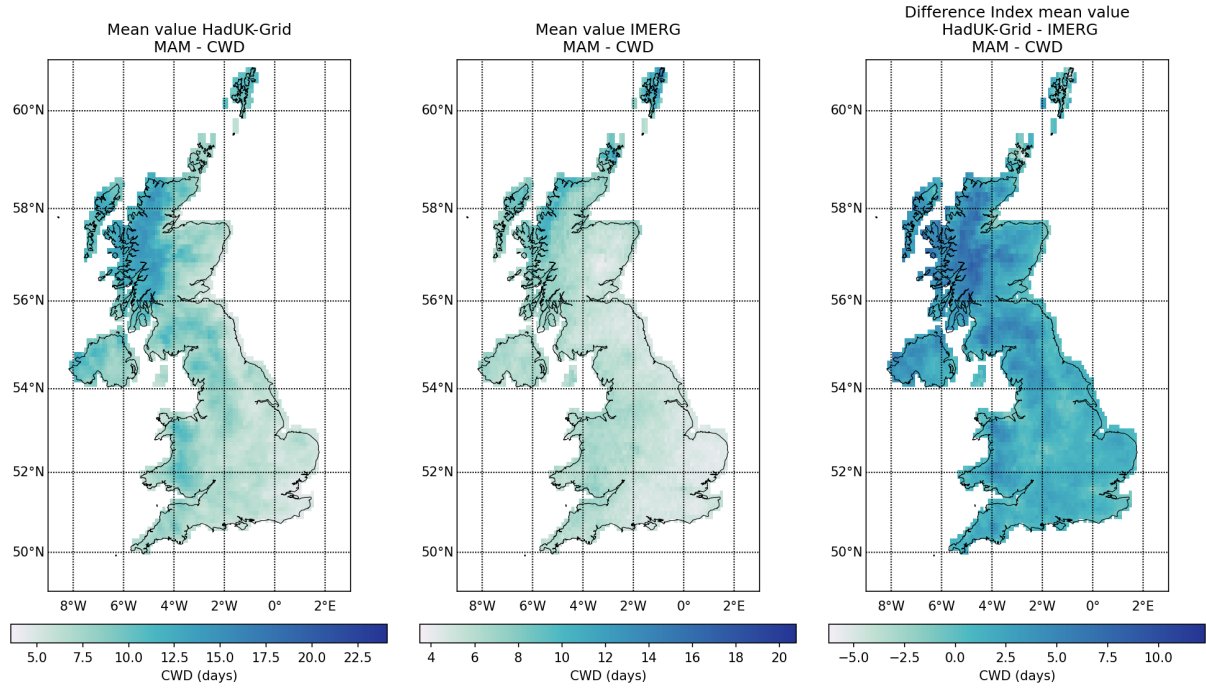


Figure 4: Spatial distribution of CWD values obtained from HadUK-Grid and IMERG and arithmetic difference between HadUK-Grid and IMERG for spring (MAM) over the 2001–2019 climatological period (cont.).

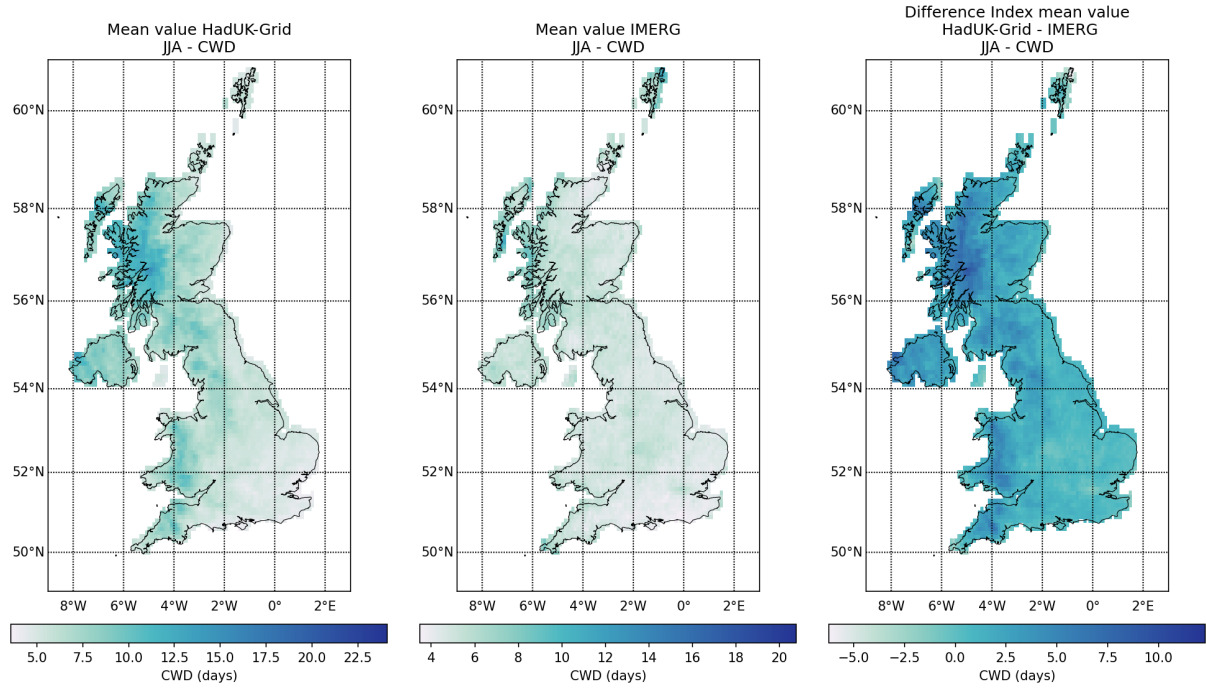


Figure 4: Spatial distribution of CWD values obtained from HadUK-Grid and IMERG and arithmetic difference between HadUK-Grid and IMERG for summer (JJA) over the 2001–2019 climatological period (cont.).

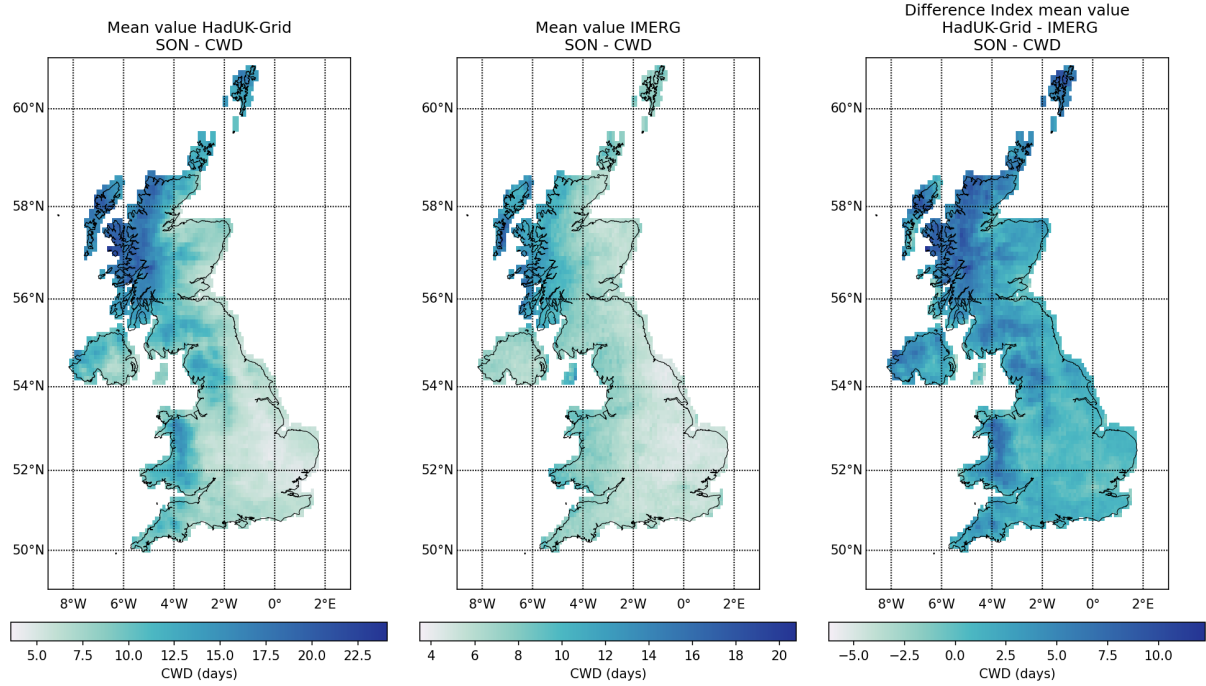


Figure 4: Spatial distribution of CWD values obtained from HadUK-Grid and IMERG and arithmetic difference between HadUK-Grid and IMERG for autumn (SON) over the 2001–2019 climatological period (cont.).

1.1.2 ERA5 DATA

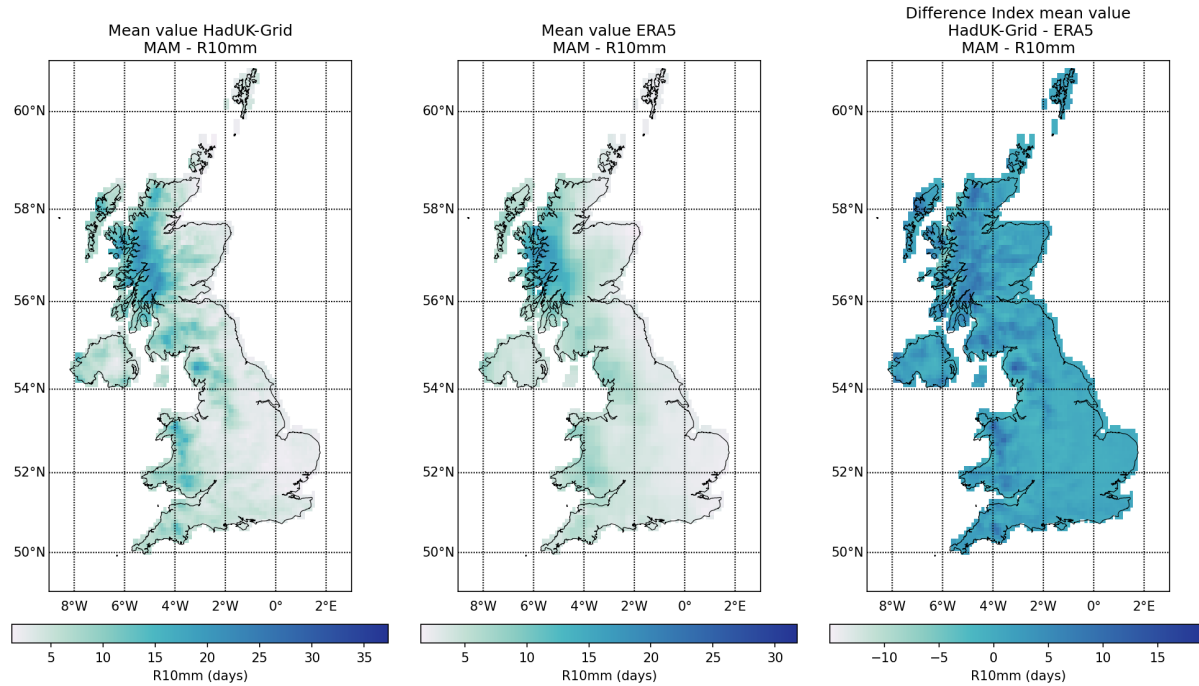


Figure 5: Spatial distribution of R10mm values obtained from HadUK-Grid and ERA5, and arithmetic difference between HadUK-Grid and ERA5 for spring (MAM) over the 2001–2019 climatological period.

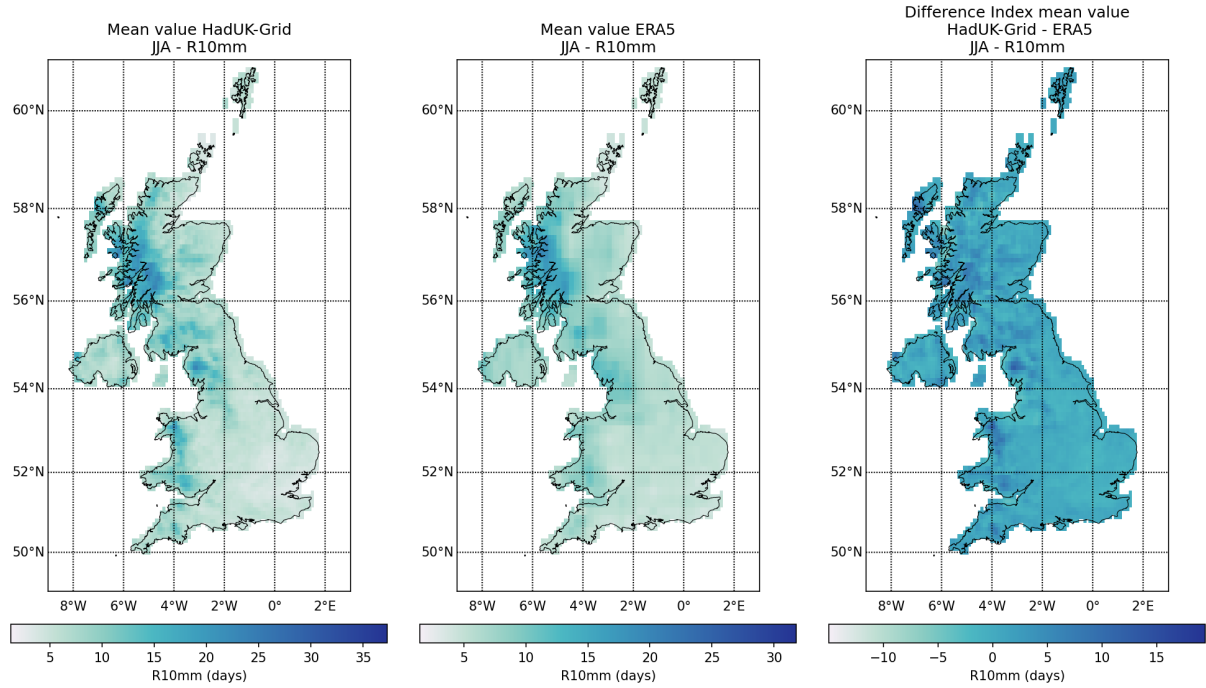


Figure 5: Spatial distribution of R10mm values obtained from HadUK-Grid and ERA5, and arithmetic difference between HadUK-Grid and ERA5 for summer (JJA) over the 2001–2019 climatological period (cont.).

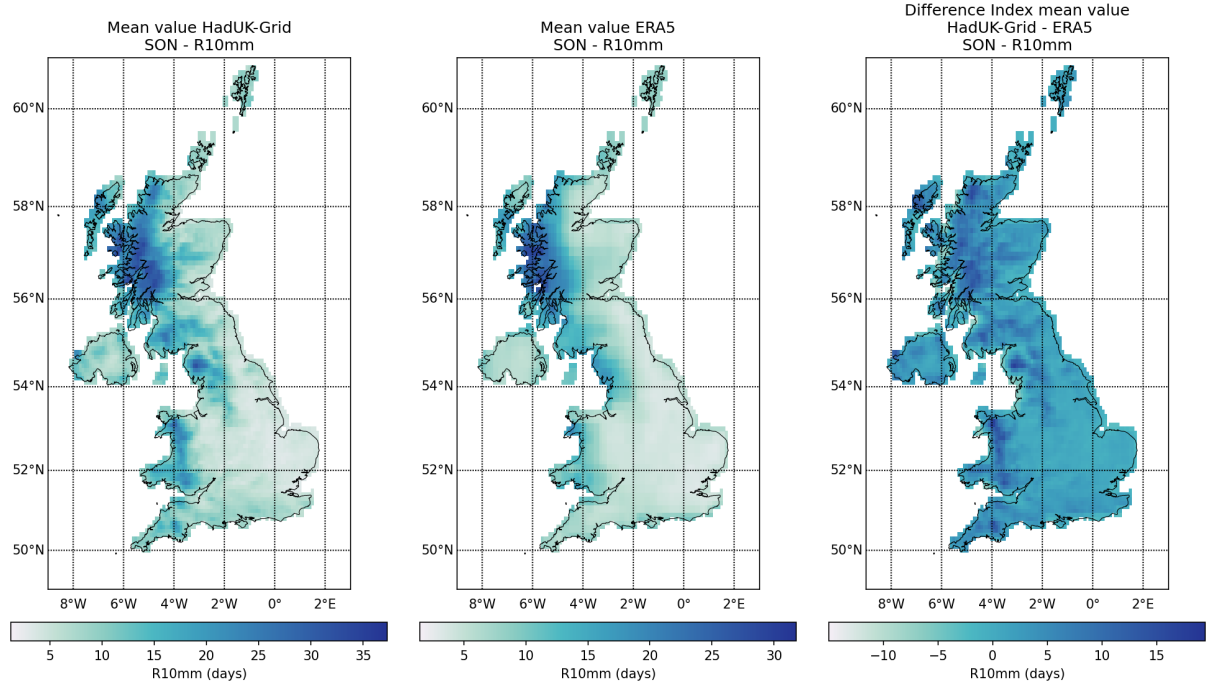


Figure 5: Spatial distribution of R10mm values obtained from HadUK-Grid and ERA5, and arithmetic difference between HadUK-Grid and ERA5 for autumn (SON) over the 2001–2019 climatological period (cont.).

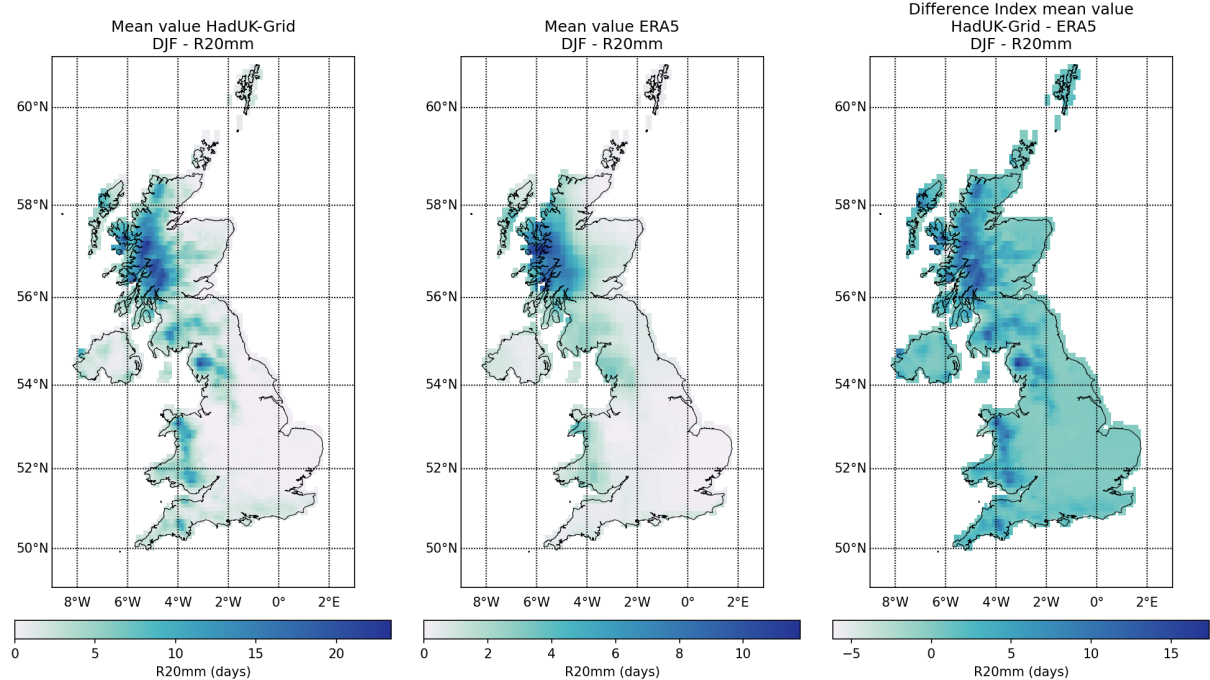


Figure 6: Spatial distribution of R20mm values obtained from HadUK-Grid and ERA5, and arithmetic difference between HadUK-Grid and ERA5 for winter (DJF) over the 2001–2019 climatological period

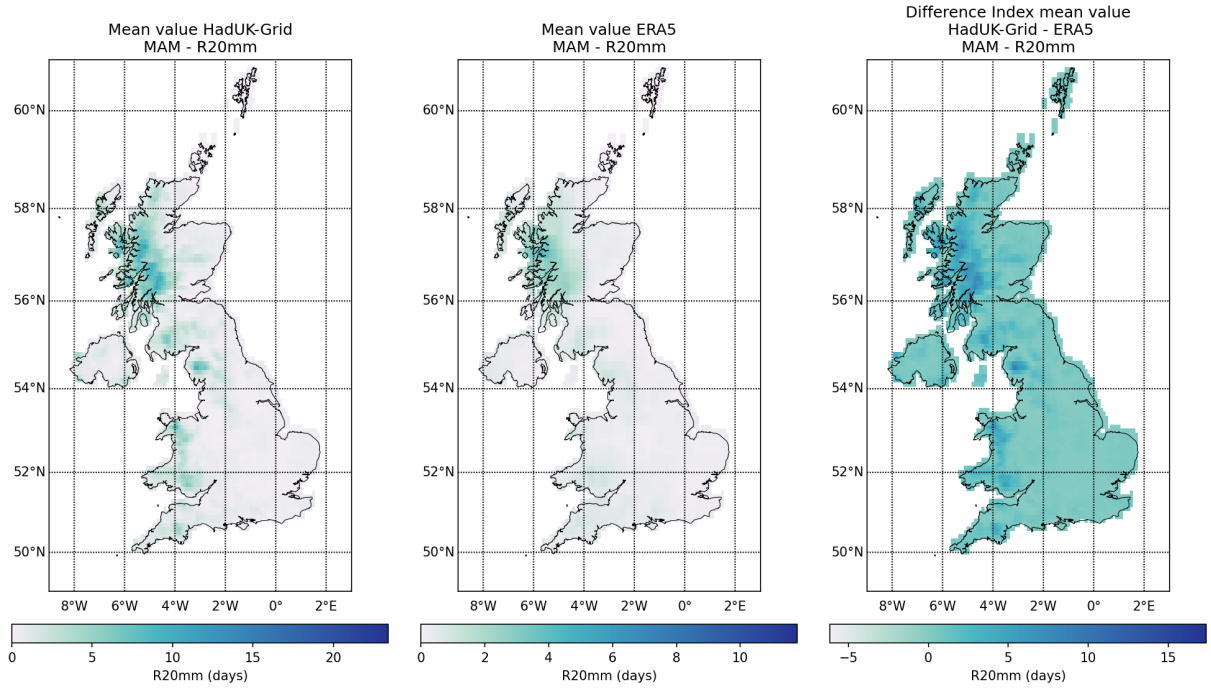


Figure 6: Spatial distribution of R20mm values obtained from HadUK-Grid and ERA5, and arithmetic difference between HadUK-Grid and ERA5 for spring (MAM) over the 2001–2019 climatological period (cont.).

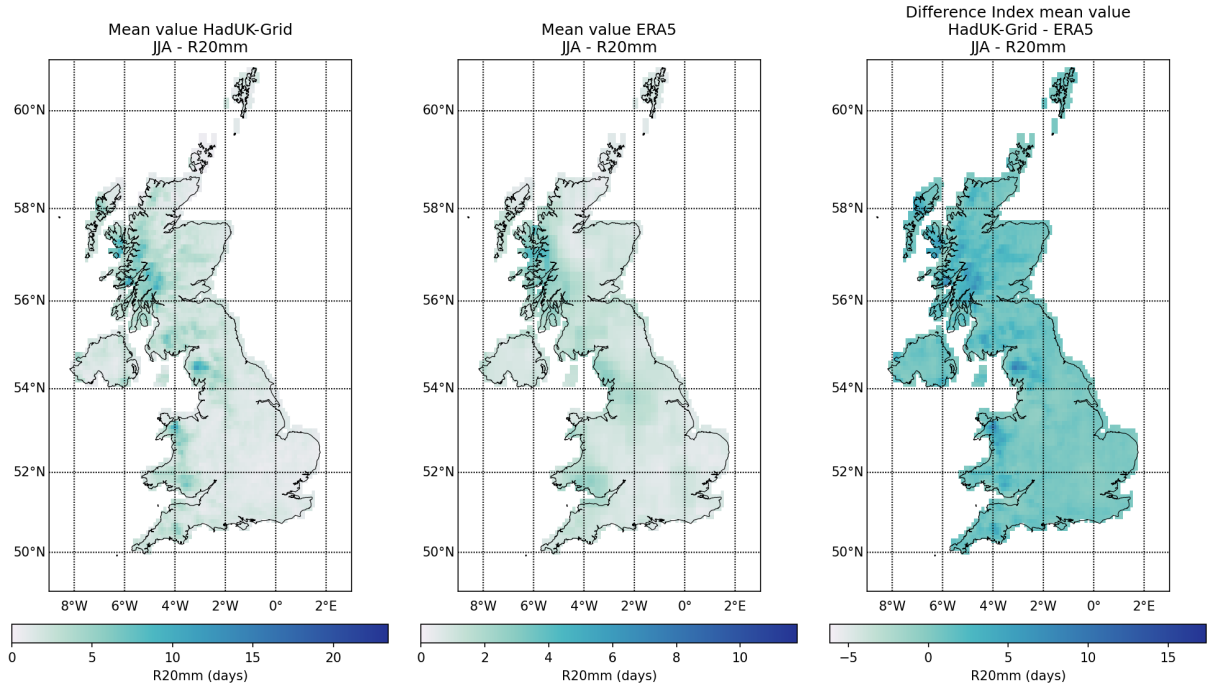


Figure 6: Spatial distribution of R20mm values obtained from HadUK-Grid and ERA5, and arithmetic difference between HadUK-Grid and ERA5 for summer (JJA) over the 2001–2019 climatological period (cont.).

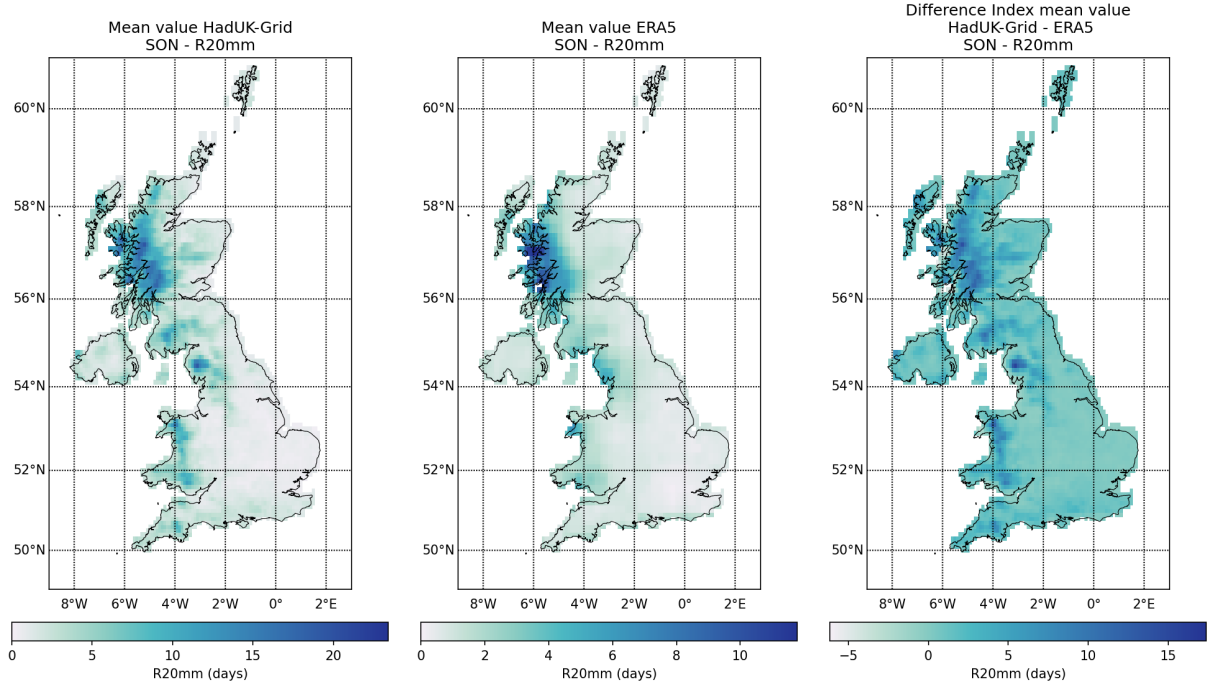


Figure 6: Spatial distribution of R20mm values obtained from HadUK-Grid and ERA5, and arithmetic difference between HadUK-Grid and ERA5 for autumn (SON) over the 2001–2019 climatological period (cont.).

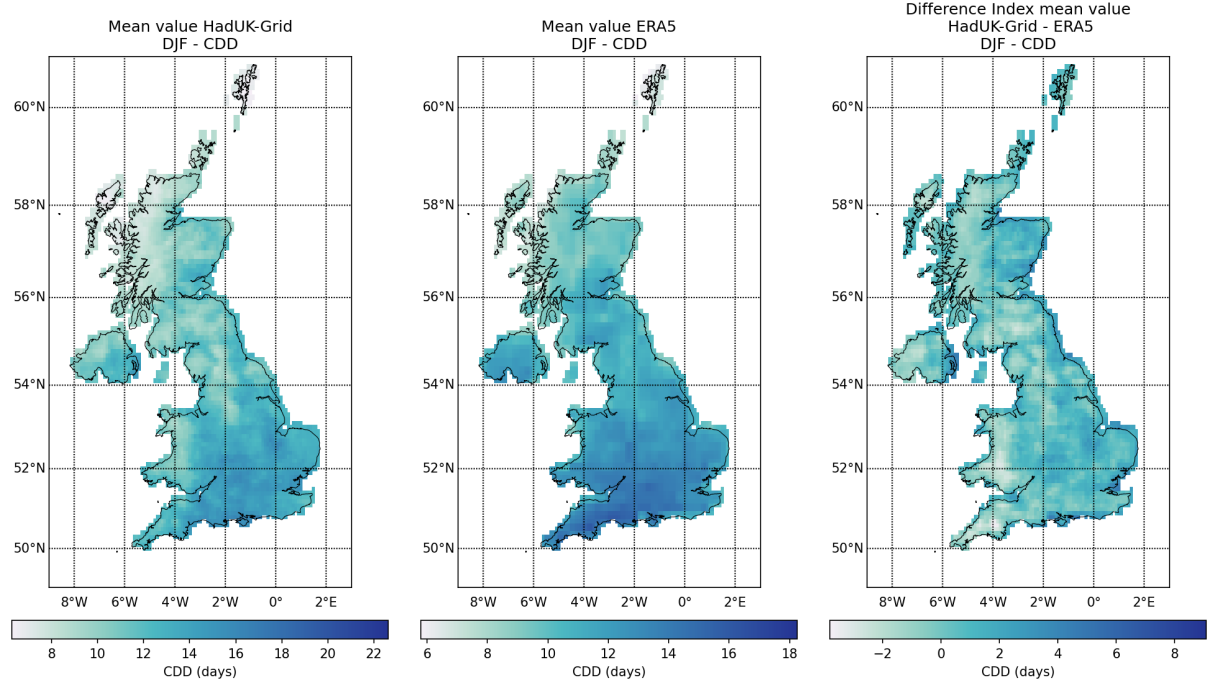


Figure 7: Spatial distribution of CDD values obtained from HadUK-Grid and ERA5, and arithmetic difference between HadUK-Grid and ERA5 for winter (DJF) over the 2001–2019 climatological period

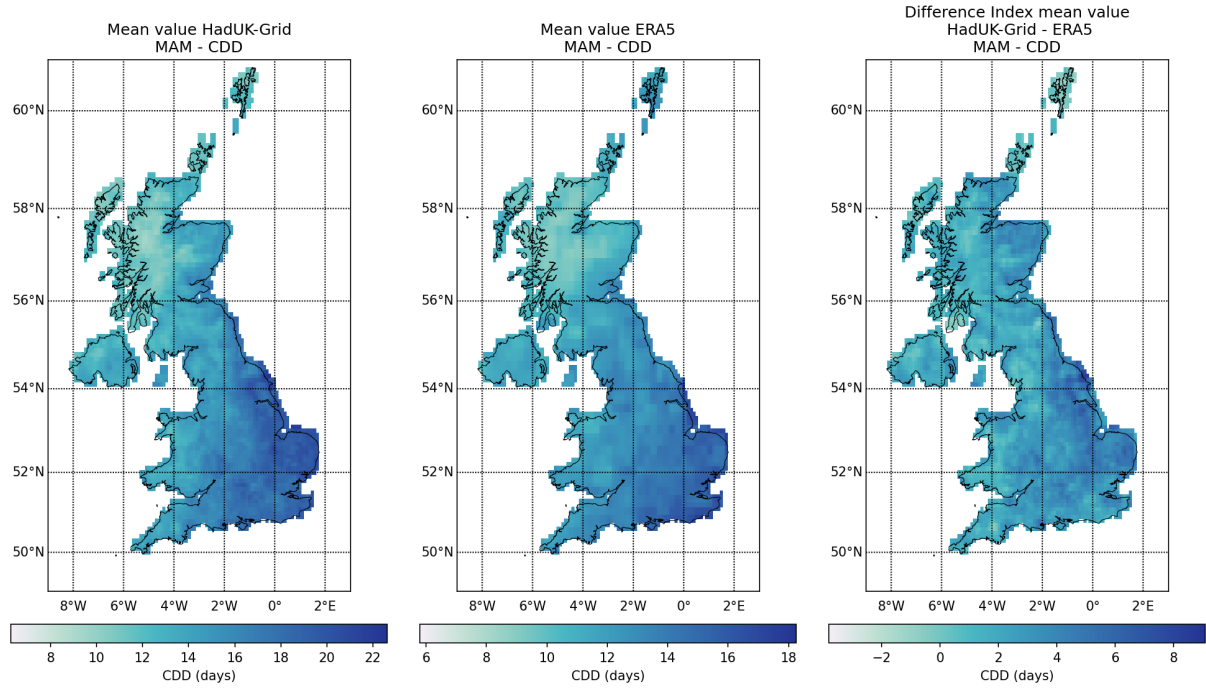


Figure 7: Spatial distribution of CDD values obtained from HadUK-Grid and ERA5, and arithmetic difference between HadUK-Grid and ERA5 for spring (MAM) over the 2001–2019 climatological period (cont.).

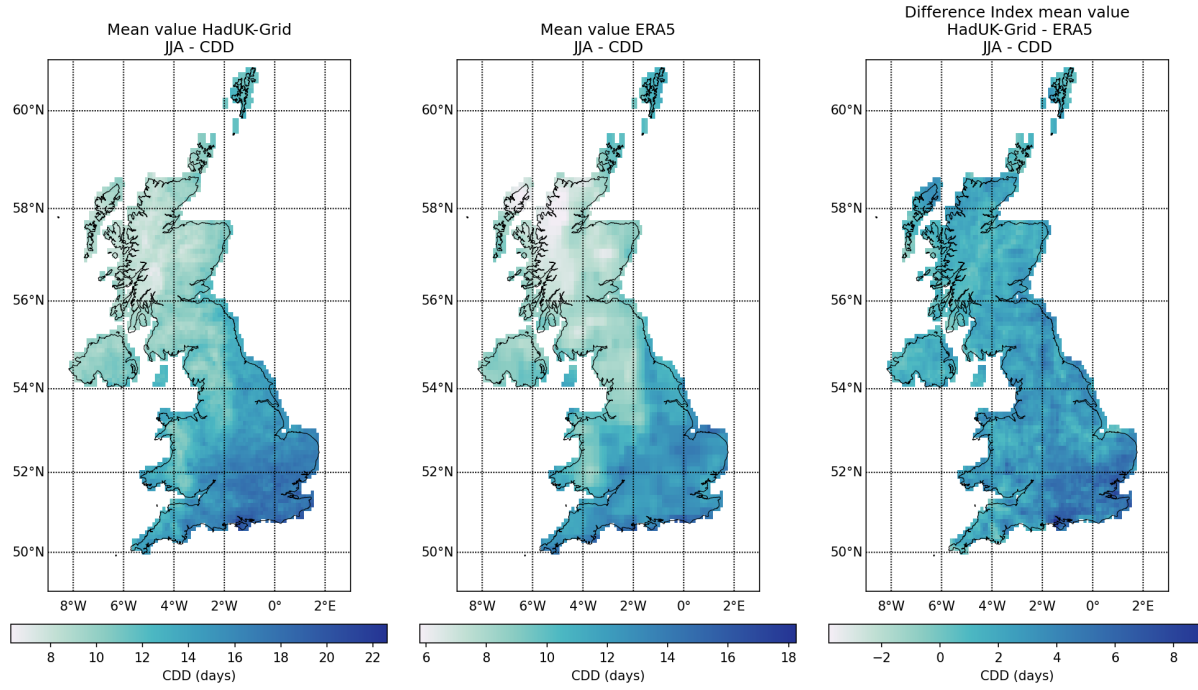


Figure 7: Spatial distribution of CDD values obtained from HadUK-Grid and ERA5, and arithmetic difference between HadUK-Grid and ERA5 for summer (JJA) over the 2001–2019 climatological period (cont.).

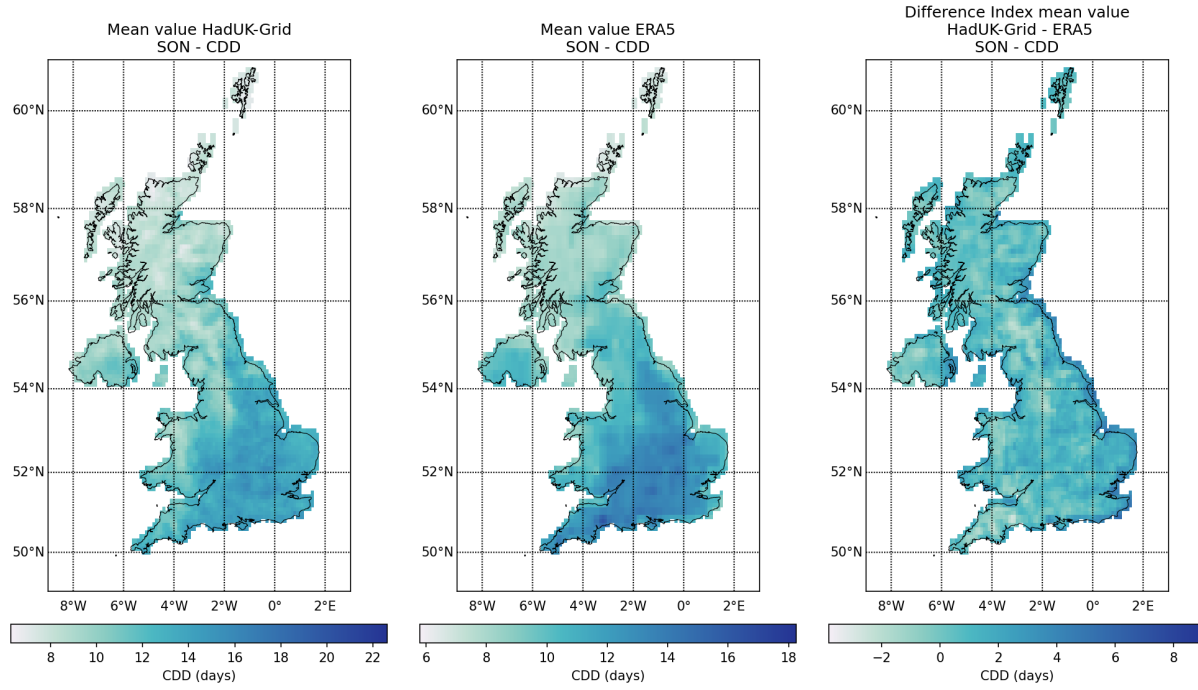


Figure 7: Spatial distribution of CDD values obtained from HadUK-Grid and ERA5, and arithmetic difference between HadUK-Grid and ERA5 for autumn (SON) over the 2001–2019 climatological period (cont.).

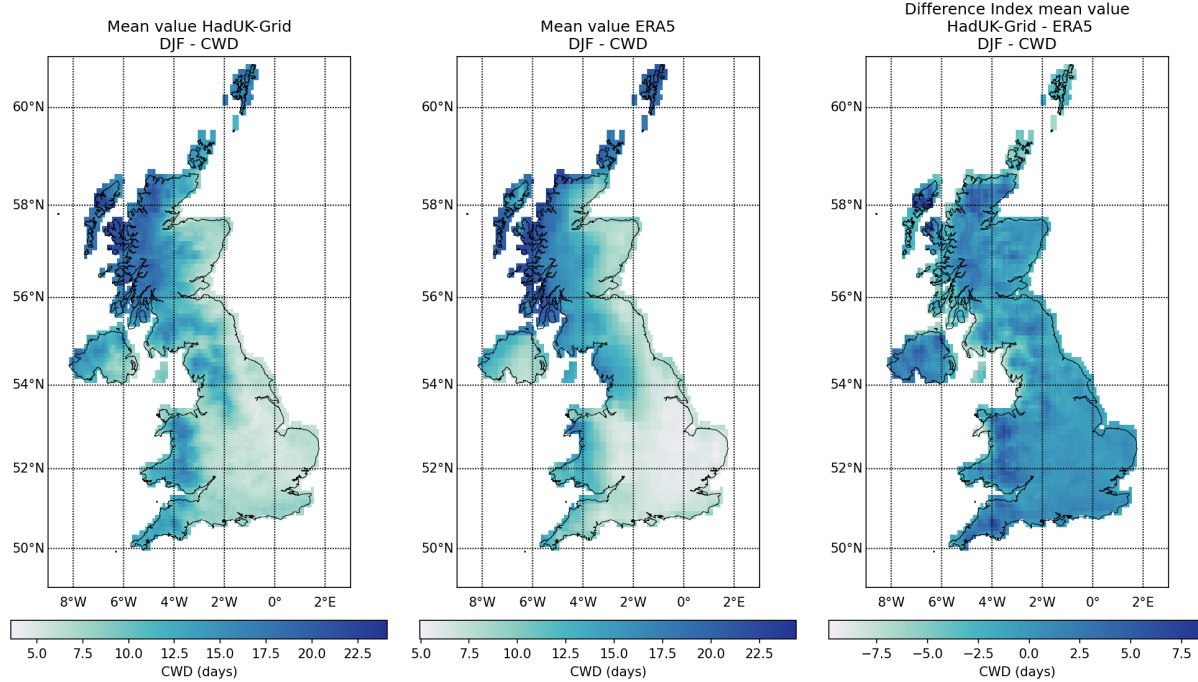


Figure 8: Spatial distribution of CWD values obtained from HadUK-Grid and ERA5, and arithmetic difference between HadUK-Grid and ERA5 for winter (DJF) over the 2001–2019 climatological period

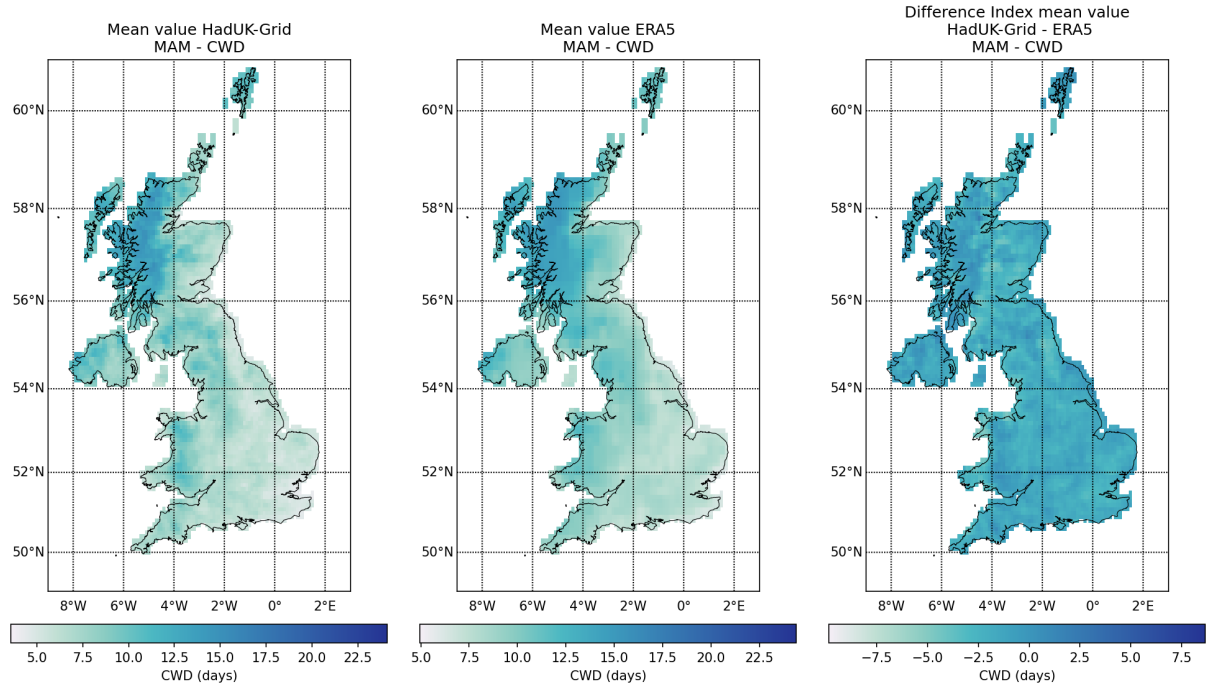


Figure 8: Spatial distribution of CWD values obtained from HadUK-Grid and ERA5, and arithmetic difference between HadUK-Grid and ERA5 for spring (MAM) over the 2001–2019 climatological period (cont.).

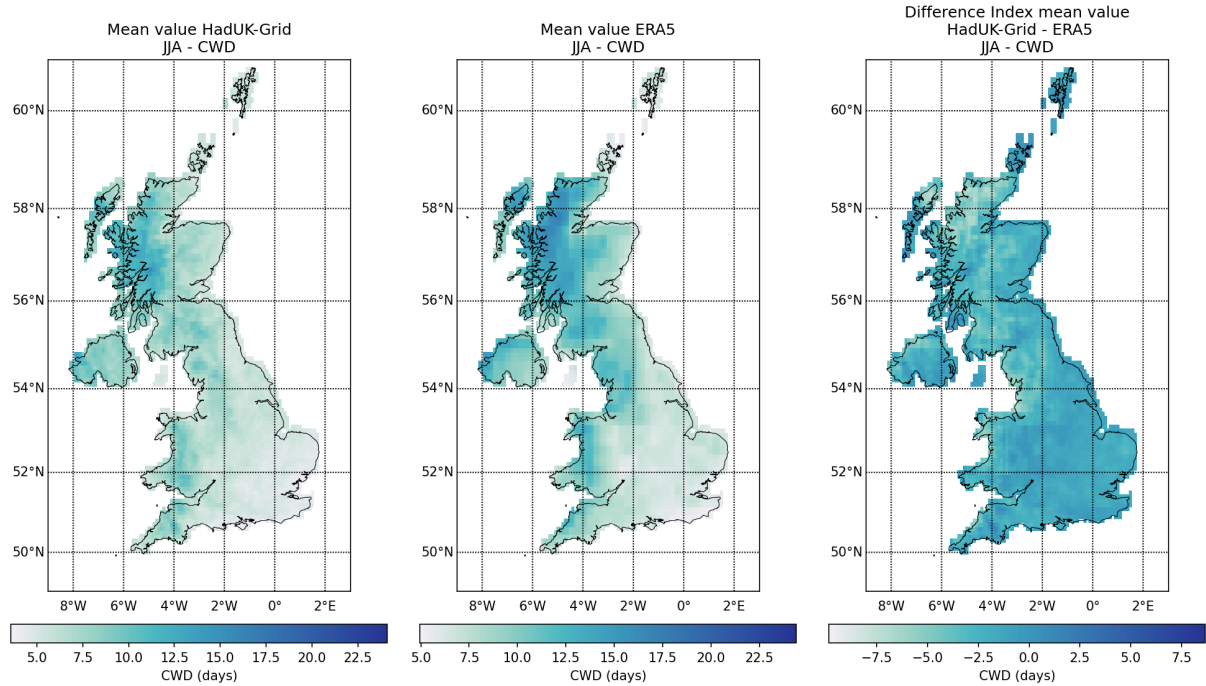


Figure 8: Spatial distribution of CWD values obtained from HadUK-Grid and ERA5, and arithmetic difference between HadUK-Grid and ERA5 for summer (JJA) over the 2001–2019 climatological period (cont.).

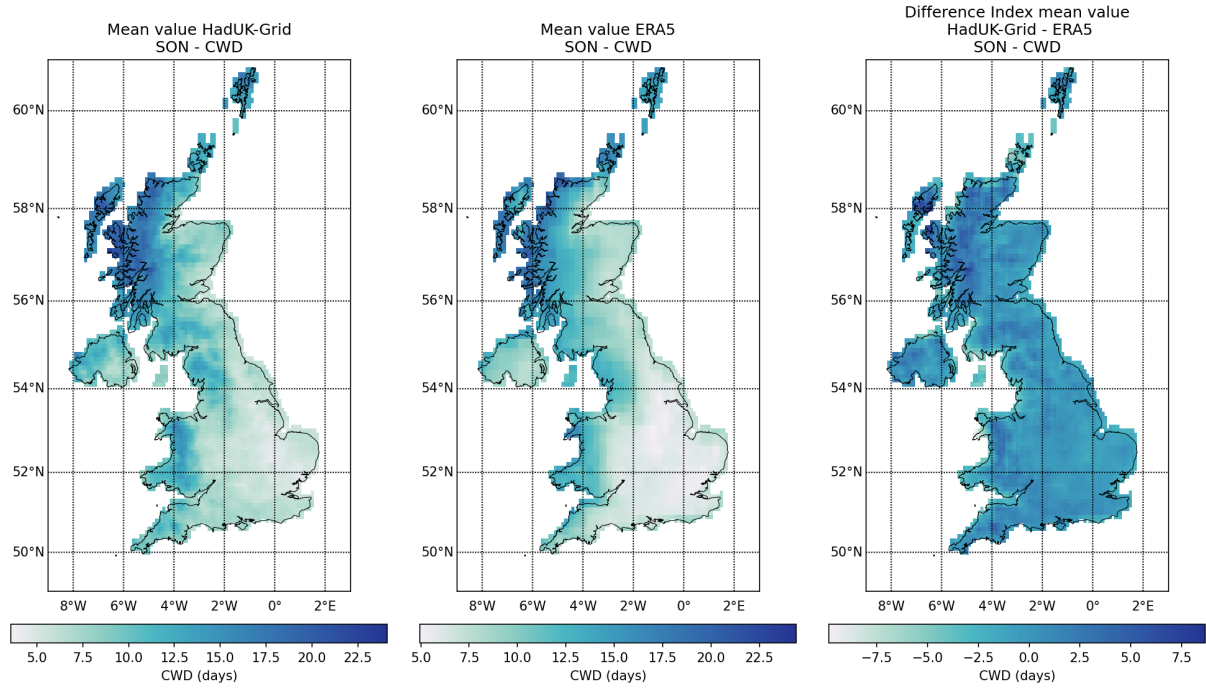


Figure 8: Spatial distribution of CWD values obtained from HadUK-Grid and ERA5, and arithmetic difference between HadUK-Grid and ERA5 for autumn (SON) over the 2001–2019 climatological period (cont.).

1.2 Indices based on station related thresholds - R95pTOT, R99TOT

1.2.1 IMERG DATA

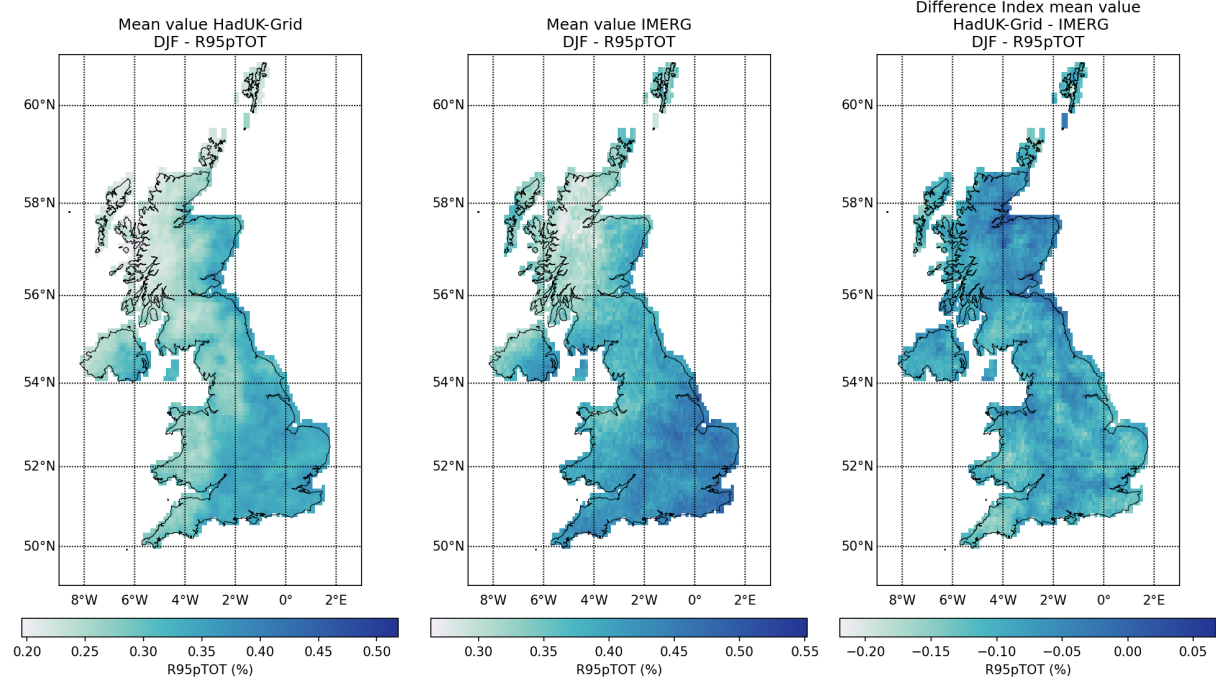


Figure 9: Spatial distribution of R95pTOT values obtained from HadUK-Grid and IMERG, and arithmetic difference between HadUK-Grid and IMERG for winter (DJF) over the 2001–2019 climatological period

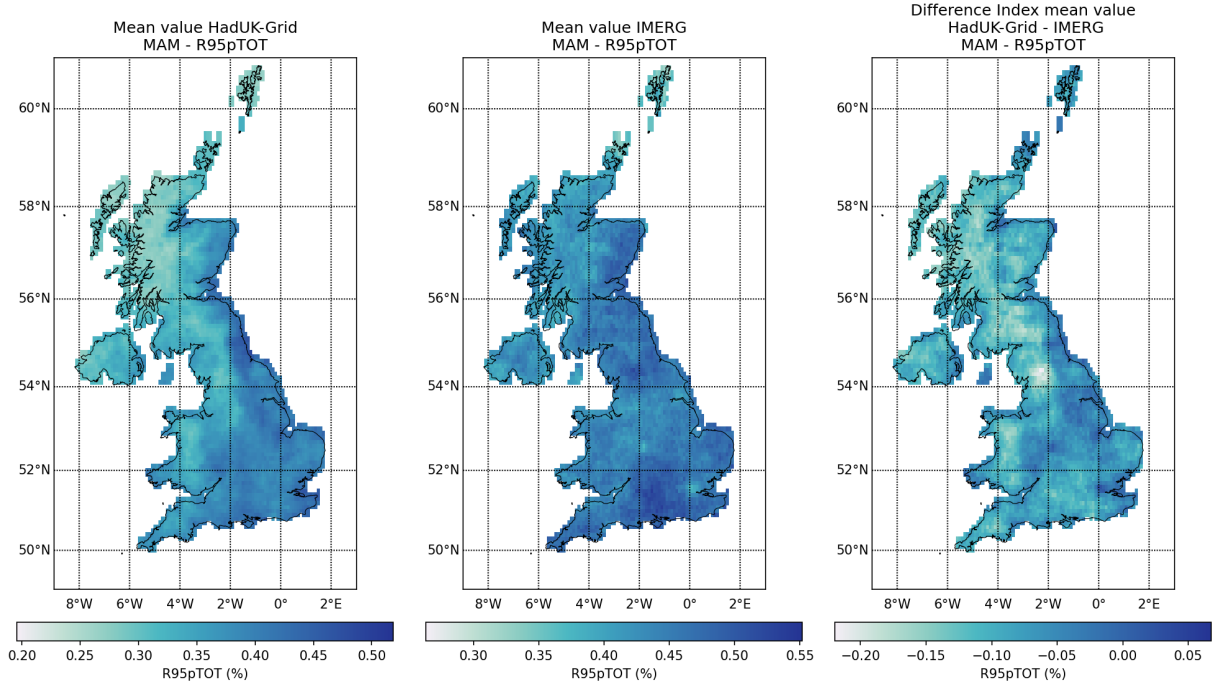


Figure 9: Spatial distribution of R95pTOT values obtained from HadUK-Grid and IMERG, and arithmetic difference between HadUK-Grid and IMERG for spring (MAM) over the 2001–2019 climatological period.

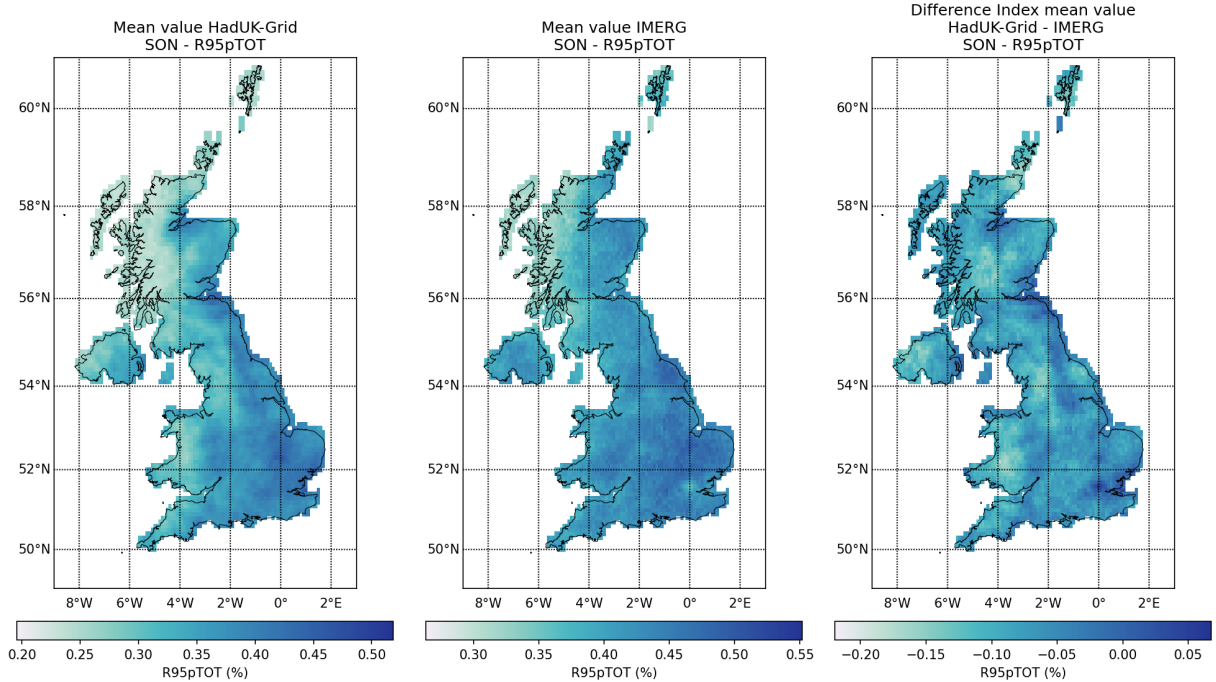


Figure 9: Spatial distribution of R95pTOT values obtained from HadUK-Grid and IMERG, and arithmetic difference between HadUK-Grid and IMERG for autumn (SON) over the 2001–2019 climatological period (cont.).

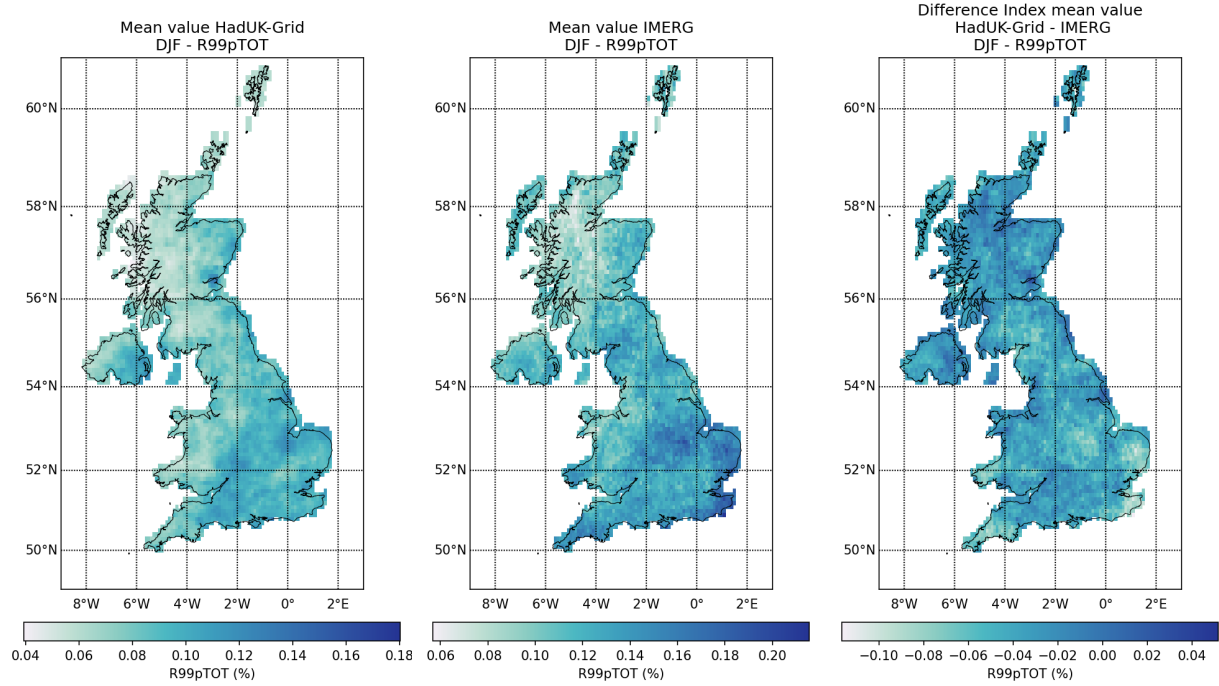


Figure 10: Spatial distribution of R99pTOT values obtained from HadUK-Grid and IMERG, and arithmetic difference between HadUK-Grid and IMERG for winter (DJF) over the 2001–2019 climatological period

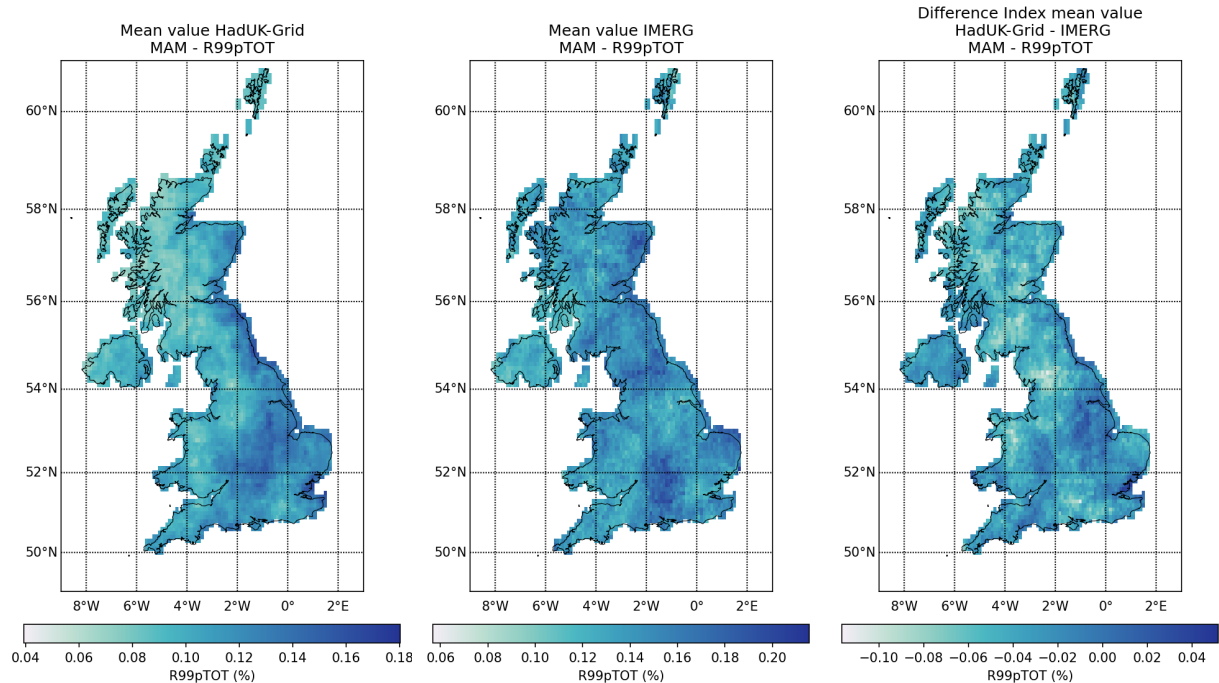


Figure 10: Spatial distribution of R99pTOT values obtained from HadUK-Grid and IMERG, and arithmetic difference between HadUK-Grid and IMERG for spring (MAM) over the 2001–2019 climatological period (cont.).

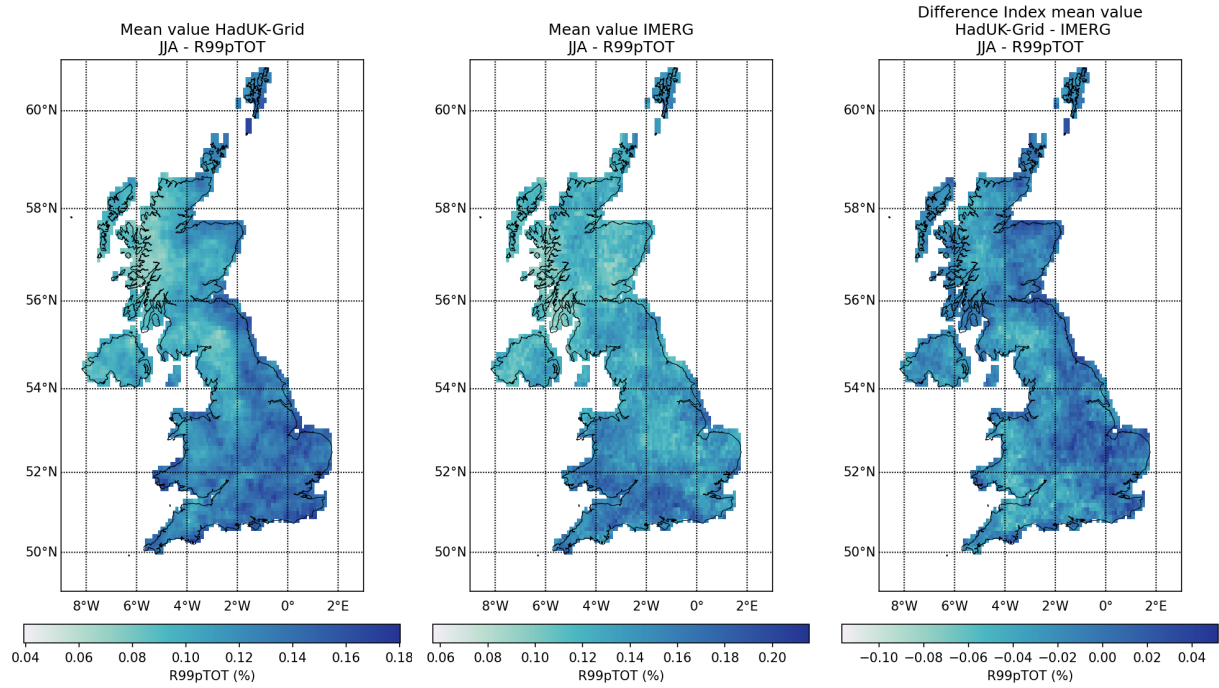


Figure 10: Spatial distribution of R99pTOT values obtained from HadUK-Grid and IMERG, and arithmetic difference between HadUK-Grid and IMERG for summer (JJA) over the 2001–2019 climatological period (cont.).

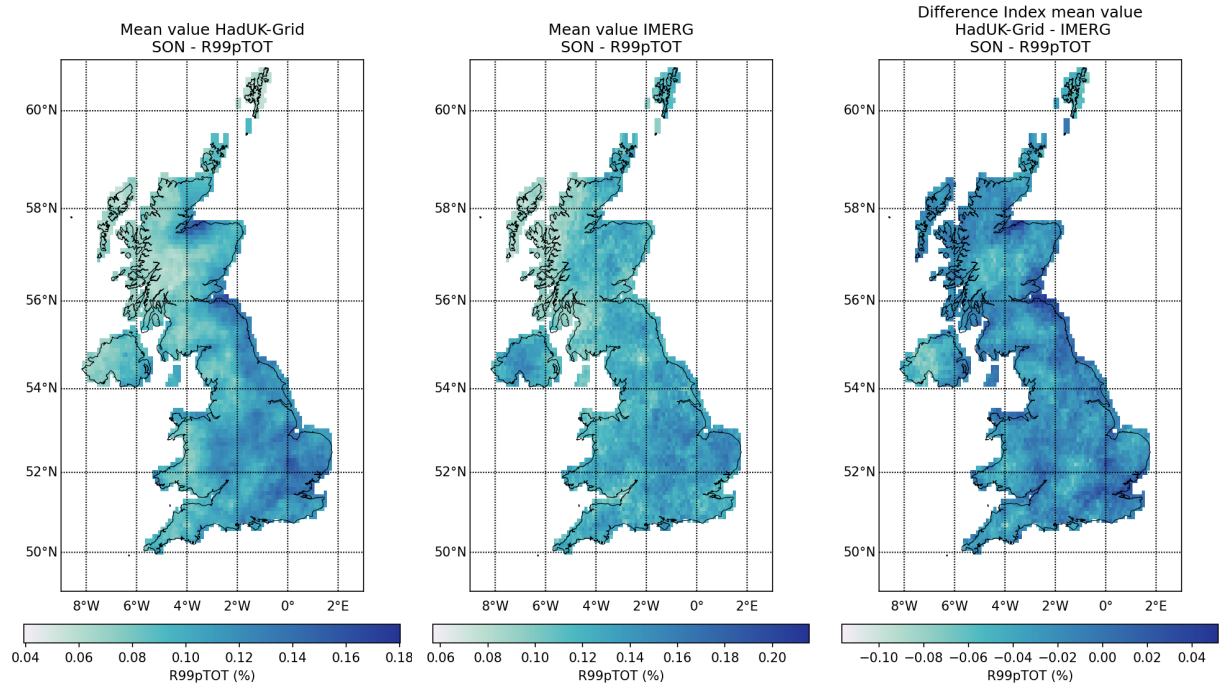


Figure 10: Spatial distribution of R99pTOT values obtained from HadUK-Grid and IMERG, and arithmetic difference between HadUK-Grid and IMERG for autumn (SON) over the 2001–2019 climatological period (cont.).

1.2.2 ERA5 DATA

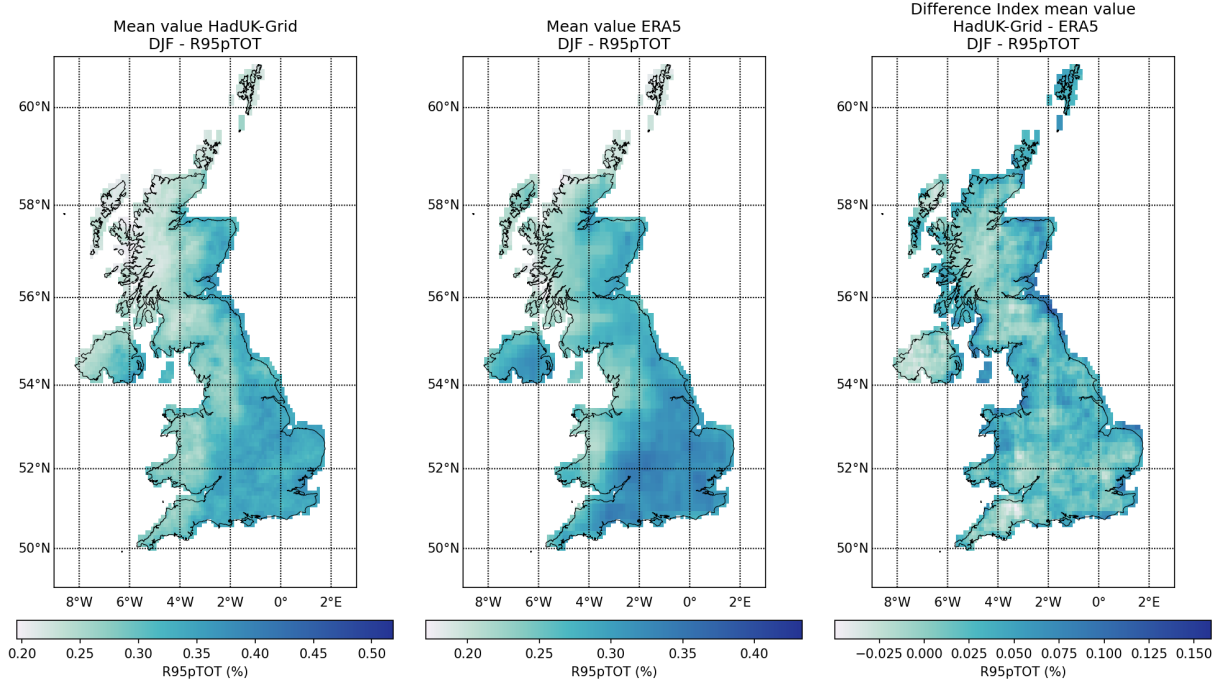


Figure 11: Spatial distribution of R95pTOT values obtained from HadUK-Grid and ERA5, and arithmetic difference between HadUK-Grid and ERA5 for winter (DJF) over the 2001–2019 climatological period

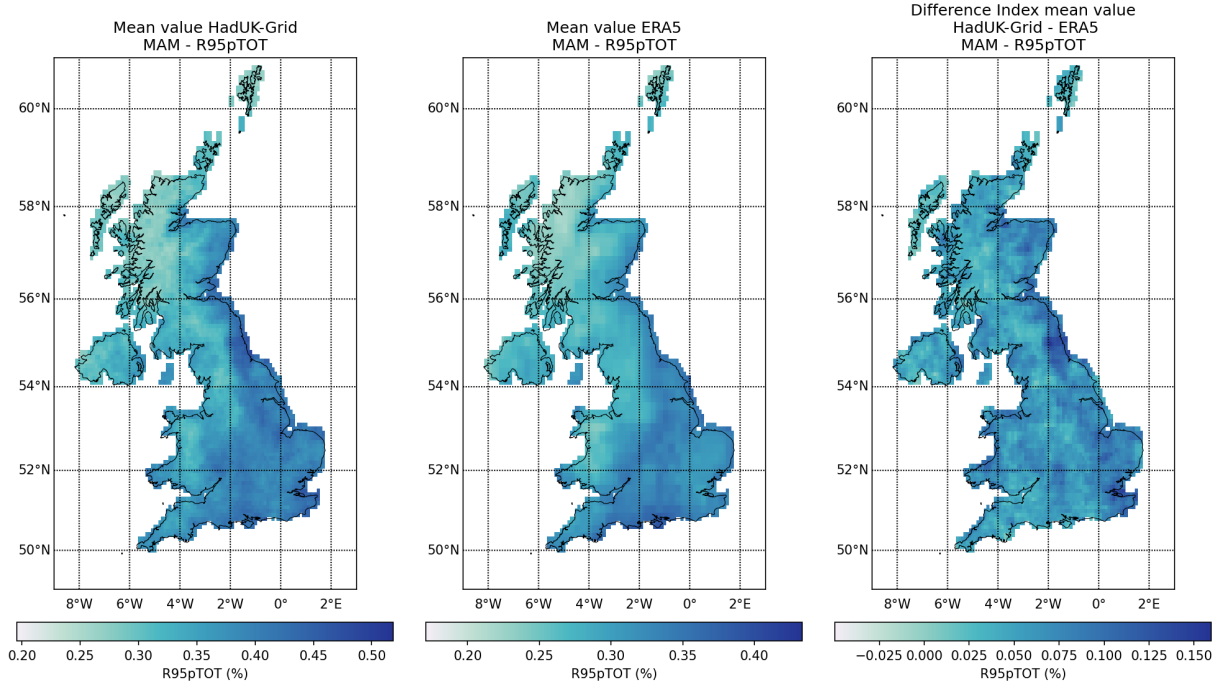


Figure 11: Spatial distribution of R95pTOT values obtained from HadUK-Grid and ERA5, and arithmetic difference between HadUK-Grid and ERA5 for spring (MAM) over the 2001–2019 climatological period.

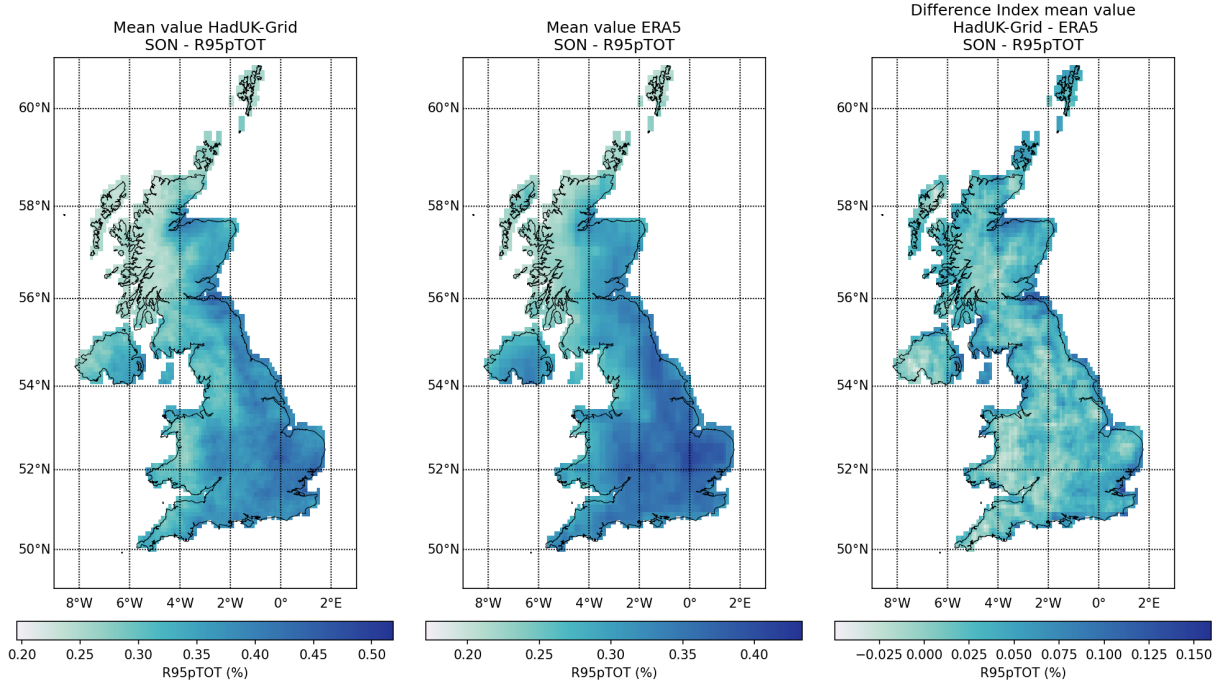


Figure 11: Spatial distribution of R95pTOT values obtained from HadUK-Grid and ERA5, and arithmetic difference between HadUK-Grid and ERA5 for autumn (SON) over the 2001–2019 climatological period (cont.).

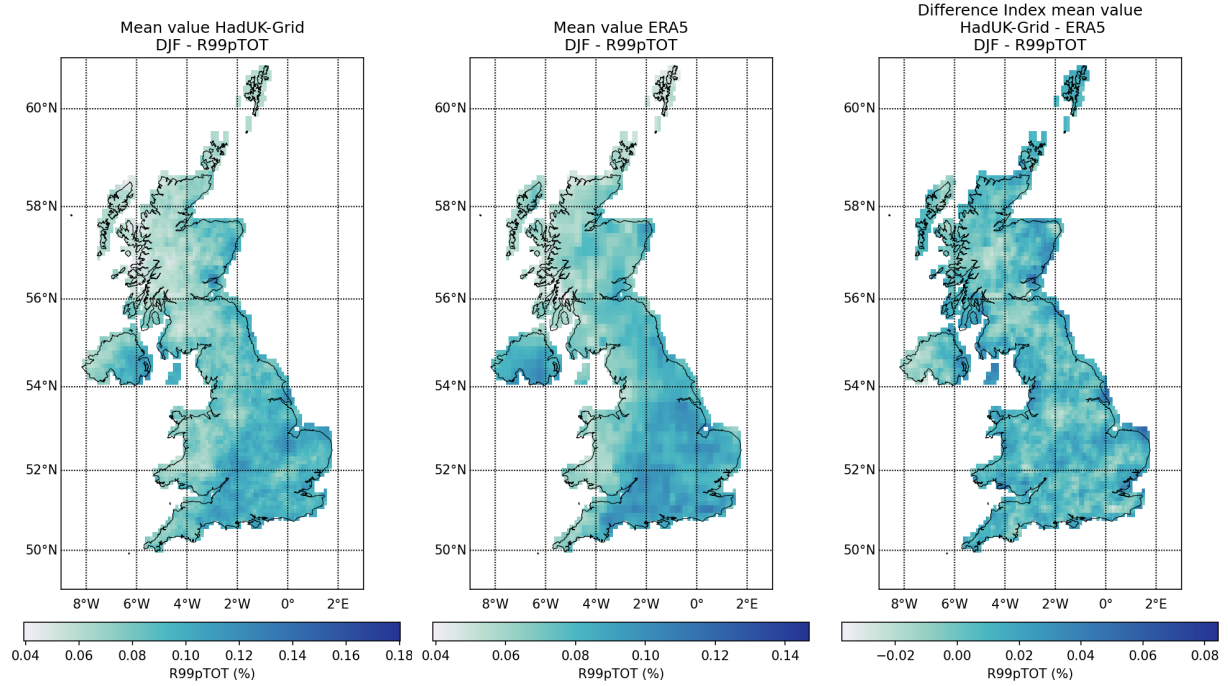


Figure 12: Spatial distribution of R99pTOT values obtained from HadUK-Grid and ERA5, and arithmetic difference between HadUK-Grid and ERA5 for winter (DJF) over the 2001–2019 climatological period

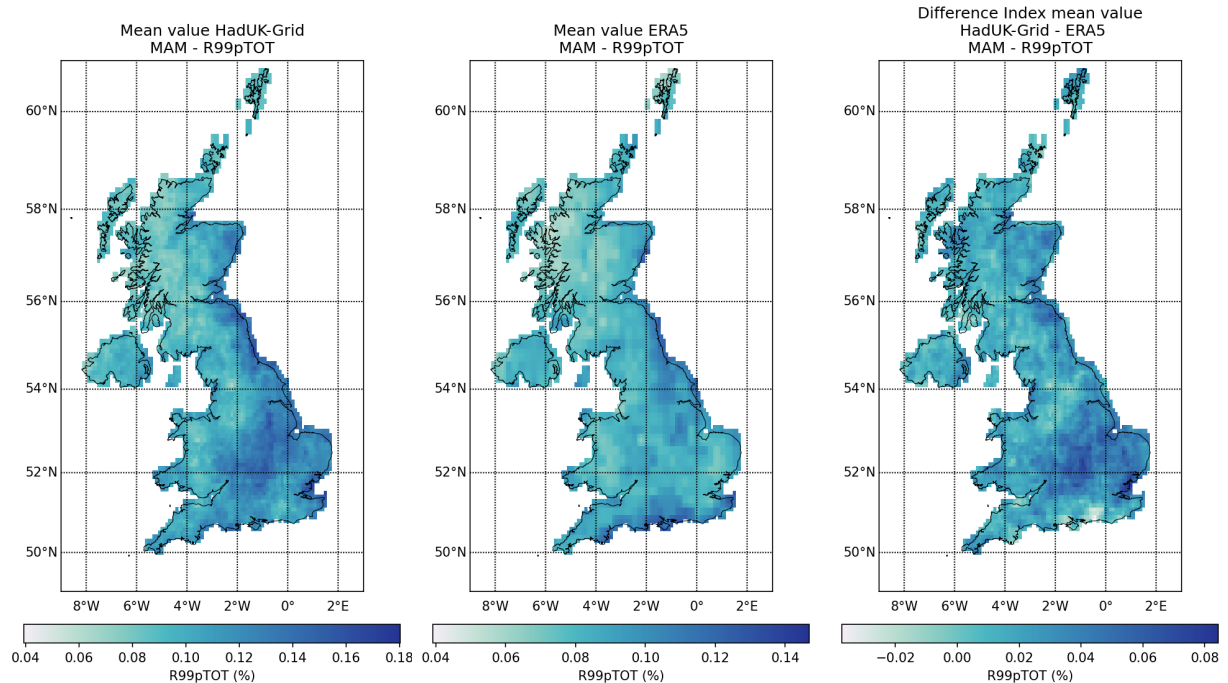


Figure 12: Spatial distribution of R99pTOT values obtained from HadUK-Grid and ERA5, and arithmetic difference between HadUK-Grid and ERA5 for spring (MAM) over the 2001–2019 climatological period (cont.).

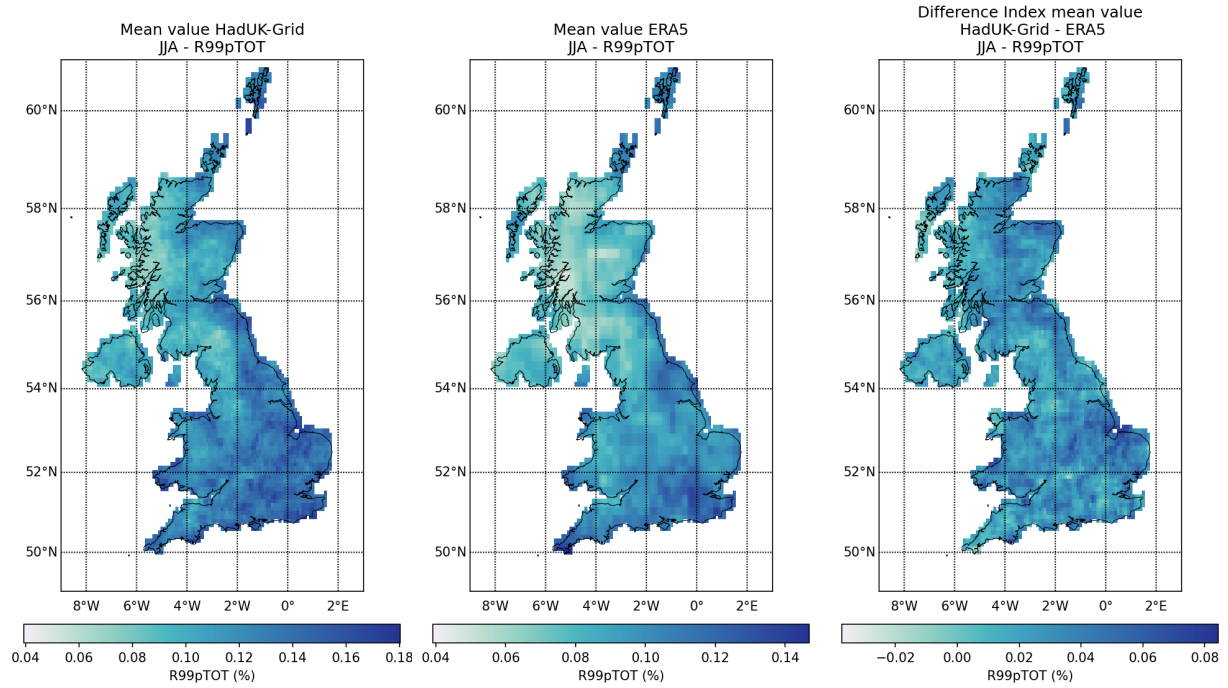


Figure 12: Spatial distribution of R99pTOT values obtained from HadUK-Grid and ERA5, and arithmetic difference between HadUK-Grid and ERA5 for summer (JJA) over the 2001–2019 climatological period (cont.).

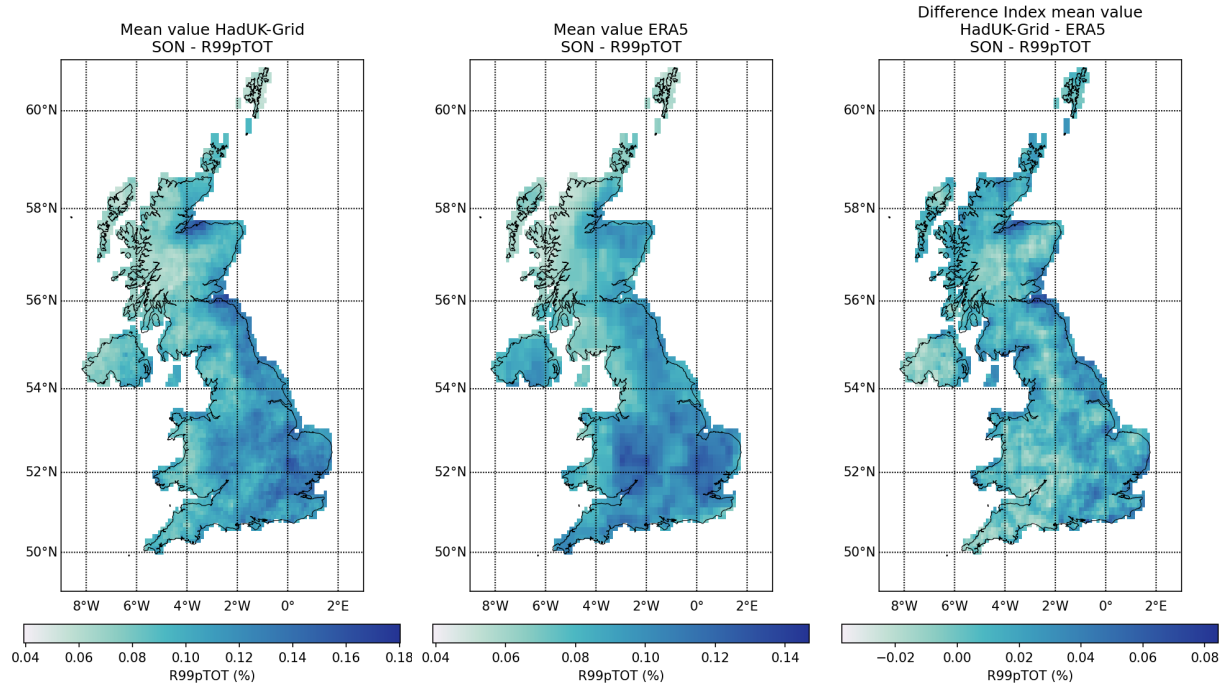


Figure 12: Spatial distribution of R99pTOT values obtained from HadUK-Grid and ERA5, and arithmetic difference between HadUK-Grid and ERA5 for autumn (SON) over the 2001–2019 climatological period (cont.).

1.3 Non-Threshold Indices - PRCPTOT, RX1day, RX5day, SDII

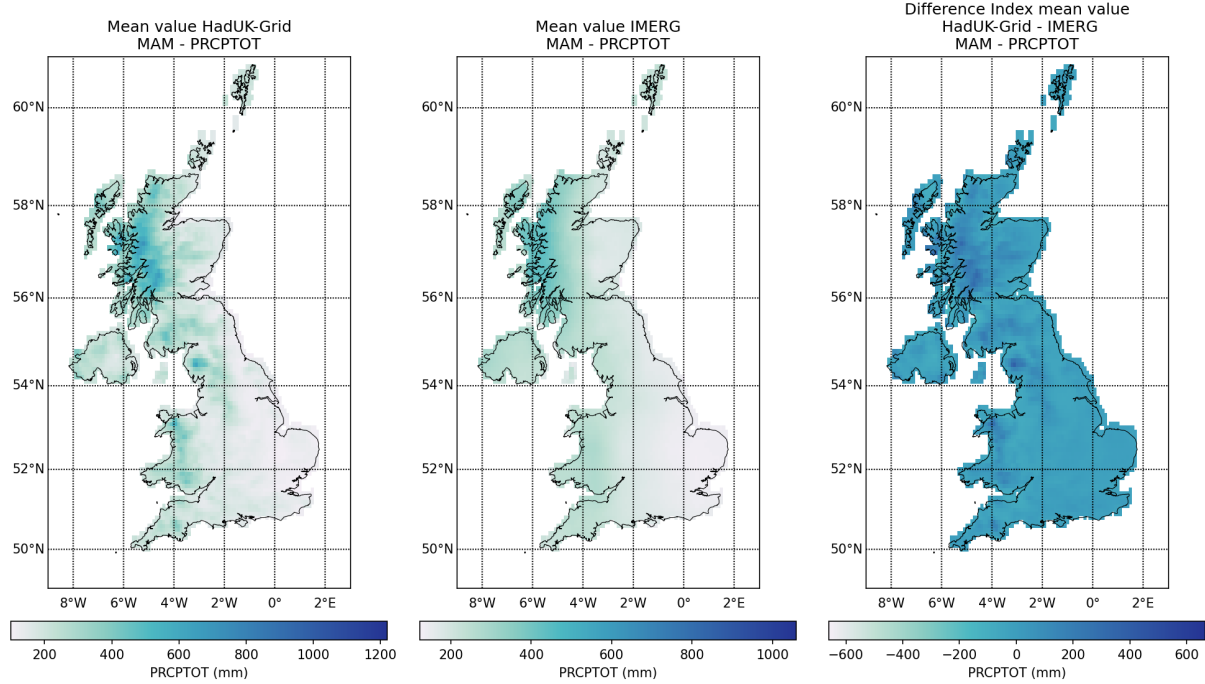


Figure 13: Spatial distribution of PRCPTOT values obtained from HadUK-Grid and IMERG and arithmetic difference between HadUK-Grid and IMERG for spring (MAM) over the 2001–2019 climatological period (cont.).

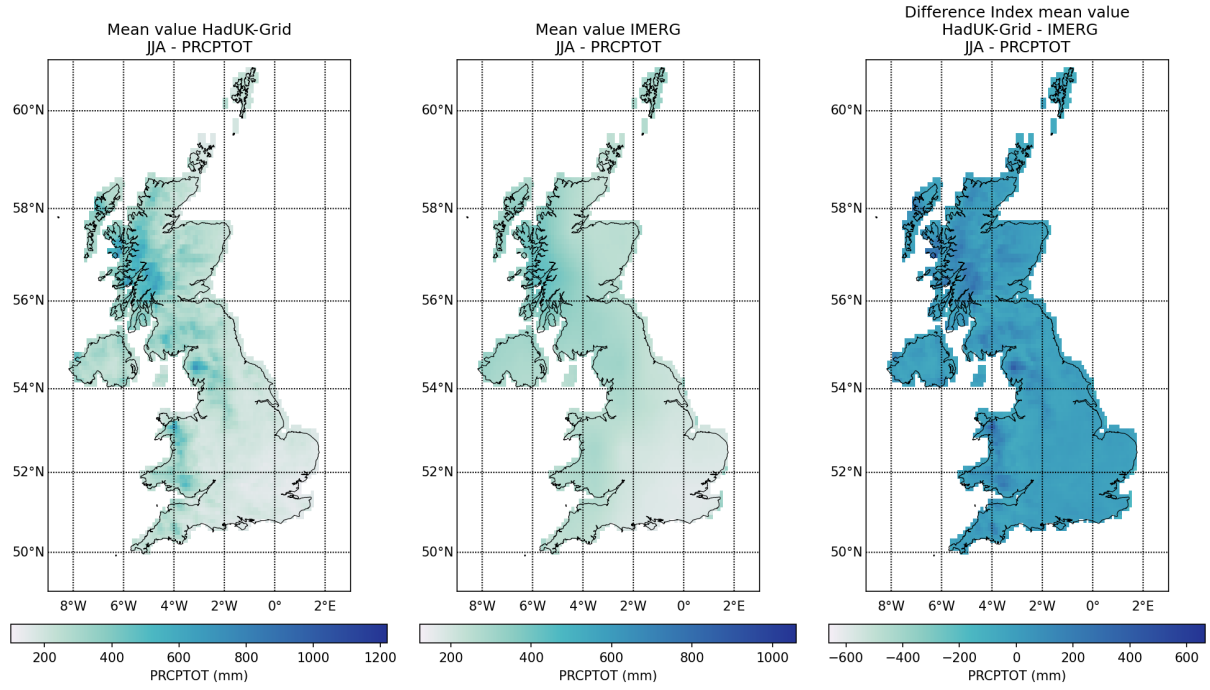


Figure 13: Spatial distribution of PRCPTOT values obtained from HadUK-Grid and IMERG and arithmetic difference between HadUK-Grid and IMERG for summer (JJA) over the 2001–2019 climatological period (cont.).

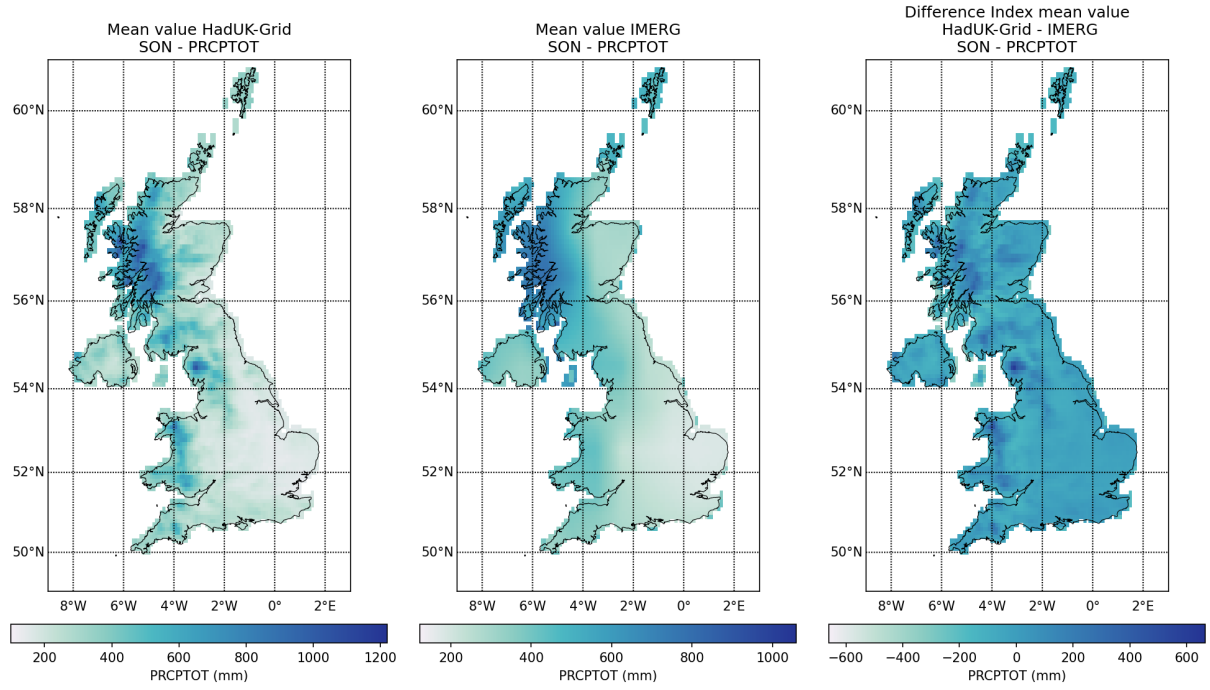


Figure 13: Spatial distribution of PRCPTOT values obtained from HadUK-Grid and IMERG and arithmetic difference between HadUK-Grid and IMERG for autumn (SON) over the 2001–2019 climatological period (cont.).

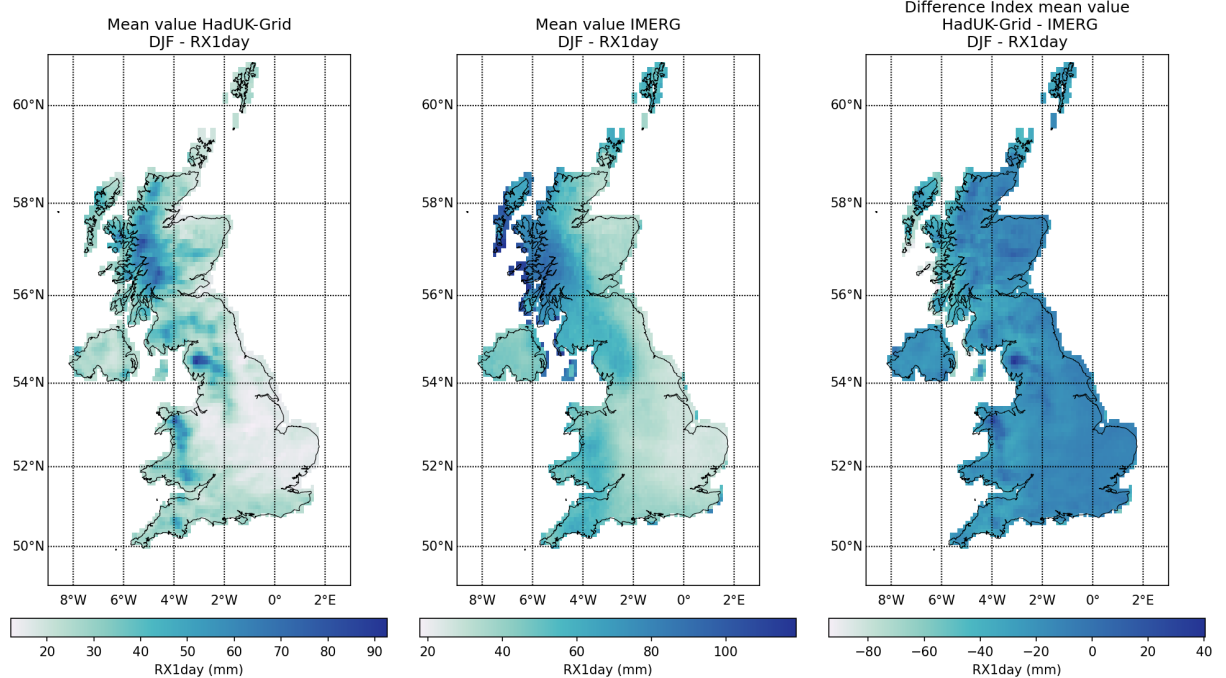


Figure 14: Spatial distribution of RX1day values obtained from HadUK-Grid and IMERG and arithmetic difference between HadUK-Grid and IMERG for winter (DJF) over the 2001–2019 climatological period

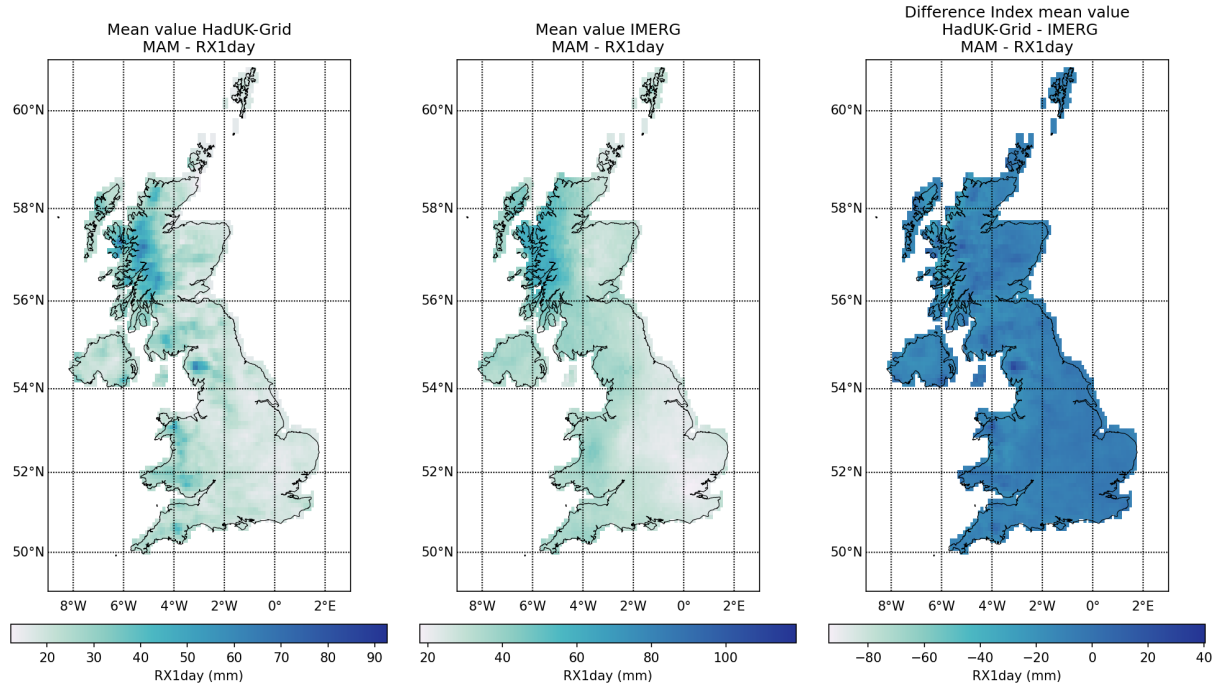


Figure 14: Spatial distribution of RX1day values obtained from HadUK-Grid and IMERG and arithmetic difference between HadUK-Grid and IMERG for spring (MAM) over the 2001–2019 climatological period (cont.).

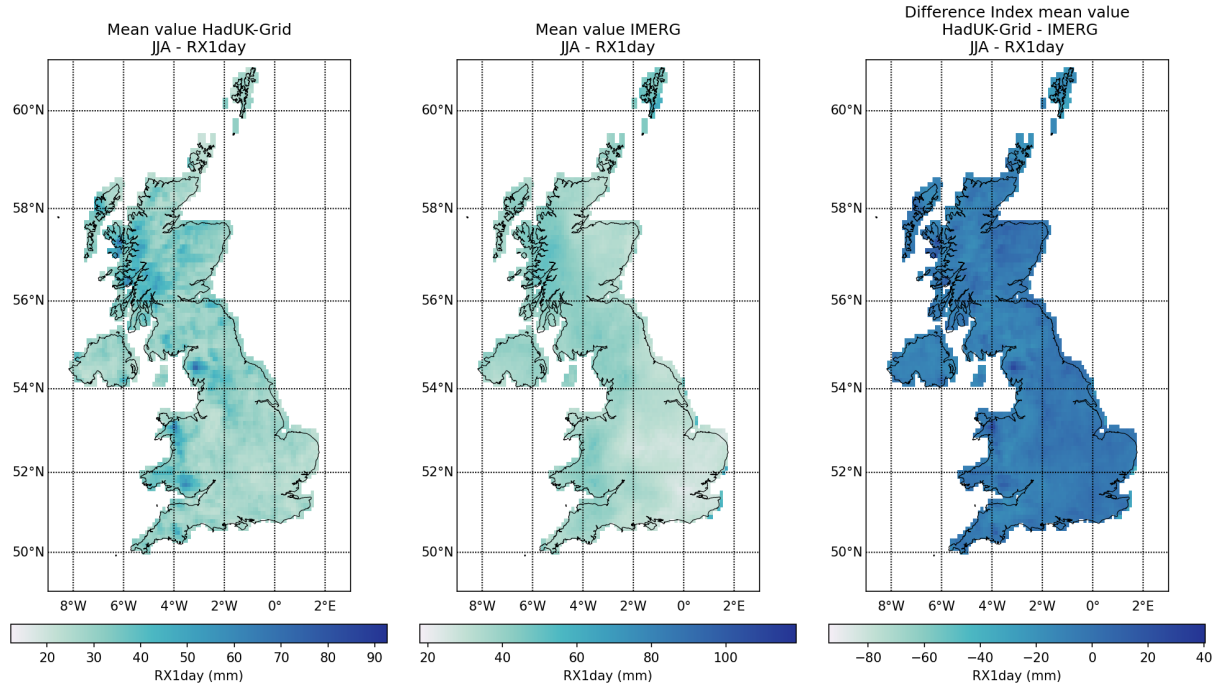


Figure 14: Spatial distribution of RX1day values obtained from HadUK-Grid and IMERG and arithmetic difference between HadUK-Grid and IMERG for summer (JJA) over the 2001–2019 climatological period (cont.).

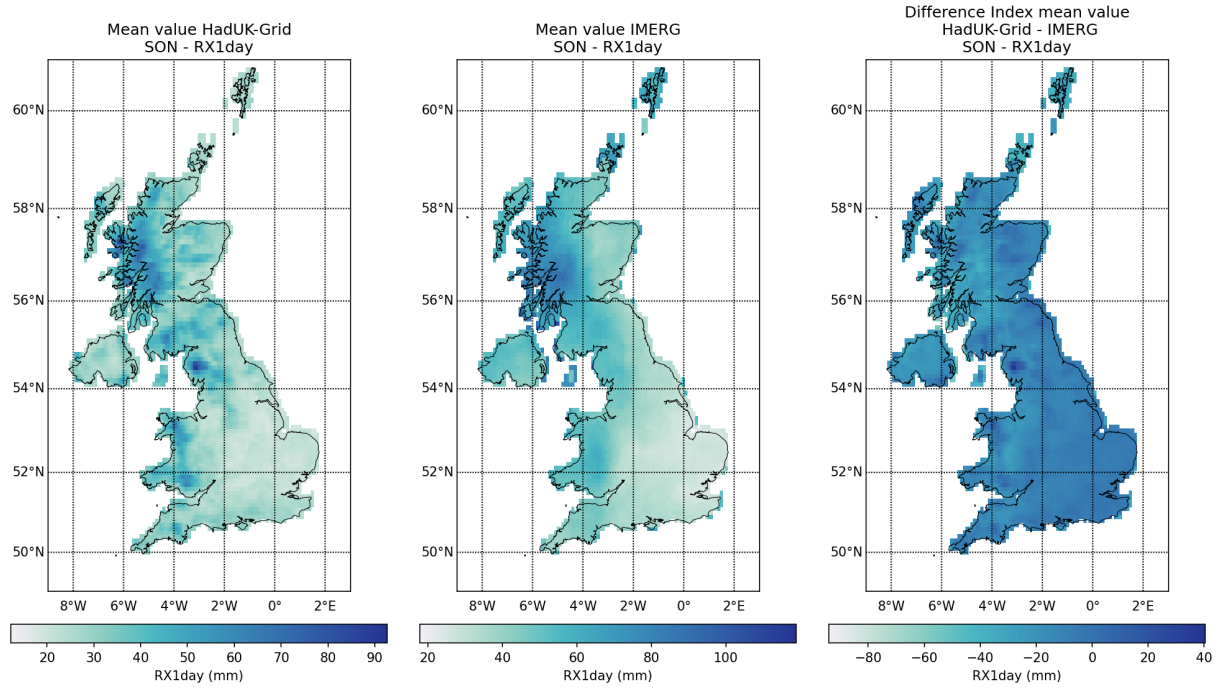


Figure 14: Spatial distribution of RX1day values obtained from HadUK-Grid and IMERG and arithmetic difference between HadUK-Grid and IMERG for autumn (SON) over the 2001–2019 climatological period (cont.).

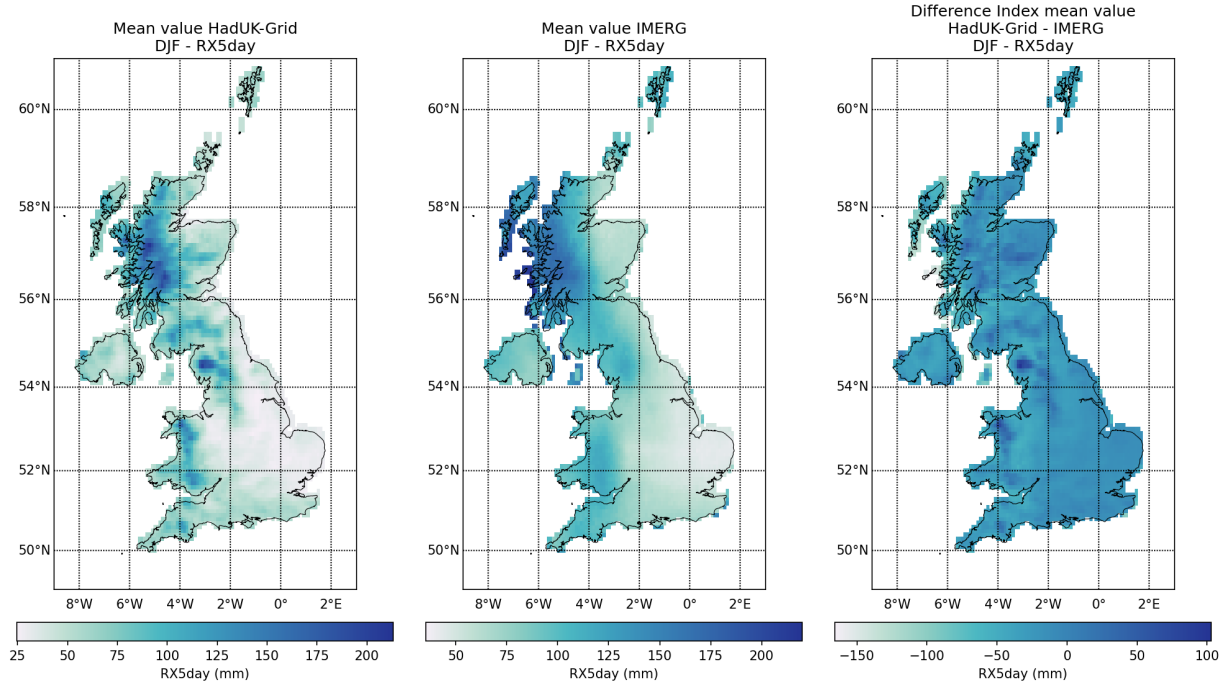


Figure 15: Spatial distribution of RX5day values obtained from HadUK-Grid and IMERG and arithmetic difference between HadUK-Grid and IMERG for winter (DJF) over the 2001–2019 climatological period

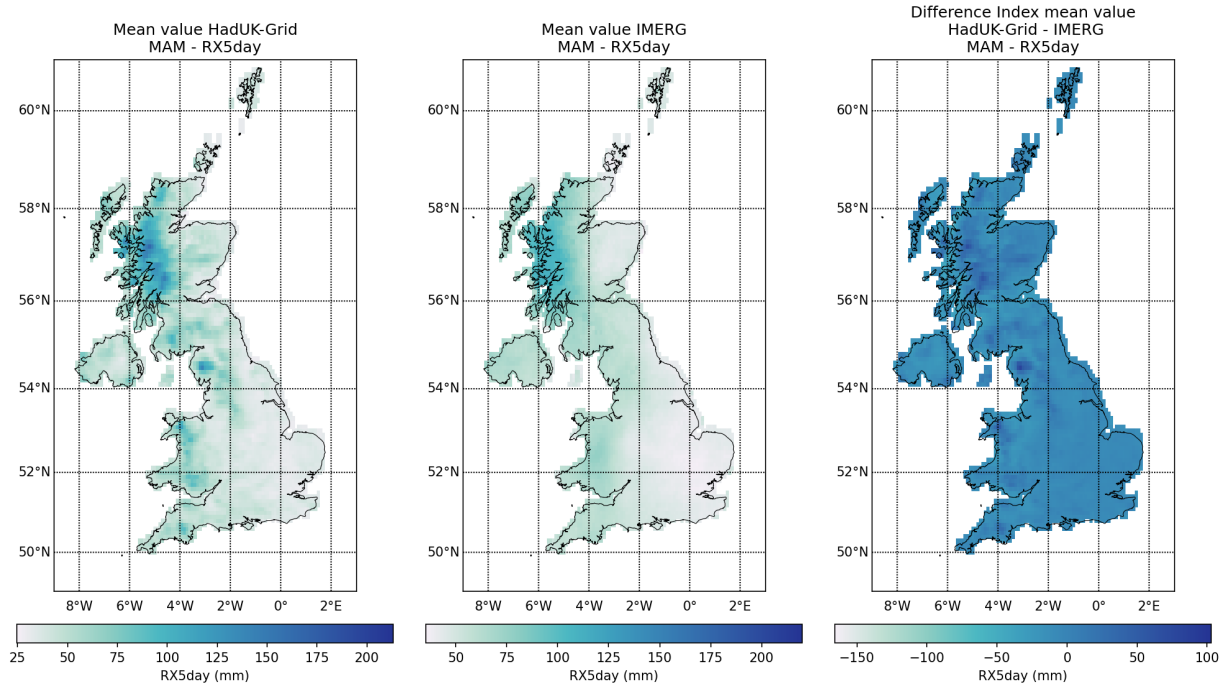


Figure 15: Spatial distribution of RX5day values obtained from HadUK-Grid and IMERG and arithmetic difference between HadUK-Grid and IMERG for spring (MAM) over the 2001–2019 climatological period (cont.).

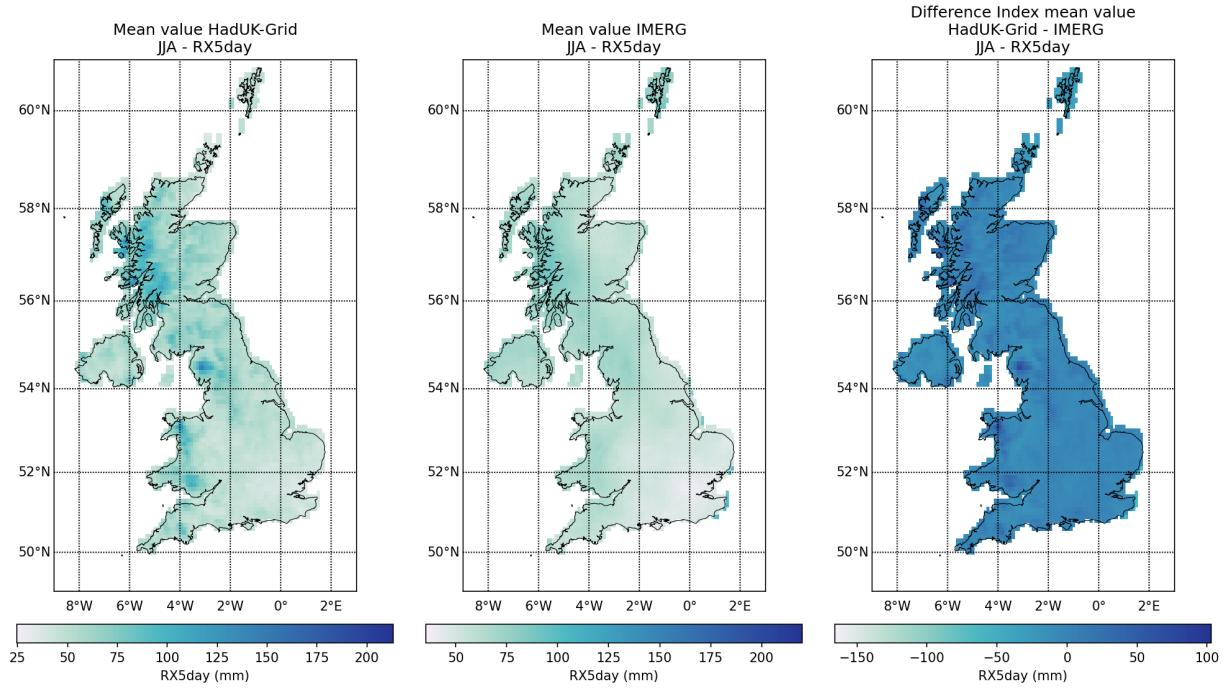


Figure 15: Spatial distribution of RX5day values obtained from HadUK-Grid and IMERG and arithmetic difference between HadUK-Grid and IMERG for summer (JJA) over the 2001–2019 climatological period (cont.).

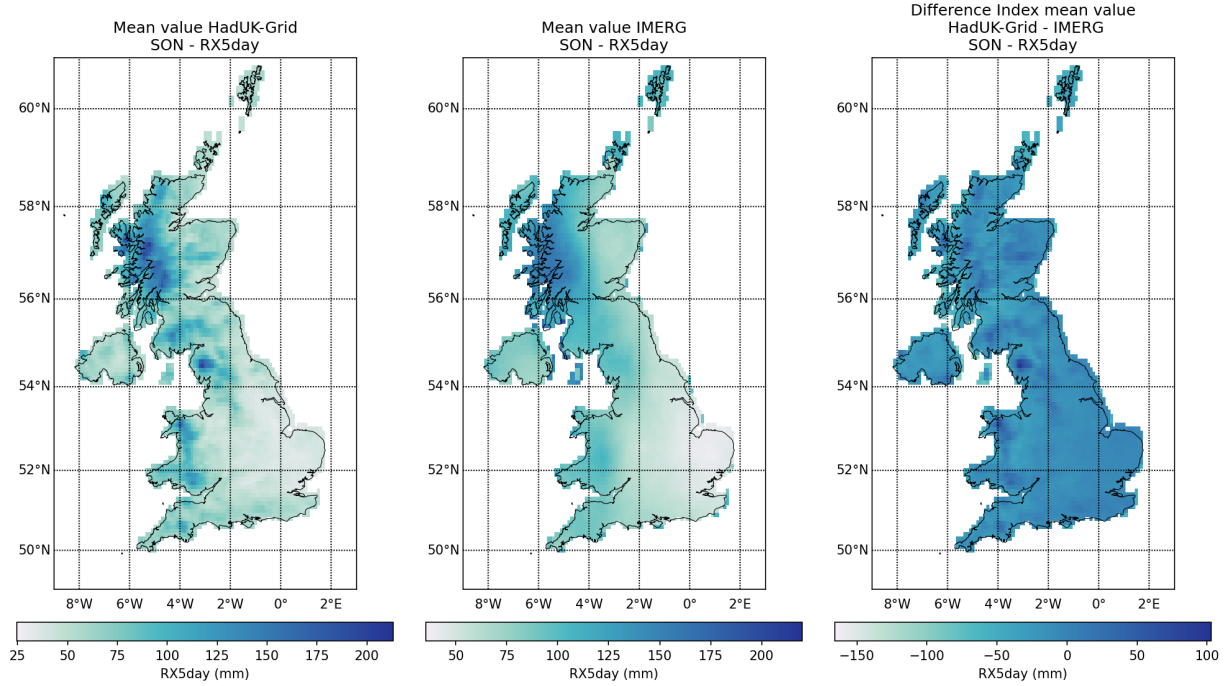


Figure 15: Spatial distribution of RX5day values obtained from HadUK-Grid and IMERG and arithmetic difference between HadUK-Grid and IMERG for autumn (SON) over the 2001–2019 climatological period (cont.).

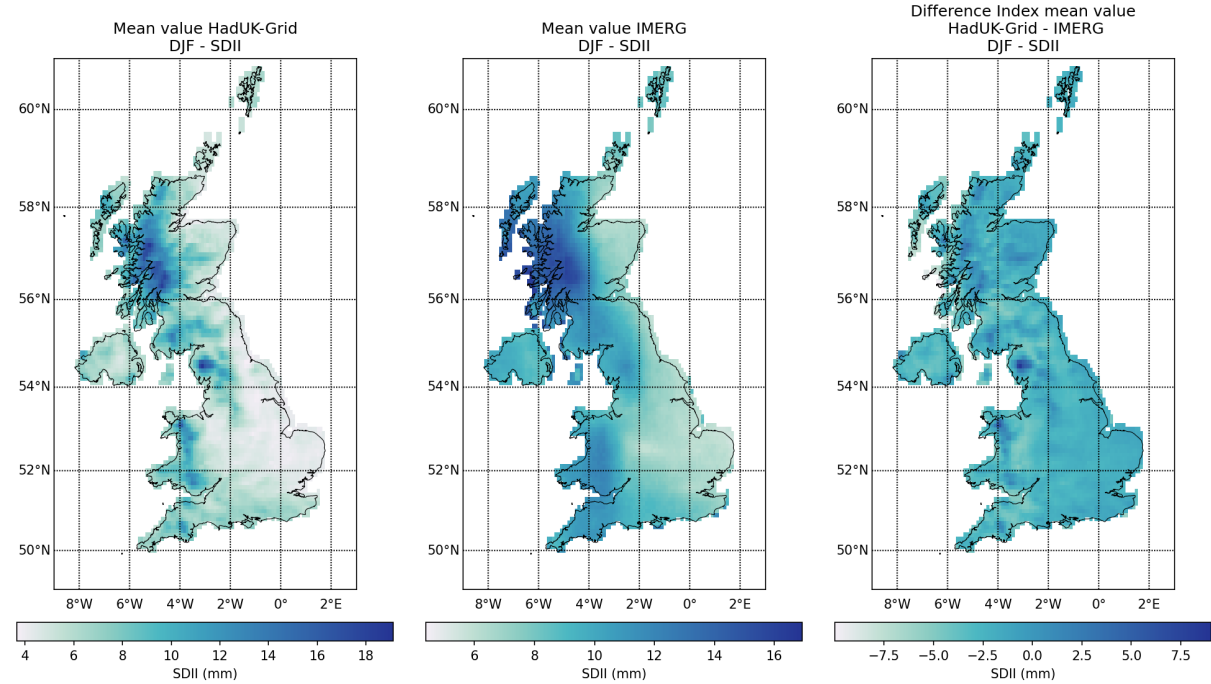


Figure 16: Spatial distribution of SDII values obtained from HadUK-Grid and IMERG and arithmetic difference between HadUK-Grid and IMERG for winter (DJF) over the 2001–2019 climatological period

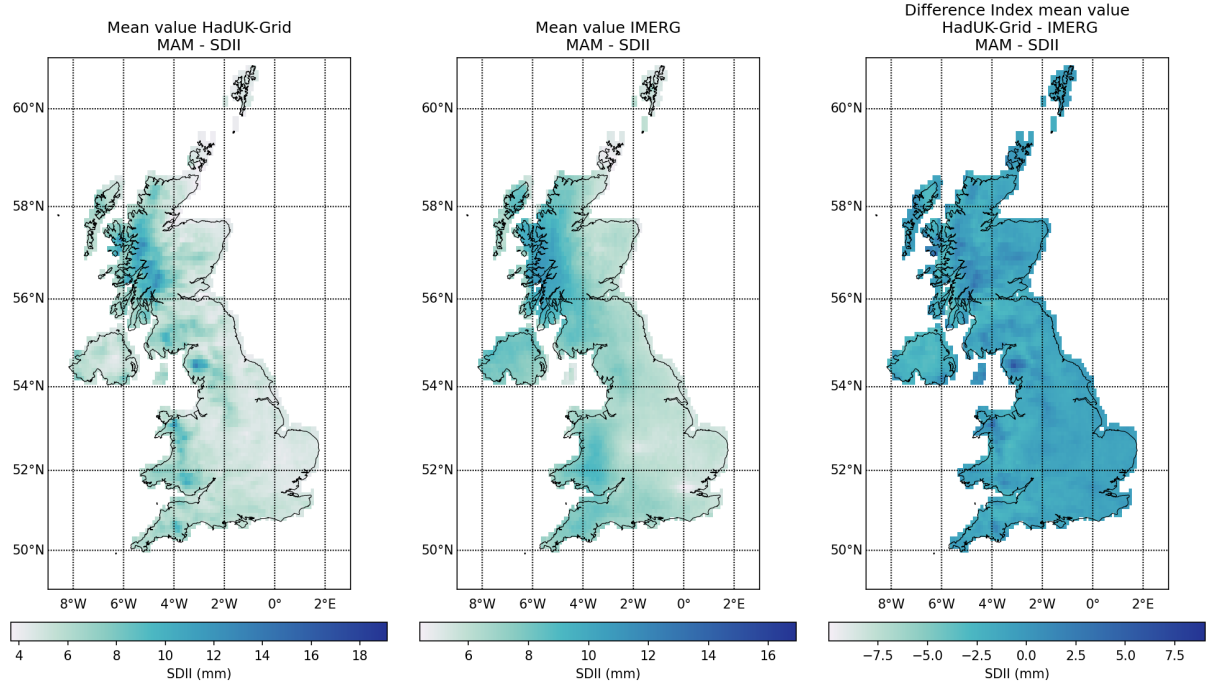


Figure 16: Spatial distribution of SDII values obtained from HadUK-Grid and IMERG and arithmetic difference between HadUK-Grid and IMERG for spring (MAM) over the 2001–2019 climatological period (cont.).

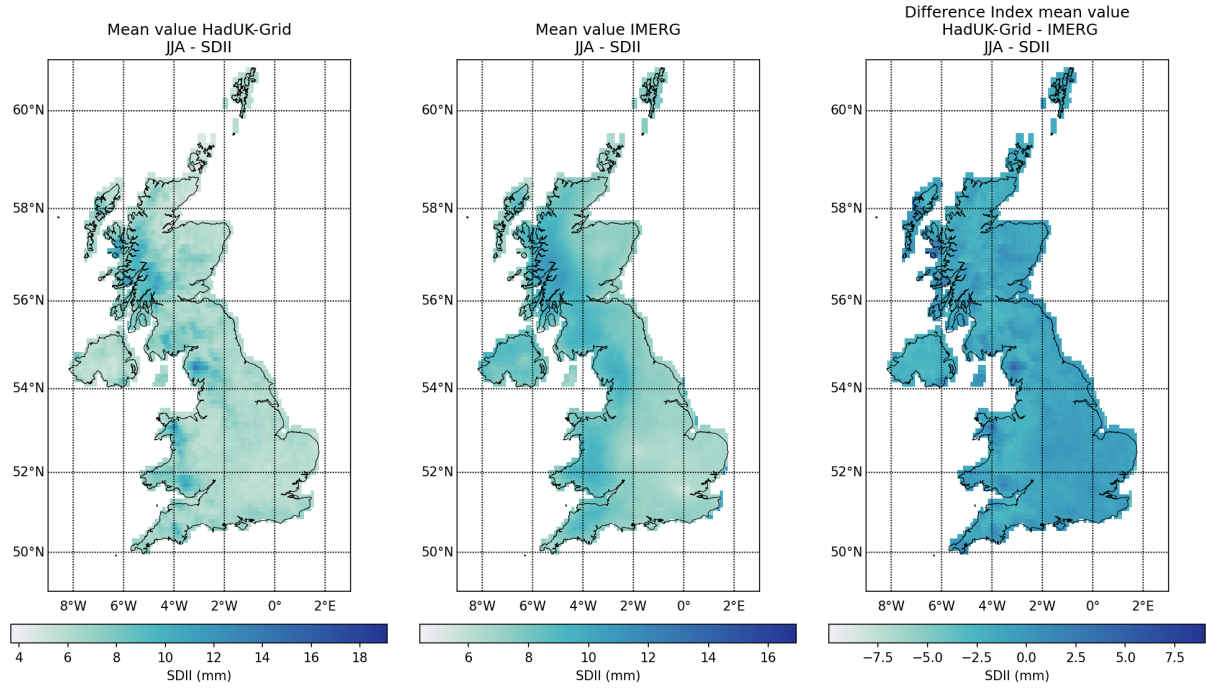


Figure 16: Spatial distribution of SDII values obtained from HadUK-Grid and IMERG and arithmetic difference between HadUK-Grid and IMERG for summer (JJA) over the 2001–2019 climatological period (cont.).

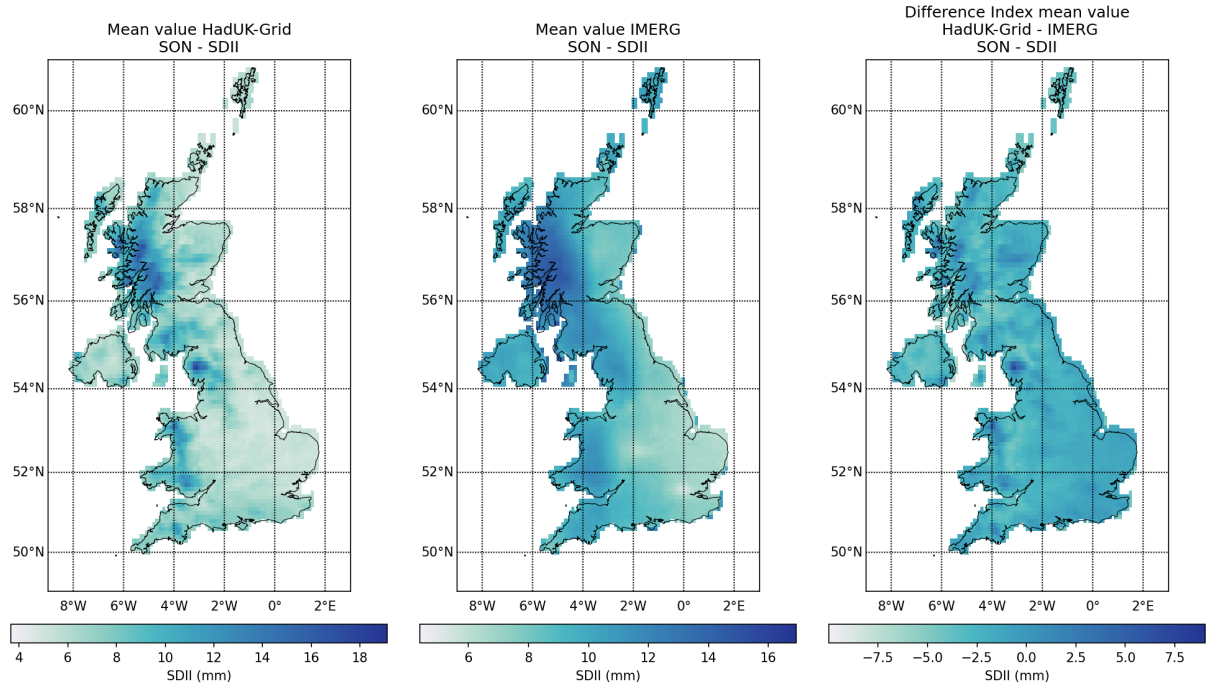


Figure 16: Spatial distribution of SDII values obtained from HadUK-Grid and IMERG and arithmetic difference between HadUK-Grid and IMERG for autumn (SON) over the 2001–2019 climatological period (cont.).

1.3.1 ERA5 DATA

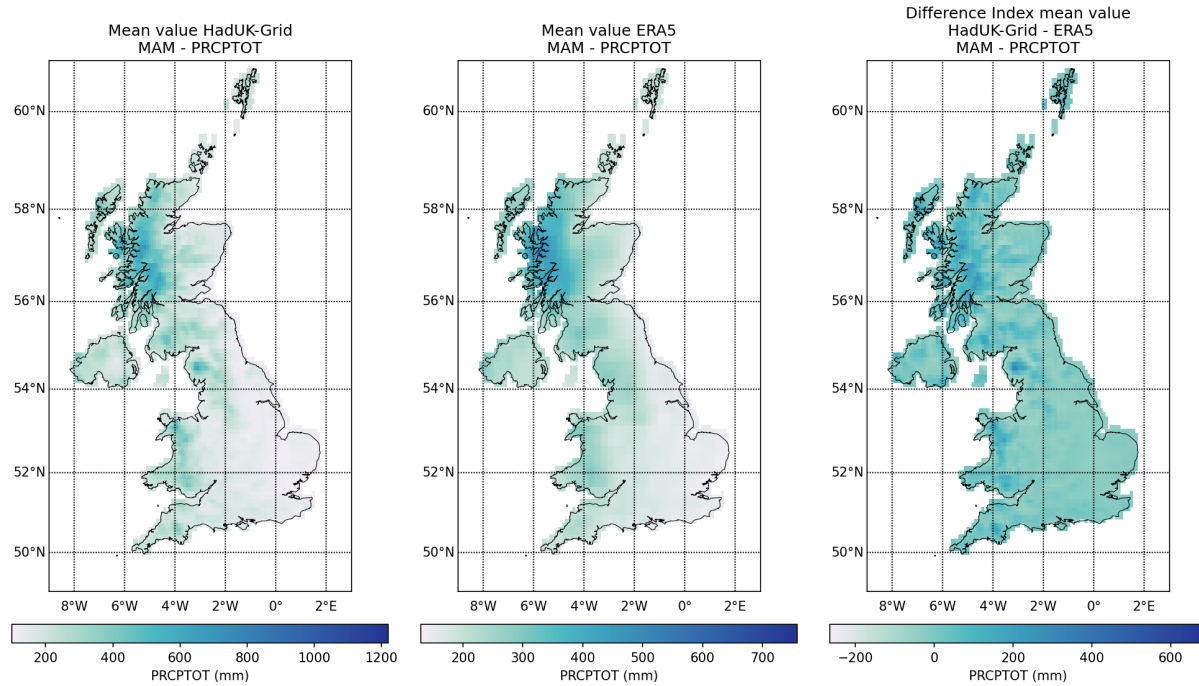


Figure 17: Spatial distribution of PRCPTOT values obtained from HadUK-Grid and ERA5 and arithmetic difference between HadUK-Grid and ERA5 for spring (MAM) over the 2001–2019 climatological period (cont.).

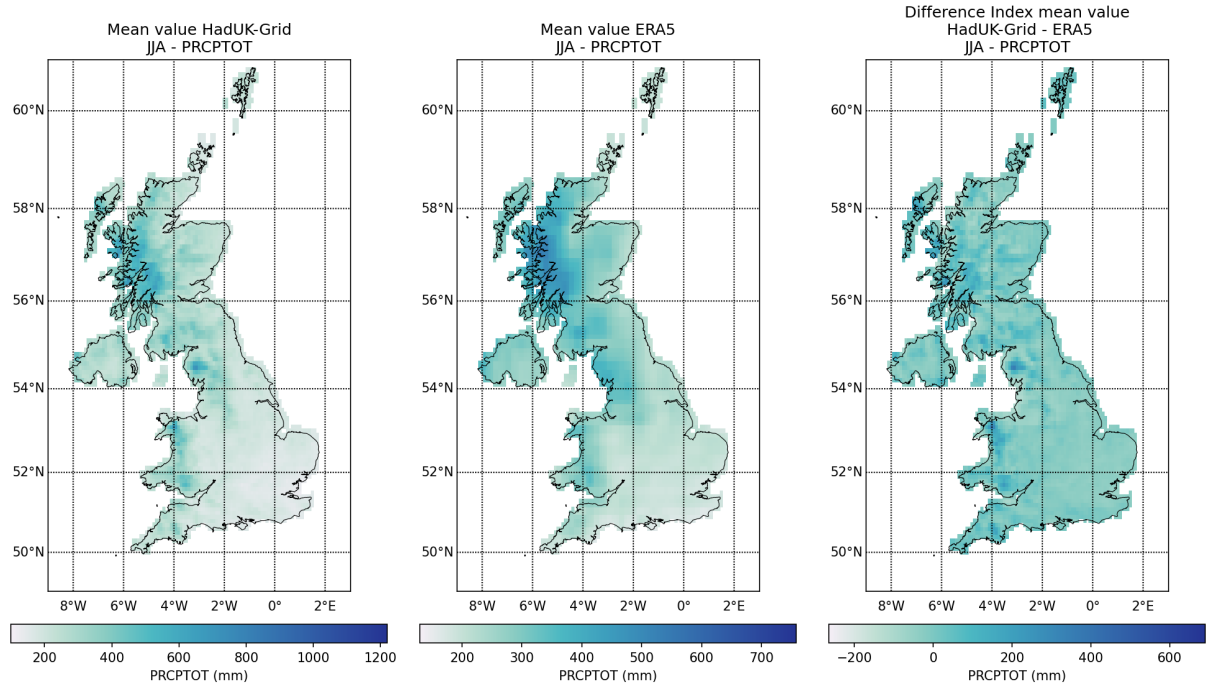


Figure 17: Spatial distribution of PRCPTOT values obtained from HadUK-Grid and ERA5 and arithmetic difference between HadUK-Grid and ERA5 for summer (JJA) over the 2001–2019 climatological period (cont.).

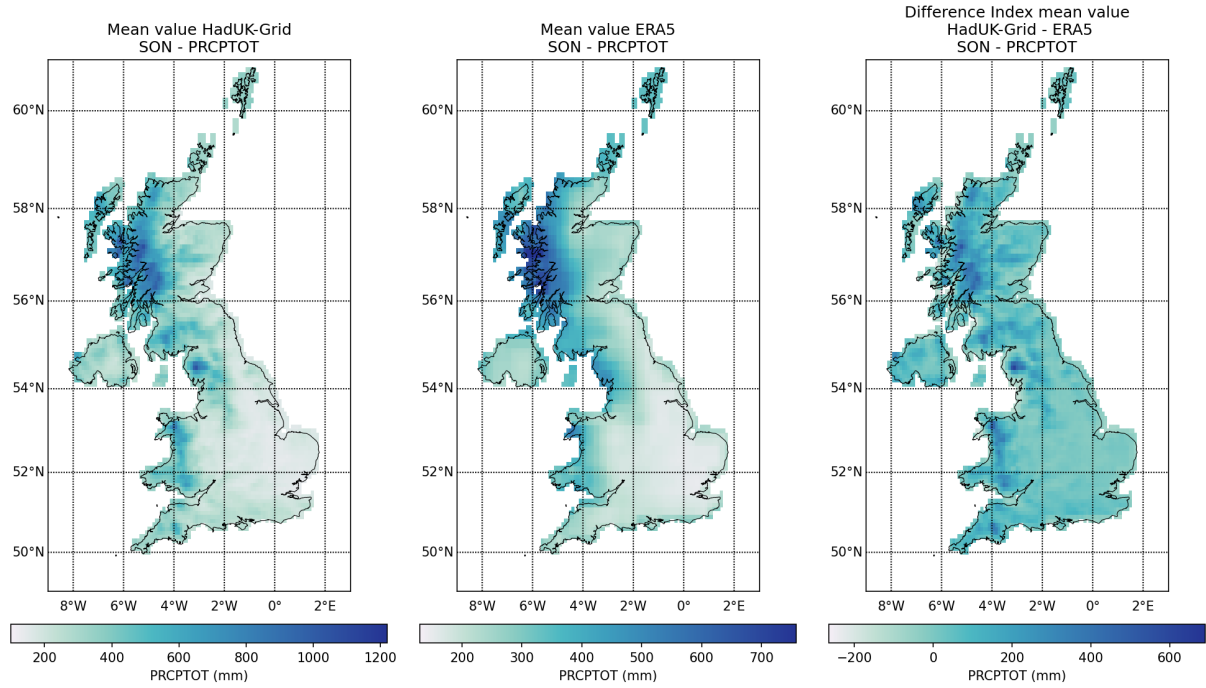


Figure 17: Spatial distribution of PRCPTOT values obtained from HadUK-Grid and ERA5 and arithmetic difference between HadUK-Grid and ERA5 for autumn (SON) over the 2001–2019 climatological period (cont.).

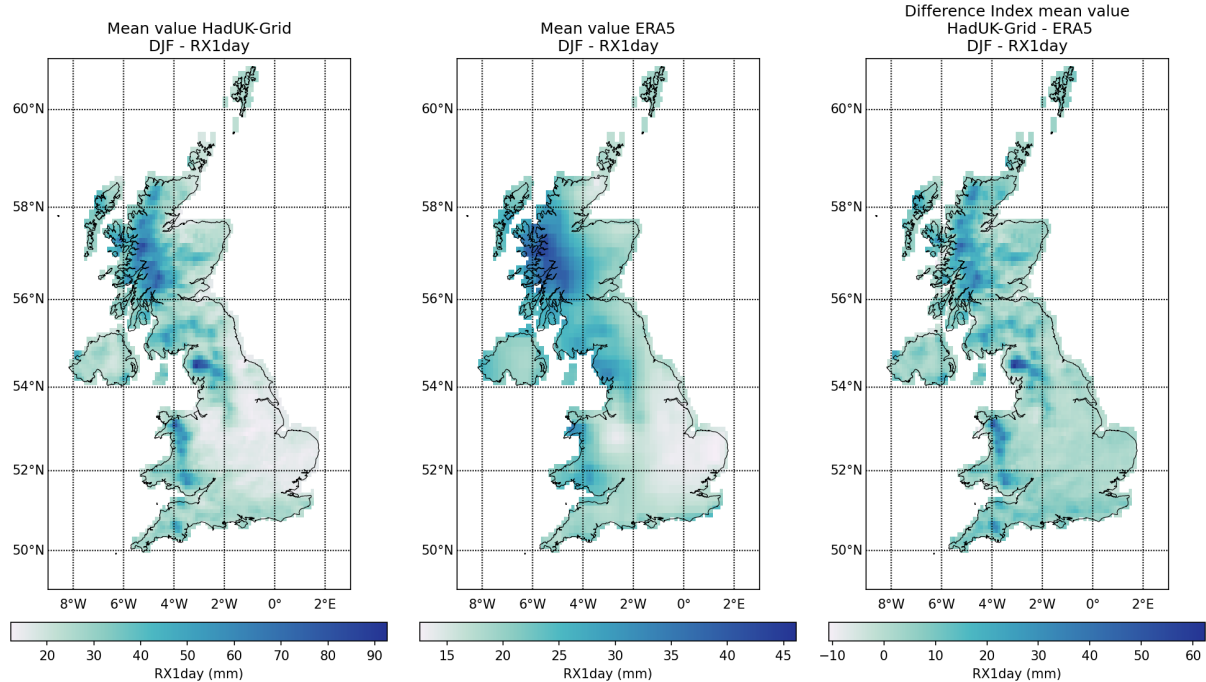


Figure 18: Spatial distribution of RX1day values obtained from HadUK-Grid and ERA5 and arithmetic difference between HadUK-Grid and ERA5 for winter (DJF) over the 2001–2019 climatological period

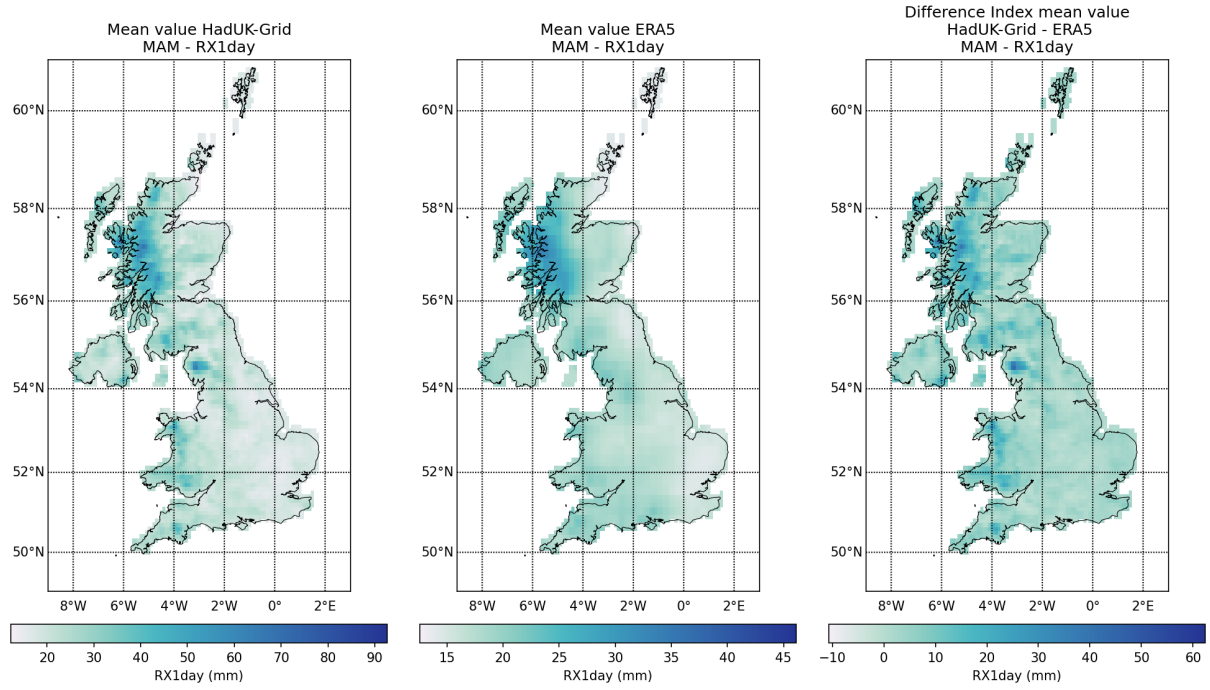


Figure 18: Spatial distribution of RX1day values obtained from HadUK-Grid and ERA5 and arithmetic difference between HadUK-Grid and ERA5 for spring (MAM) over the 2001–2019 climatological period (cont.).

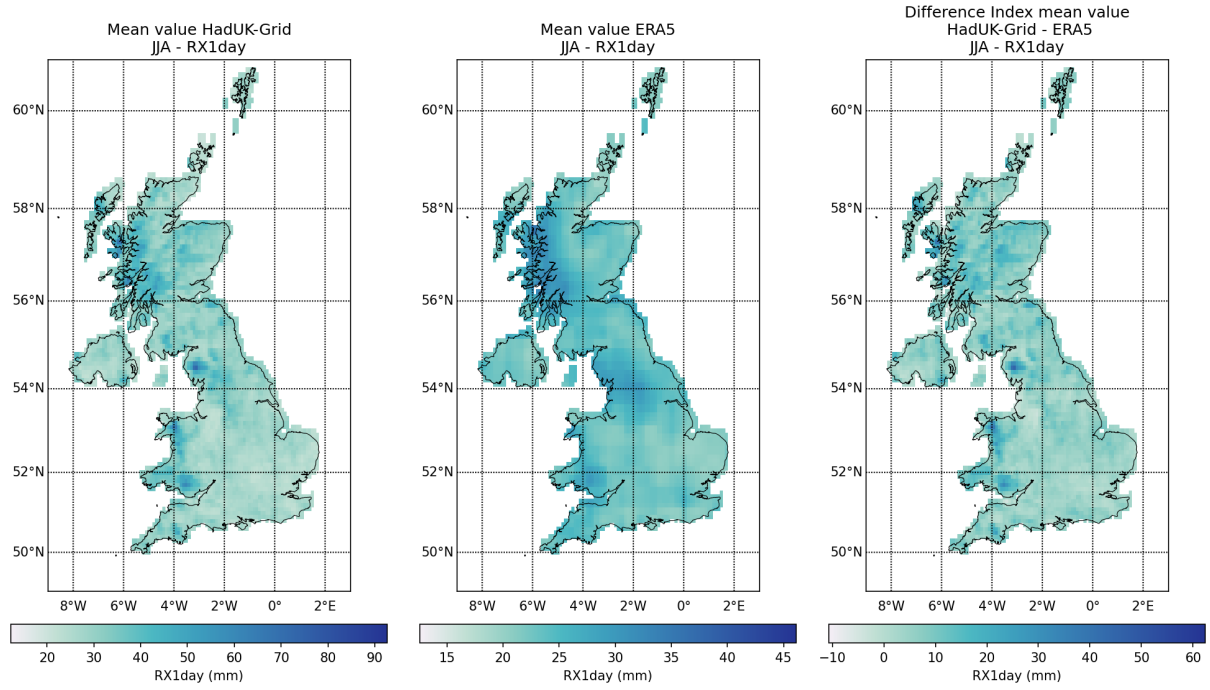


Figure 18: Spatial distribution of RX1day values obtained from HadUK-Grid and ERA5 and arithmetic difference between HadUK-Grid and ERA5 for summer (JJA) over the 2001–2019 climatological period (cont.).

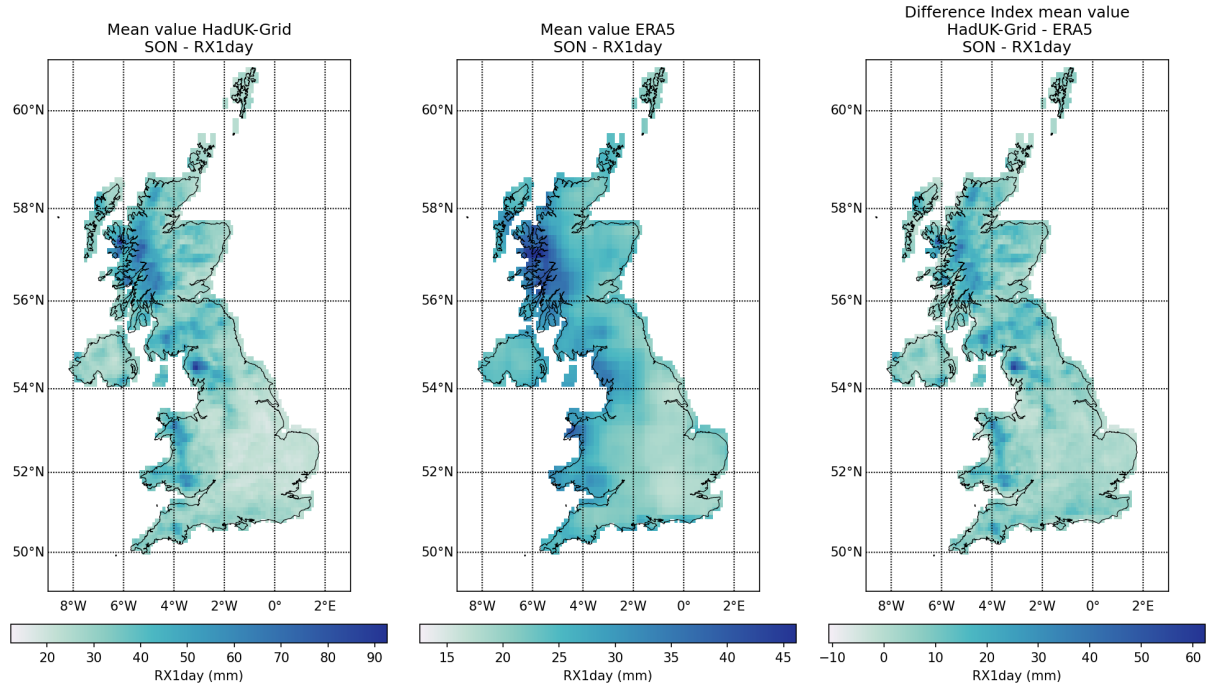


Figure 18: Spatial distribution of RX1day values obtained from HadUK-Grid and ERA5 and arithmetic difference between HadUK-Grid and ERA5 for autumn (SON) over the 2001–2019 climatological period (cont.).

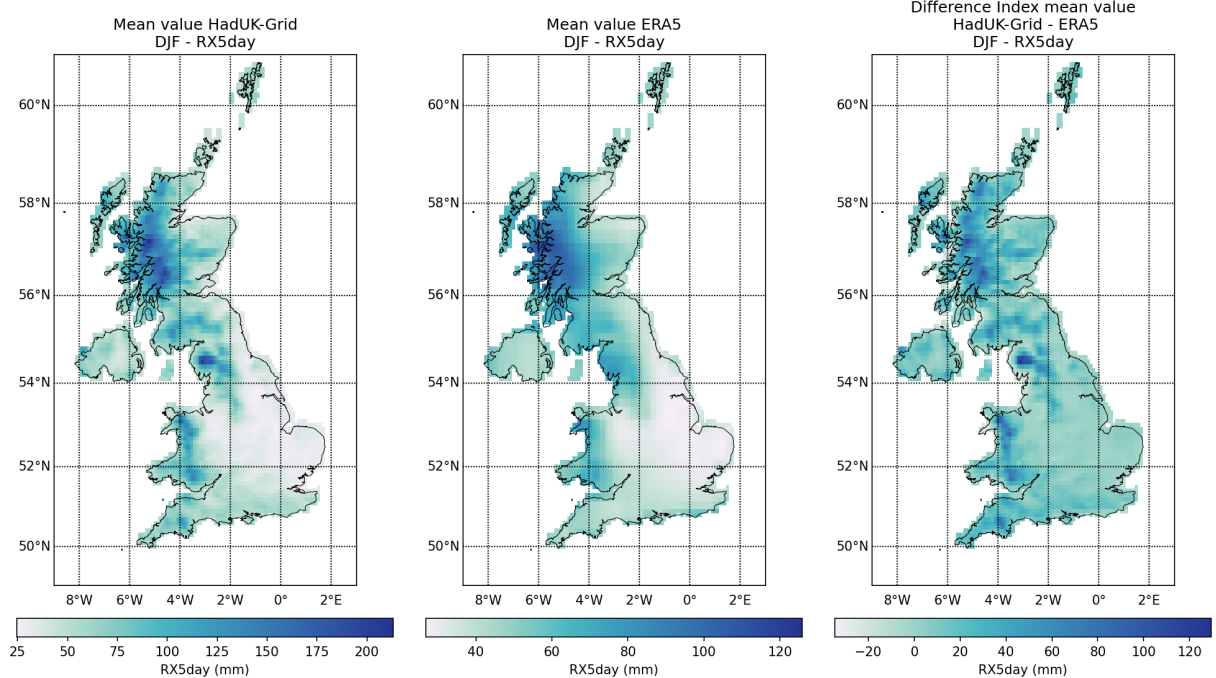


Figure 19: Spatial distribution of RX5day values obtained from HadUK-Grid and ERA5 and arithmetic difference between HadUK-Grid and ERA5 for winter (DJF) over the 2001–2019 climatological period

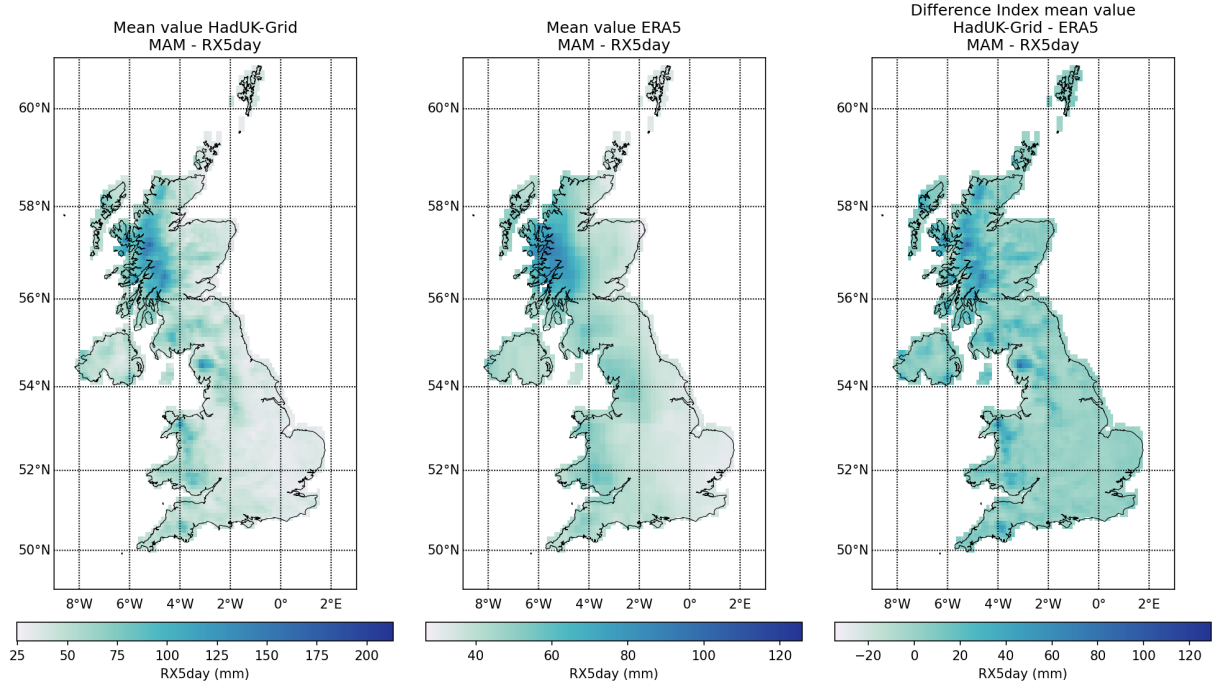


Figure 19: Spatial distribution of RX5day values obtained from HadUK-Grid and ERA5 and arithmetic difference between HadUK-Grid and ERA5 for spring (MAM) over the 2001–2019 climatological period (cont.).

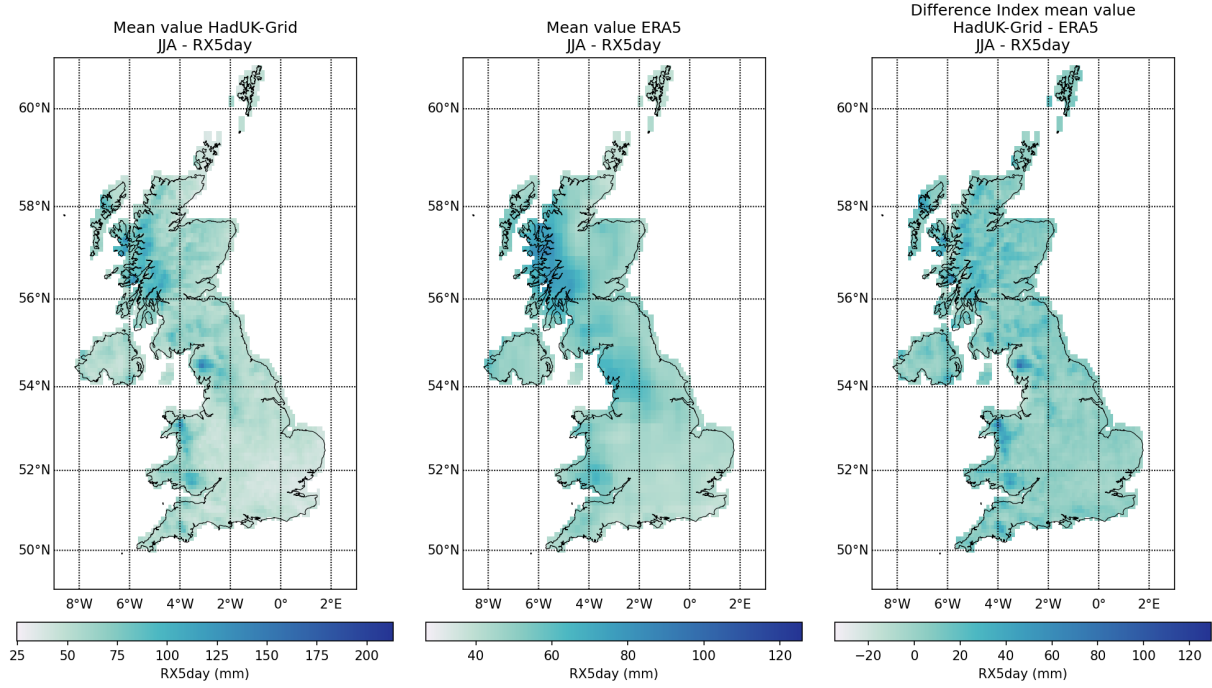


Figure 19: Spatial distribution of RX5day values obtained from HadUK-Grid and ERA5 and arithmetic difference between HadUK-Grid and ERA5 for summer (JJA) over the 2001–2019 climatological period (cont.).

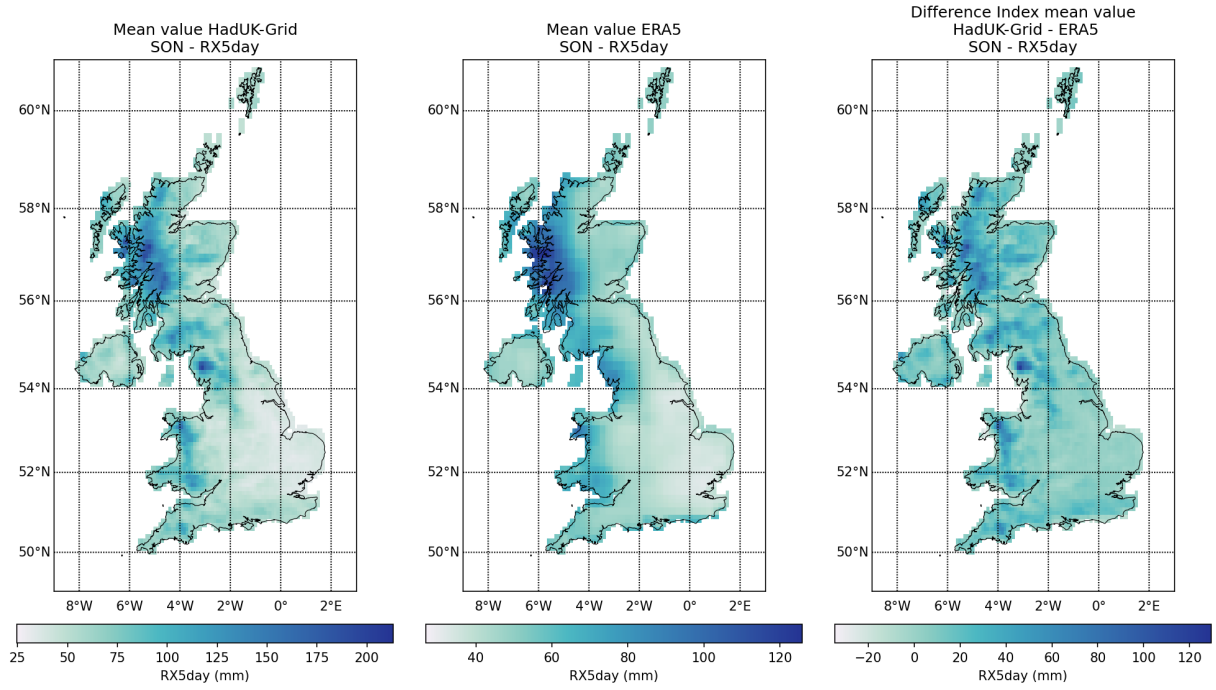


Figure 19: Spatial distribution of RX5day values obtained from HadUK-Grid and ERA5 and arithmetic difference between HadUK-Grid and ERA5 for autumn (SON) over the 2001–2019 climatological period (cont.).

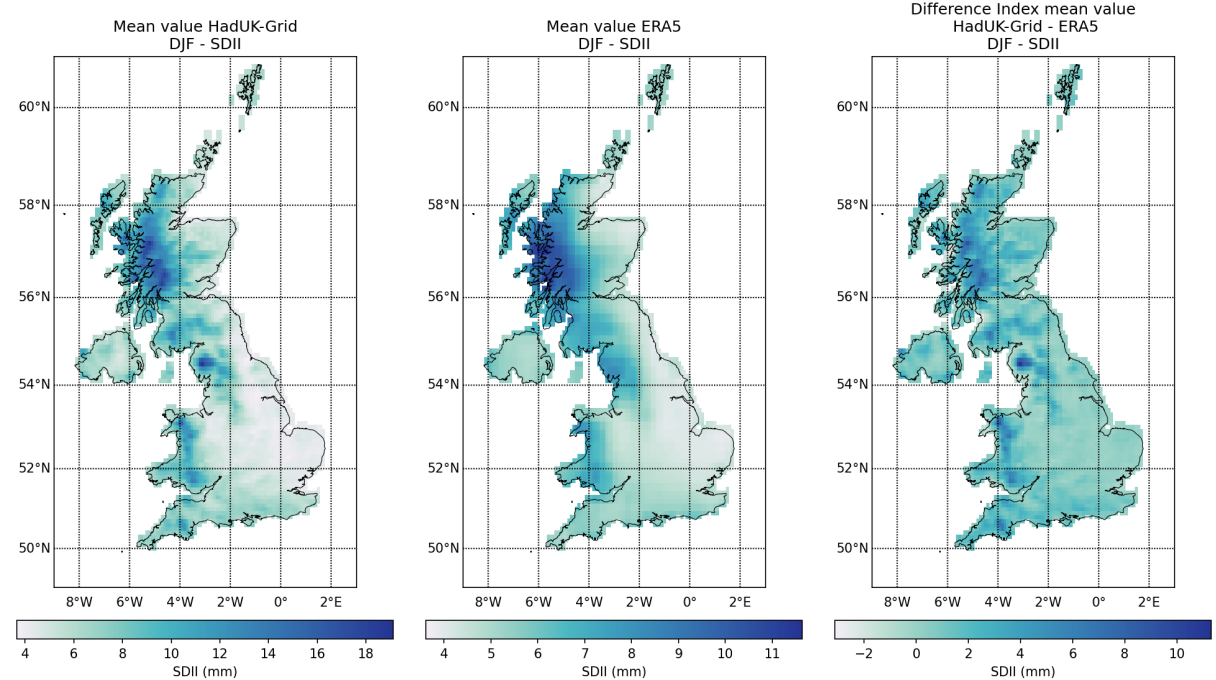


Figure 20: Spatial distribution of SDII values obtained from HadUK-Grid and ERA5 and arithmetic difference between HadUK-Grid and ERA5 for winter (DJF) over the 2001–2019 climatological period

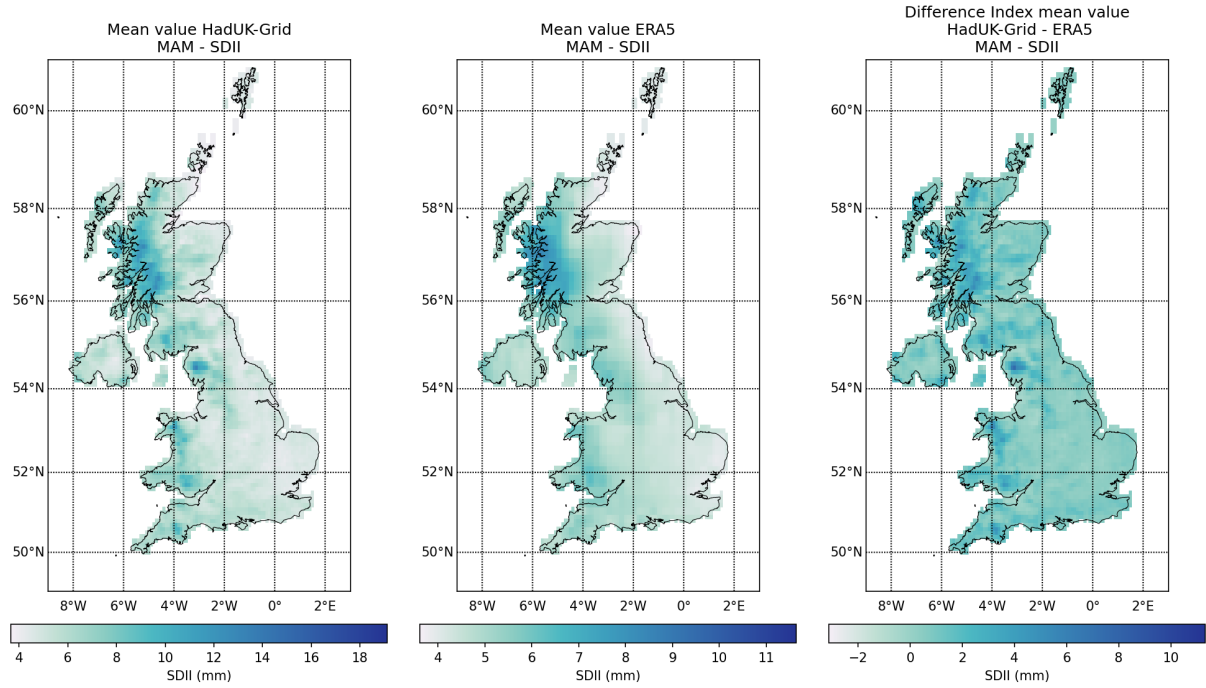


Figure 20: Spatial distribution of SDII values obtained from HadUK-Grid and ERA5 and arithmetic difference between HadUK-Grid and ERA5 for spring (MAM) over the 2001–2019 climatological period (cont.).

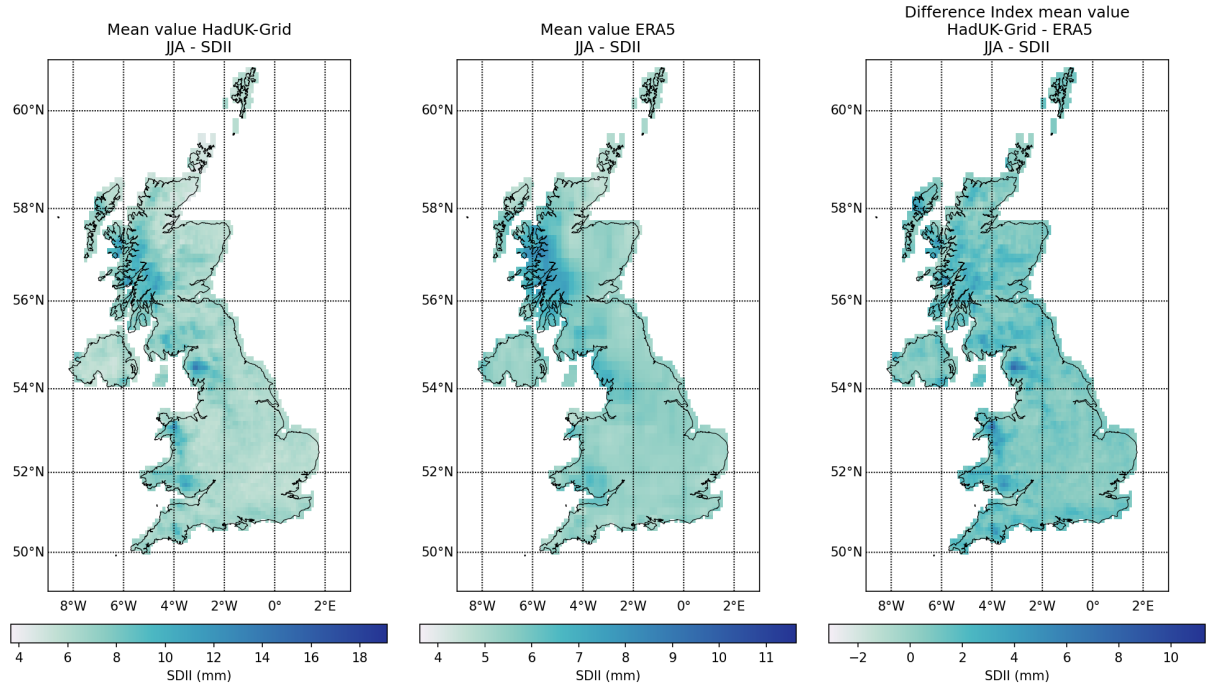


Figure 20: Spatial distribution of SDII values obtained from HadUK-Grid and ERA5 and arithmetic difference between HadUK-Grid and ERA5 for summer (JJA) over the 2001–2019 climatological period (cont.).

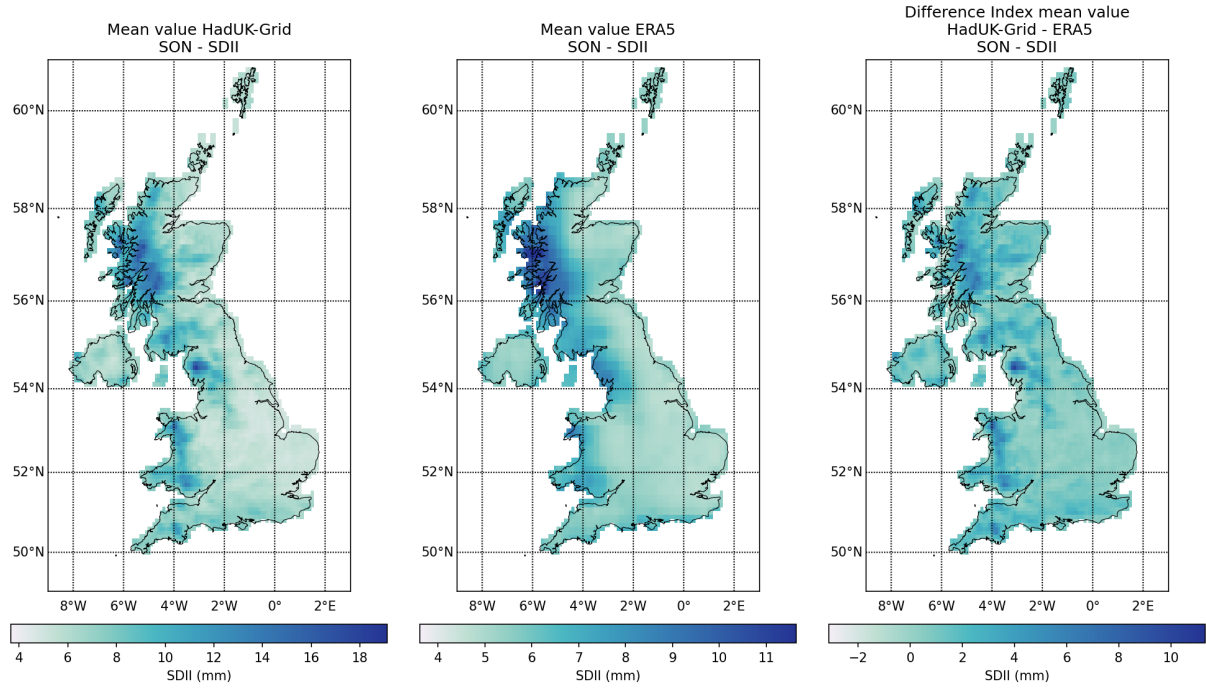


Figure 20: Spatial distribution of SDII values obtained from HadUK-Grid and ERA5 and arithmetic difference between HadUK-Grid and ERA5 for autumn (SON) over the 2001–2019 climatological period (cont.).

2 Comparative Assessment

2.1 Indices based on fixed thresholds - R10mm, R20mm, CWD, CDD

2.1.1 IMERG DATA

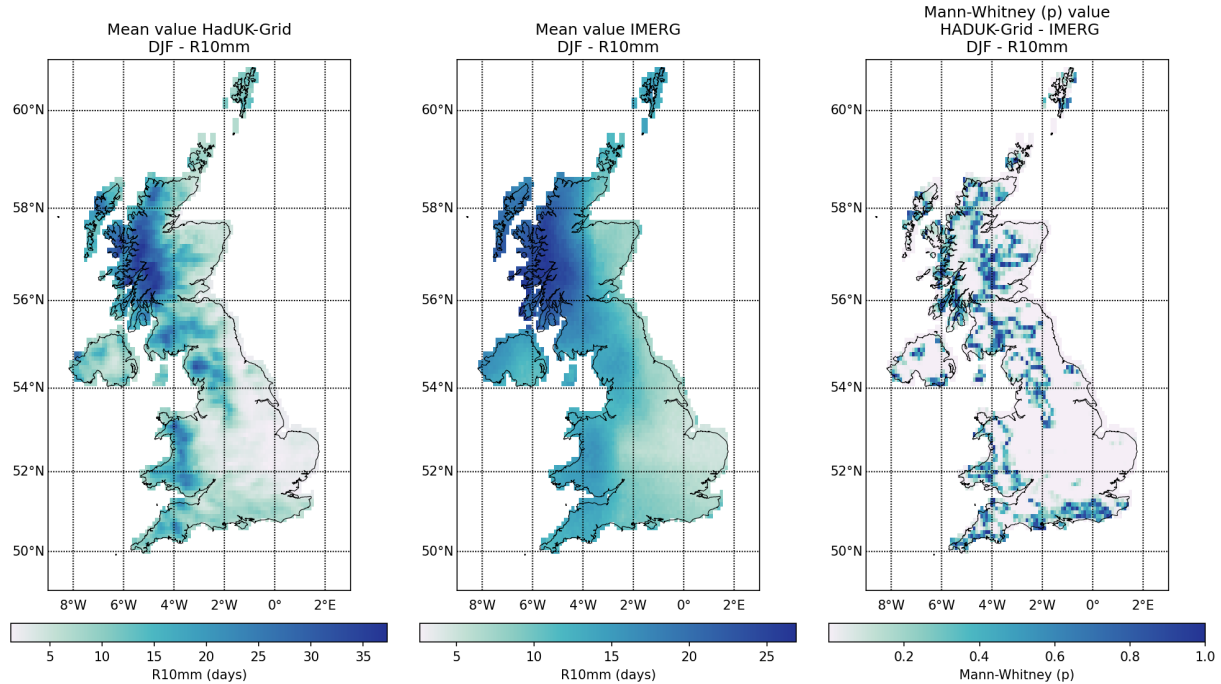


Figure 21: Spatial distribution of R10mm values obtained from HadUK-Grid and IMERG with Mann-Whitney test p value, Levene -center in the median- p value, and Pearson and Spearman correlation coefficient (r), for winter (DJF) over the 2001-2019 climatological period.

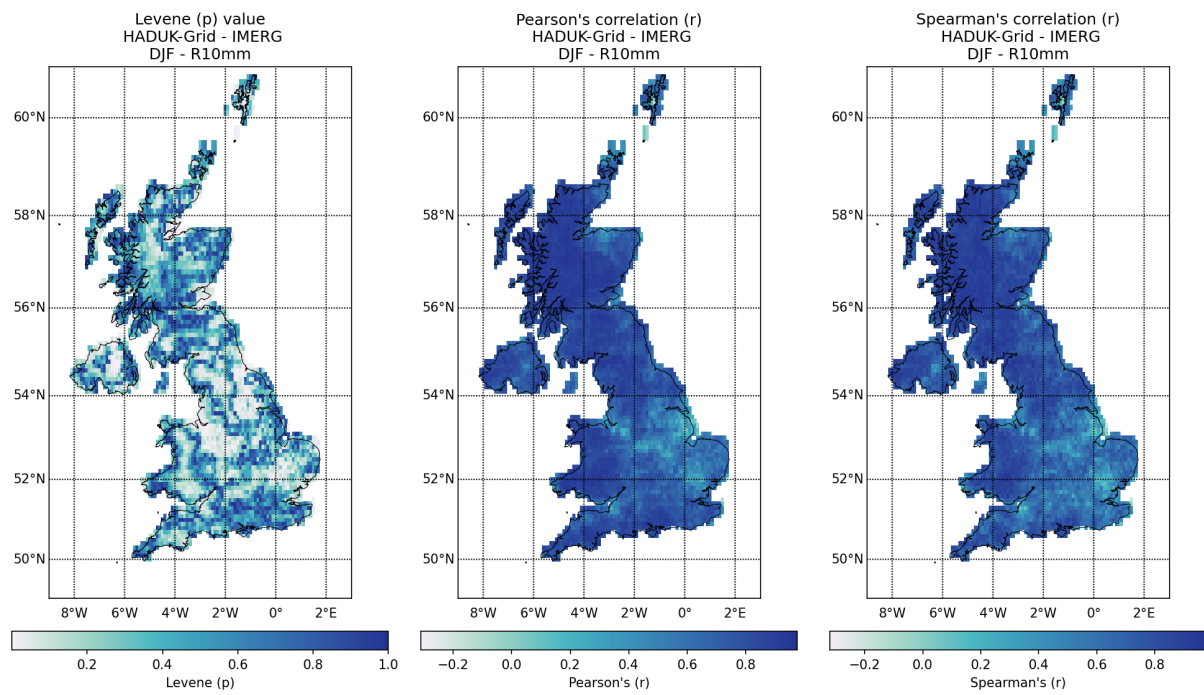


Figure 21: Spatial distribution of R10mm values obtained from HadUK-Grid and IMERG with Mann-Whitney test p value, Levene -center in the median- p value, and Pearson and Spearman correlation coefficient (r), for spring (DJF) over the 2001-2019 climatological period (cont.).

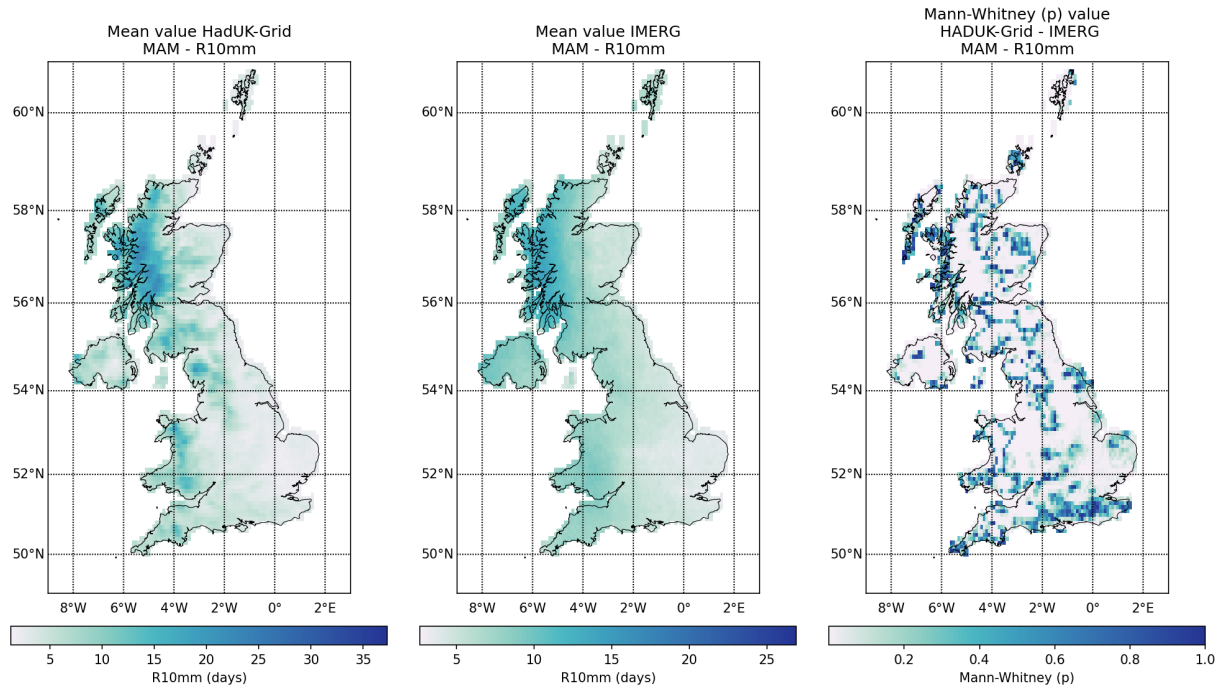


Figure 21: Spatial distribution of R10mm values obtained from HadUK-Grid and IMERG with Mann-Whitney test p value, Levene -center in the median- p value, and Pearson and Spearman correlation coefficient (r), for spring (MAM) over the 2001-2019 climatological period (cont.).

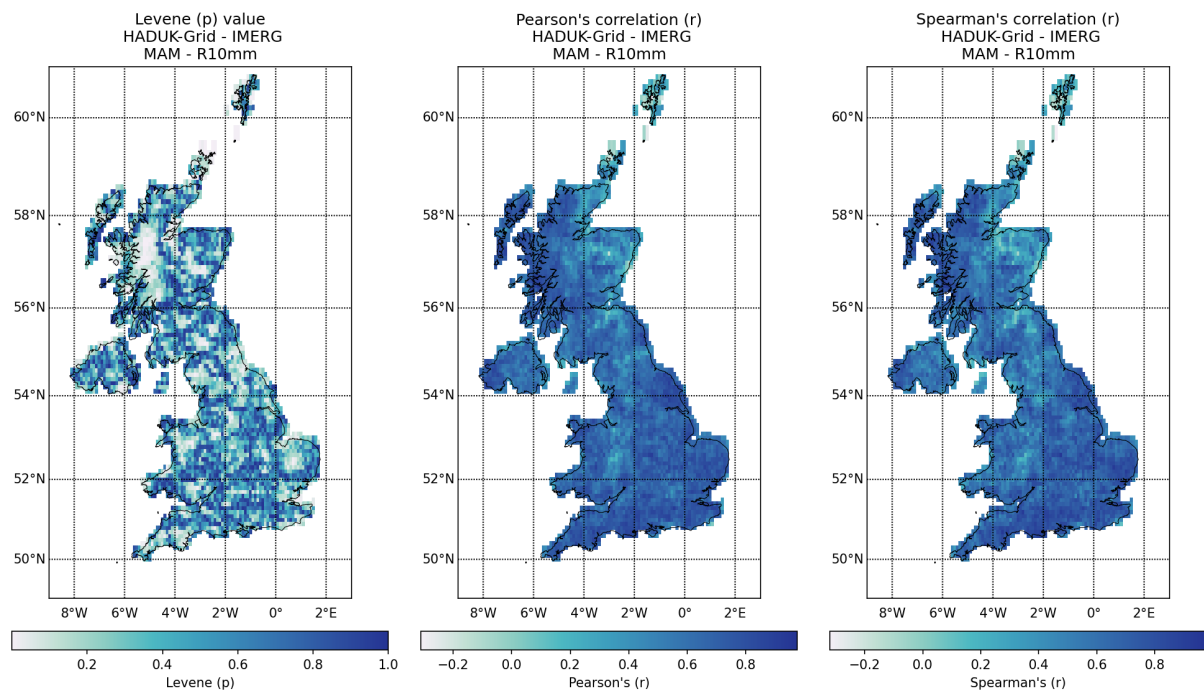


Figure 21: Spatial distribution of R10mm values obtained from HadUK-Grid and IMERG with Mann-Whitney test p value, Levene -center in the median- p value, and Pearson and Spearman correlation coefficient (r), for spring (MAM) over the 2001-2019 climatological period (cont.).

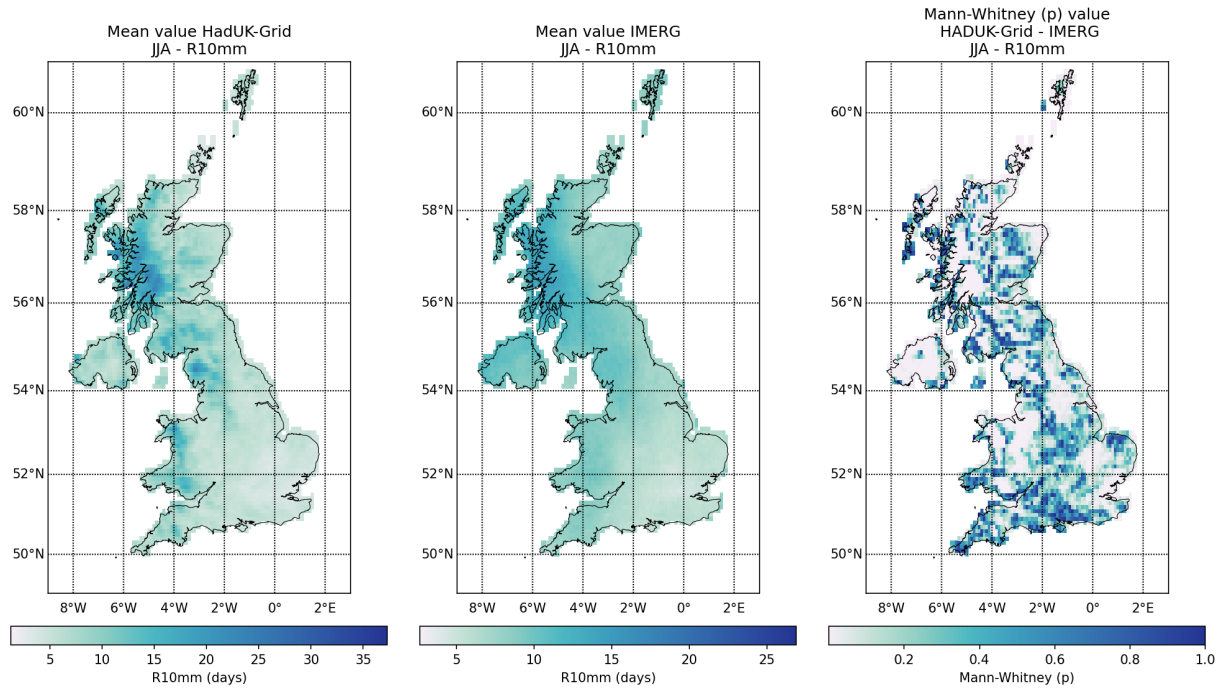


Figure 21: Spatial distribution of R10mm values obtained from HadUK-Grid and IMERG with Mann-Whitney test p value, Levene -center in the median- p value, and Pearson and Spearman correlation coefficient (r), for summer (JJA) over the 2001-2019 climatological period (cont.).

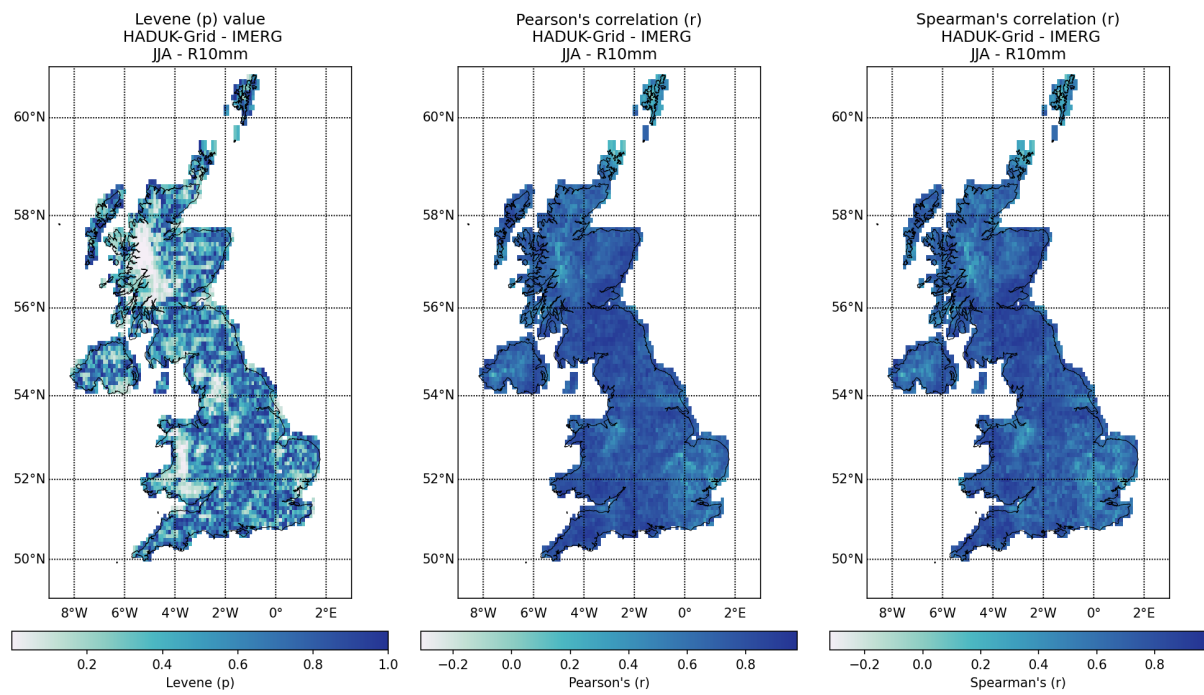


Figure 21: Spatial distribution of R10mm values obtained from HadUK-Grid and IMERG with Mann-Whitney test p value, Levene -center in the median- p value, and Pearson and Spearman correlation coefficient (r), for summer (JJA) over the 2001-2019 climatological period (cont.).

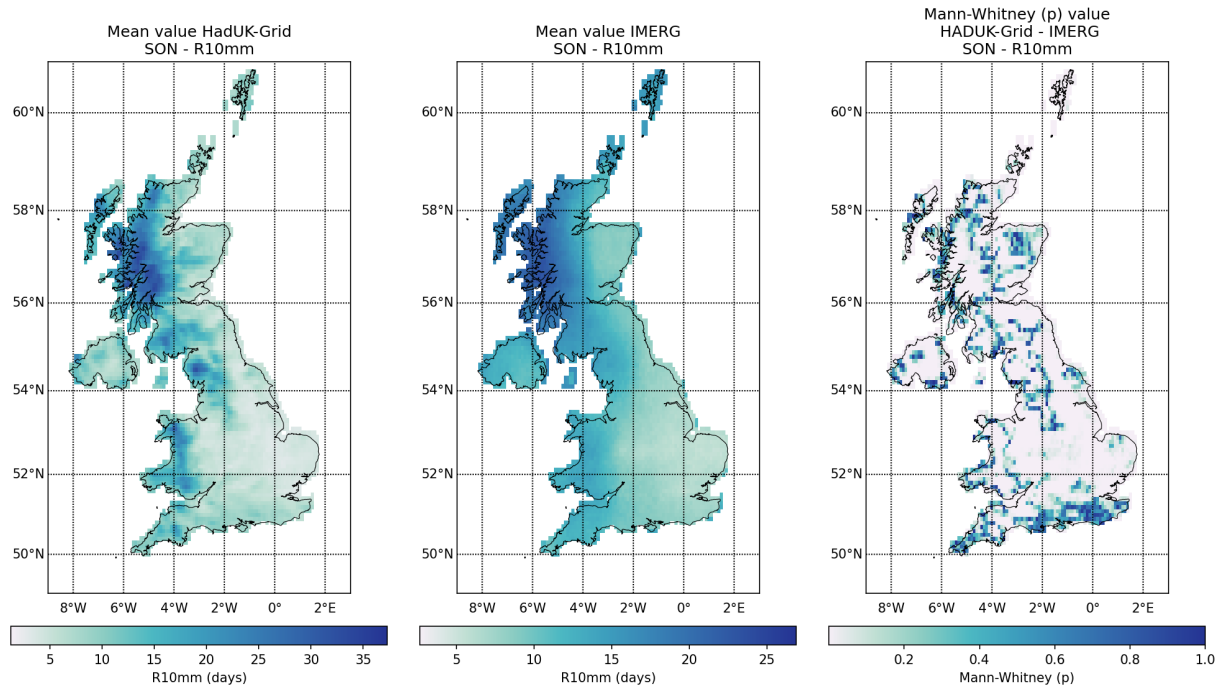


Figure 21: Spatial distribution of R10mm values obtained from HadUK-Grid and IMERG with Mann-Whitney test p value, Levene -center in the median- p value, and Pearson and Spearman correlation coefficient (r), for autumn (SON) over the 2001-2019 climatological period (cont.).

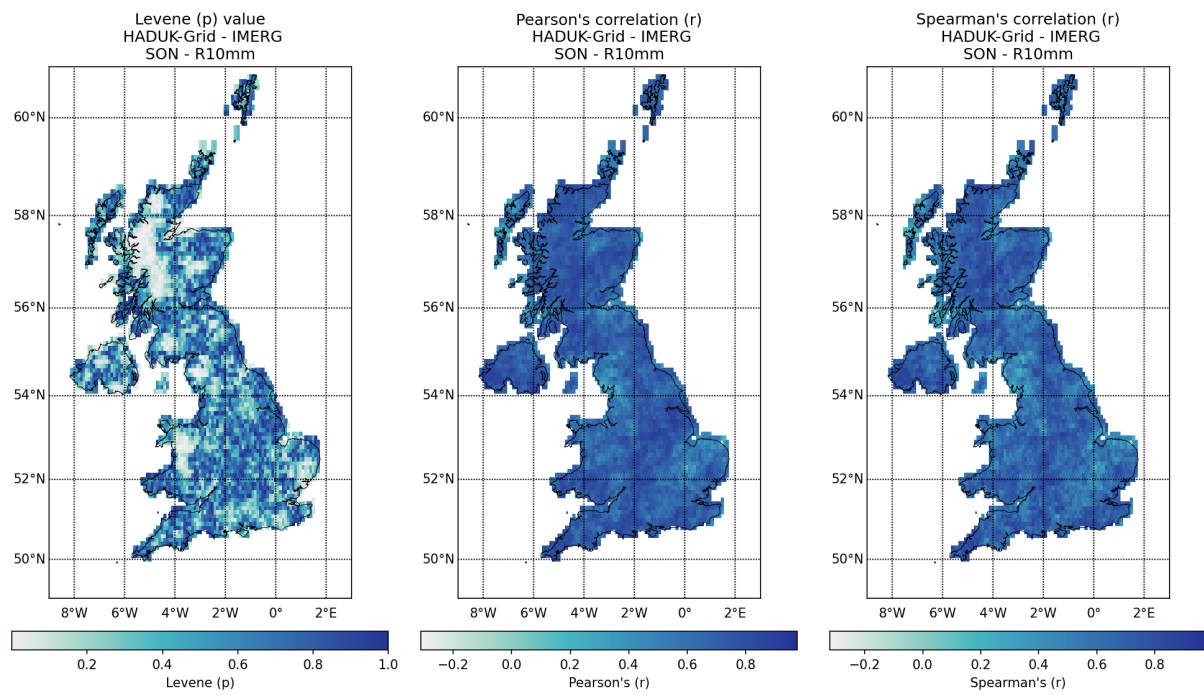


Figure 21: Spatial distribution of R10mm values obtained from HadUK-Grid and IMERG with Mann-Whitney test p value, Levene -center in the median- p value, and Pearson and Spearman correlation coefficient (r), for autumn (SON) over the 2001-2019 climatological period.

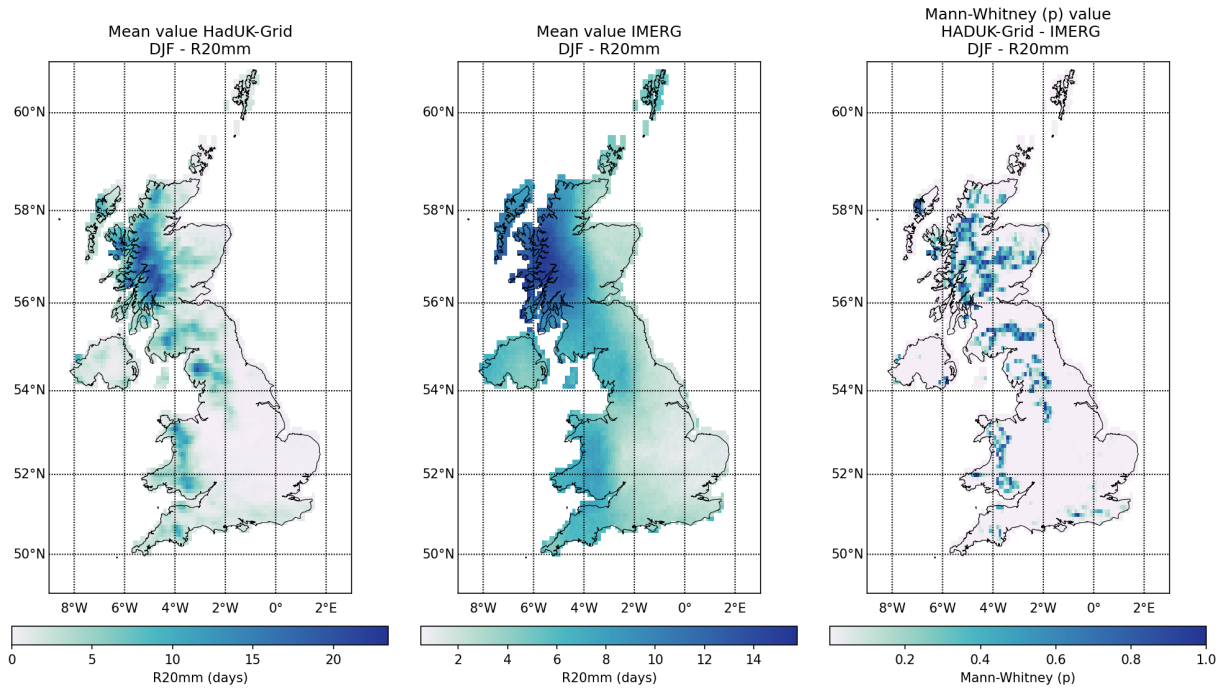


Figure 22: Spatial distribution of R20mm values obtained from HadUK-Grid and IMERG with Mann-Whitney test p value, Levene -center in the median- p value, and Pearson and Spearman correlation coefficient (r), for winter (DJF) over the 2001-2019 climatological period.

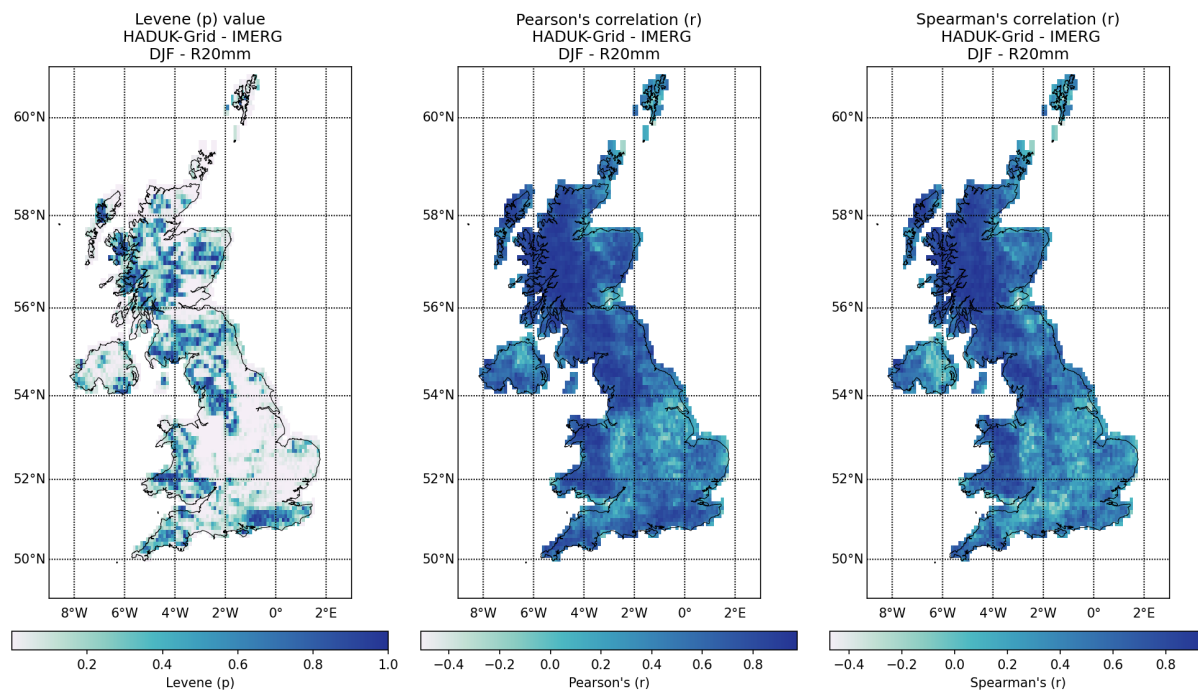


Figure 22: Spatial distribution of R20mm values obtained from HadUK-Grid and IMERG with Mann-Whitney test p value, Levene -center in the median- p value, and Pearson and Spearman correlation coefficient (r), for spring (DJF) over the 2001-2019 climatological period (cont.).

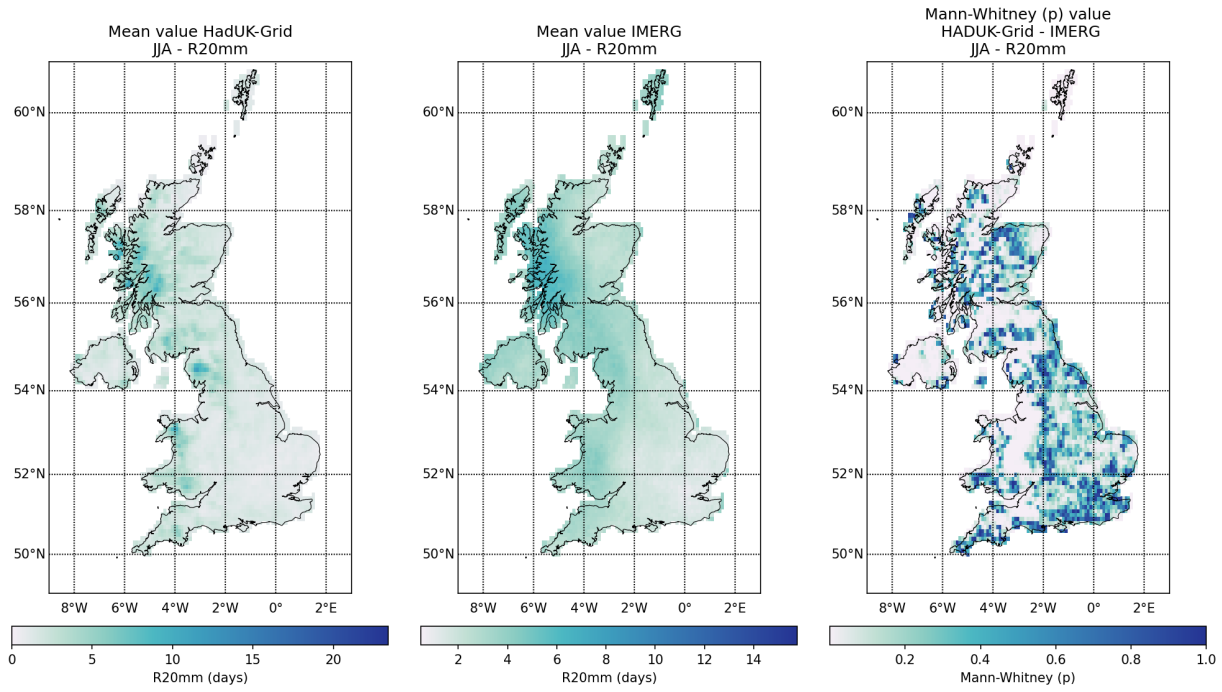


Figure 22: Spatial distribution of R20mm values obtained from HadUK-Grid and IMERG with Mann-Whitney test p value, Levene -center in the median- p value, and Pearson and Spearman correlation coefficient (r), for summer (JJA) over the 2001-2019 climatological period (cont.).

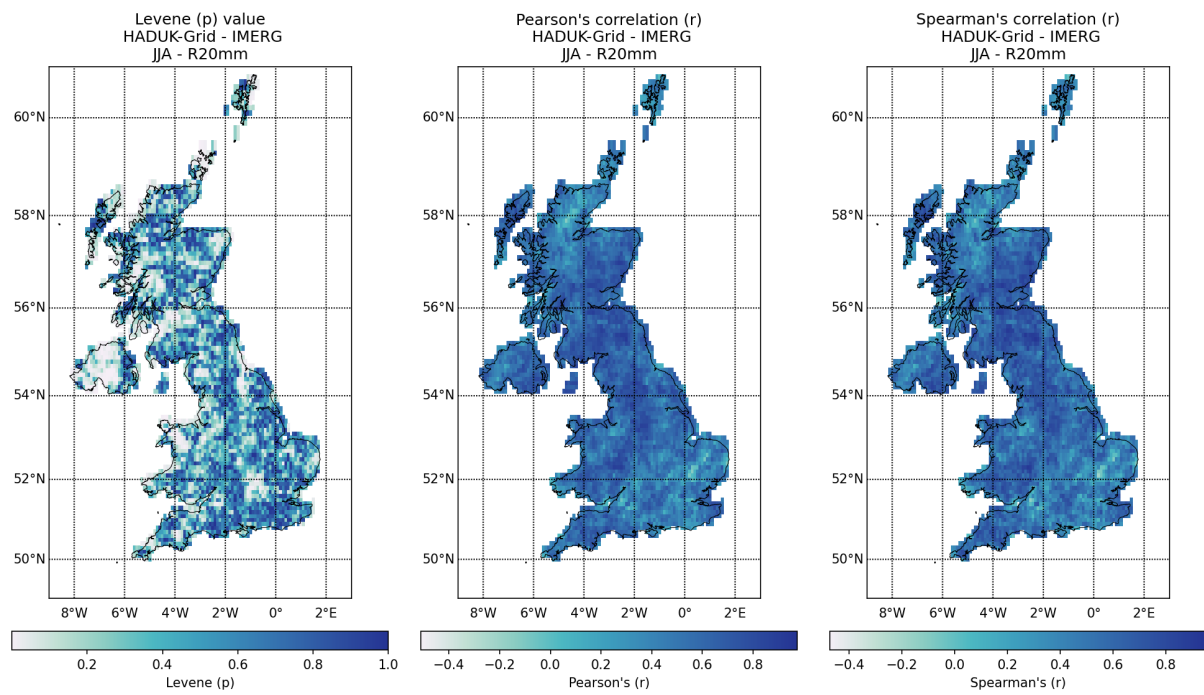


Figure 22: Spatial distribution of R20mm values obtained from HadUK-Grid and IMERG with Mann-Whitney test p value, Levene -center in the median- p value, and Pearson and Spearman correlation coefficient (r), for summer (JJA) over the 2001-2019 climatological period (cont.).

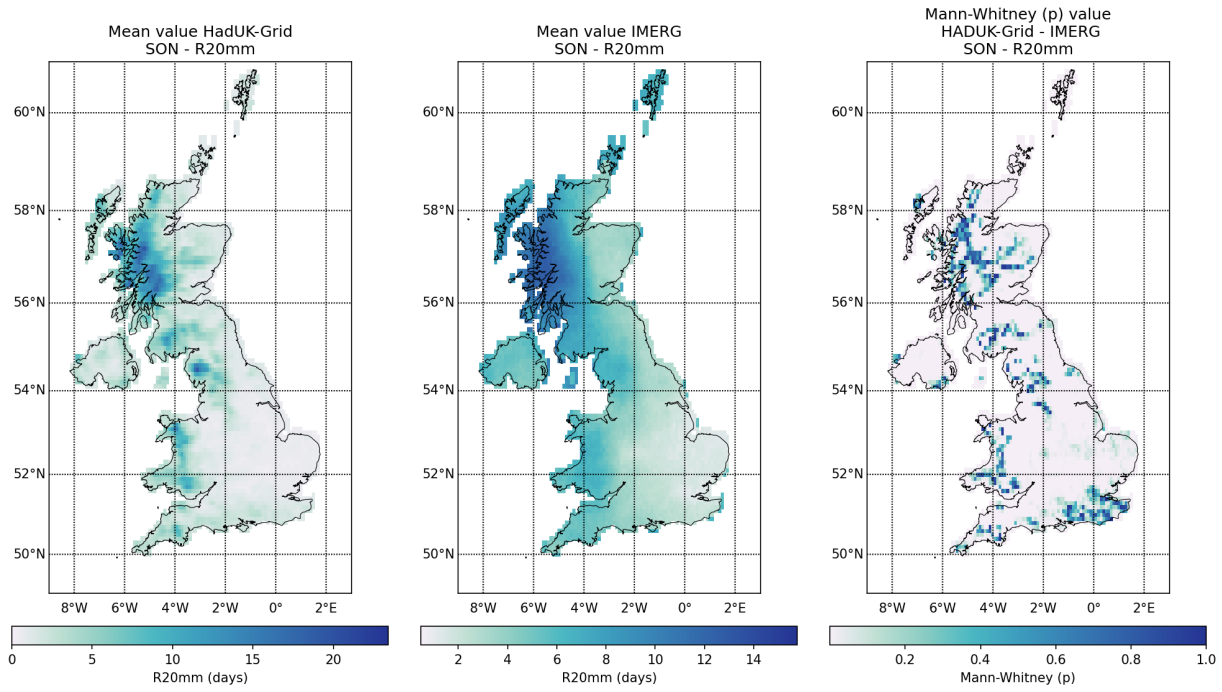


Figure 22: Spatial distribution of R20mm values obtained from HadUK-Grid and IMERG with Mann-Whitney test p value, Levene -center in the median- p value, and Pearson and Spearman correlation coefficient (r), for autumn (SON) over the 2001-2019 climatological period (cont.).

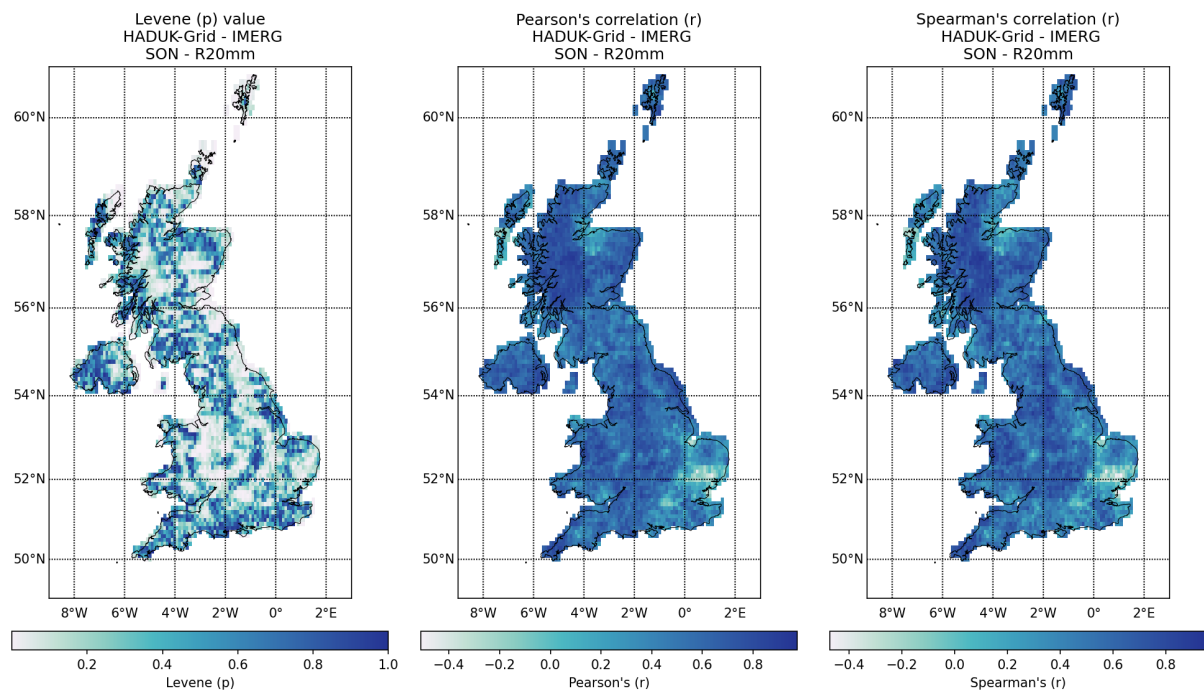


Figure 22: Spatial distribution of R20mm values obtained from HadUK-Grid and IMERG with Mann-Whitney test p value, Levene -center in the median- p value, and Pearson and Spearman correlation coefficient (r), for autumn (SON) over the 2001-2019 climatological period.

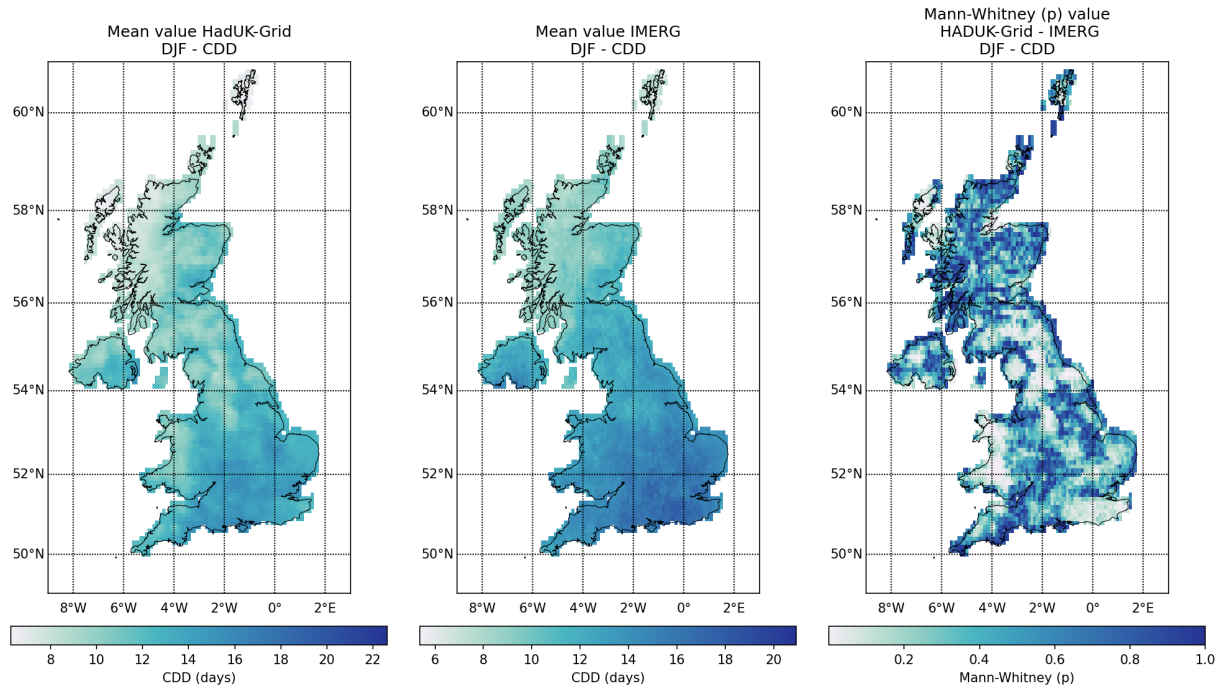


Figure 23: Spatial distribution of CDD values obtained from HadUK-Grid and IMERG with Mann-Whitney test p value, Levene -center in the median- p value, and Pearson and Spearman correlation coefficient (r), for winter (DJF) over the 2001-2019 climatological period.

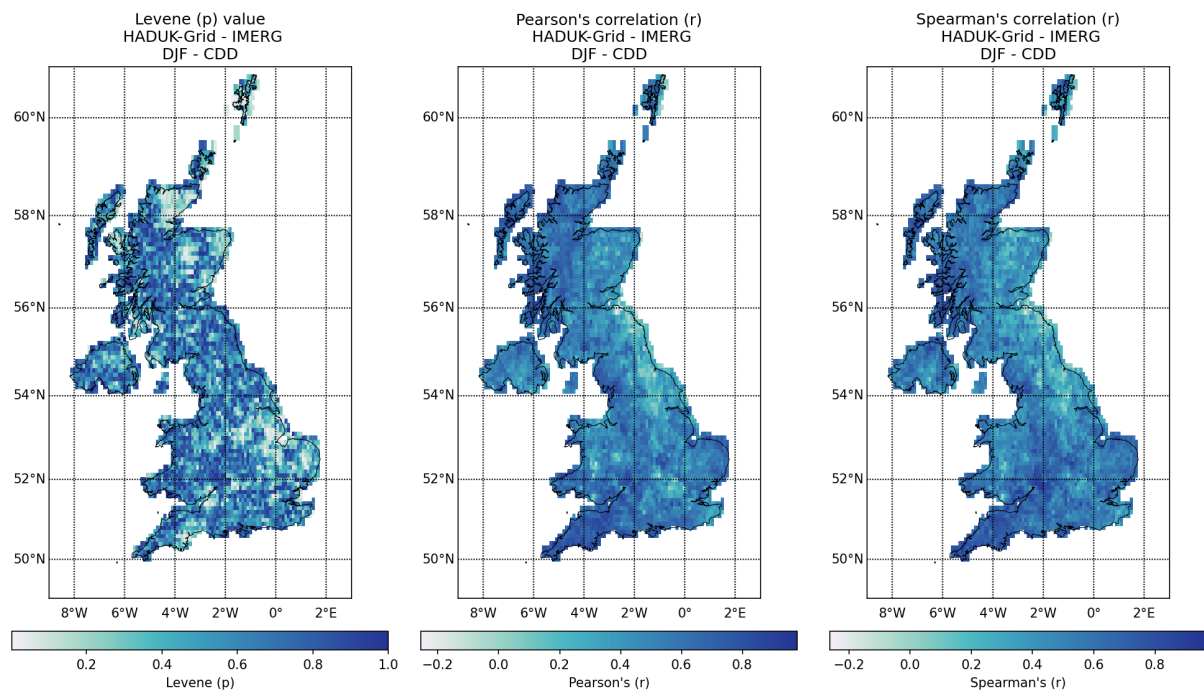


Figure 23: Spatial distribution of CDD values obtained from HadUK-Grid and IMERG with Mann-Whitney test p value, Levene -center in the median- p value, and Pearson and Spearman correlation coefficient (r), for spring (DJF) over the 2001-2019 climatological period (cont.).

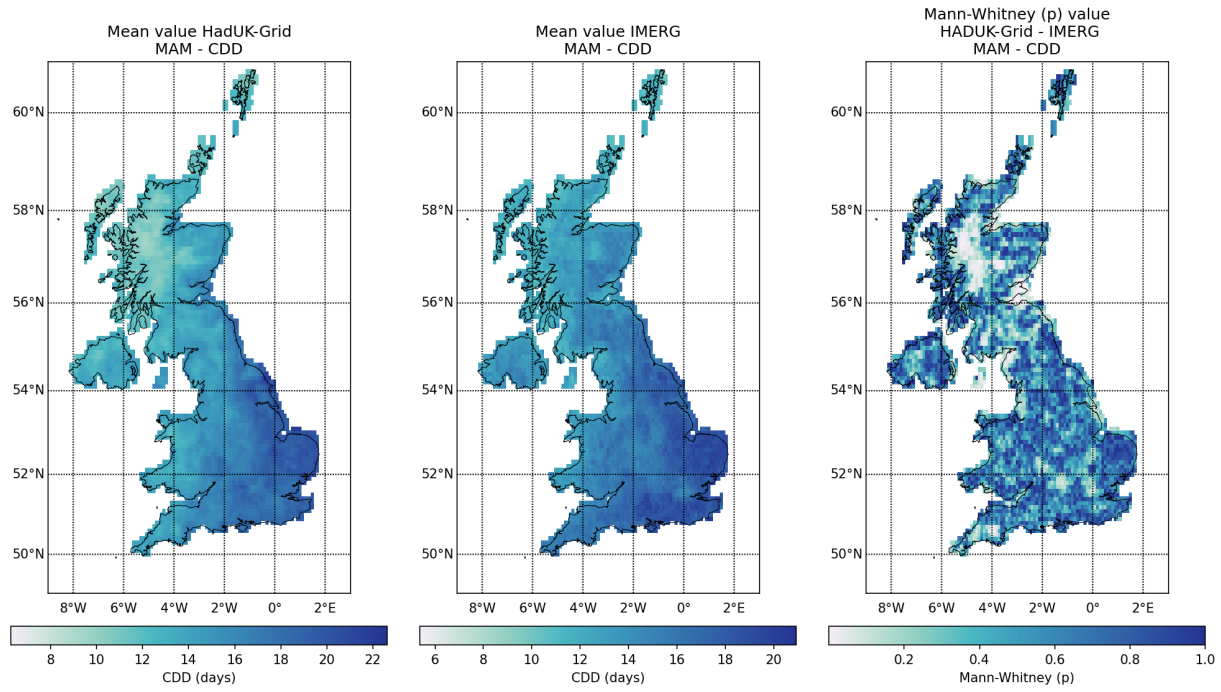


Figure 23: Spatial distribution of CDD values obtained from HadUK-Grid and IMERG with Mann-Whitney test p value, Levene -center in the median- p value, and Pearson and Spearman correlation coefficient (r), for spring (MAM) over the 2001-2019 climatological period (cont.).

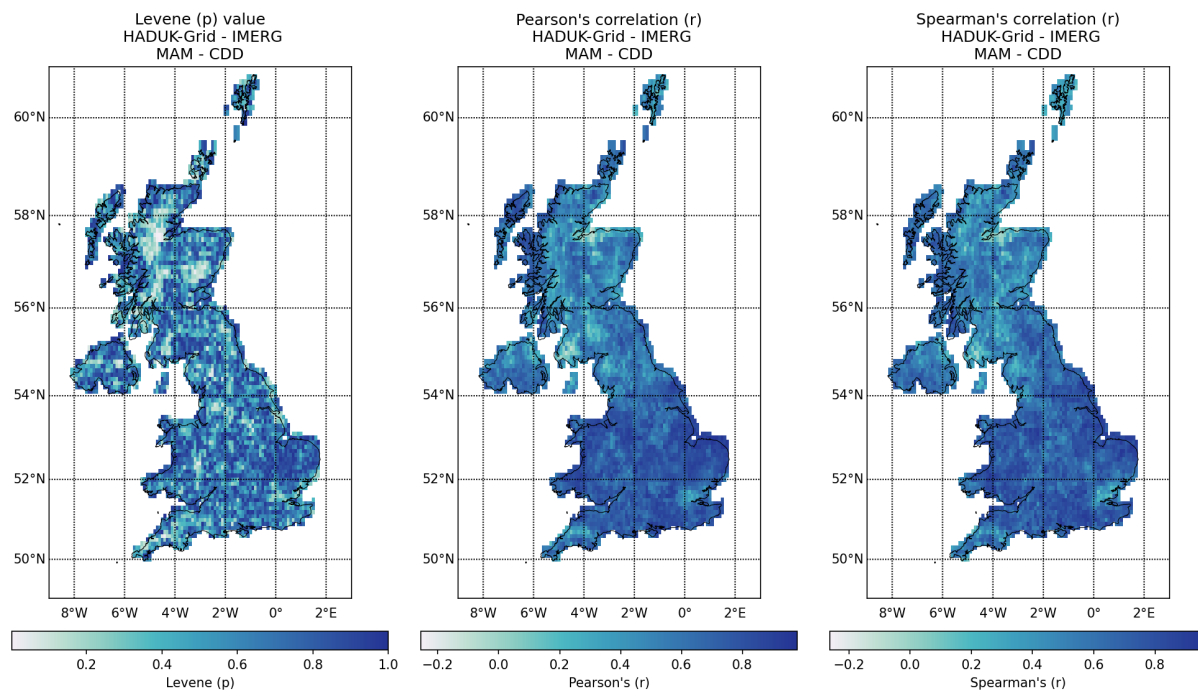


Figure 23: Spatial distribution of CDD values obtained from HadUK-Grid and IMERG with Mann-Whitney test p value, Levene -center in the median- p value, and Pearson and Spearman correlation coefficient (r), for spring (MAM) over the 2001-2019 climatological period (cont.).

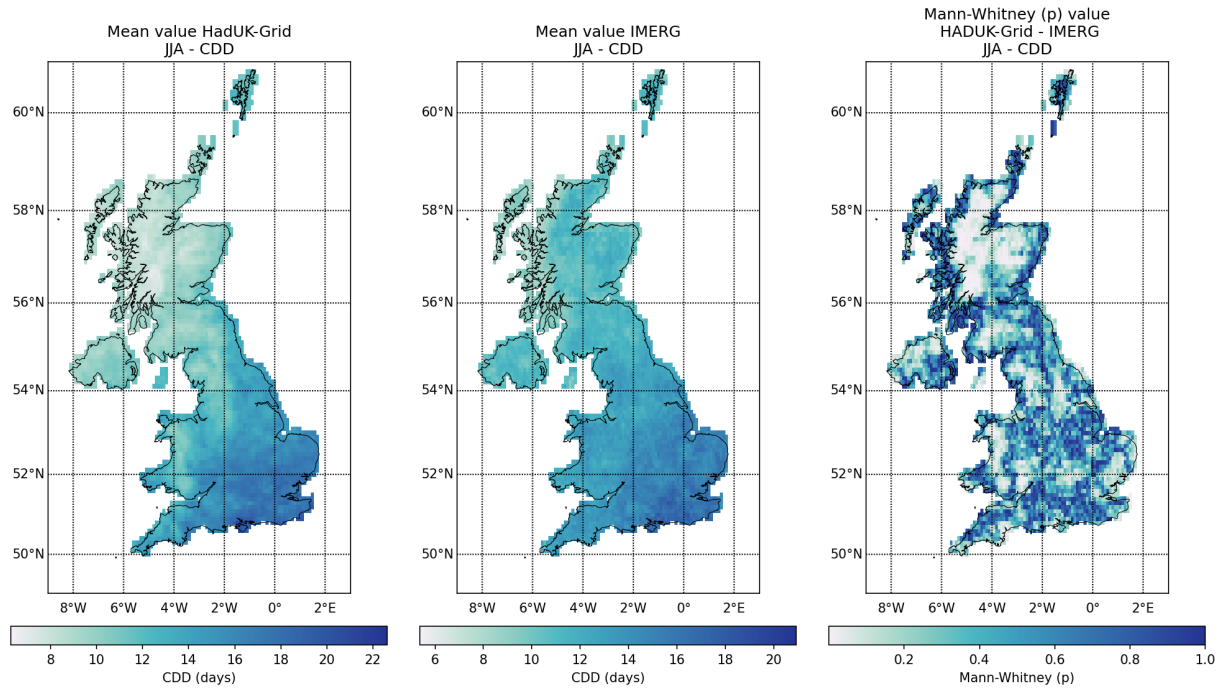


Figure 23: Spatial distribution of CDD values obtained from HadUK-Grid and IMERG with Mann-Whitney test p value, Levene -center in the median- p value, and Pearson and Spearman correlation coefficient (r), for summer (JJA) over the 2001-2019 climatological period (cont.).

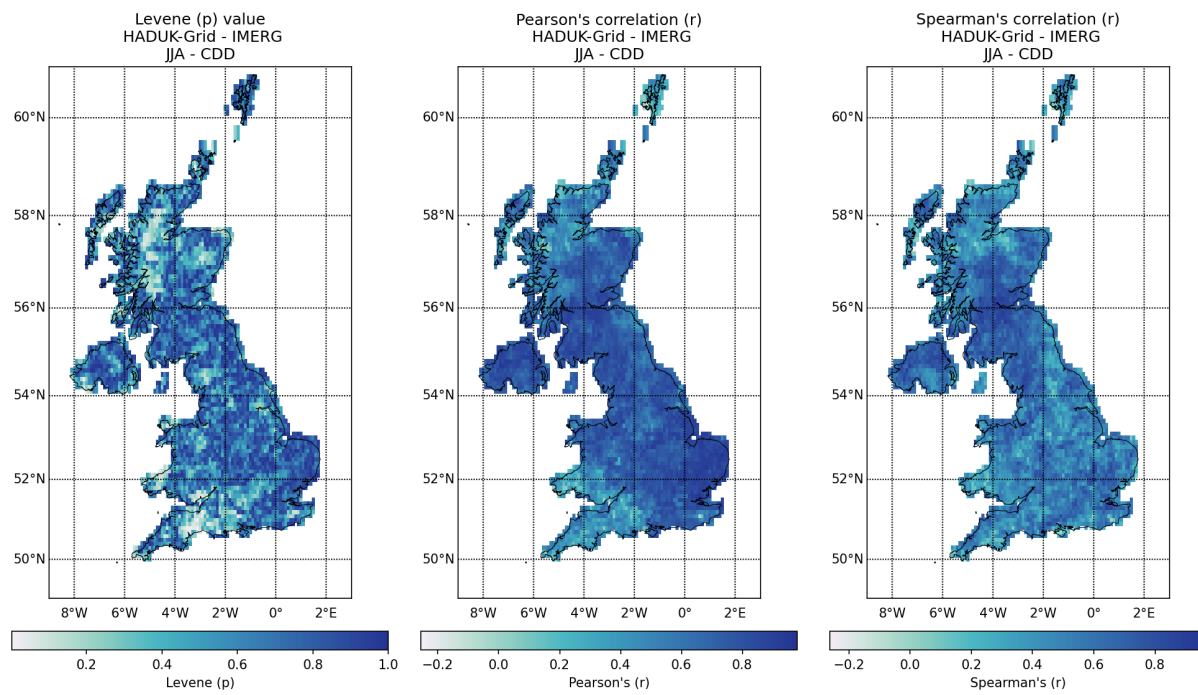


Figure 23: Spatial distribution of CDD values obtained from HadUK-Grid and IMERG with Mann-Whitney test p value, Levene -center in the median- p value, and Pearson and Spearman correlation coefficient (r), for summer (JJA) over the 2001-2019 climatological period (cont.).

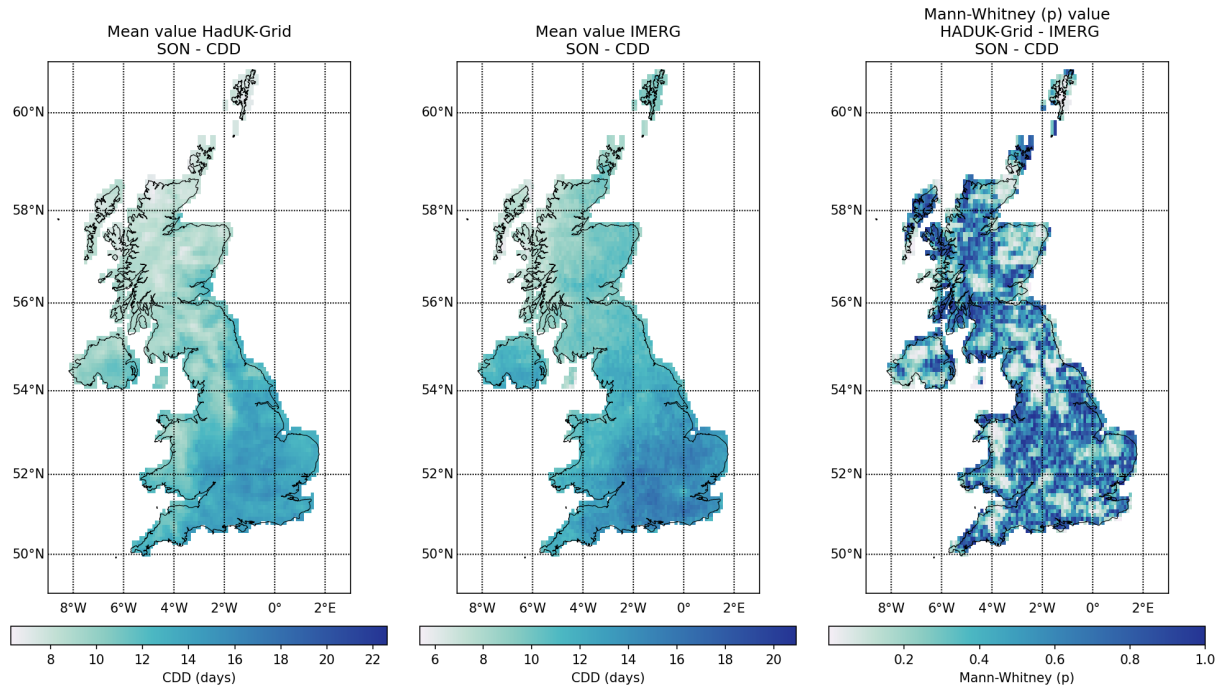


Figure 23: Spatial distribution of CDD values obtained from HadUK-Grid and IMERG with Mann-Whitney test p value, Levene -center in the median- p value, and Pearson and Spearman correlation coefficient (r), for autumn (SON) over the 2001-2019 climatological period (cont.).

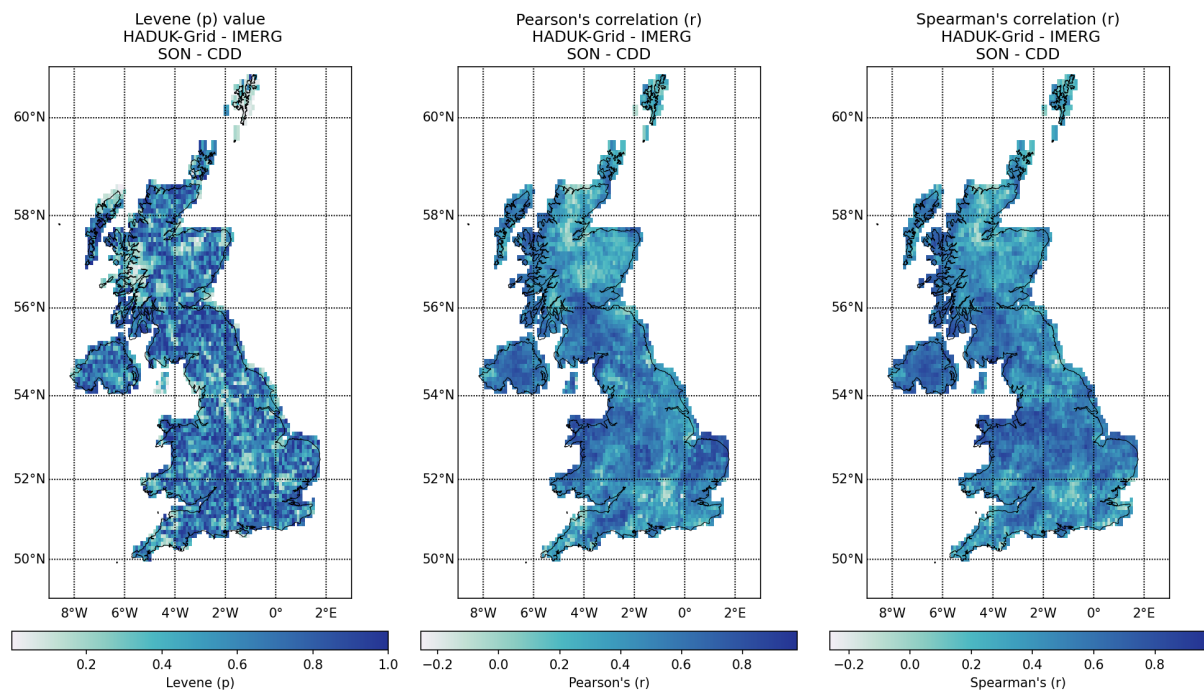


Figure 23: Spatial distribution of CDD values obtained from HadUK-Grid and IMERG with Mann-Whitney test p value, Levene -center in the median- p value, and Pearson and Spearman correlation coefficient (r), for autumn (SON) over the 2001-2019 climatological period.

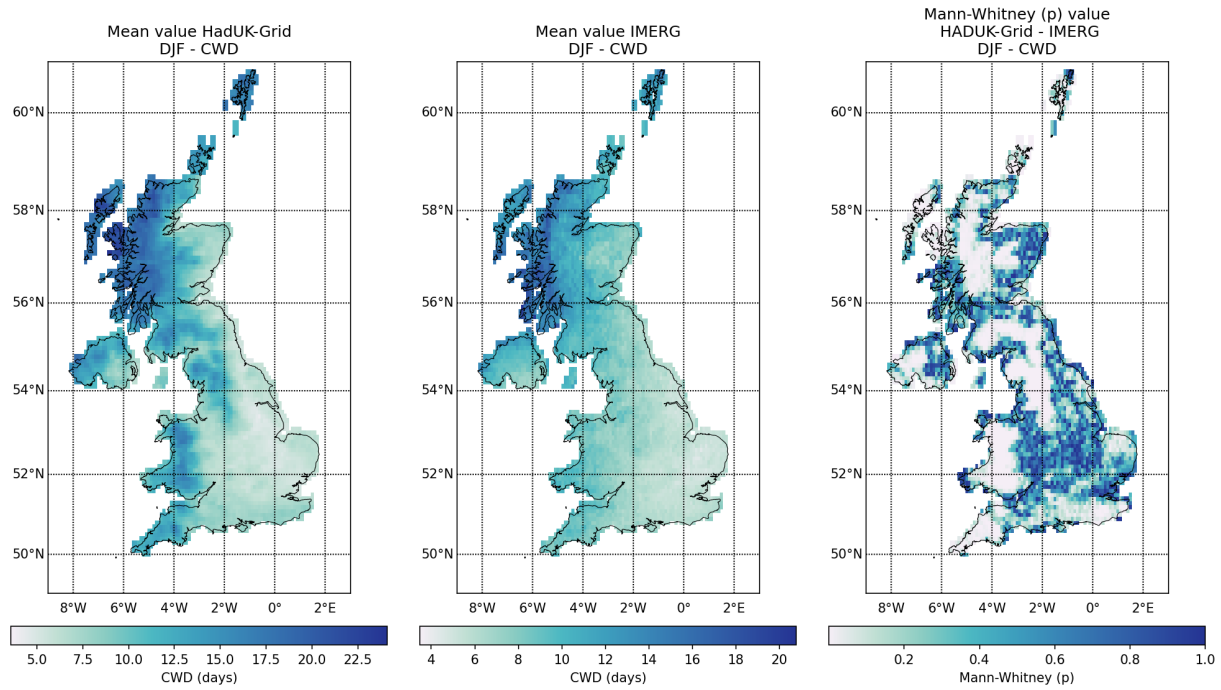


Figure 24: Spatial distribution of CWD values obtained from HadUK-Grid and IMERG with Mann-Whitney test p value, Levene -center in the median- p value, and Pearson and Spearman correlation coefficient (r), for winter (DJF) over the 2001-2019 climatological period.

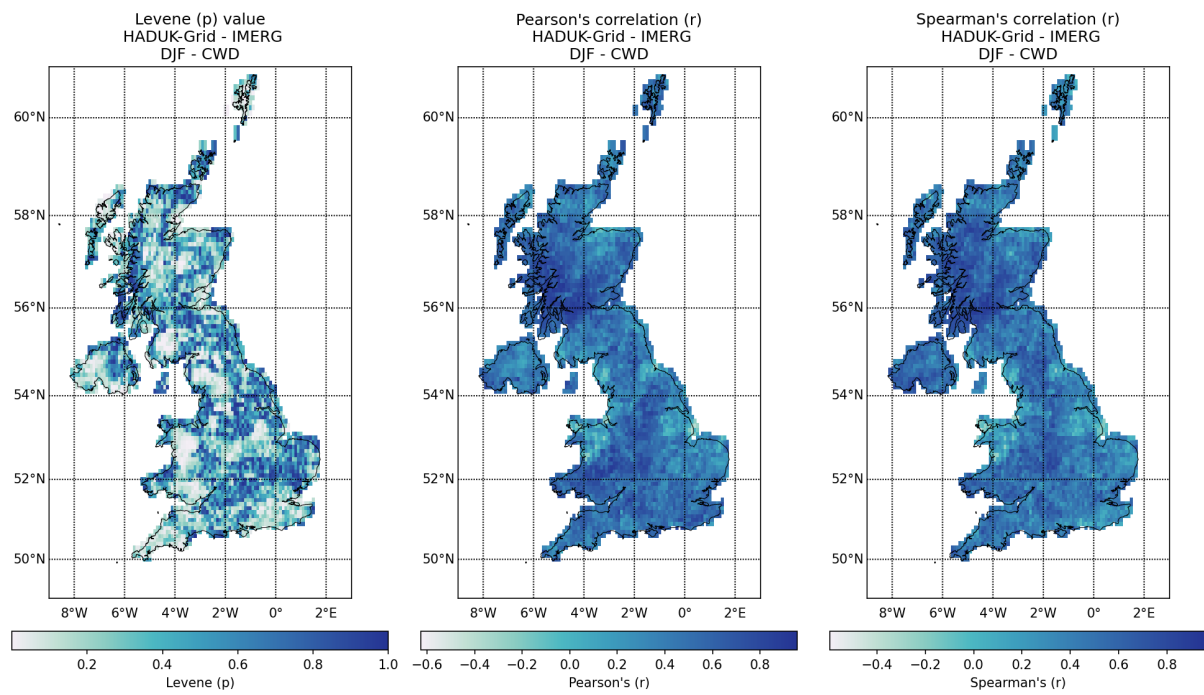


Figure 24: Spatial distribution of CWD values obtained from HadUK-Grid and IMERG with Mann-Whitney test p value, Levene -center in the median- p value, and Pearson and Spearman correlation coefficient (r), for spring (DJF) over the 2001-2019 climatological period (cont.).

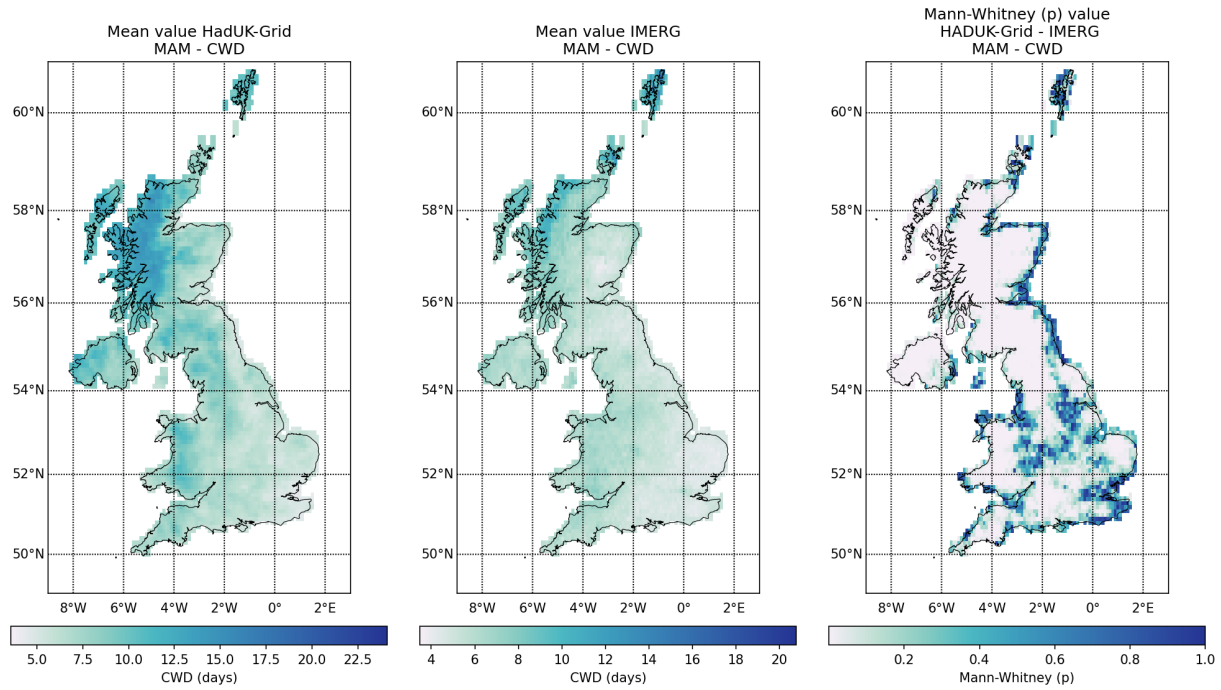


Figure 24: Spatial distribution of CWD values obtained from HadUK-Grid and IMERG with Mann-Whitney test p value, Levene -center in the median- p value, and Pearson and Spearman correlation coefficient (r), for spring (MAM) over the 2001-2019 climatological period (cont.).

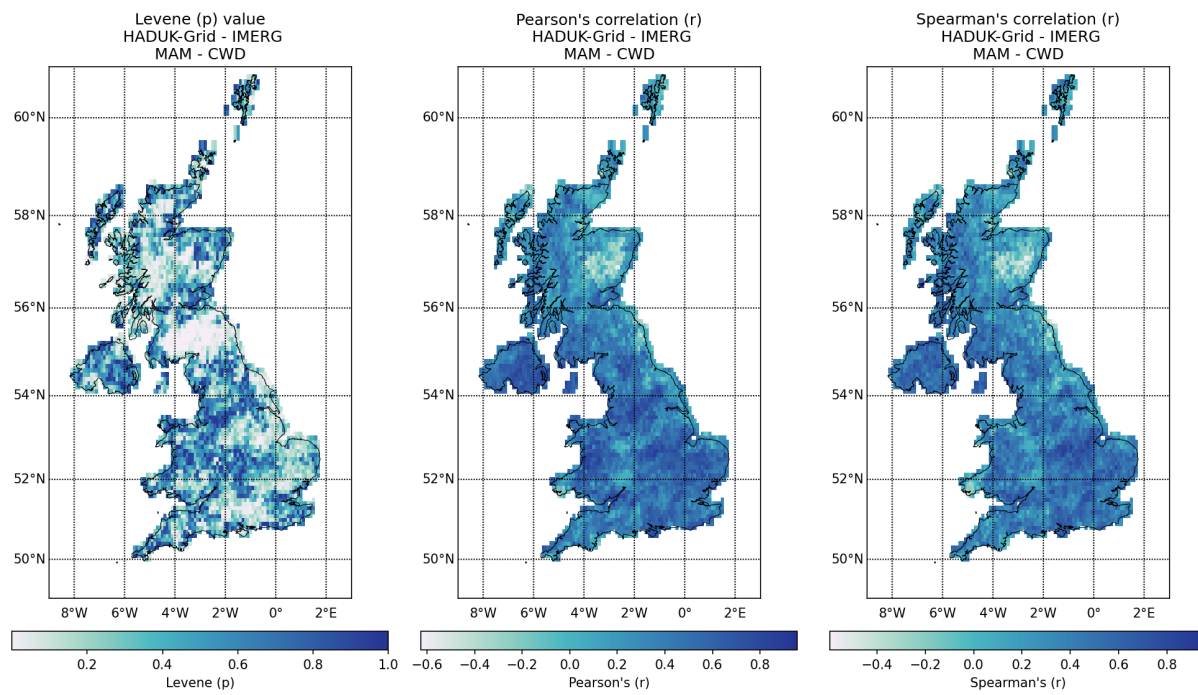


Figure 24: Spatial distribution of CWD values obtained from HadUK-Grid and IMERG with Mann-Whitney test p value, Levene -center in the median- p value, and Pearson and Spearman correlation coefficient (r), for spring (MAM) over the 2001-2019 climatological period (cont.).

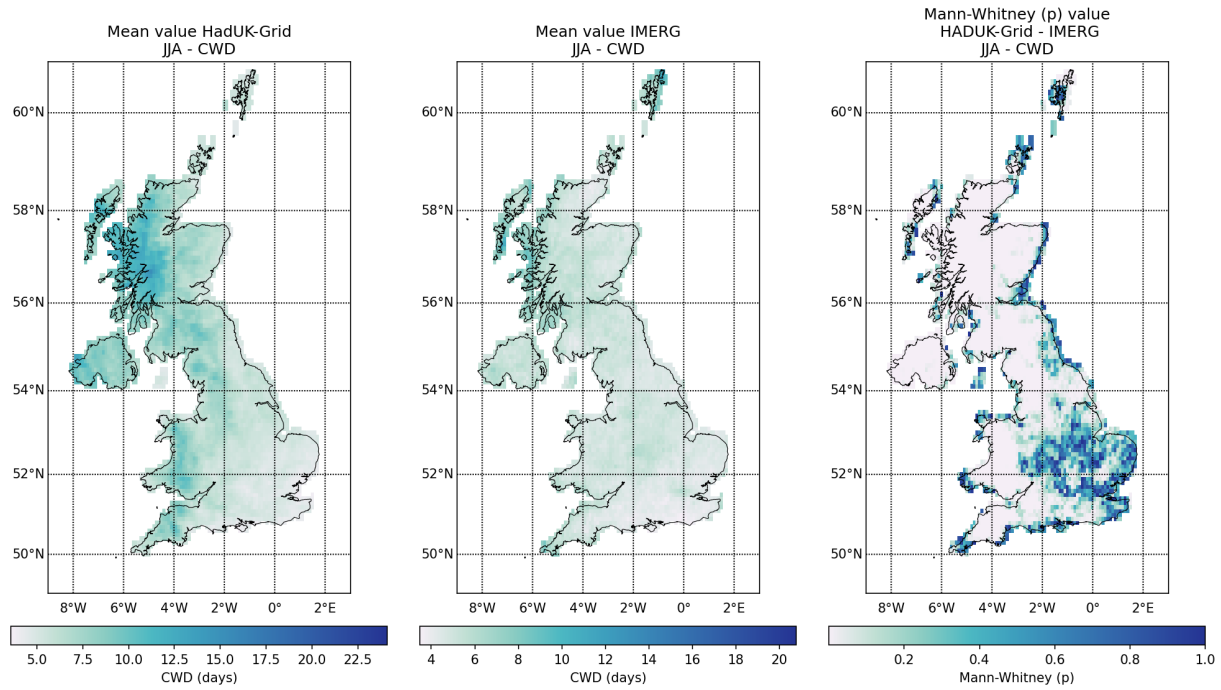


Figure 24: Spatial distribution of CWD values obtained from HadUK-Grid and IMERG with Mann-Whitney test p value, Levene -center in the median- p value, and Pearson and Spearman correlation coefficient (r), for summer (JJA) over the 2001-2019 climatological period (cont.).

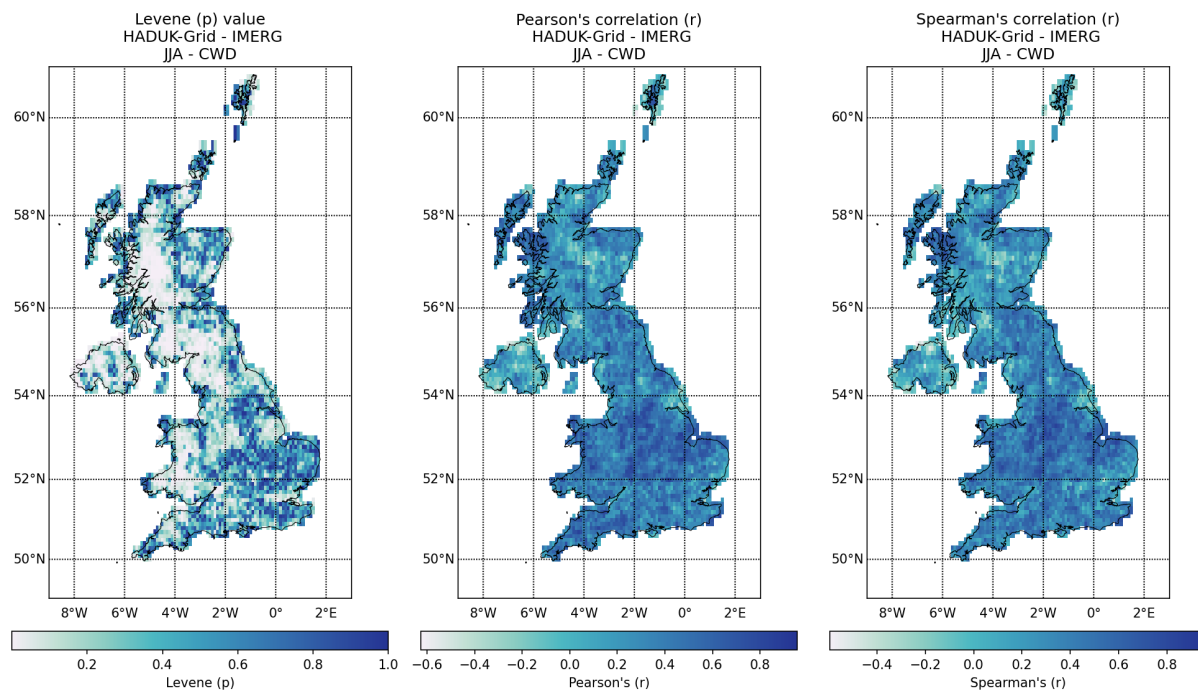


Figure 24: Spatial distribution of CWD values obtained from HadUK-Grid and IMERG with Mann-Whitney test p value, Levene -center in the median- p value, and Pearson and Spearman correlation coefficient (r), for summer (JJA) over the 2001-2019 climatological period (cont.).

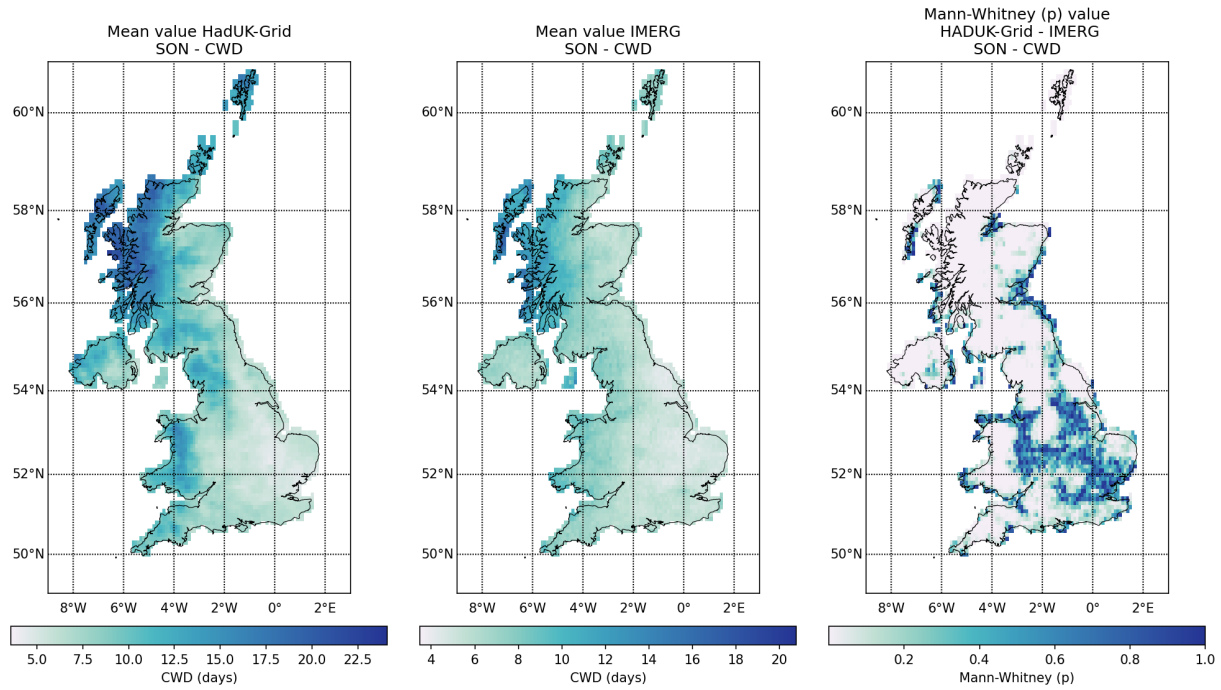


Figure 24: Spatial distribution of CWD values obtained from HadUK-Grid and IMERG with Mann-Whitney test p value, Levene -center in the median- p value, and Pearson and Spearman correlation coefficient (r), for autumn (SON) over the 2001-2019 climatological period (cont.).

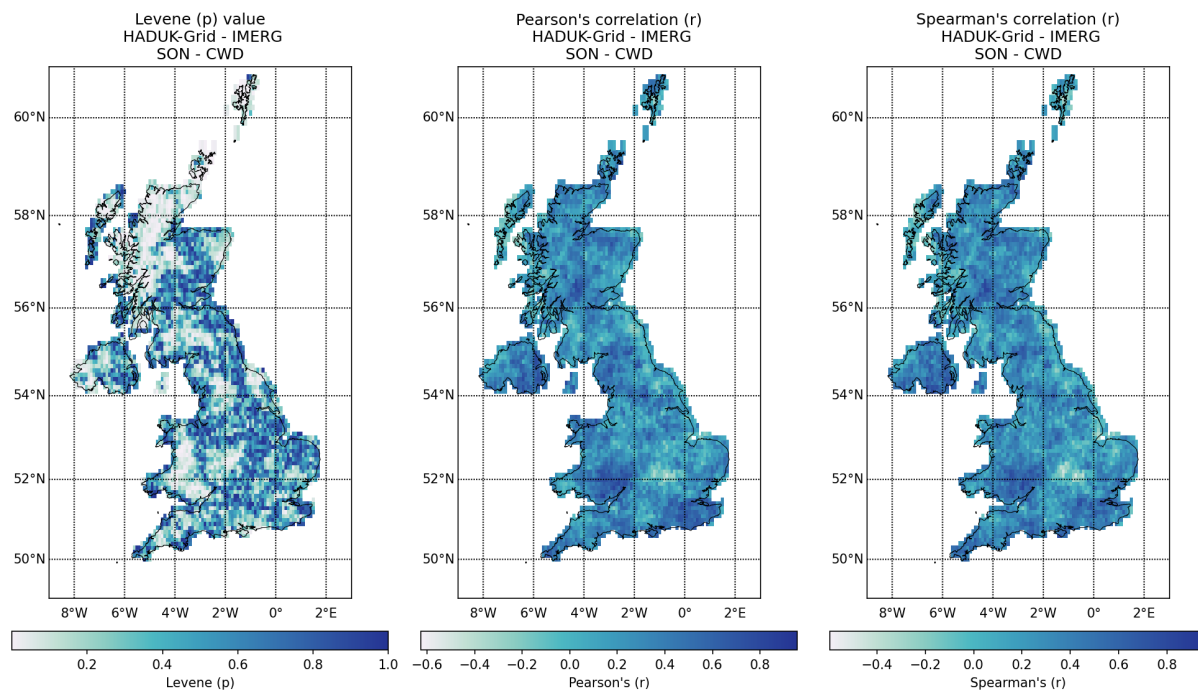


Figure 24: Spatial distribution of CWD values obtained from HadUK-Grid and IMERG with Mann-Whitney test p value, Levene -center in the median- p value, and Pearson and Spearman correlation coefficient (r), for autumn (SON) over the 2001-2019 climatological period.

2.1.2 ERA5 DATA

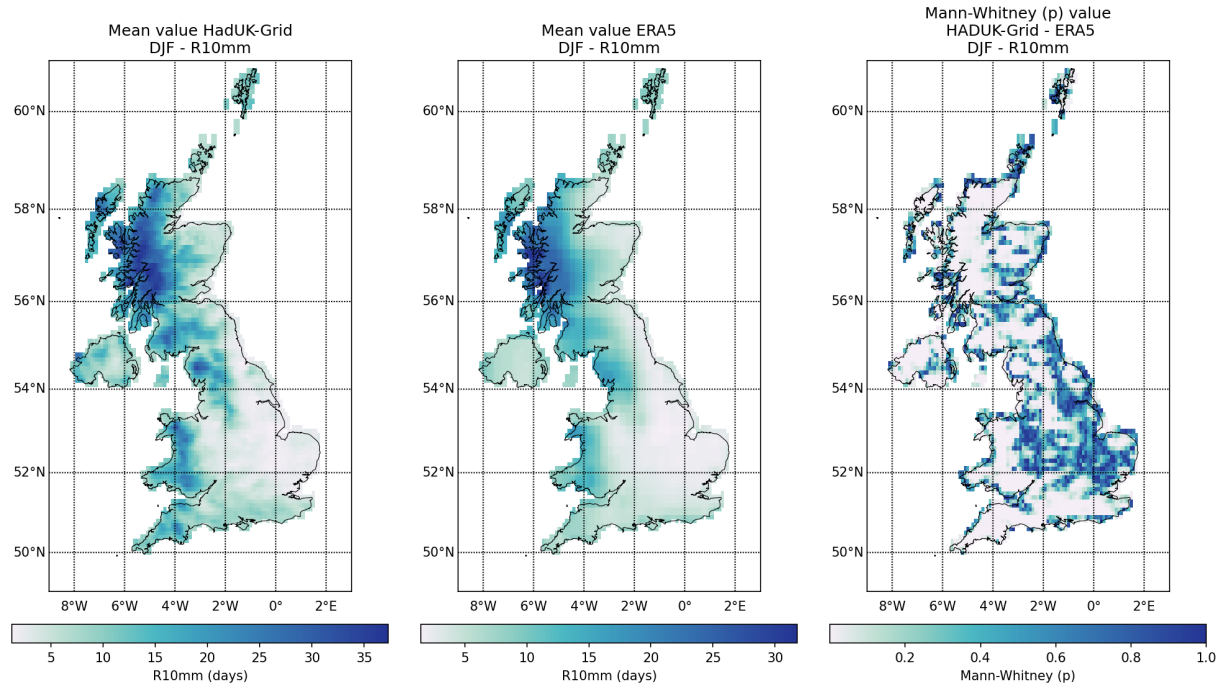


Figure 25: Spatial distribution of R10mm values obtained from HadUK-Grid and ERA5 with Mann-Whitney test p value, Levene -center in the median- p value, and Pearson and Spearman correlation coefficient (r), for winter (DJF) over the 2001-2019 climatological period.

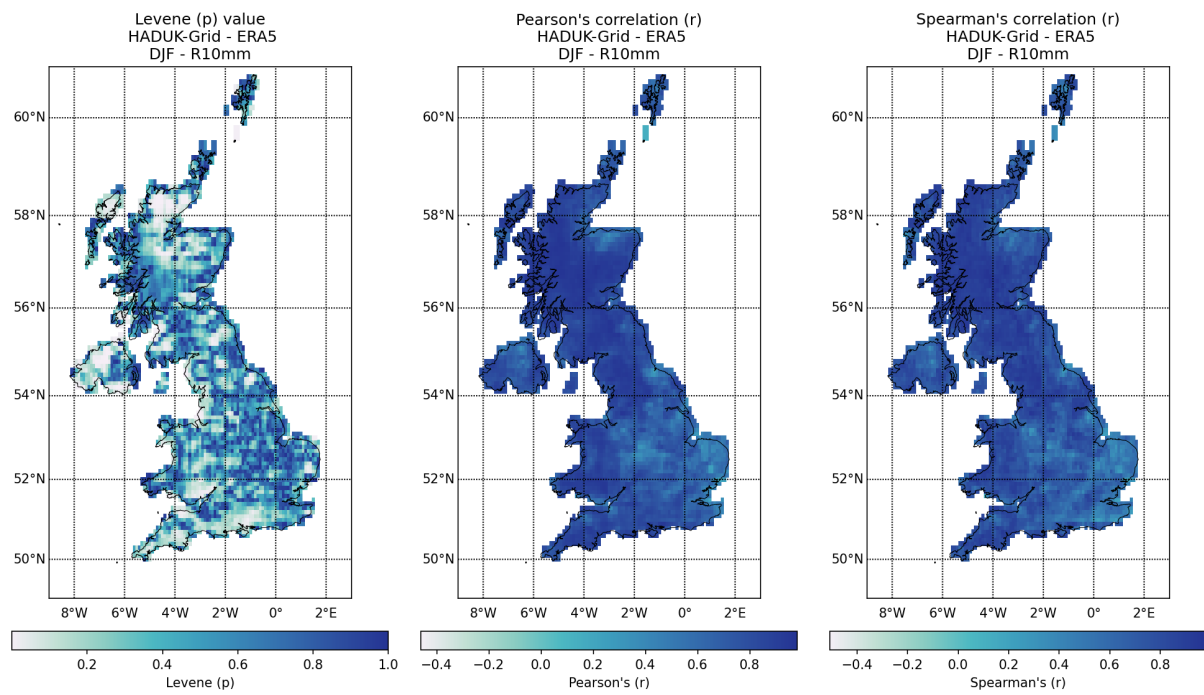


Figure 25: Spatial distribution of R10mm values obtained from HadUK-Grid and ERA5 with Mann-Whitney test p value, Levene -center in the median- p value, and Pearson and Spearman correlation coefficient (r), for spring (DJF) over the 2001-2019 climatological period (cont.).

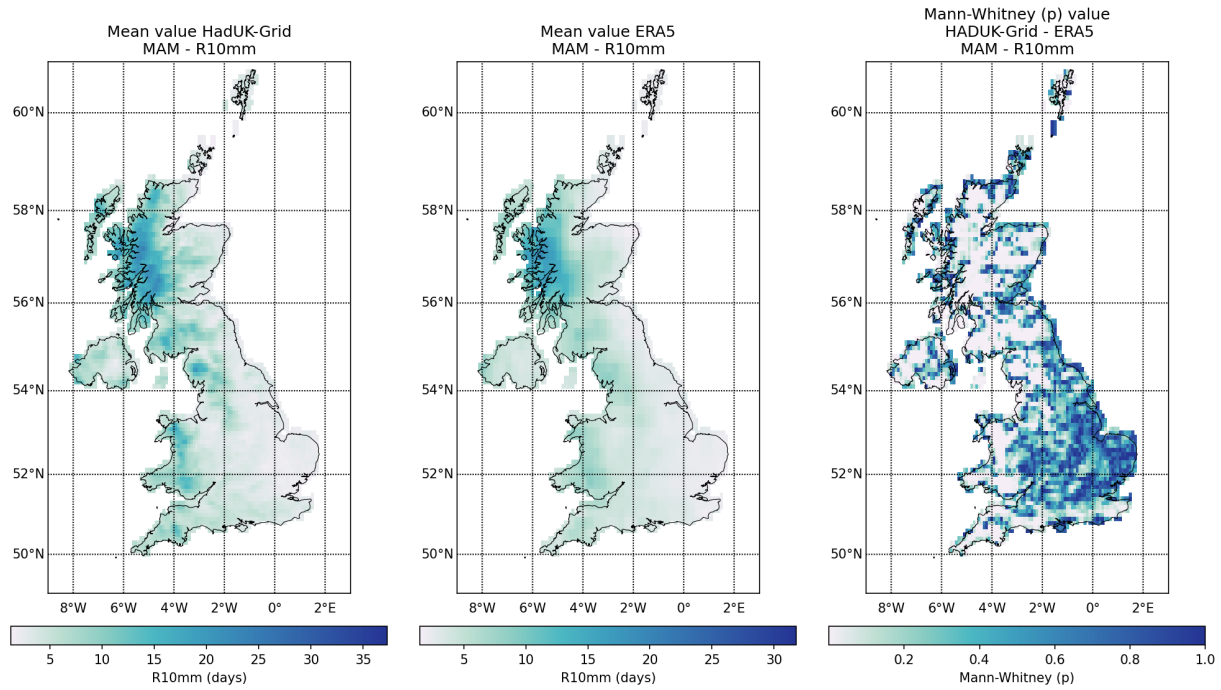


Figure 25: Spatial distribution of R10mm values obtained from HadUK-Grid and ERA5 with Mann-Whitney test p value, Levene -center in the median- p value, and Pearson and Spearman correlation coefficient (r), for spring (MAM) over the 2001-2019 climatological period (cont.).

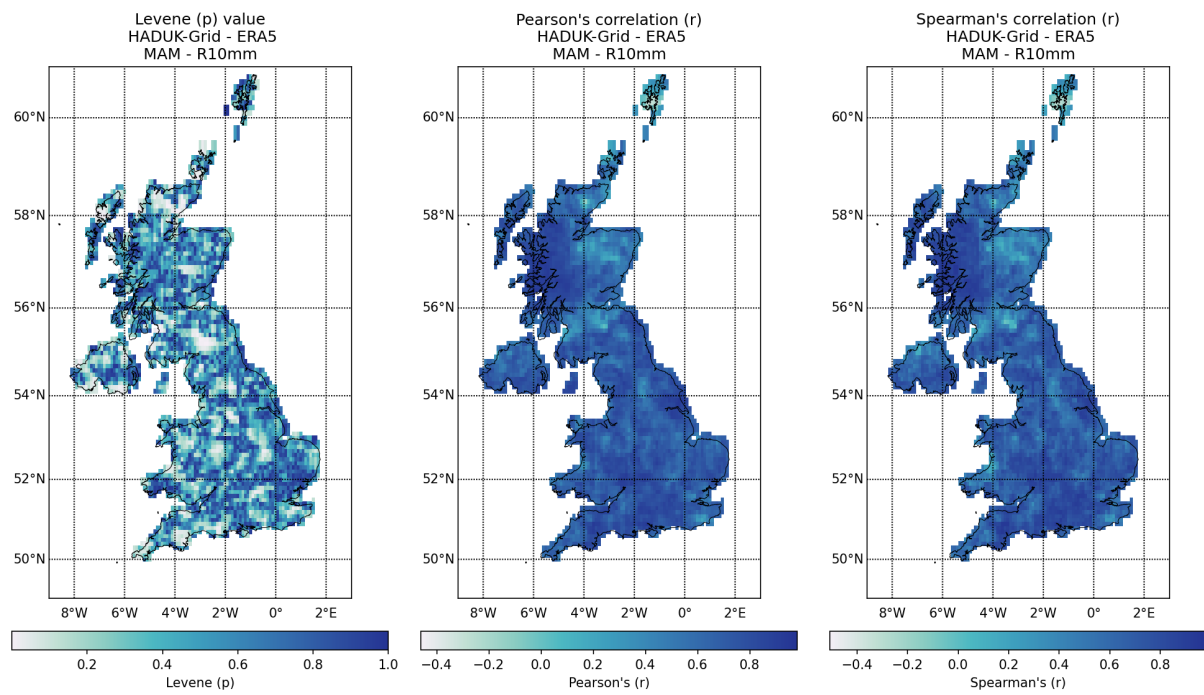


Figure 25: Spatial distribution of R10mm values obtained from HadUK-Grid and ERA5 with Mann-Whitney test p value, Levene -center in the median- p value, and Pearson and Spearman correlation coefficient (r), for spring (MAM) over the 2001-2019 climatological period (cont.).

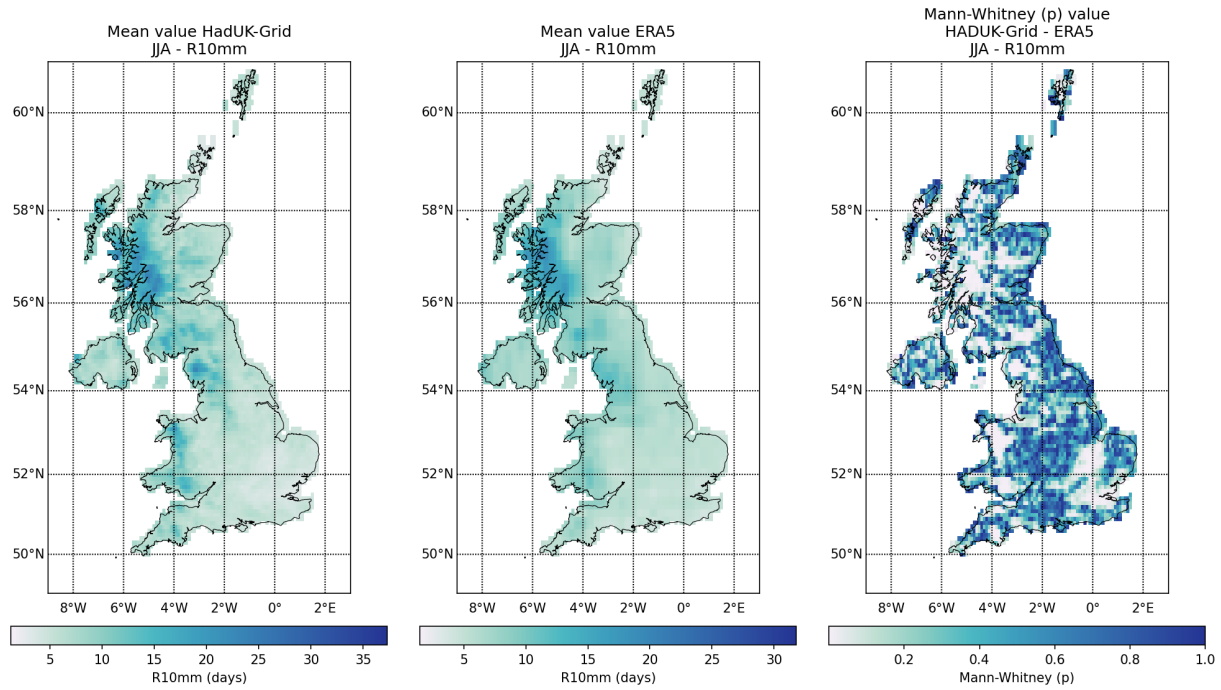


Figure 25: Spatial distribution of R10mm values obtained from HadUK-Grid and ERA5 with Mann-Whitney test p value, Levene -center in the median- p value, and Pearson and Spearman correlation coefficient (r), for summer (JJA) over the 2001-2019 climatological period (cont.).

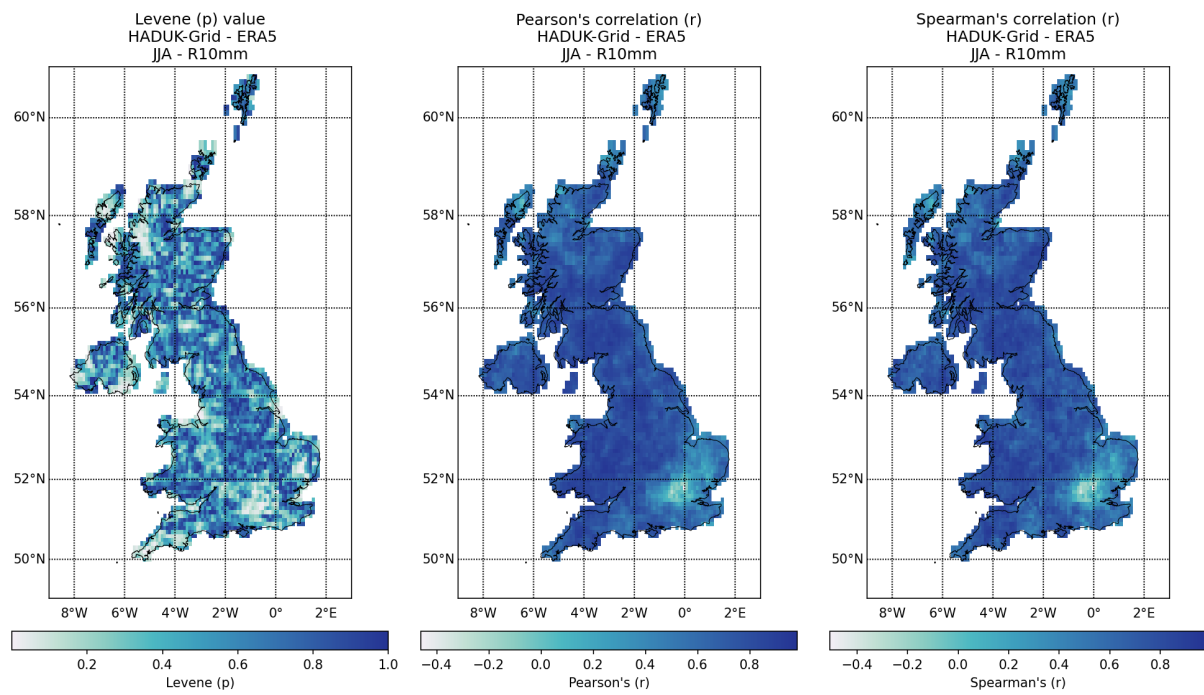


Figure 25: Spatial distribution of R10mm values obtained from HadUK-Grid and ERA5 with Mann-Whitney test p value, Levene -center in the median- p value, and Pearson and Spearman correlation coefficient (r), for summer (JJA) over the 2001-2019 climatological period (cont.).

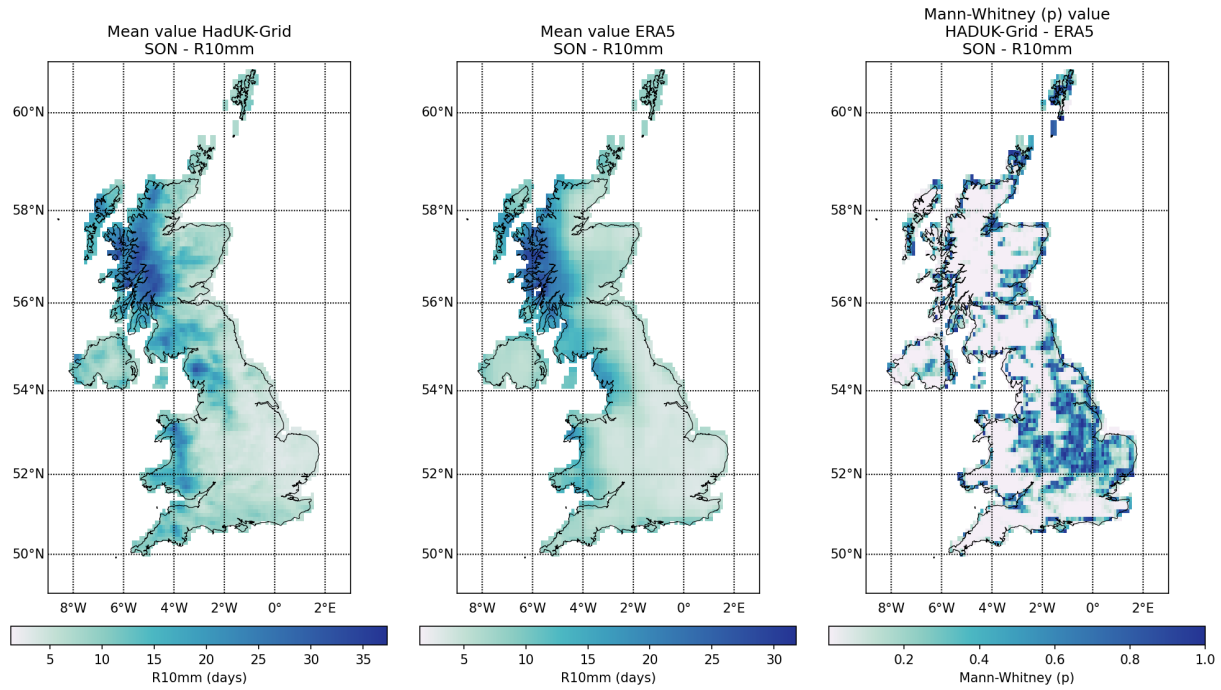


Figure 25: Spatial distribution of R10mm values obtained from HadUK-Grid and ERA5 with Mann-Whitney test p value, Levene -center in the median- p value, and Pearson and Spearman correlation coefficient (r), for autumn (SON) over the 2001-2019 climatological period (cont.).

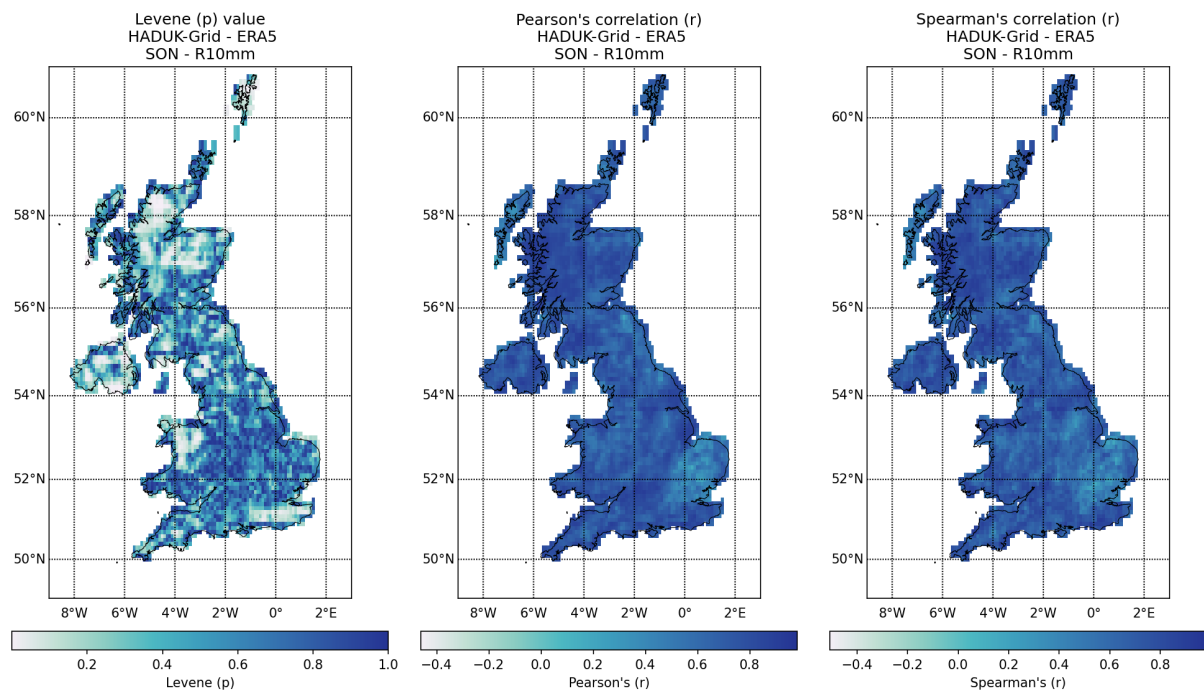


Figure 25: Spatial distribution of R10mm values obtained from HadUK-Grid and ERA5 with Mann-Whitney test p value, Levene -center in the median- p value, and Pearson and Spearman correlation coefficient (r), for autumn (SON) over the 2001-2019 climatological period.

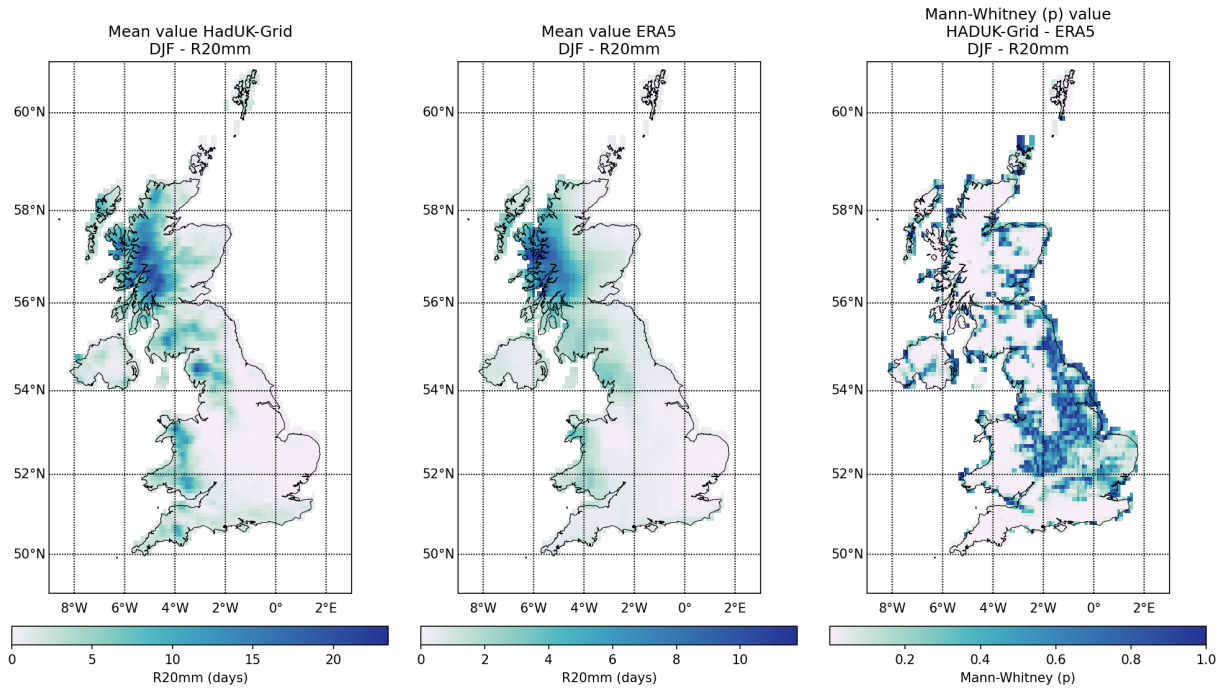


Figure 26: Spatial distribution of R20mm values obtained from HadUK-Grid and ERA5 with Mann-Whitney test p value, Levene -center in the median- p value, and Pearson and Spearman correlation coefficient (r), for winter (DJF) over the 2001-2019 climatological period.

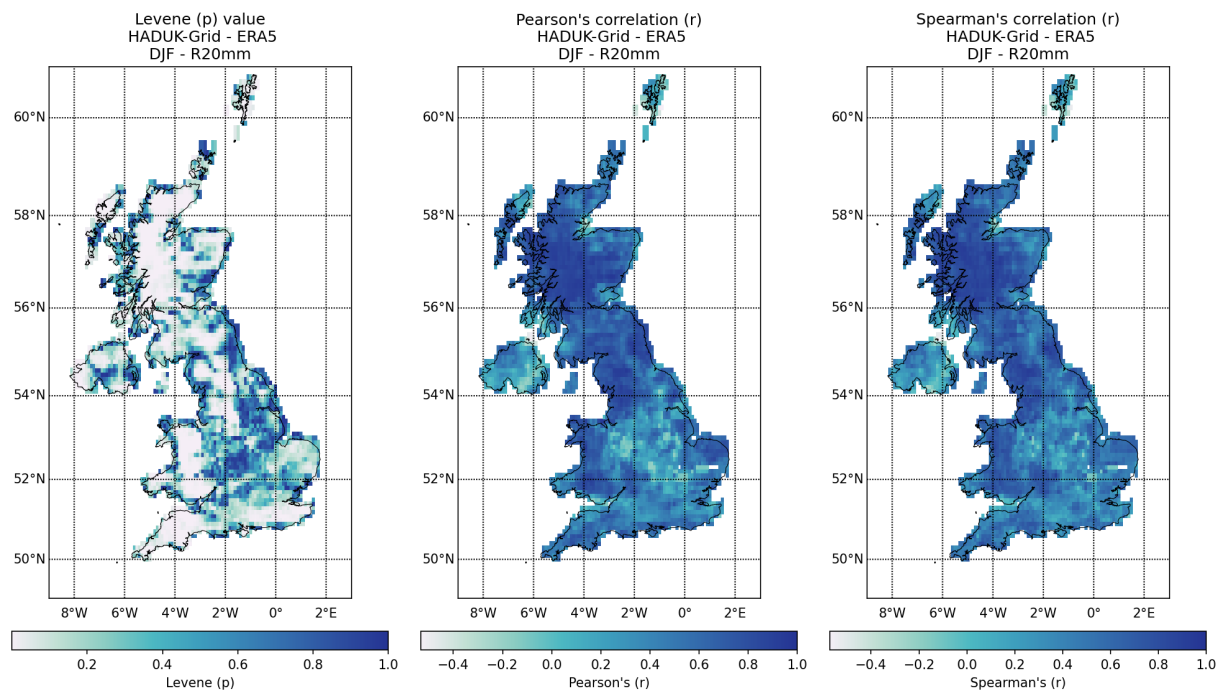


Figure 26: Spatial distribution of R20mm values obtained from HadUK-Grid and ERA5 with Mann-Whitney test p value, Levene -center in the median- p value, and Pearson and Spearman correlation coefficient (r), for spring (DJF) over the 2001-2019 climatological period (cont.).

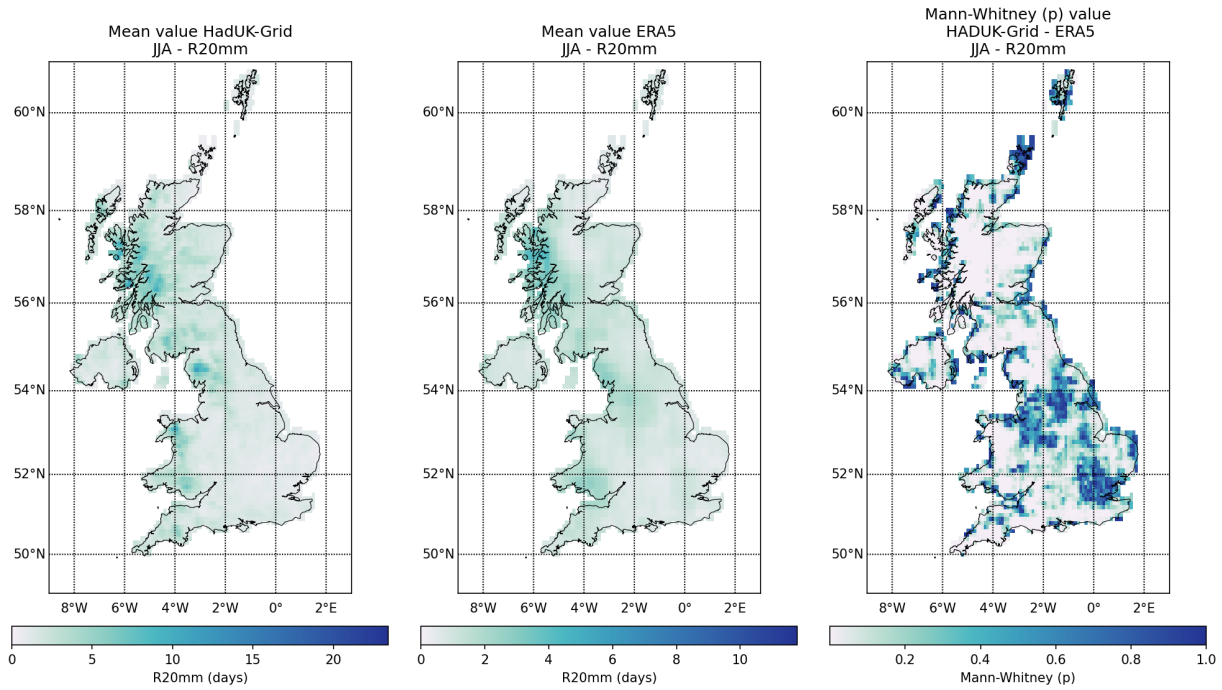


Figure 26: Spatial distribution of R20mm values obtained from HadUK-Grid and ERA5 with Mann-Whitney test p value, Levene -center in the median- p value, and Pearson and Spearman correlation coefficient (r), for summer (JJA) over the 2001-2019 climatological period (cont.).

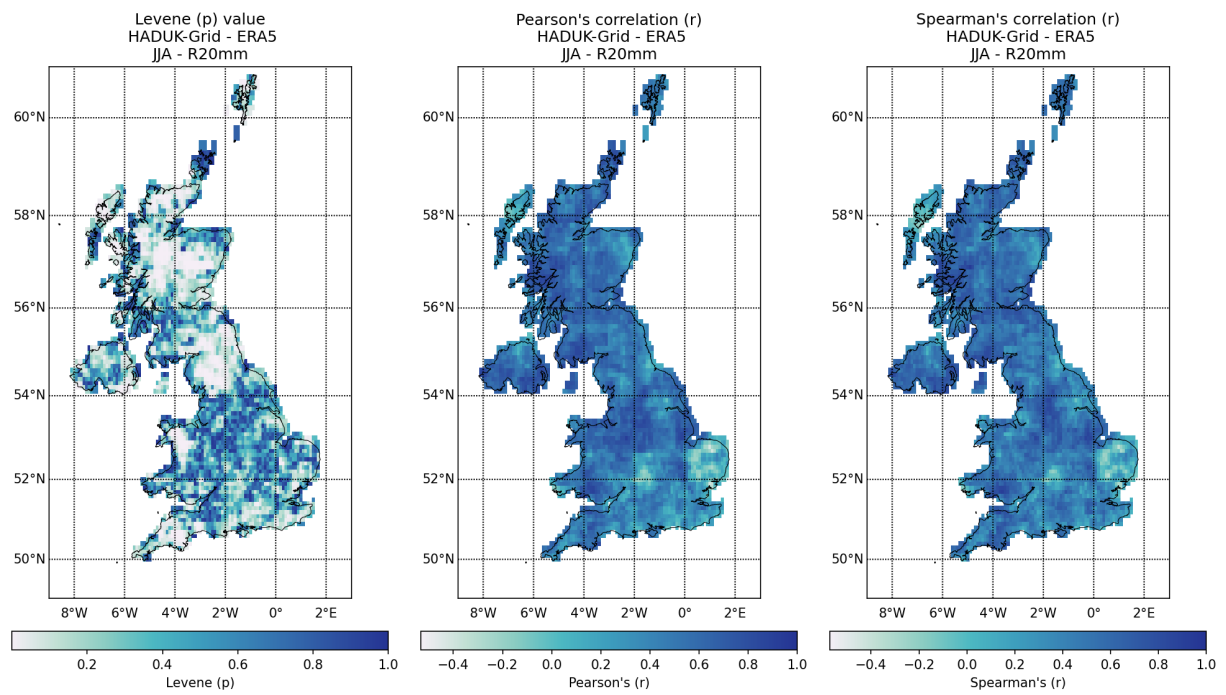


Figure 26: Spatial distribution of R20mm values obtained from HadUK-Grid and ERA5 with Mann-Whitney test p value, Levene -center in the median- p value, and Pearson and Spearman correlation coefficient (r), for summer (JJA) over the 2001-2019 climatological period (cont.).

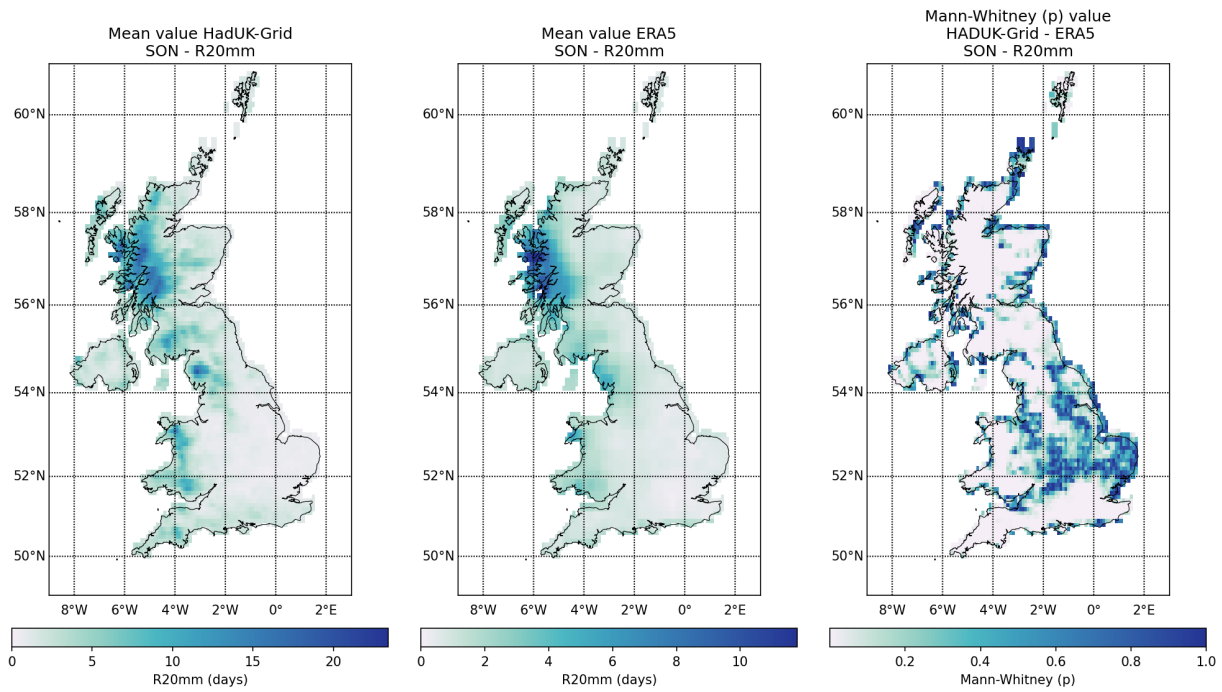


Figure 26: Spatial distribution of R20mm values obtained from HadUK-Grid and ERA5 with Mann-Whitney test p value, Levene -center in the median- p value, and Pearson and Spearman correlation coefficient (r), for autumn (SON) over the 2001-2019 climatological period (cont.).

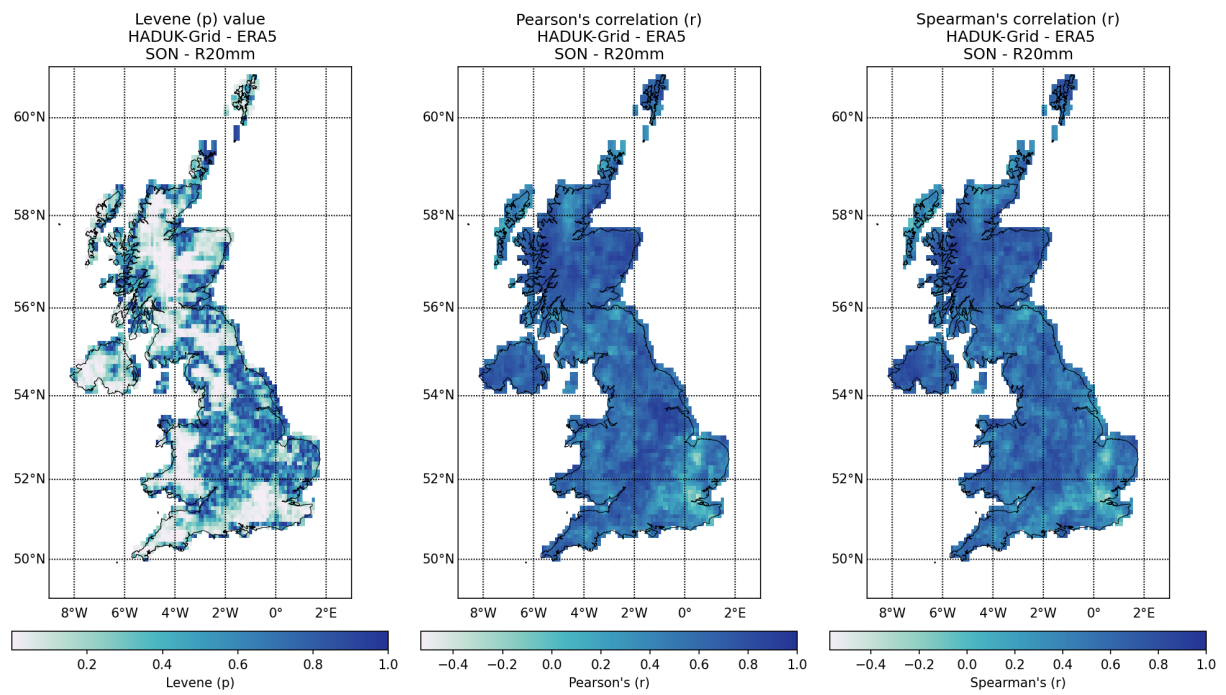


Figure 26: Spatial distribution of R20mm values obtained from HadUK-Grid and ERA5 with Mann-Whitney test p value, Levene -center in the median- p value, and Pearson and Spearman correlation coefficient (r), for autumn (SON) over the 2001-2019 climatological period.

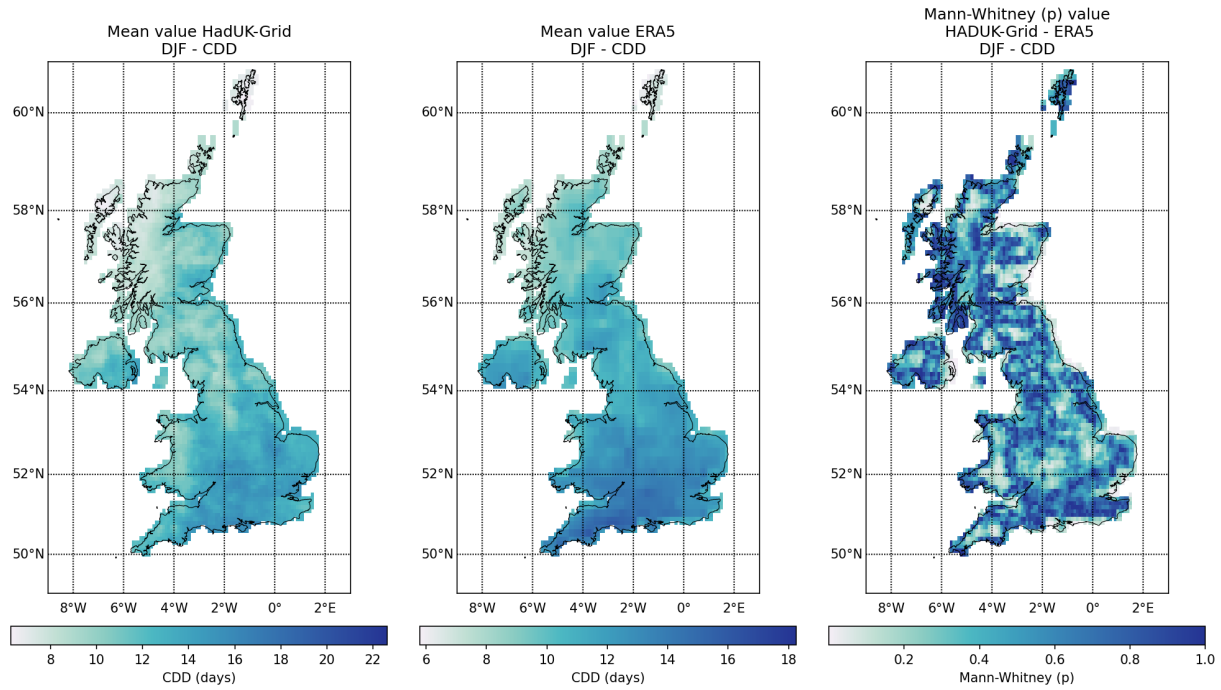


Figure 27: Spatial distribution of CDD values obtained from HadUK-Grid and ERA5 with Mann-Whitney test p value, Levene -center in the median- p value, and Pearson and Spearman correlation coefficient (r), for winter (DJF) over the 2001-2019 climatological period.

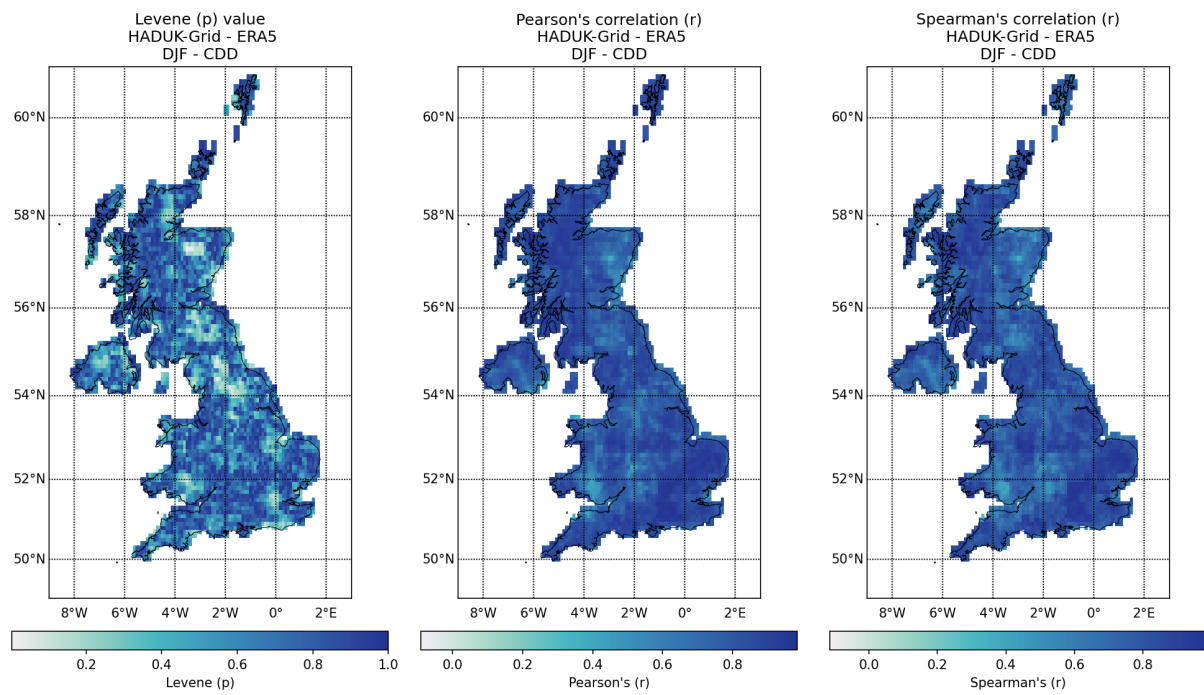


Figure 27: Spatial distribution of CDD values obtained from HadUK-Grid and ERA5 with Mann-Whitney test p value, Levene -center in the median- p value, and Pearson and Spearman correlation coefficient (r), for spring (DJF) over the 2001-2019 climatological period (cont.).

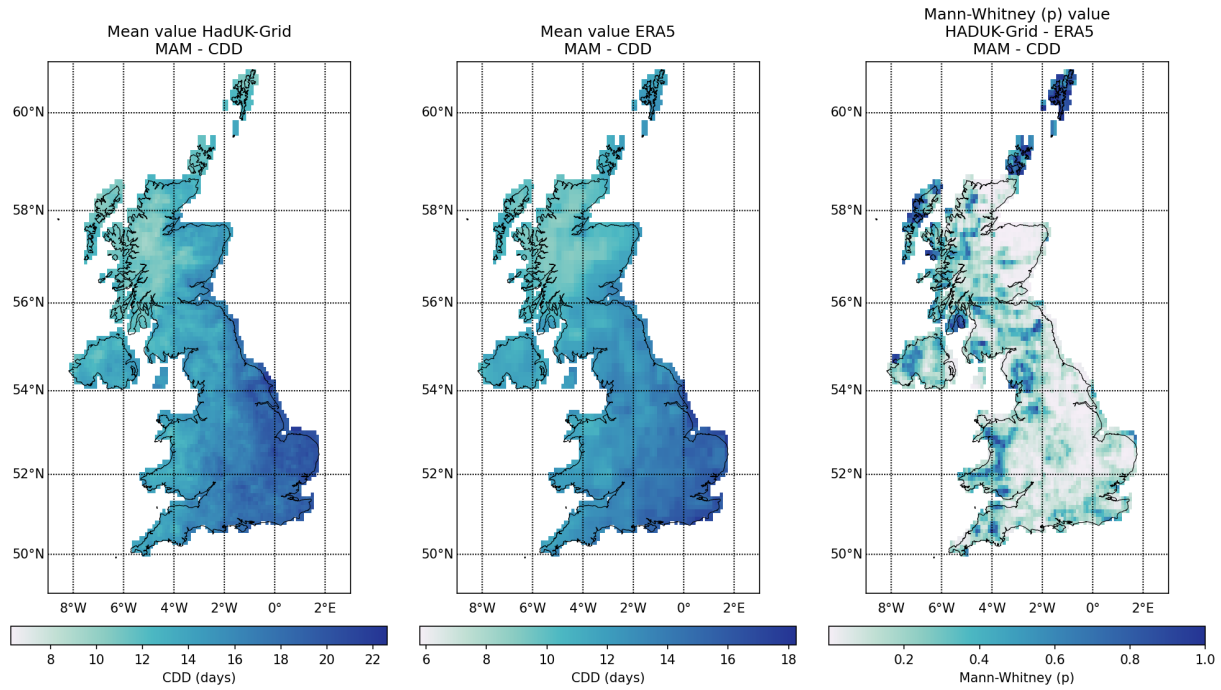


Figure 27: Spatial distribution of CDD values obtained from HadUK-Grid and ERA5 with Mann-Whitney test p value, Levene -center in the median- p value, and Pearson and Spearman correlation coefficient (r), for spring (MAM) over the 2001-2019 climatological period (cont.).

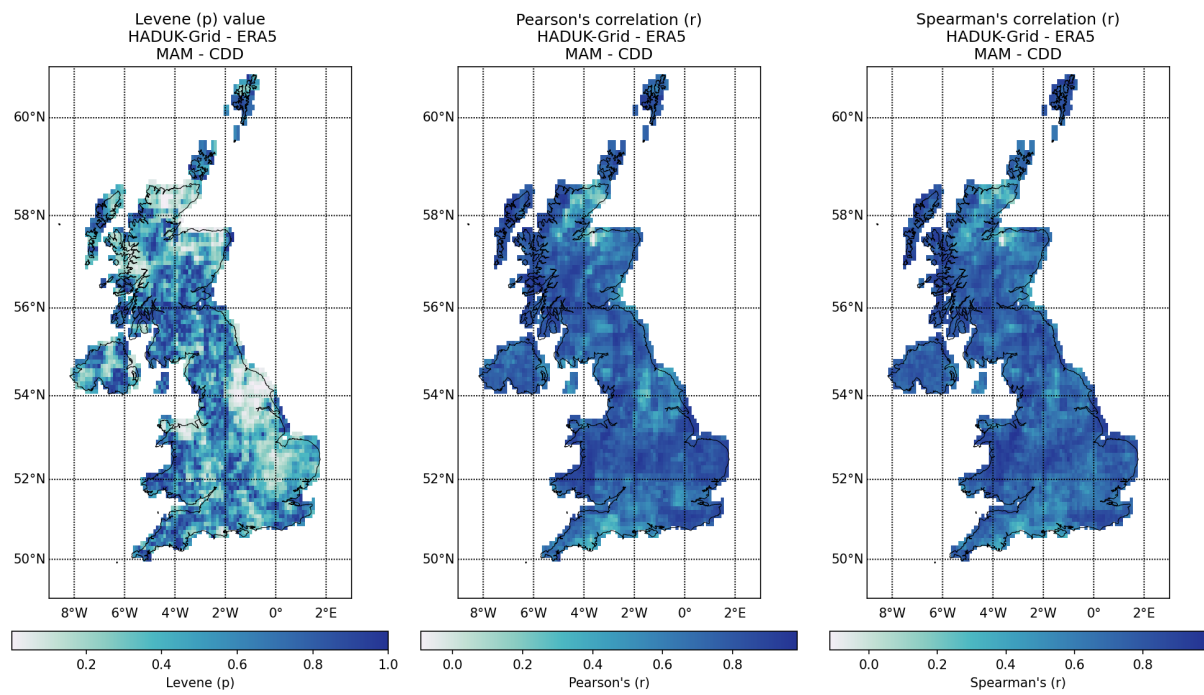


Figure 27: Spatial distribution of CDD values obtained from HadUK-Grid and ERA5 with Mann-Whitney test p value, Levene -center in the median- p value, and Pearson and Spearman correlation coefficient (r), for spring (MAM) over the 2001-2019 climatological period (cont.).

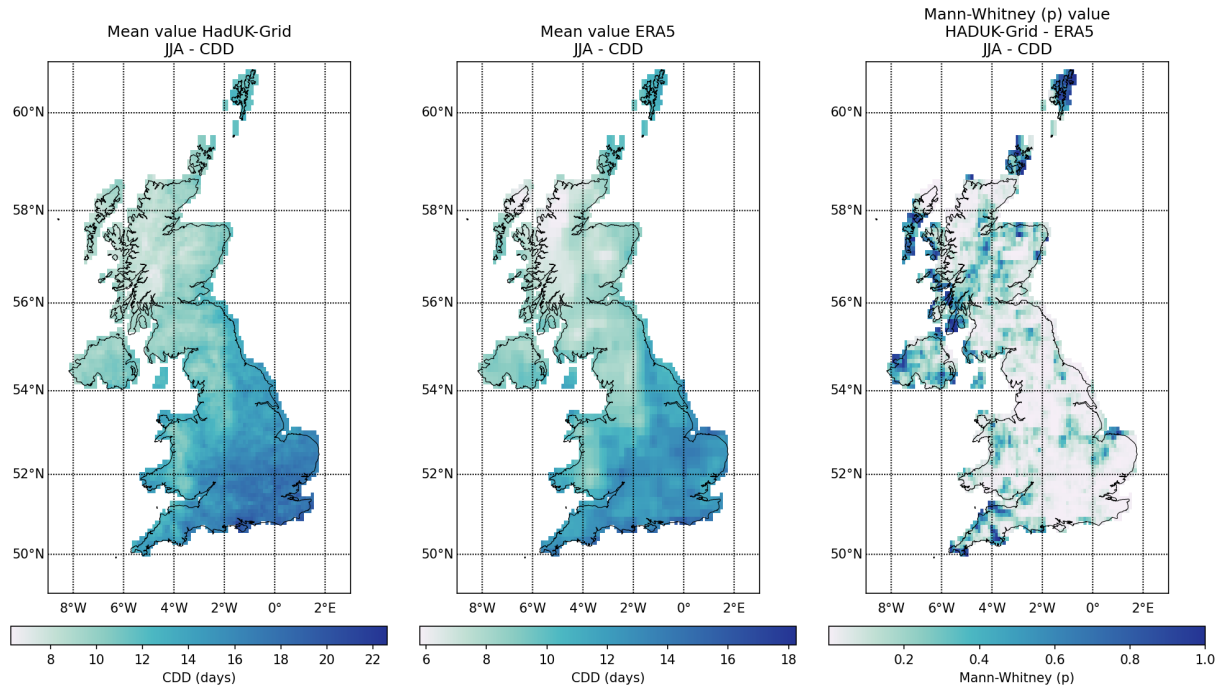


Figure 27: Spatial distribution of CDD values obtained from HadUK-Grid and ERA5 with Mann-Whitney test p value, Levene -center in the median- p value, and Pearson and Spearman correlation coefficient (r), for summer (JJA) over the 2001-2019 climatological period (cont.).

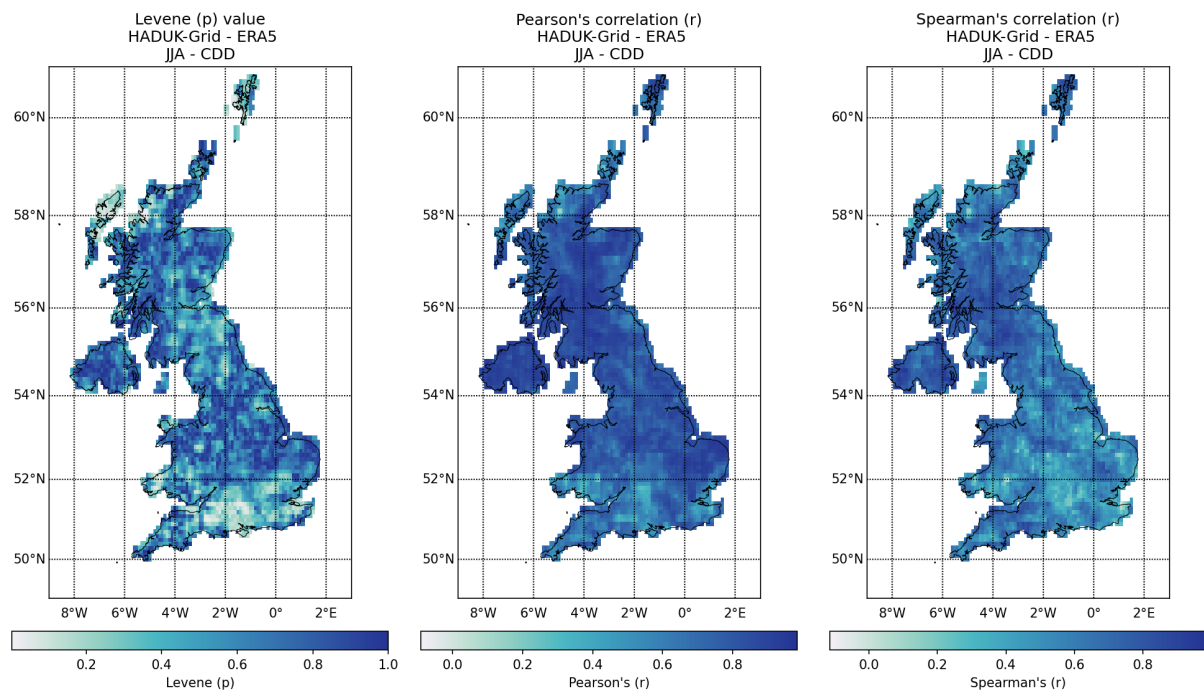


Figure 27: Spatial distribution of CDD values obtained from HadUK-Grid and ERA5 with Mann-Whitney test p value, Levene -center in the median- p value, and Pearson and Spearman correlation coefficient (r), for summer (JJA) over the 2001-2019 climatological period (cont.).

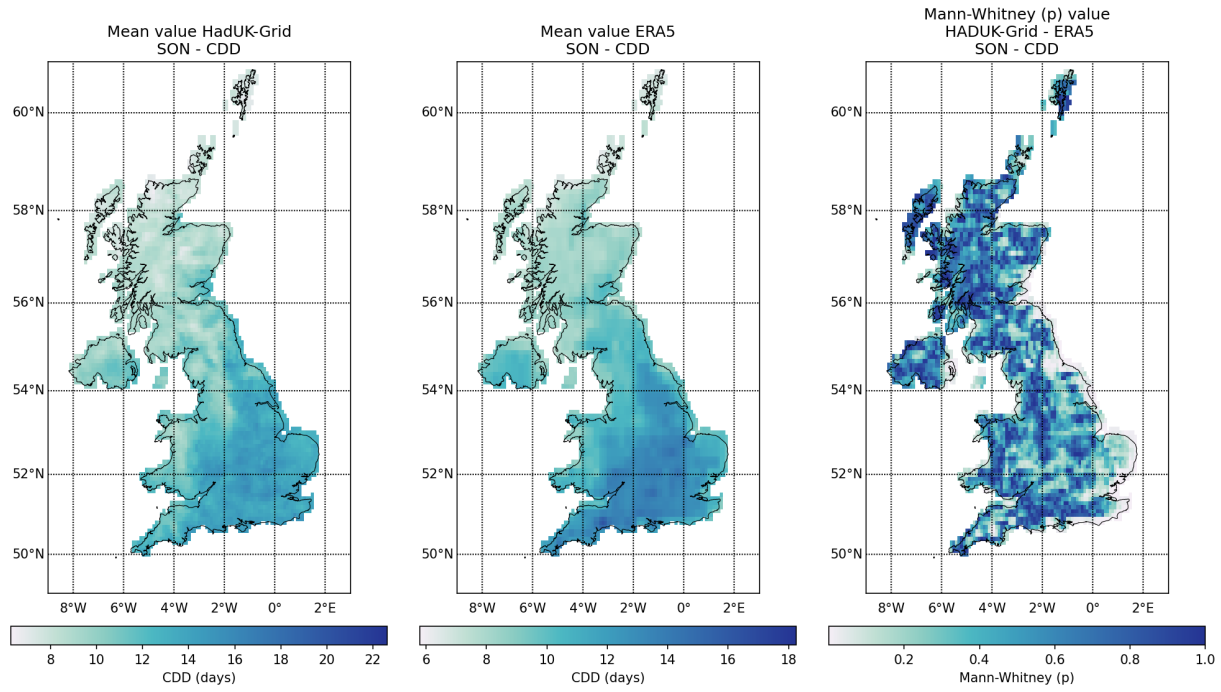


Figure 27: Spatial distribution of CDD values obtained from HadUK-Grid and ERA5 with Mann-Whitney test p value, Levene -center in the median- p value, and Pearson and Spearman correlation coefficient (r), for autumn (SON) over the 2001-2019 climatological period (cont.).

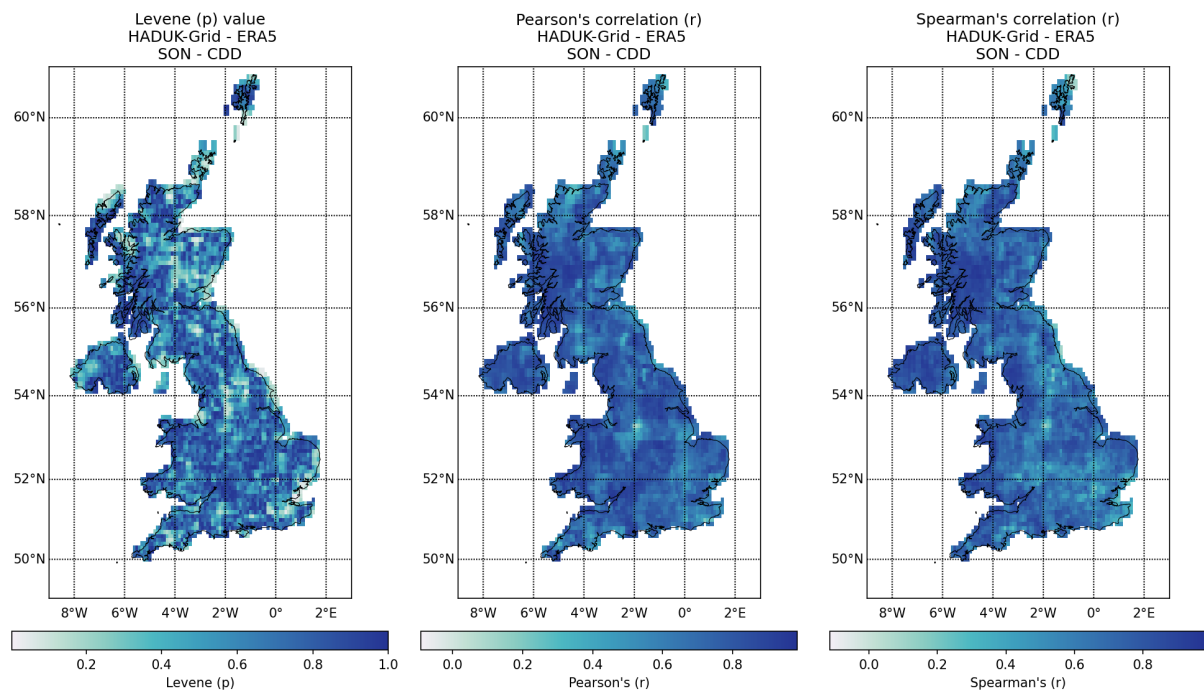


Figure 27: Spatial distribution of CDD values obtained from HadUK-Grid and ERA5 with Mann-Whitney test p value, Levene -center in the median- p value, and Pearson and Spearman correlation coefficient (r), for autumn (SON) over the 2001-2019 climatological period.

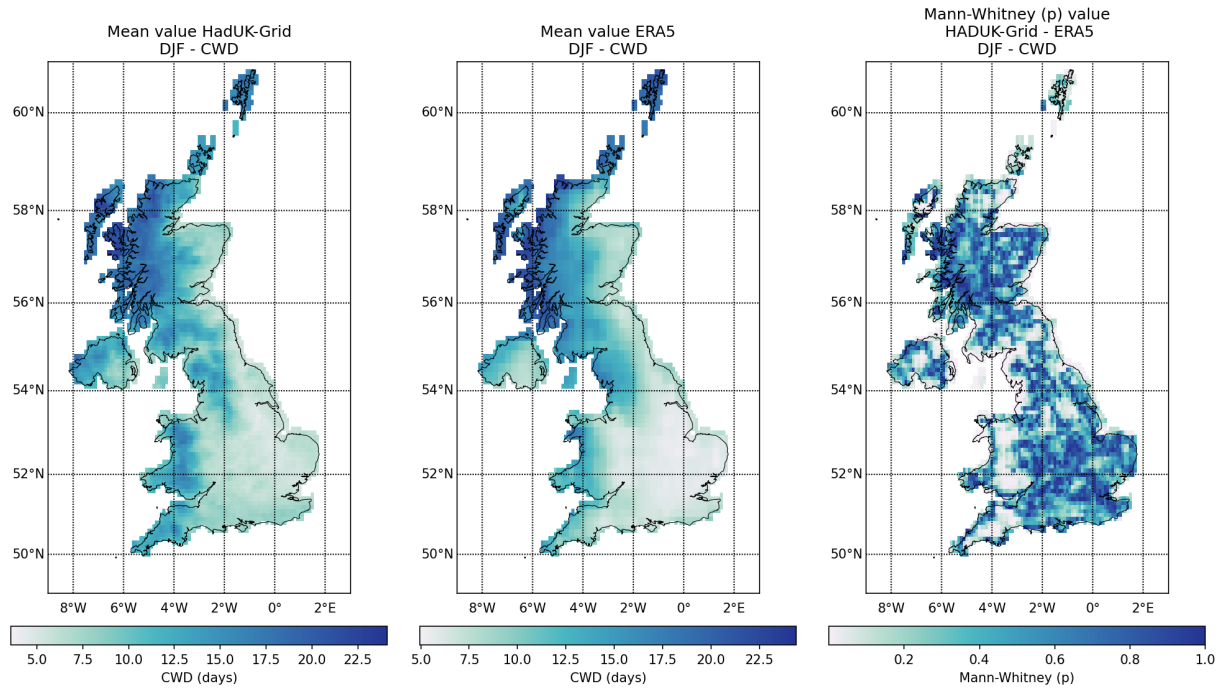


Figure 28: Spatial distribution of CWD values obtained from HadUK-Grid and ERA5 with Mann-Whitney test p value, Levene -center in the median- p value, and Pearson and Spearman correlation coefficient (r), for winter (DJF) over the 2001-2019 climatological period.

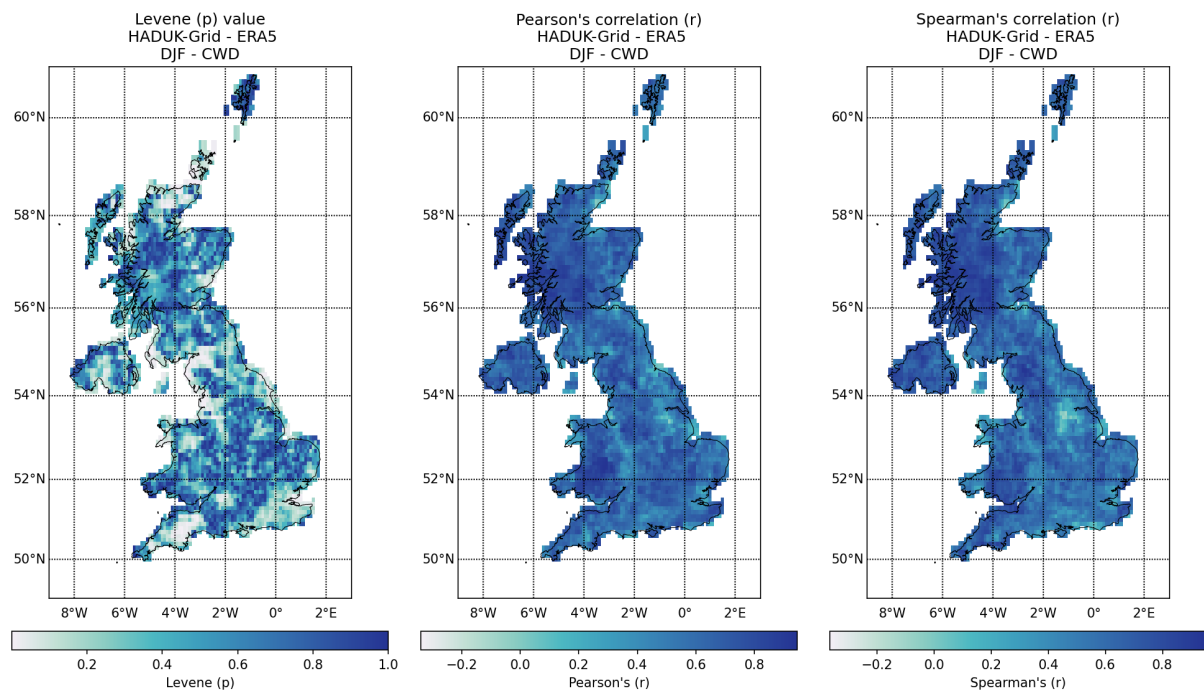


Figure 28: Spatial distribution of CWD values obtained from HadUK-Grid and ERA5 with Mann-Whitney test p value, Levene -center in the median- p value, and Pearson and Spearman correlation coefficient (r), for spring (DJF) over the 2001-2019 climatological period (cont.).

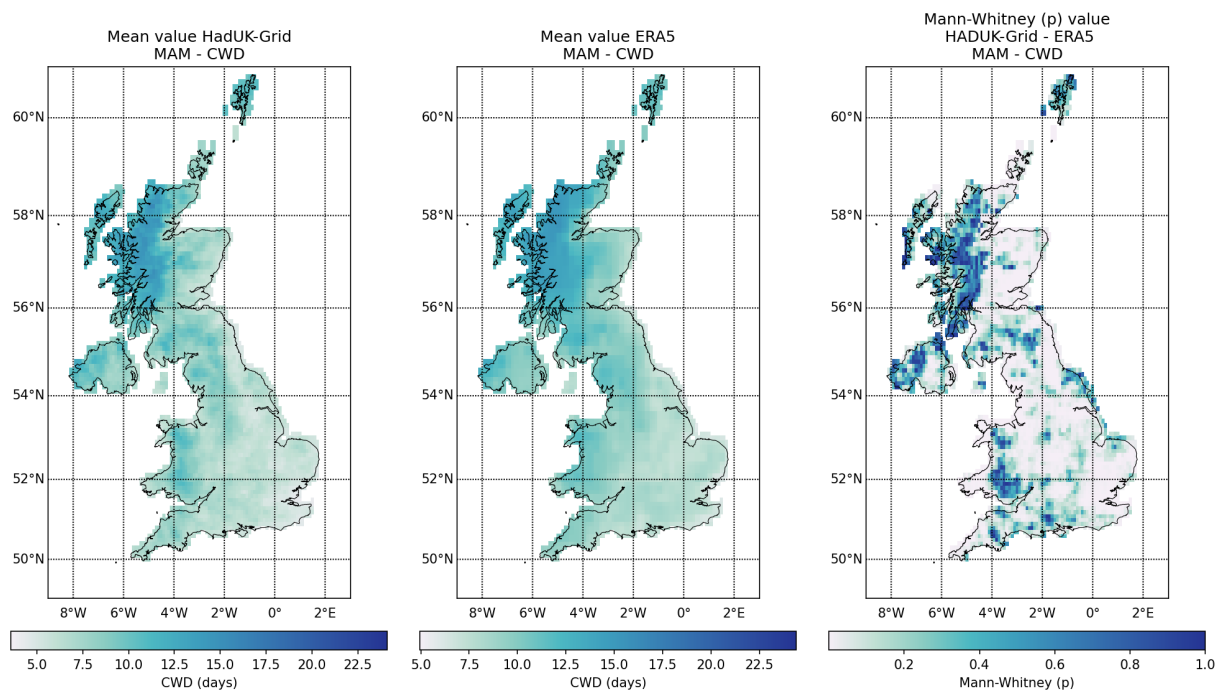


Figure 28: Spatial distribution of CWD values obtained from HadUK-Grid and ERA5 with Mann-Whitney test p value, Levene -center in the median- p value, and Pearson and Spearman correlation coefficient (r), for spring (MAM) over the 2001-2019 climatological period (cont.).

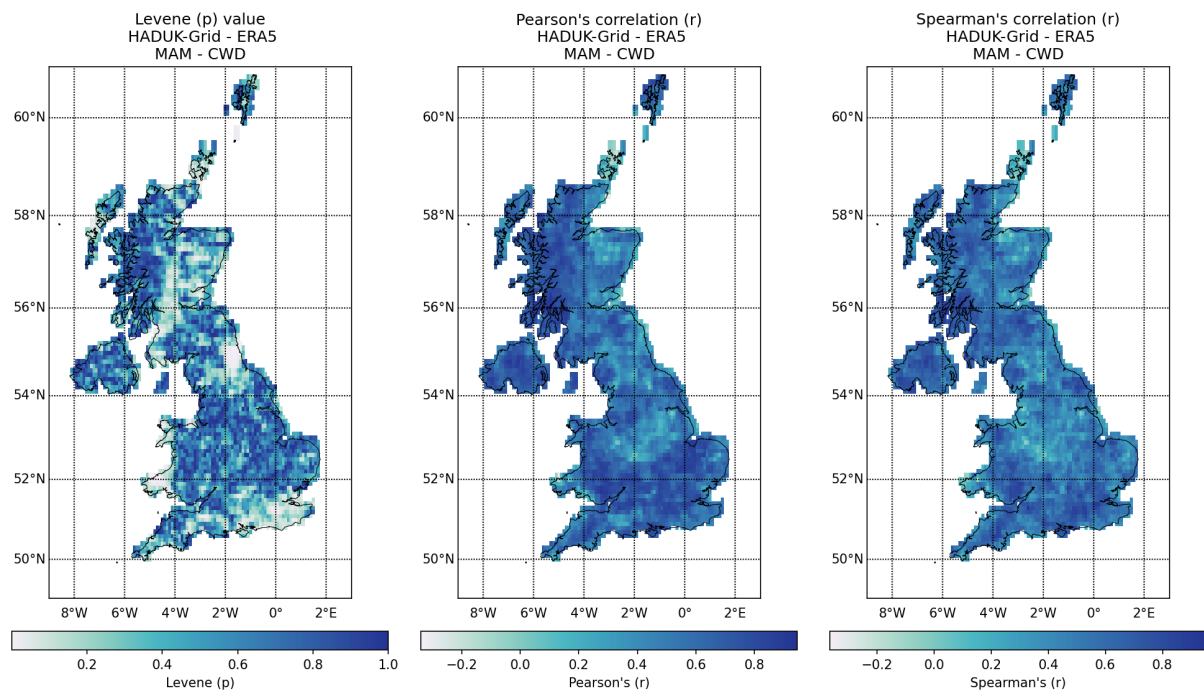


Figure 28: Spatial distribution of CWD values obtained from HadUK-Grid and ERA5 with Mann-Whitney test p value, Levene -center in the median- p value, and Pearson and Spearman correlation coefficient (r), for spring (MAM) over the 2001-2019 climatological period (cont.).

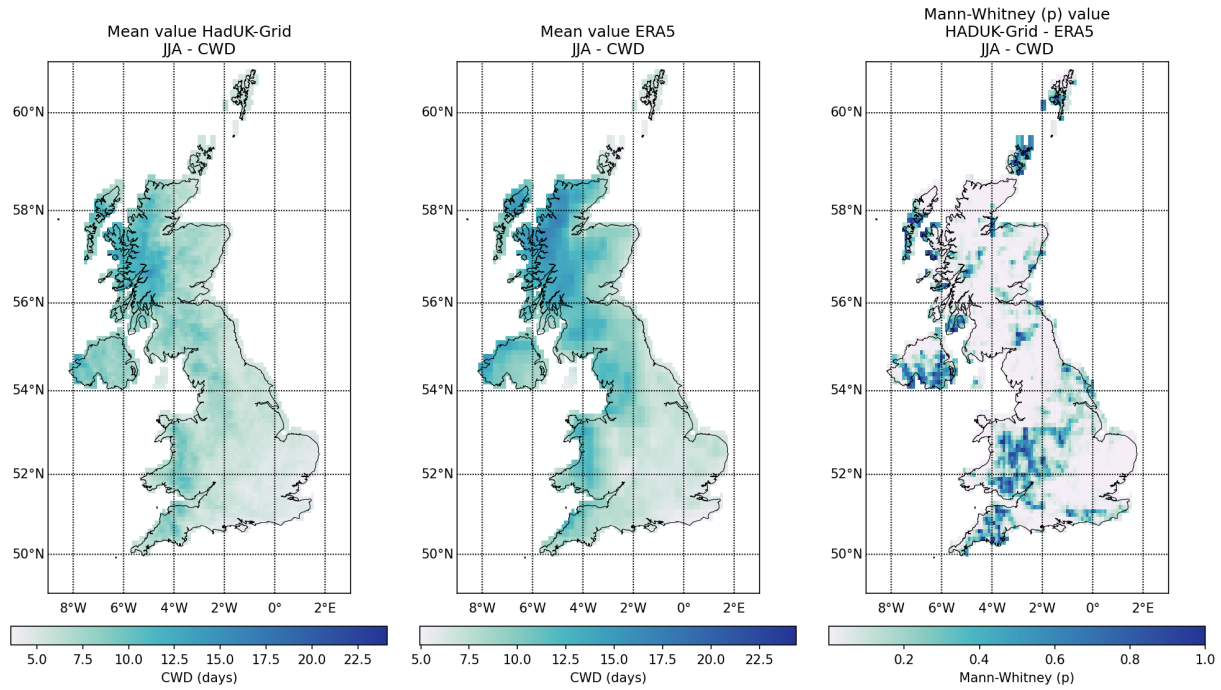


Figure 28: Spatial distribution of CWD values obtained from HadUK-Grid and ERA5 with Mann-Whitney test p value, Levene -center in the median- p value, and Pearson and Spearman correlation coefficient (r), for summer (JJA) over the 2001-2019 climatological period (cont.).

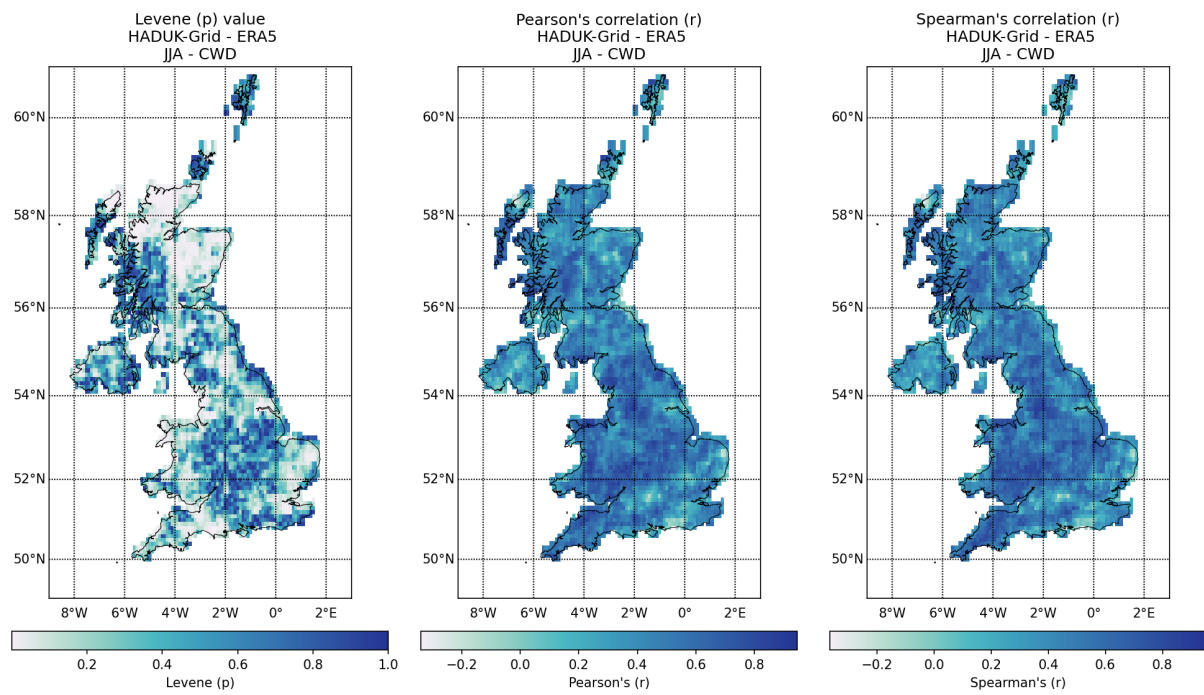


Figure 28: Spatial distribution of CWD values obtained from HadUK-Grid and ERA5 with Mann-Whitney test p value, Levene -center in the median- p value, and Pearson and Spearman correlation coefficient (r), for summer (JJA) over the 2001-2019 climatological period (cont.).

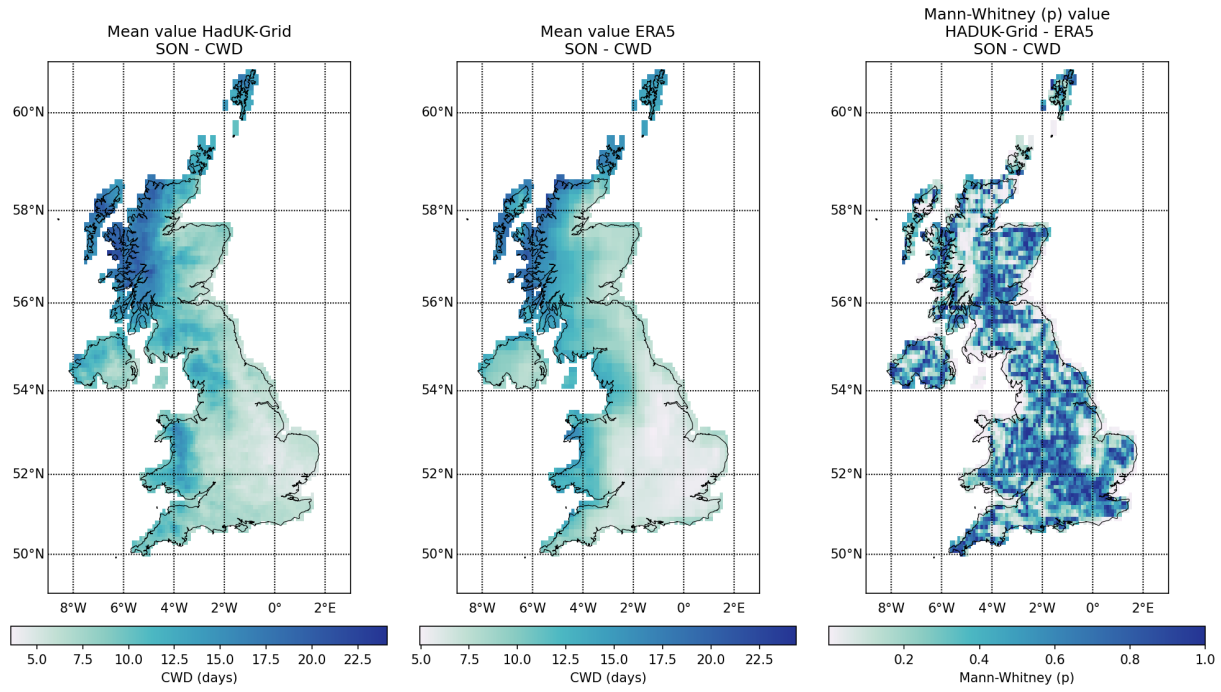


Figure 28: Spatial distribution of CWD values obtained from HadUK-Grid and ERA5 with Mann-Whitney test p value, Levene -center in the median- p value, and Pearson and Spearman correlation coefficient (r), for autumn (SON) over the 2001-2019 climatological period (cont.).

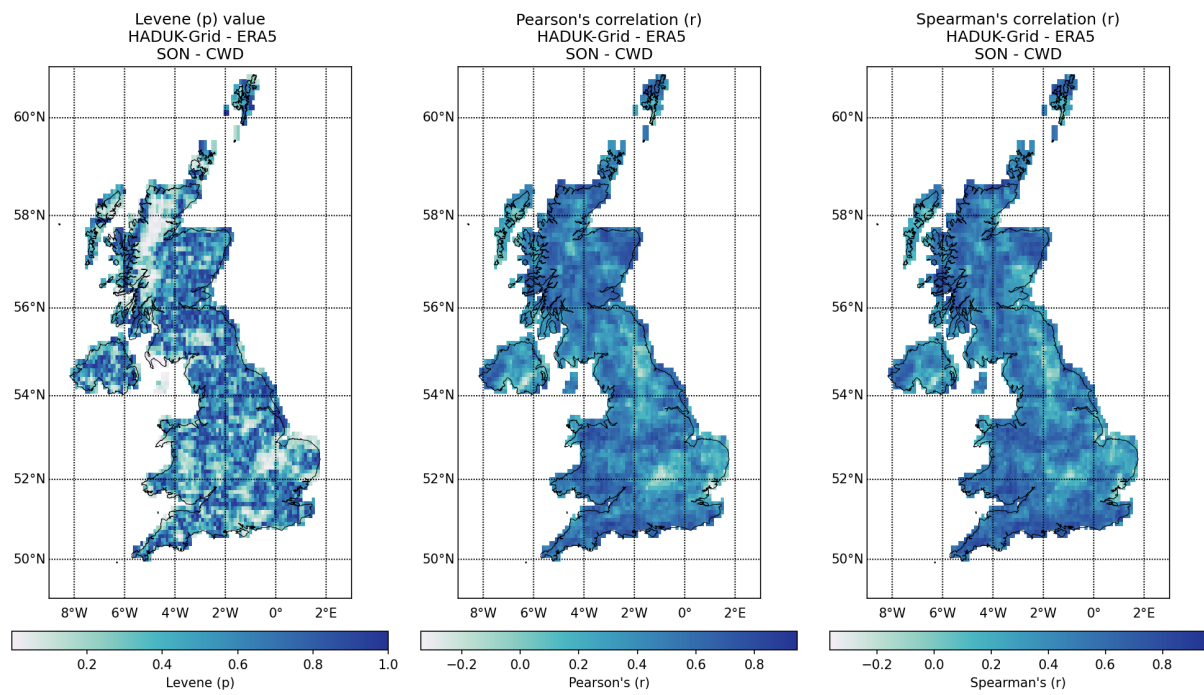


Figure 28: Spatial distribution of CWD values obtained from HadUK-Grid and ERA5 with Mann-Whitney test p value, Levene -center in the median- p value, and Pearson and Spearman correlation coefficient (r), for autumn (SON) over the 2001-2019 climatological period.

2.2 Indices based on station related thresholds - R95pTOT, R99TOT

2.2.1 IMERG DATA

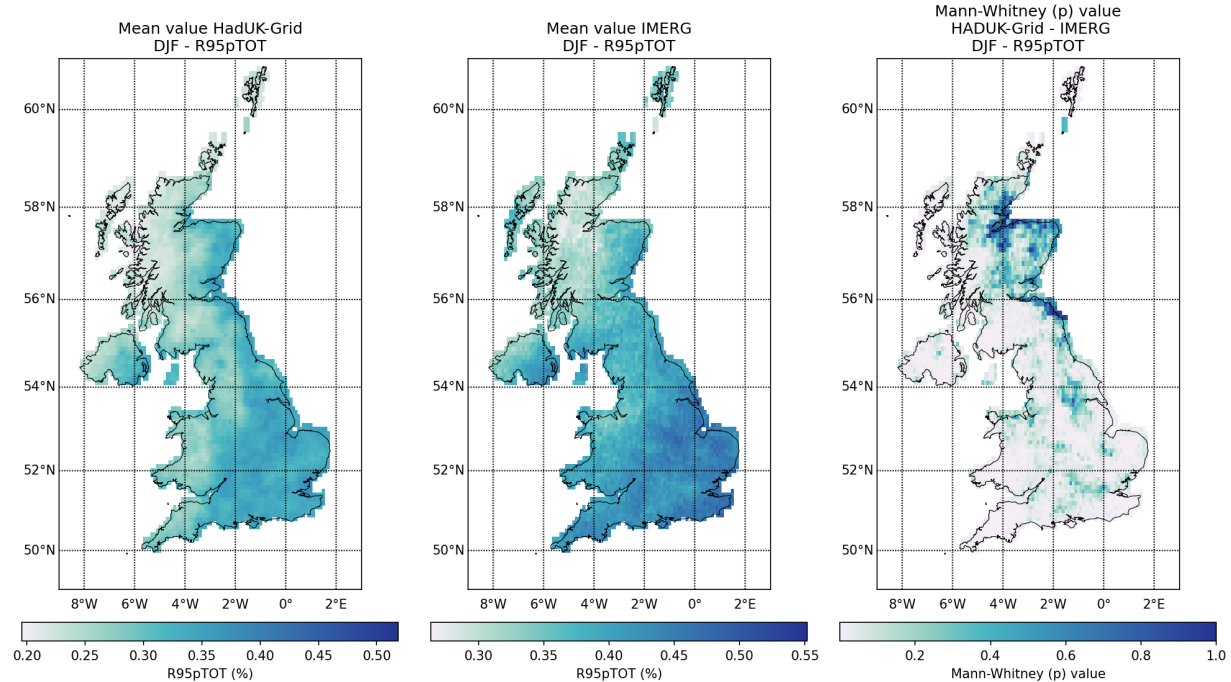


Figure 29: Spatial distribution of R95pTOT values obtained from HadUK-Grid and IMERG with Mann-Whitney test p value, Levene -center in the median- p value, and Pearson and Spearman correlation coefficient (r), for winter (DJF) over the 2001-2019 climatological period.

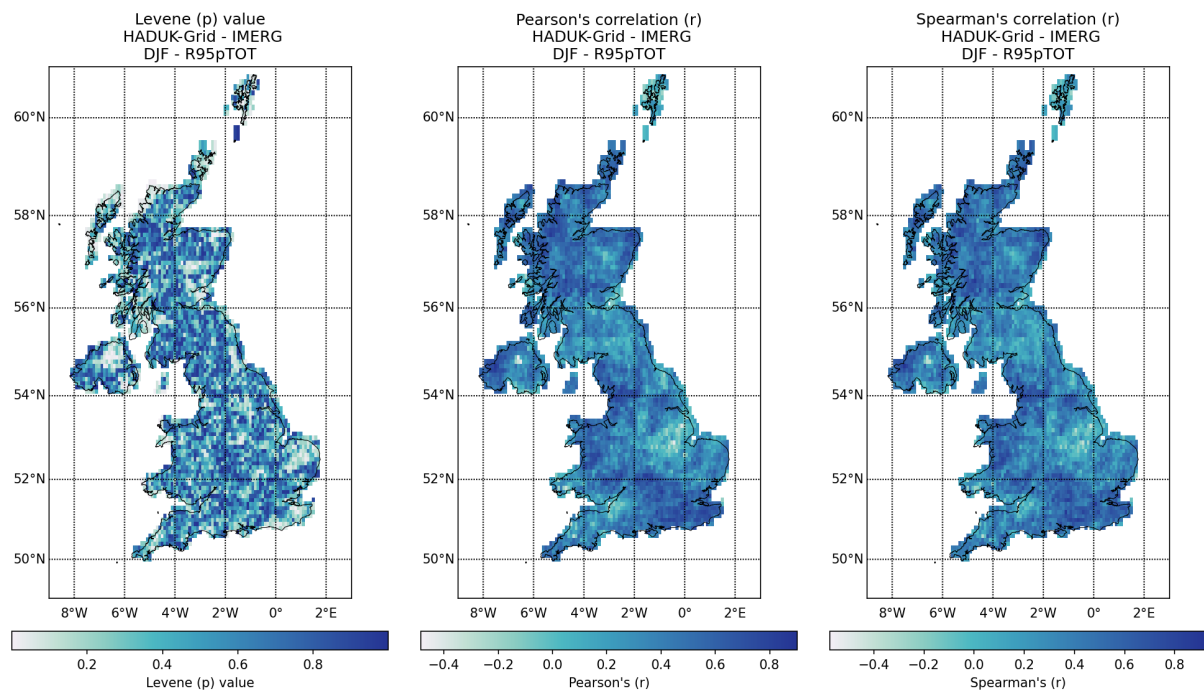


Figure 29: Spatial distribution of R95pTOT values obtained from HadUK-Grid and IMERG with Mann-Whitney test p value, Levene -center in the median- p value, and Pearson and Spearman correlation coefficient (r), for spring (DJF) over the 2001-2019 climatological period (cont.).

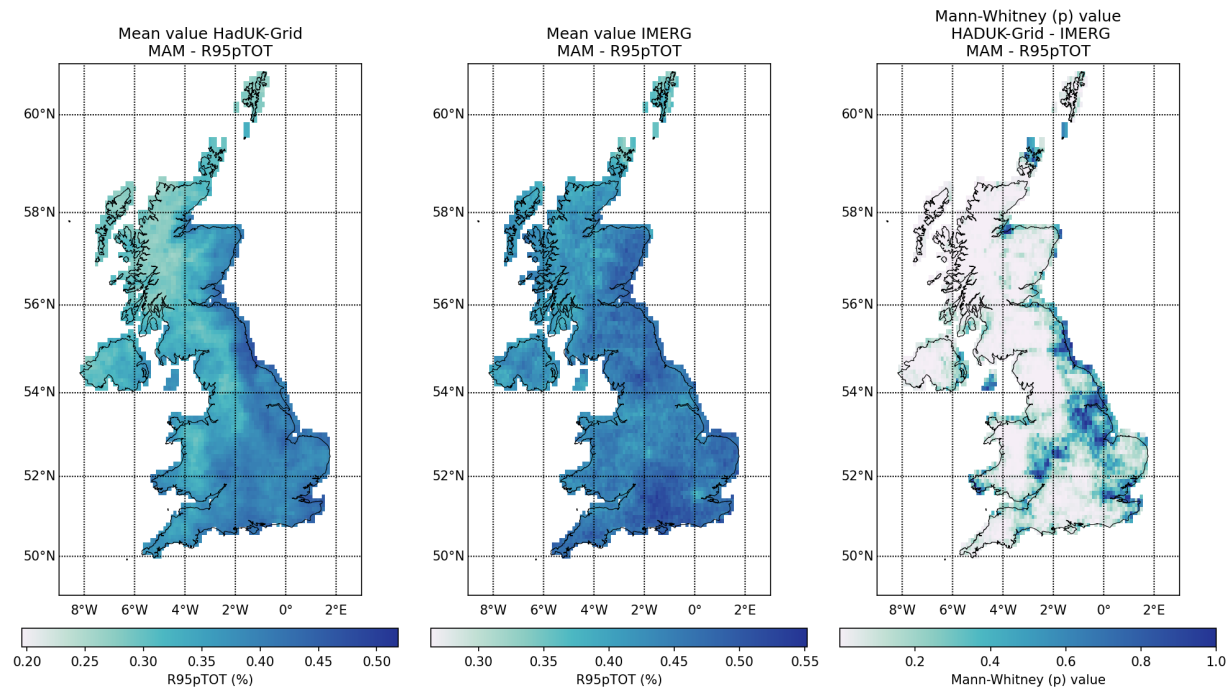


Figure 29: Spatial distribution of R95pTOT values obtained from HadUK-Grid and IMERG with Mann-Whitney test p value, Levene -center in the median- p value, and Pearson and Spearman correlation coefficient (r), for spring (MAM) over the 2001-2019 climatological period (cont.).

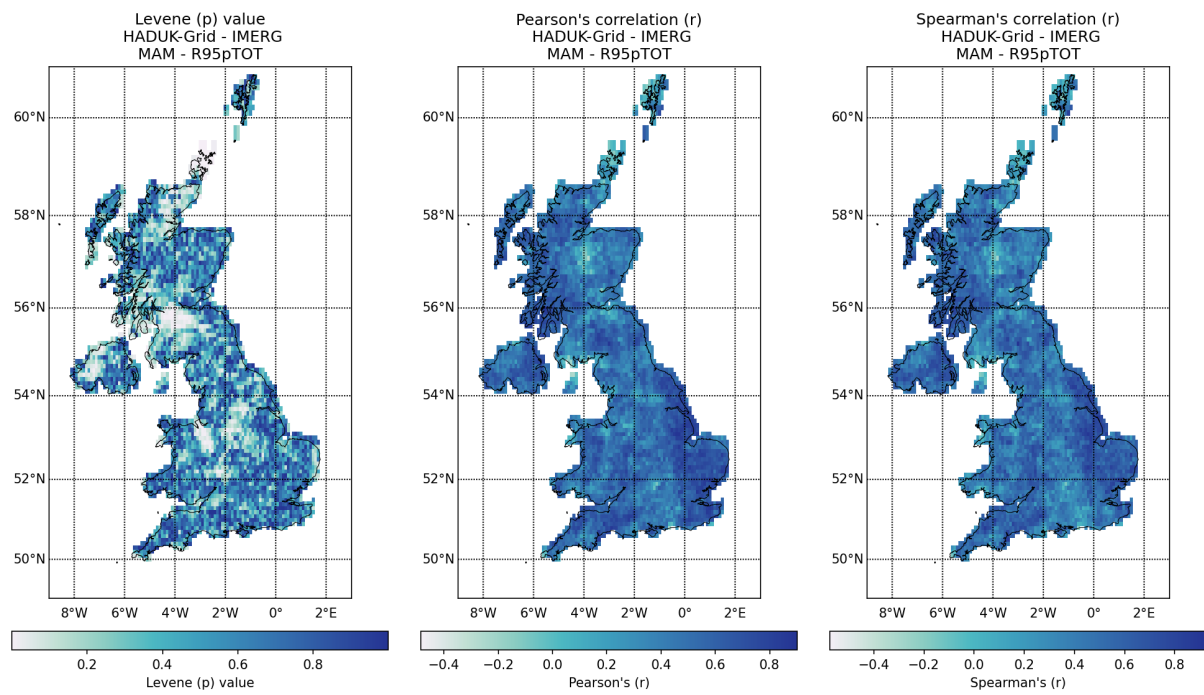


Figure 29: Spatial distribution of R95pTOT values obtained from HadUK-Grid and IMERG with Mann-Whitney test p value, Levene -center in the median- p value, and Pearson and Spearman correlation coefficient (r), for spring (MAM) over the 2001-2019 climatological period (cont.).

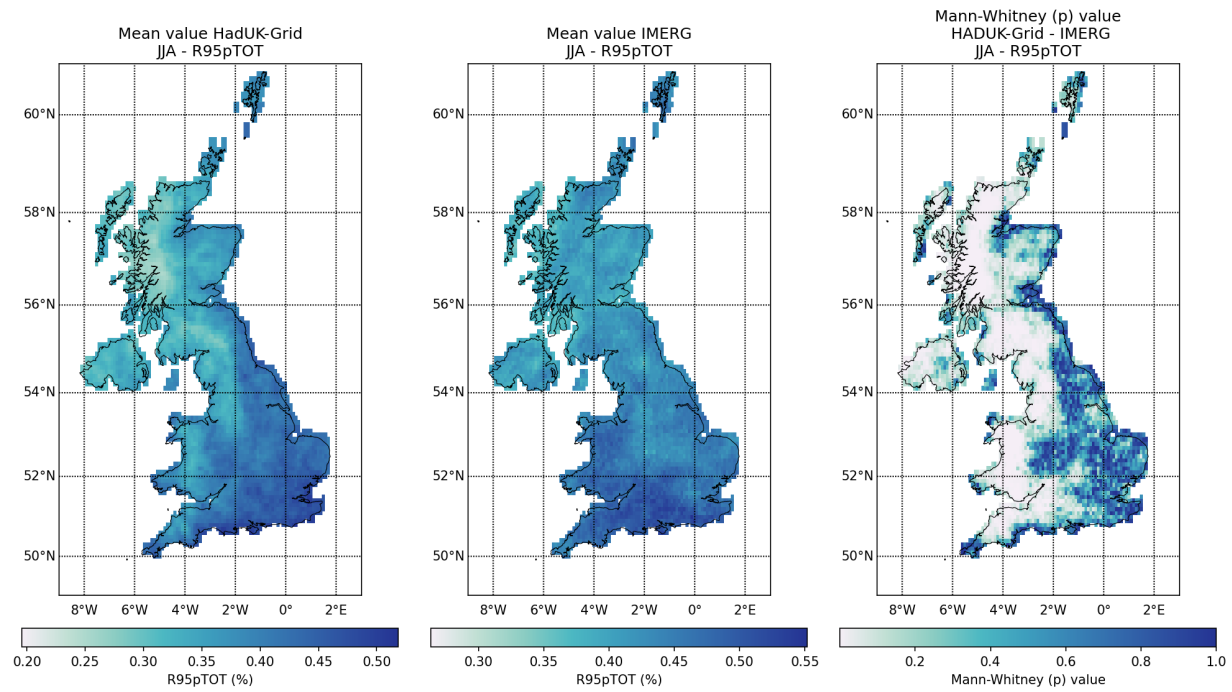


Figure 29: Spatial distribution of R95pTOT values obtained from HadUK-Grid and IMERG with Mann-Whitney test p value, Levene -center in the median- p value, and Pearson and Spearman correlation coefficient (r), for summer (JJA) over the 2001-2019 climatological period (cont.).

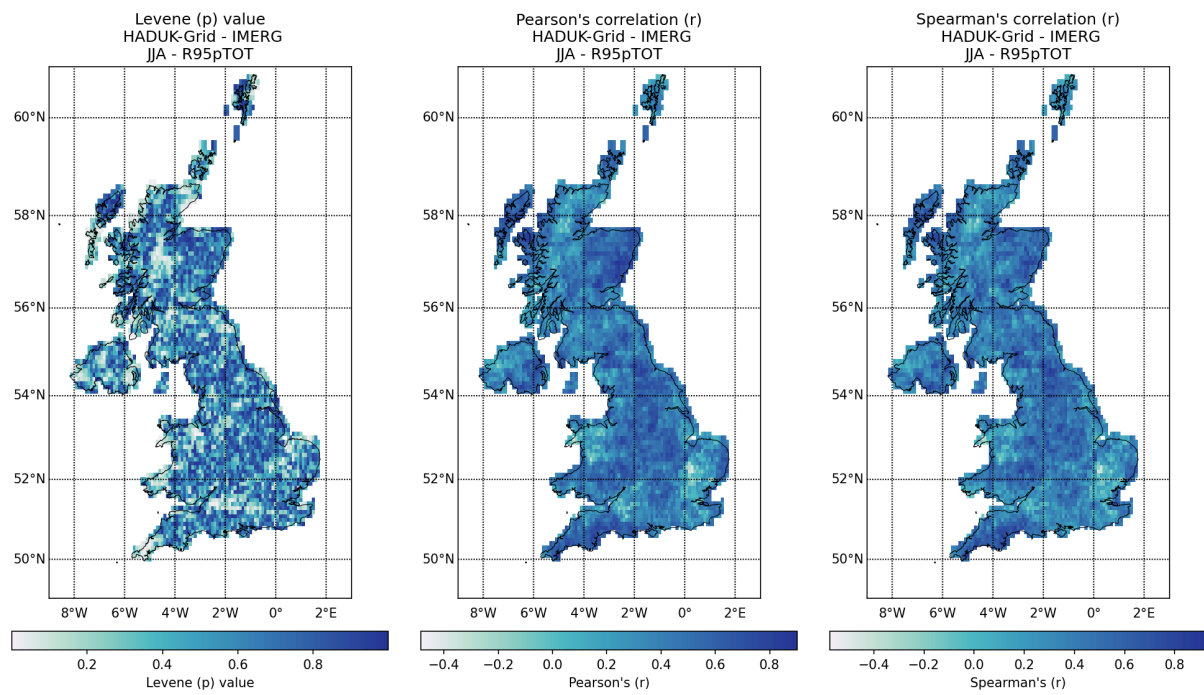


Figure 29: Spatial distribution of R95pTOT values obtained from HadUK-Grid and IMERG with Mann-Whitney test p value, Levene -center in the median- p value, and Pearson and Spearman correlation coefficient (r), for summer (JJA) over the 2001-2019 climatological period (cont.).

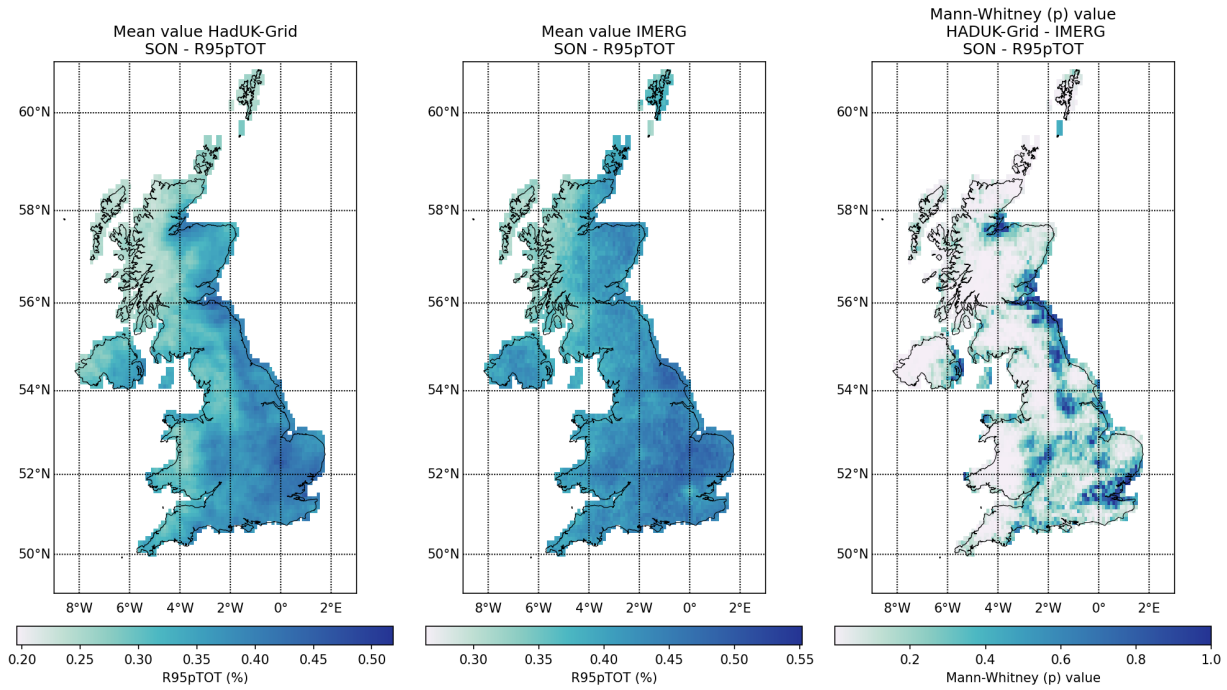


Figure 29: Spatial distribution of R95pTOT values obtained from HadUK-Grid and IMERG with Mann-Whitney test p value, Levene -center in the median- p value, and Pearson and Spearman correlation coefficient (r), for autumn (SON) over the 2001-2019 climatological period (cont.).

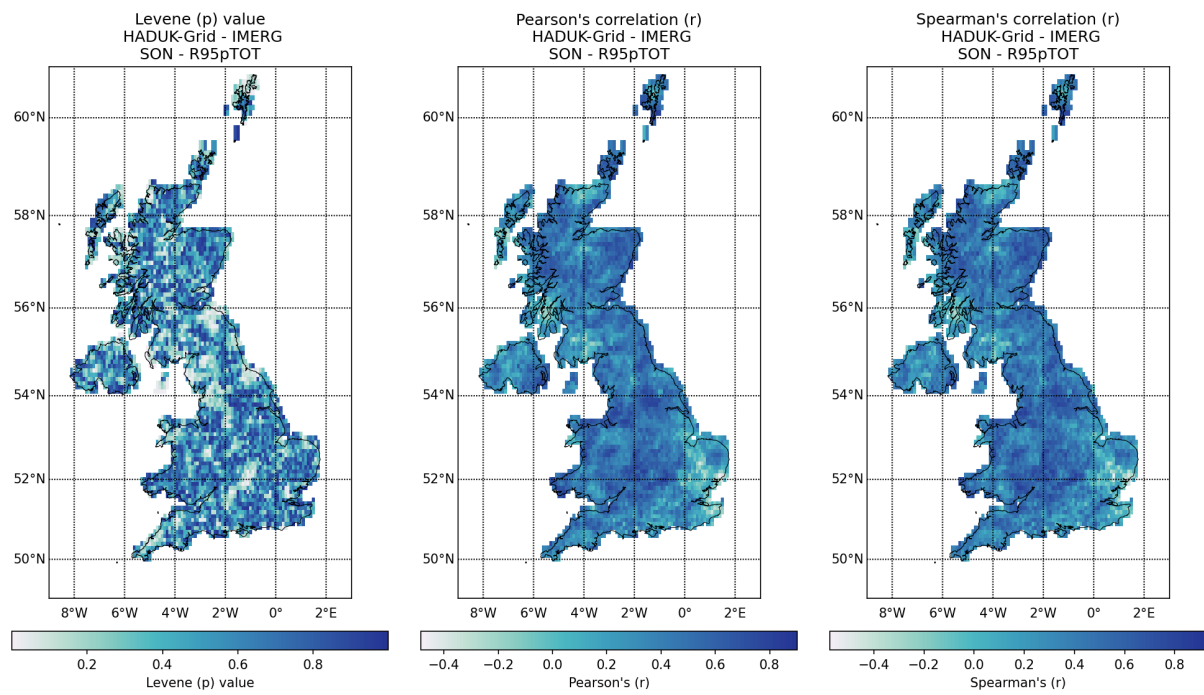


Figure 29: Spatial distribution of R95pTOT values obtained from HadUK-Grid and IMERG with Mann-Whitney test p value, Levene -center in the median- p value, and Pearson and Spearman correlation coefficient (r), for autumn (SON) over the 2001-2019 climatological period.

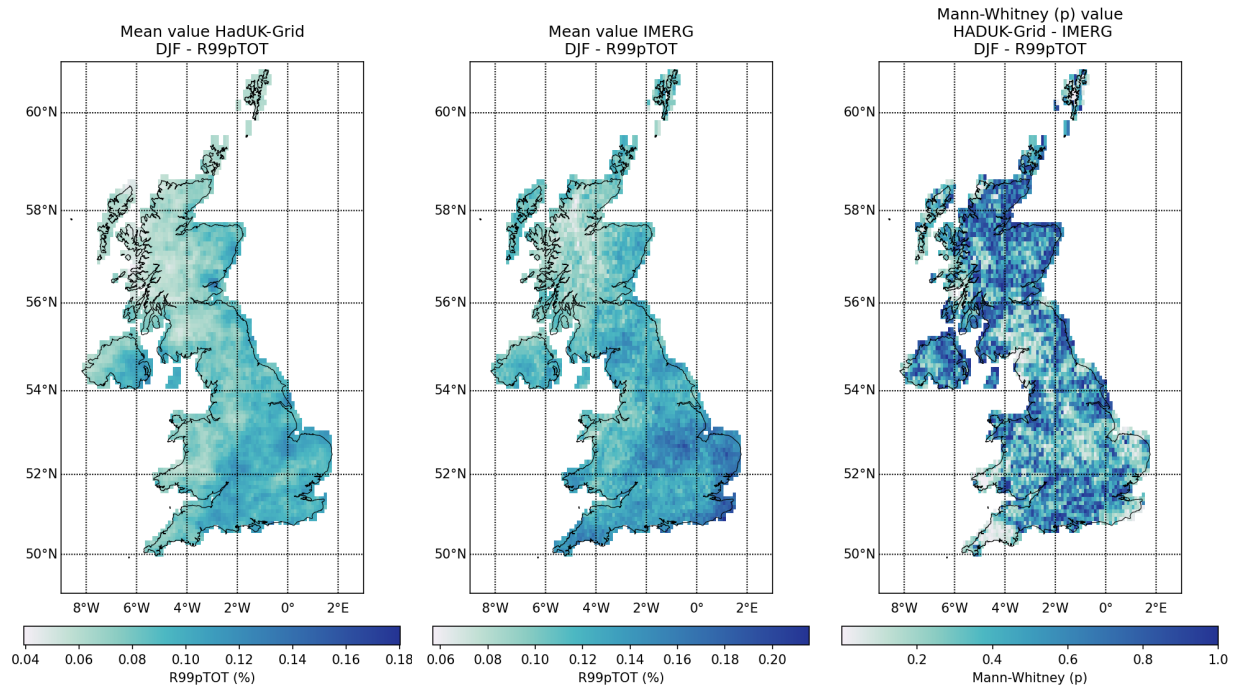


Figure 30: Spatial distribution of R99pTOT values obtained from HadUK-Grid and IMERG with Mann-Whitney test p value, Levene -center in the median- p value, and Pearson and Spearman correlation coefficient (r), for winter (DJF) over the 2001-2019 climatological period.

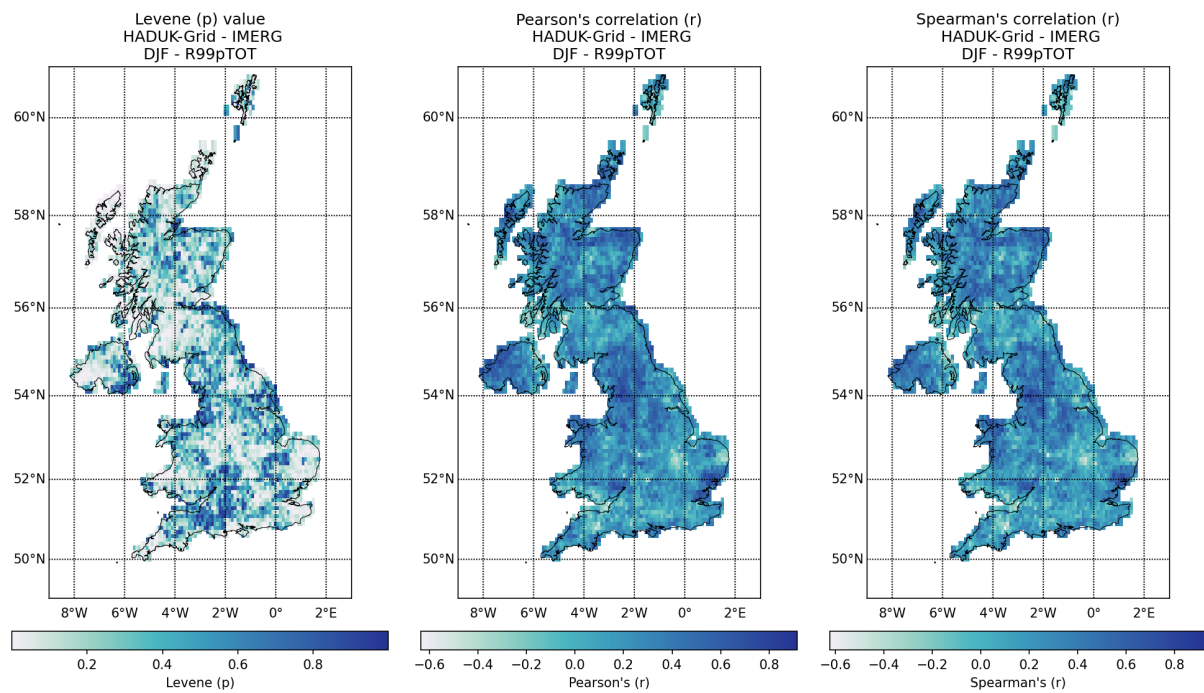


Figure 30: Spatial distribution of R99pTOT values obtained from HadUK-Grid and IMERG with Mann-Whitney test p value, Levene -center in the median- p value, and Pearson and Spearman correlation coefficient (r), for spring (DJF) over the 2001-2019 climatological period (cont.).

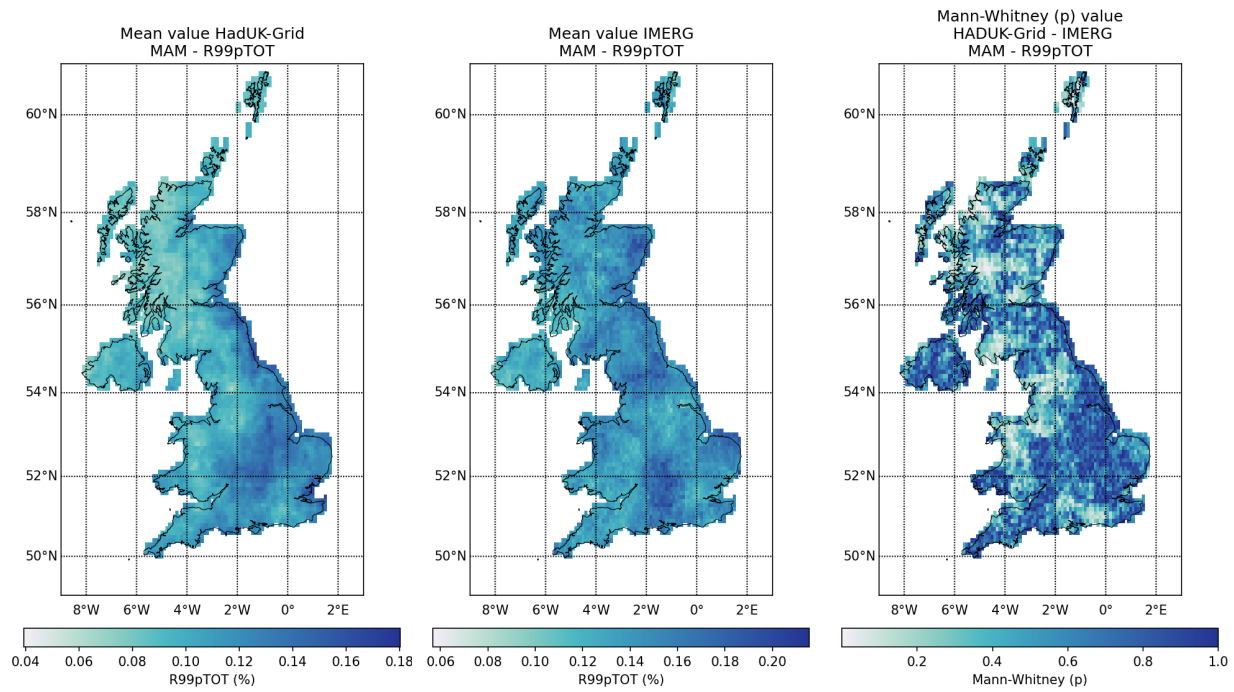


Figure 30: Spatial distribution of R99pTOT values obtained from HadUK-Grid and IMERG with Mann-Whitney test p value, Levene -center in the median- p value, and Pearson and Spearman correlation coefficient (r), for spring (MAM) over the 2001-2019 climatological period (cont.).

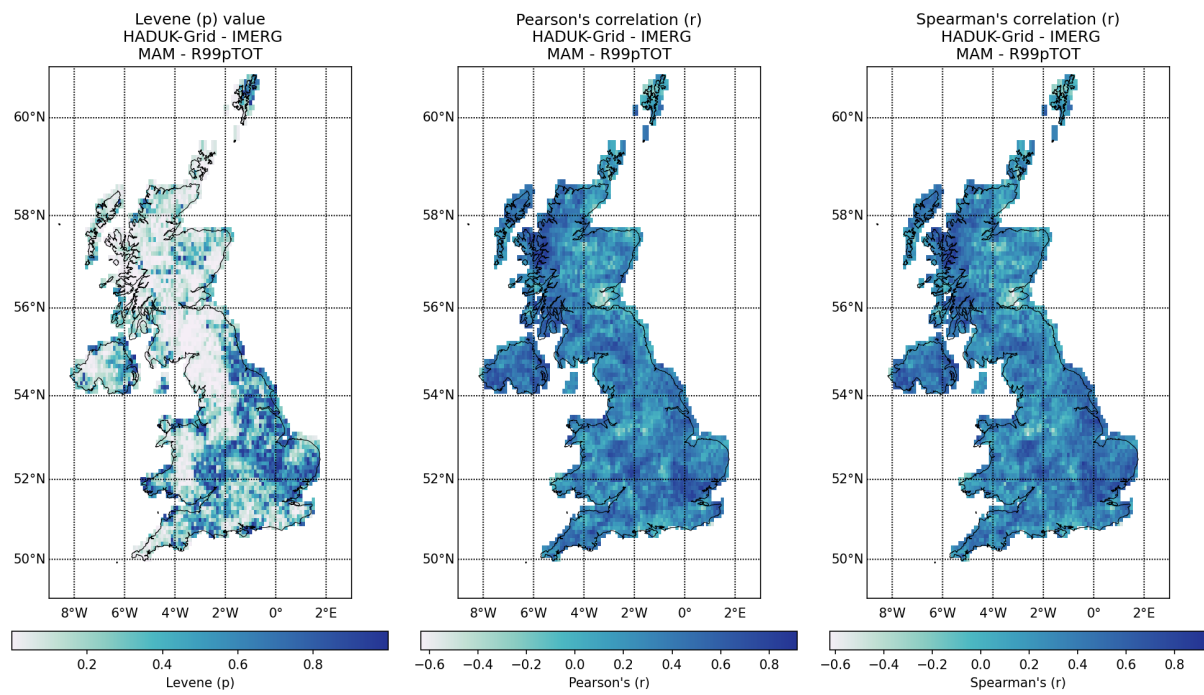


Figure 30: Spatial distribution of R99pTOT values obtained from HadUK-Grid and IMERG with Mann-Whitney test p value, Levene -center in the median- p value, and Pearson and Spearman correlation coefficient (r), for spring (MAM) over the 2001-2019 climatological period (cont.).

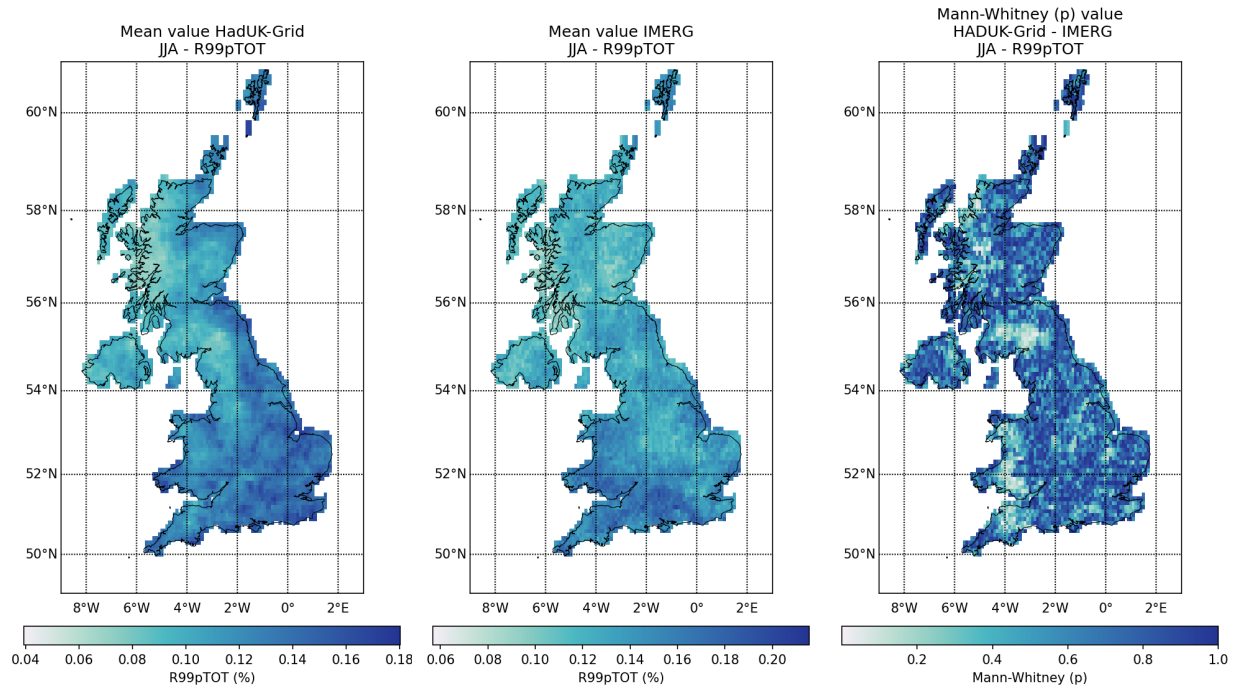


Figure 30: Spatial distribution of R99pTOT values obtained from HadUK-Grid and IMERG with Mann-Whitney test p value, Levene -center in the median- p value, and Pearson and Spearman correlation coefficient (r), for summer (JJA) over the 2001-2019 climatological period (cont.).

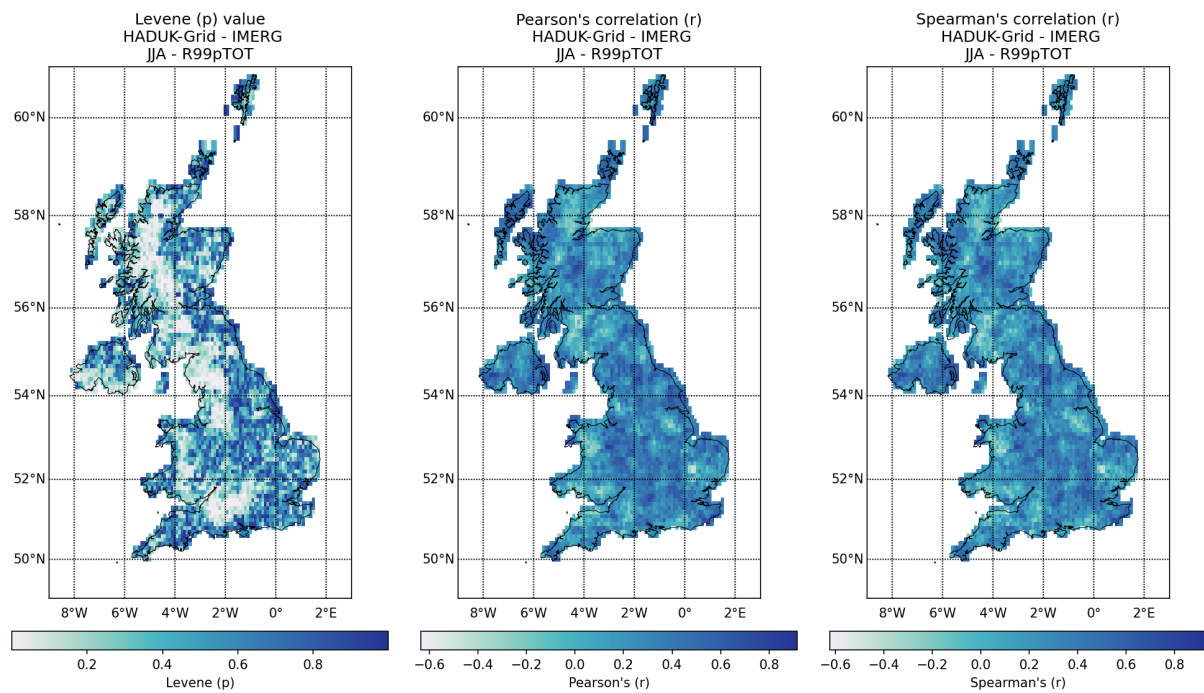


Figure 30: Spatial distribution of R99pTOT values obtained from HadUK-Grid and IMERG with Mann-Whitney test p value, Levene -center in the median- p value, and Pearson and Spearman correlation coefficient (r), for summer (JJA) over the 2001-2019 climatological period (cont.).

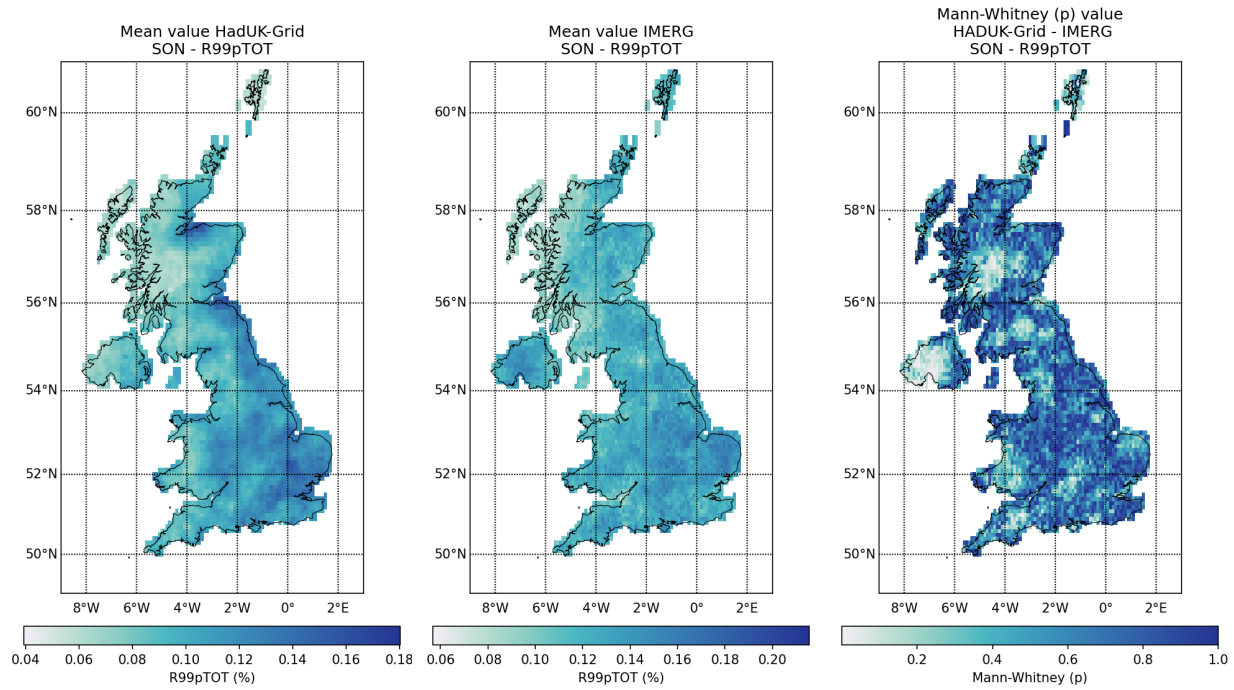


Figure 30: Spatial distribution of R99pTOT values obtained from HadUK-Grid and IMERG with Mann-Whitney test p value, Levene -center in the median- p value, and Pearson and Spearman correlation coefficient (r), for autumn (SON) over the 2001-2019 climatological period (cont.).

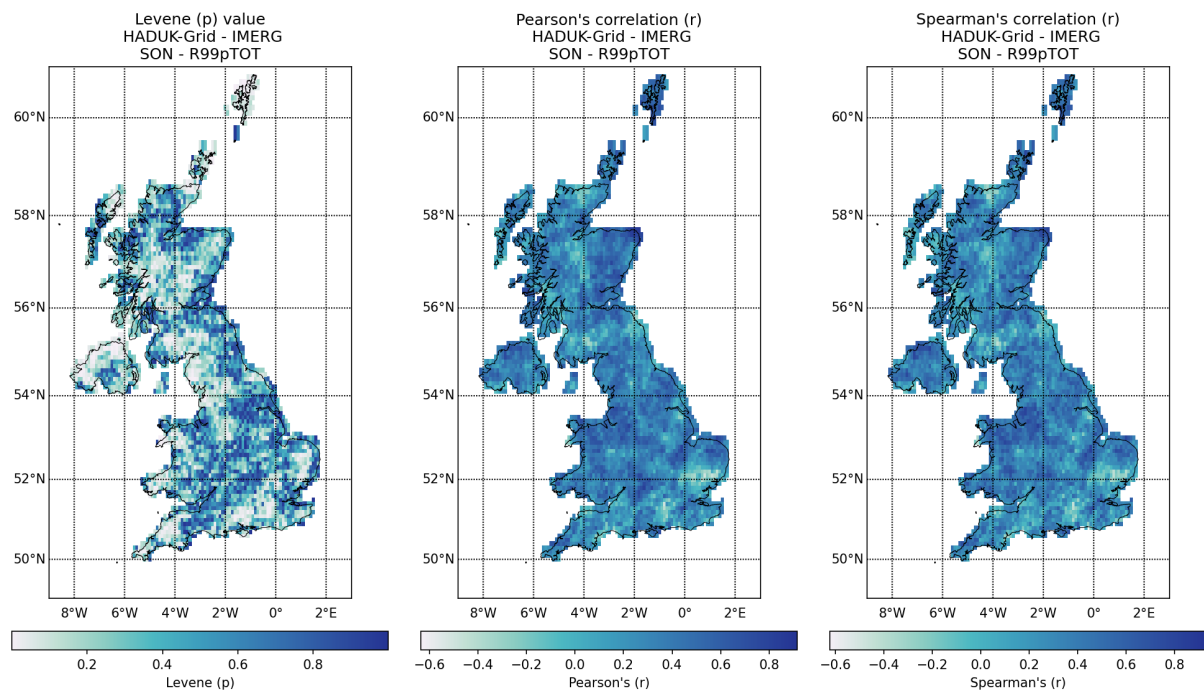


Figure 30: Spatial distribution of R99pTOT values obtained from HadUK-Grid and IMERG with Mann-Whitney test p value, Levene -center in the median- p value, and Pearson and Spearman correlation coefficient (r), for autumn (SON) over the 2001-2019 climatological period.

2.2.2 ERA5 DATA

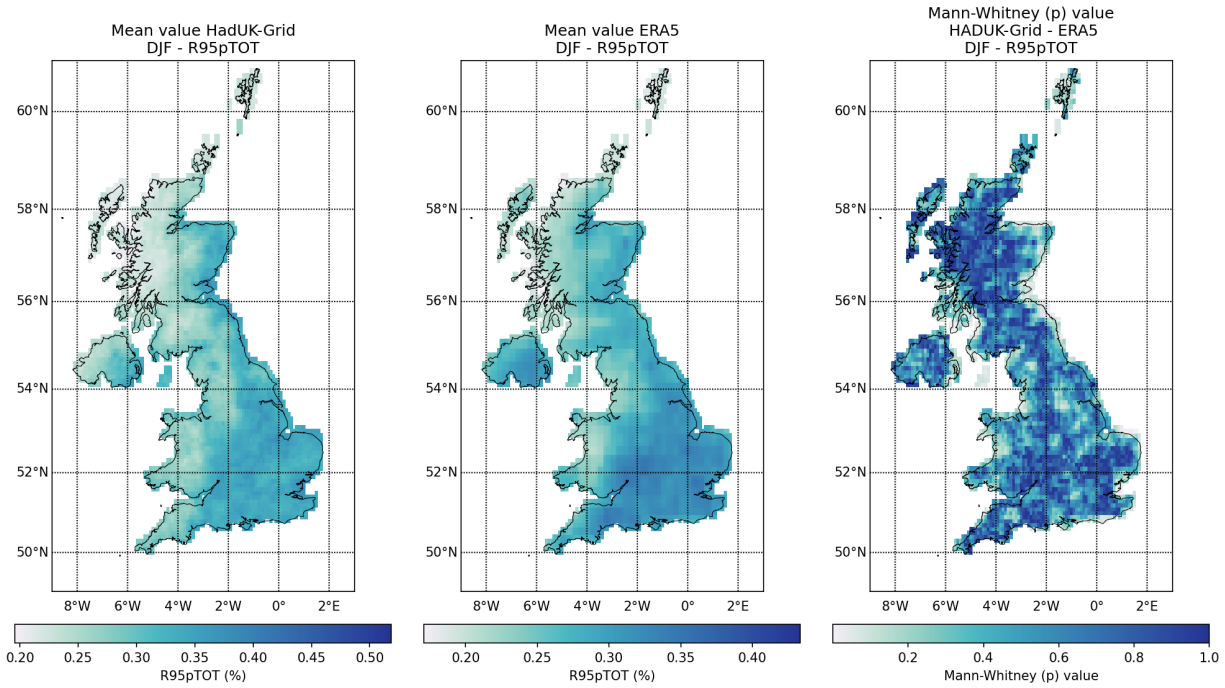


Figure 31: Spatial distribution of R95pTOT values obtained from HadUK-Grid and ERA5 with Mann-Whitney test p value, Levene -center in the median- p value, and Pearson and Spearman correlation coefficient (r), for winter (DJF) over the 2001-2019 climatological period.

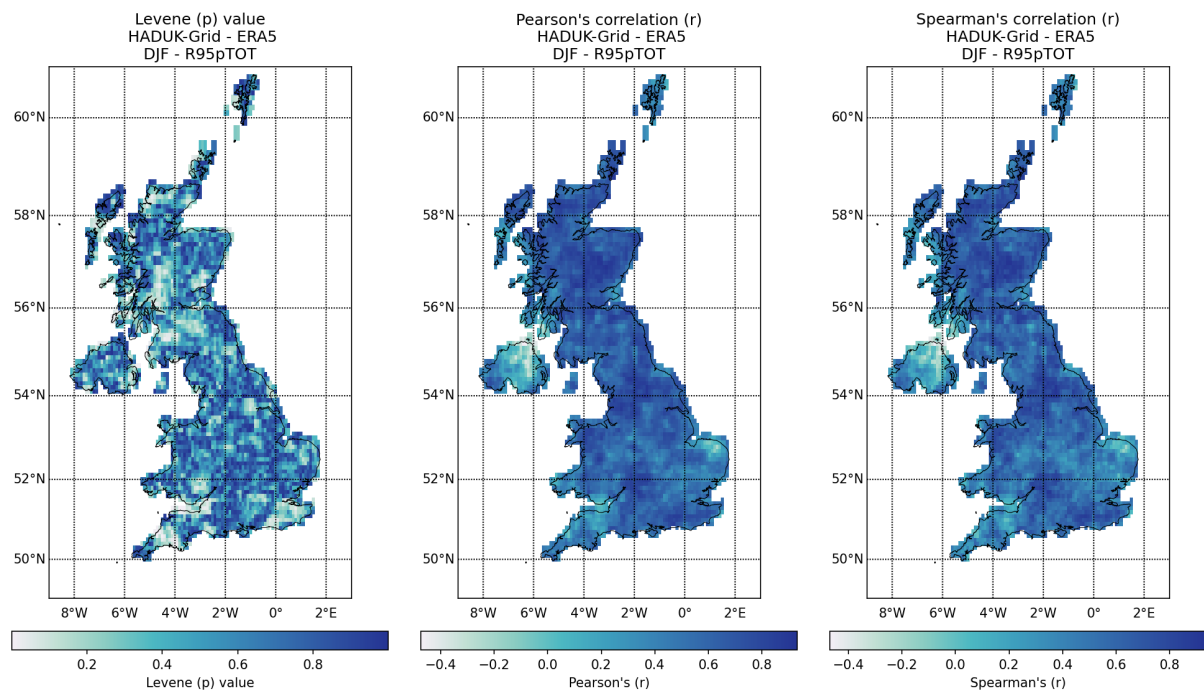


Figure 31: Spatial distribution of R95pTOT values obtained from HadUK-Grid and ERA5 with Mann-Whitney test p value, Levene -center in the median- p value, and Pearson and Spearman correlation coefficient (r), for spring (DJF) over the 2001-2019 climatological period (cont.).

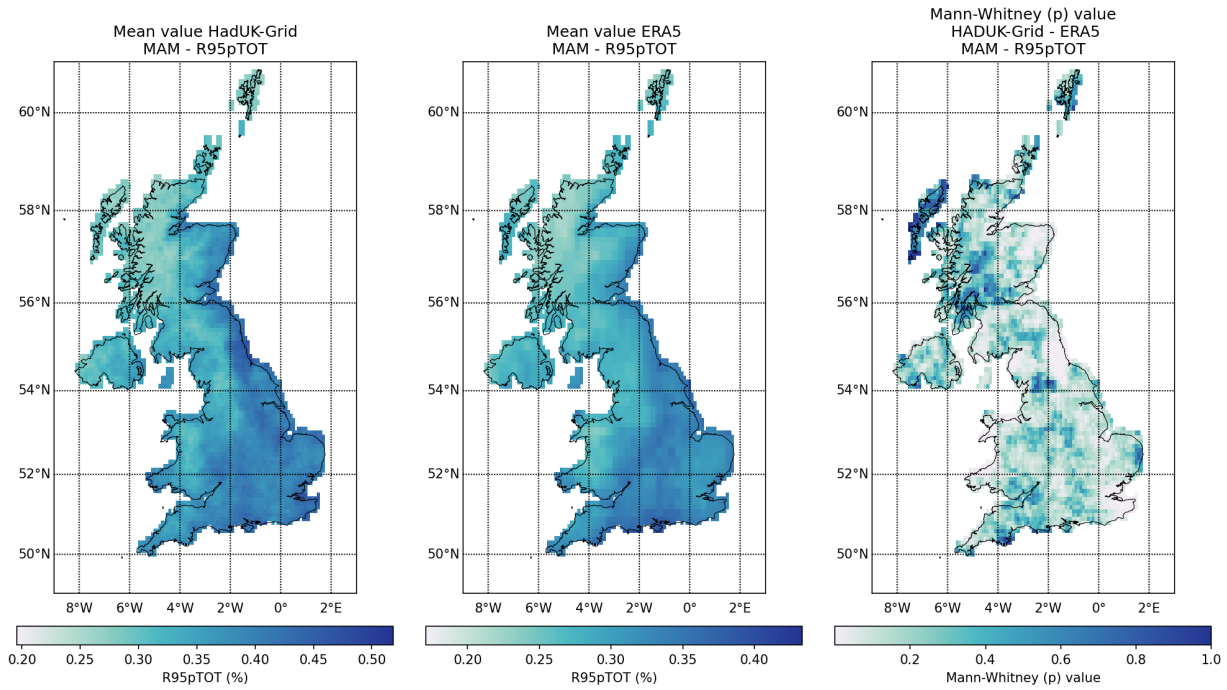


Figure 31: Spatial distribution of R95pTOT values obtained from HadUK-Grid and ERA5 with Mann-Whitney test p value, Levene -center in the median- p value, and Pearson and Spearman correlation coefficient (r), for spring (MAM) over the 2001-2019 climatological period (cont.).

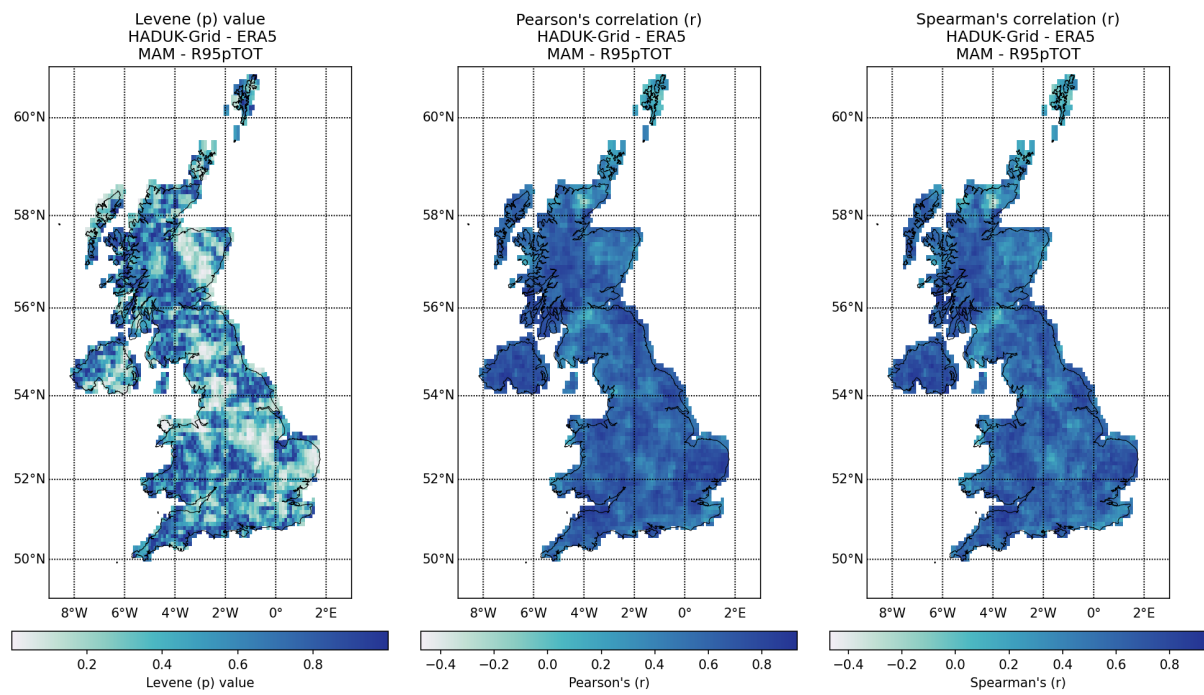


Figure 31: Spatial distribution of R95pTOT values obtained from HadUK-Grid and ERA5 with Mann-Whitney test p value, Levene -center in the median- p value, and Pearson and Spearman correlation coefficient (r), for spring (MAM) over the 2001-2019 climatological period (cont.).

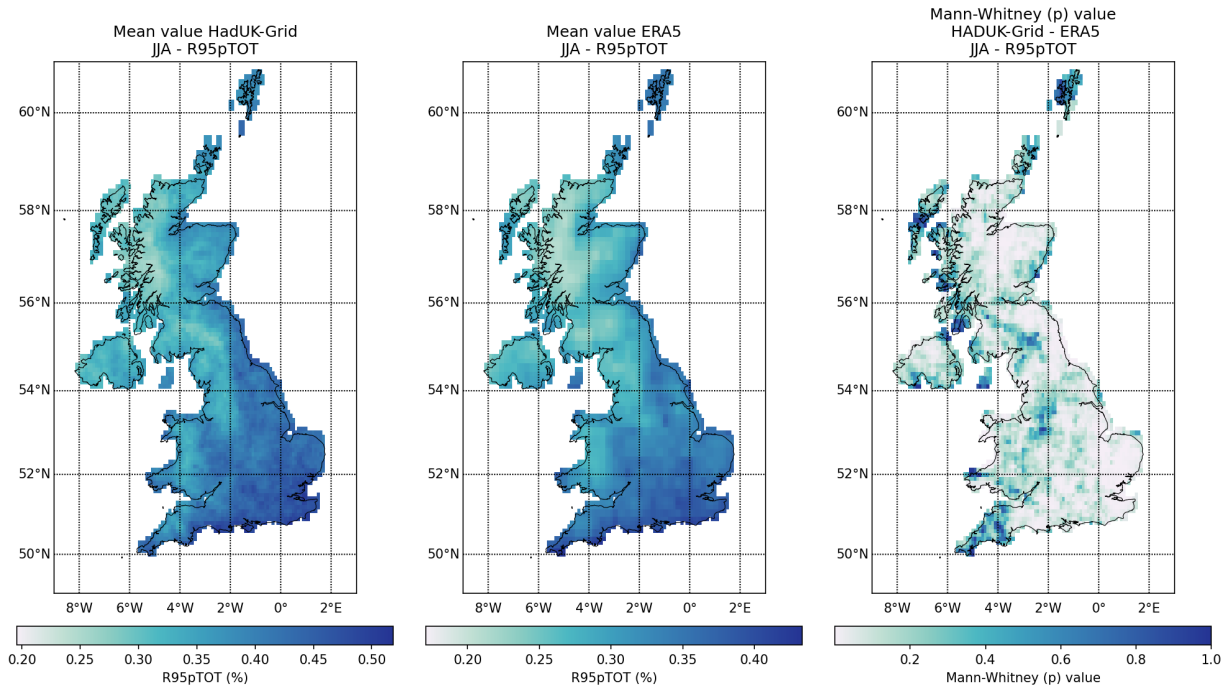


Figure 31: Spatial distribution of R95pTOT values obtained from HadUK-Grid and ERA5 with Mann-Whitney test p value, Levene -center in the median- p value, and Pearson and Spearman correlation coefficient (r), for summer (JJA) over the 2001-2019 climatological period (cont.).

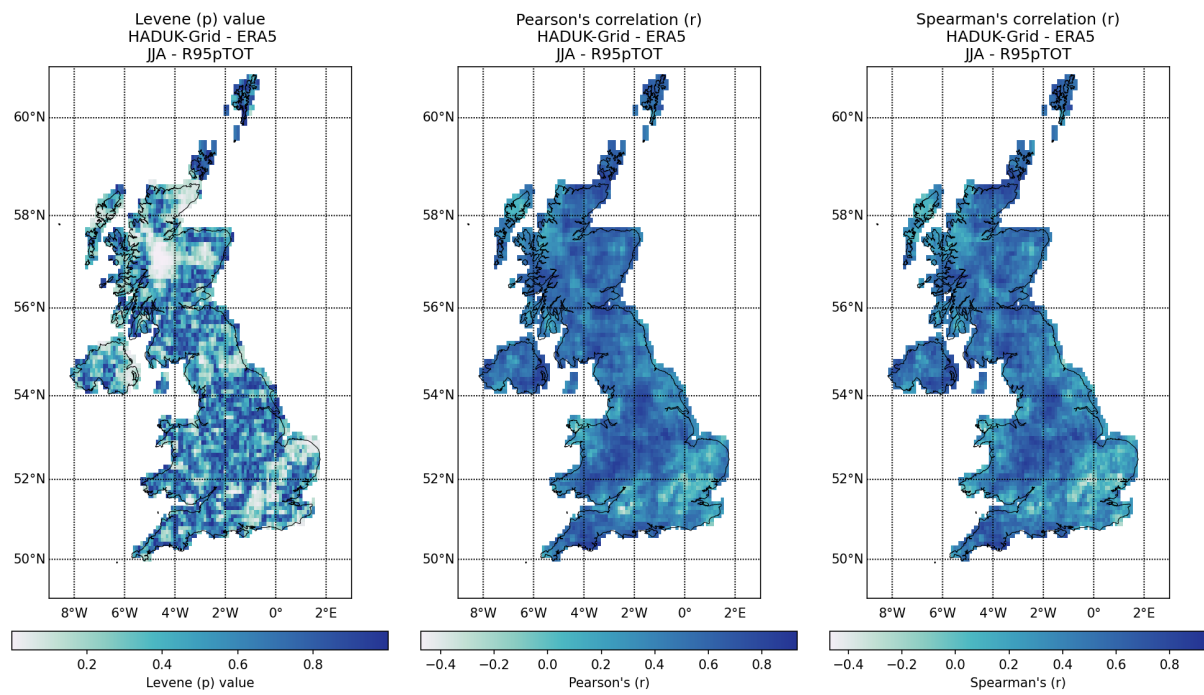


Figure 31: Spatial distribution of R95pTOT values obtained from HadUK-Grid and ERA5 with Mann-Whitney test p value, Levene -center in the median- p value, and Pearson and Spearman correlation coefficient (r), for summer (JJA) over the 2001-2019 climatological period (cont.).

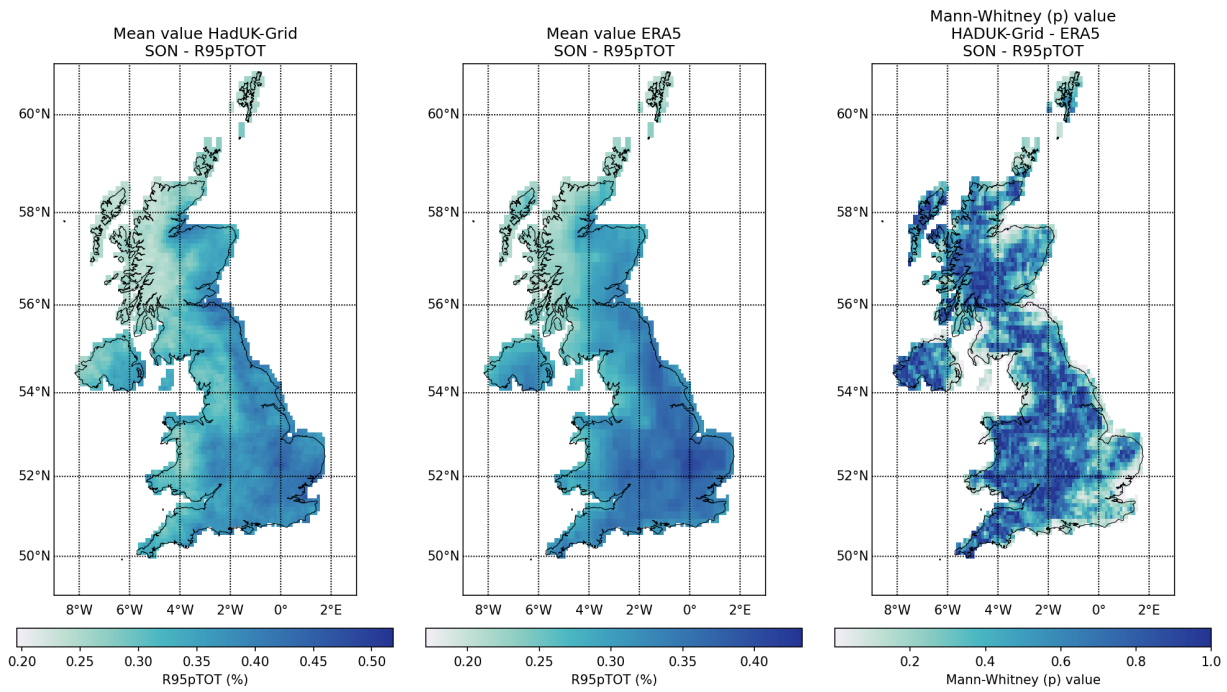


Figure 31: Spatial distribution of R95pTOT values obtained from HadUK-Grid and ERA5 with Mann-Whitney test p value, Levene -center in the median- p value, and Pearson and Spearman correlation coefficient (r), for autumn (SON) over the 2001-2019 climatological period (cont.).

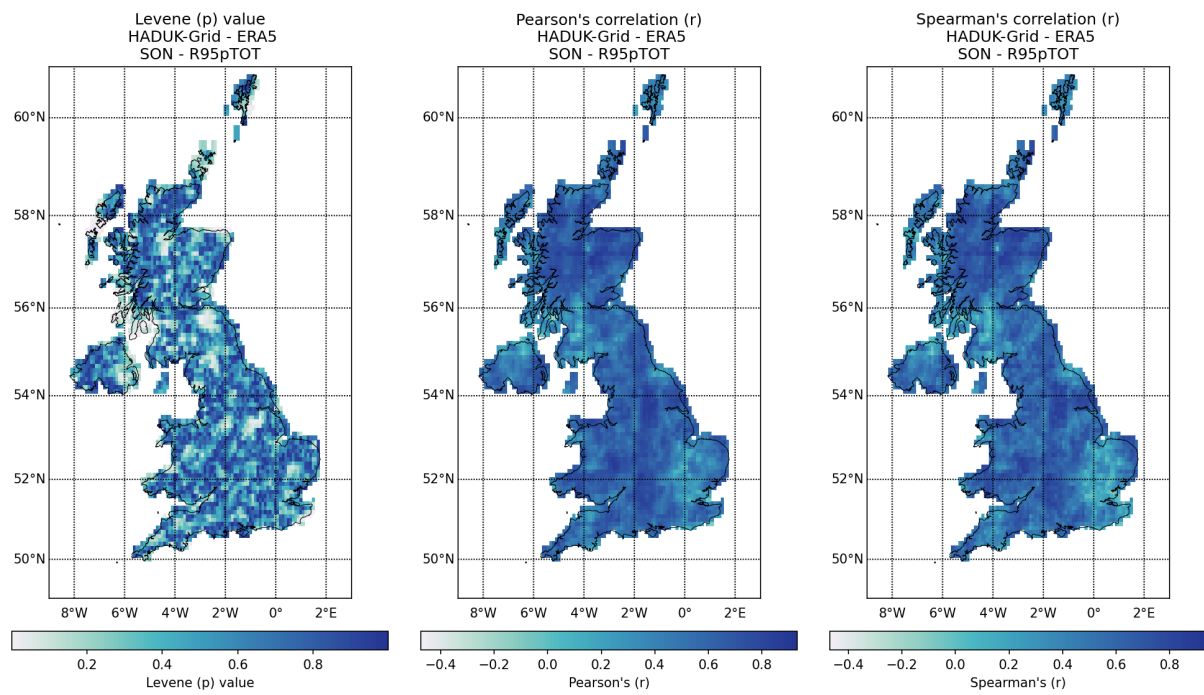


Figure 31: Spatial distribution of R95pTOT values obtained from HadUK-Grid and ERA5 with Mann-Whitney test p value, Levene -center in the median- p value, and Pearson and Spearman correlation coefficient (r), for autumn (SON) over the 2001-2019 climatological period.

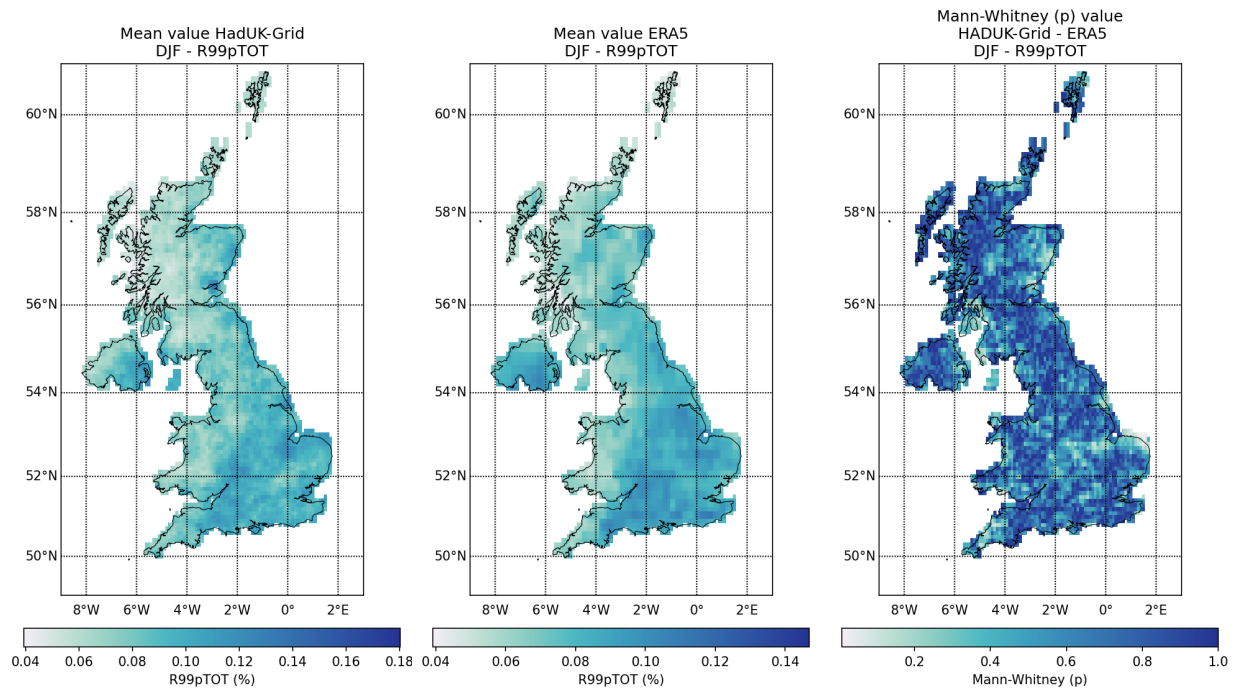


Figure 32: Spatial distribution of R99pTOT values obtained from HadUK-Grid and ERA5 with Mann-Whitney test p value, Levene -center in the median- p value, and Pearson and Spearman correlation coefficient (r), for winter (DJF) over the 2001-2019 climatological period.

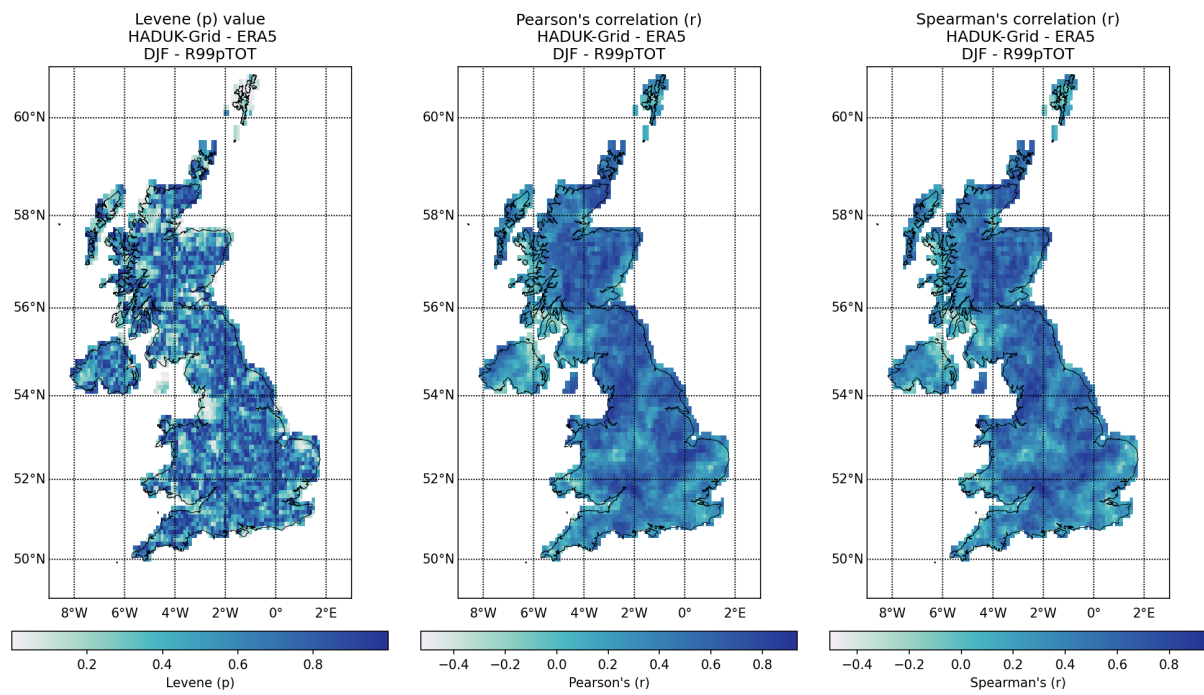


Figure 32: Spatial distribution of R99pTOT values obtained from HadUK-Grid and ERA5 with Mann-Whitney test p value, Levene -center in the median- p value, and Pearson and Spearman correlation coefficient (r), for spring (DJF) over the 2001-2019 climatological period (cont.).

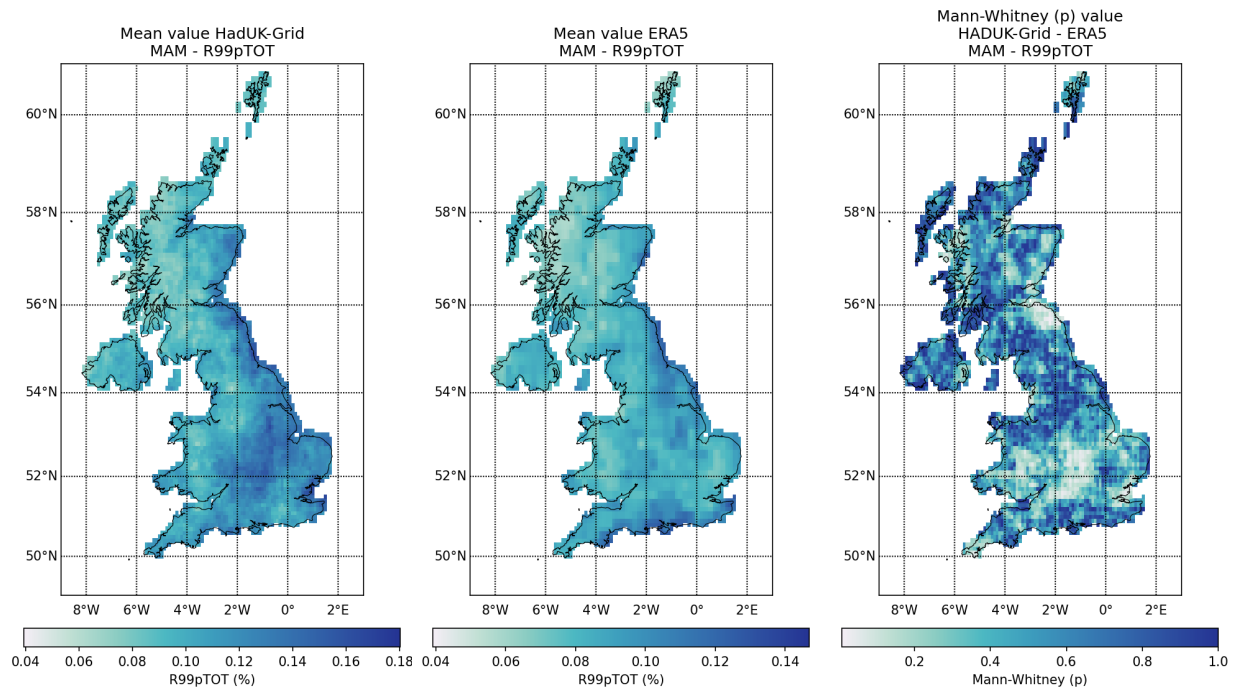


Figure 32: Spatial distribution of R99pTOT values obtained from HadUK-Grid and ERA5 with Mann-Whitney test p value, Levene -center in the median- p value, and Pearson and Spearman correlation coefficient (r), for spring (MAM) over the 2001-2019 climatological period (cont.).

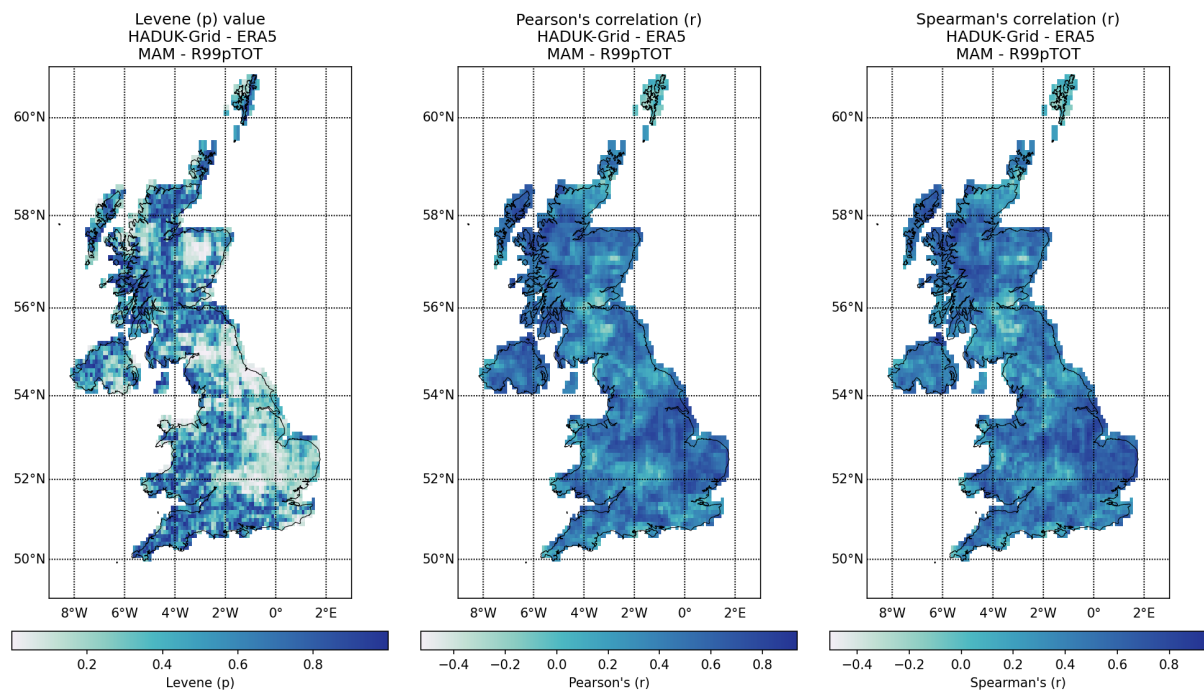


Figure 32: Spatial distribution of R99pTOT values obtained from HadUK-Grid and ERA5 with Mann-Whitney test p value, Levene -center in the median- p value, and Pearson and Spearman correlation coefficient (r), for spring (MAM) over the 2001-2019 climatological period (cont.).

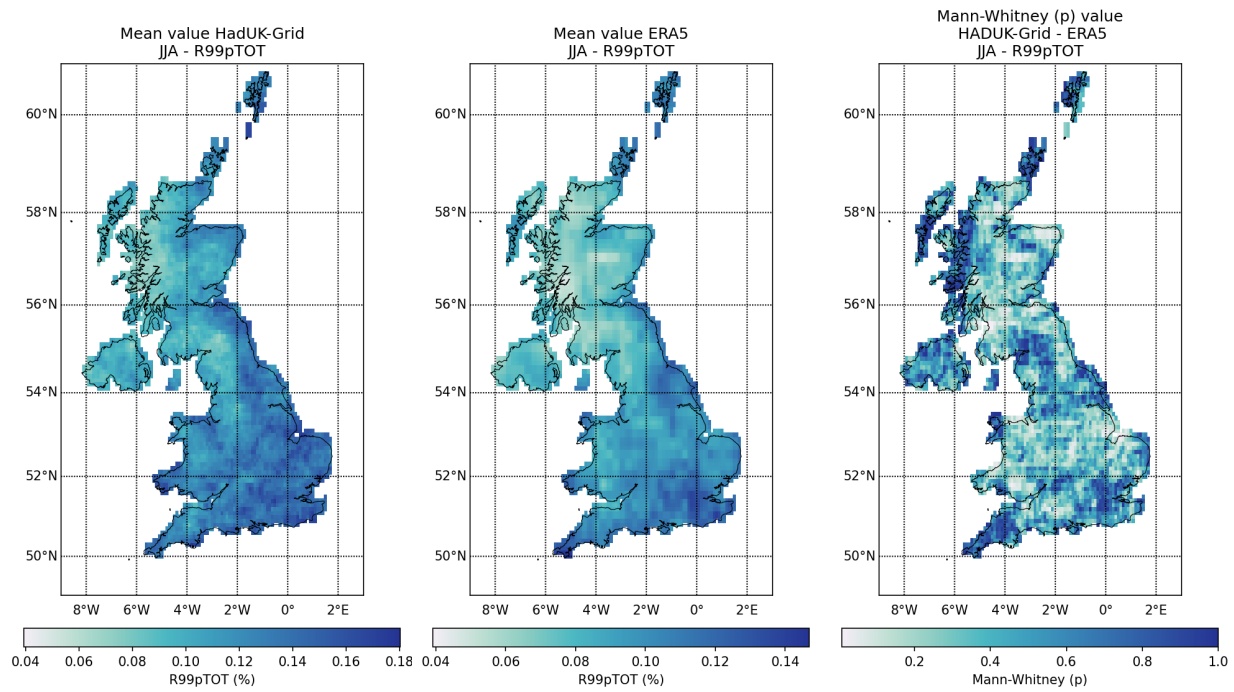


Figure 32: Spatial distribution of R99pTOT values obtained from HadUK-Grid and ERA5 with Mann-Whitney test p value, Levene -center in the median- p value, and Pearson and Spearman correlation coefficient (r), for summer (JJA) over the 2001-2019 climatological period (cont.).

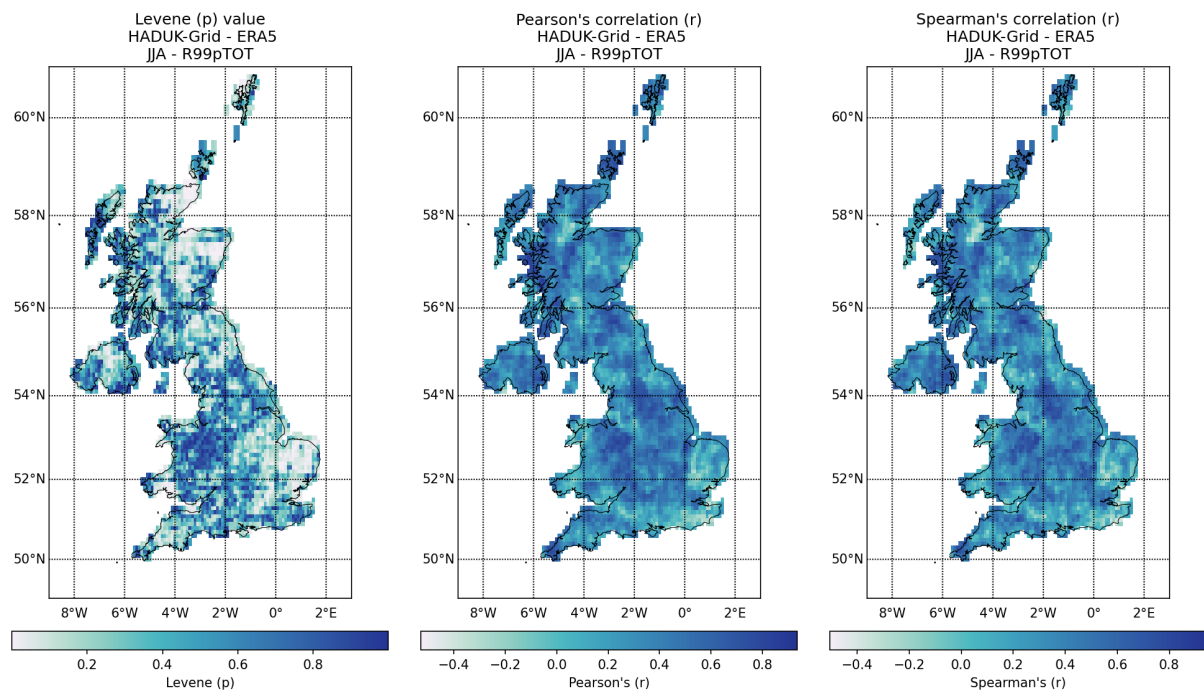


Figure 32: Spatial distribution of R99pTOT values obtained from HadUK-Grid and ERA5 with Mann-Whitney test p value, Levene -center in the median- p value, and Pearson and Spearman correlation coefficient (r), for summer (JJA) over the 2001-2019 climatological period (cont.).

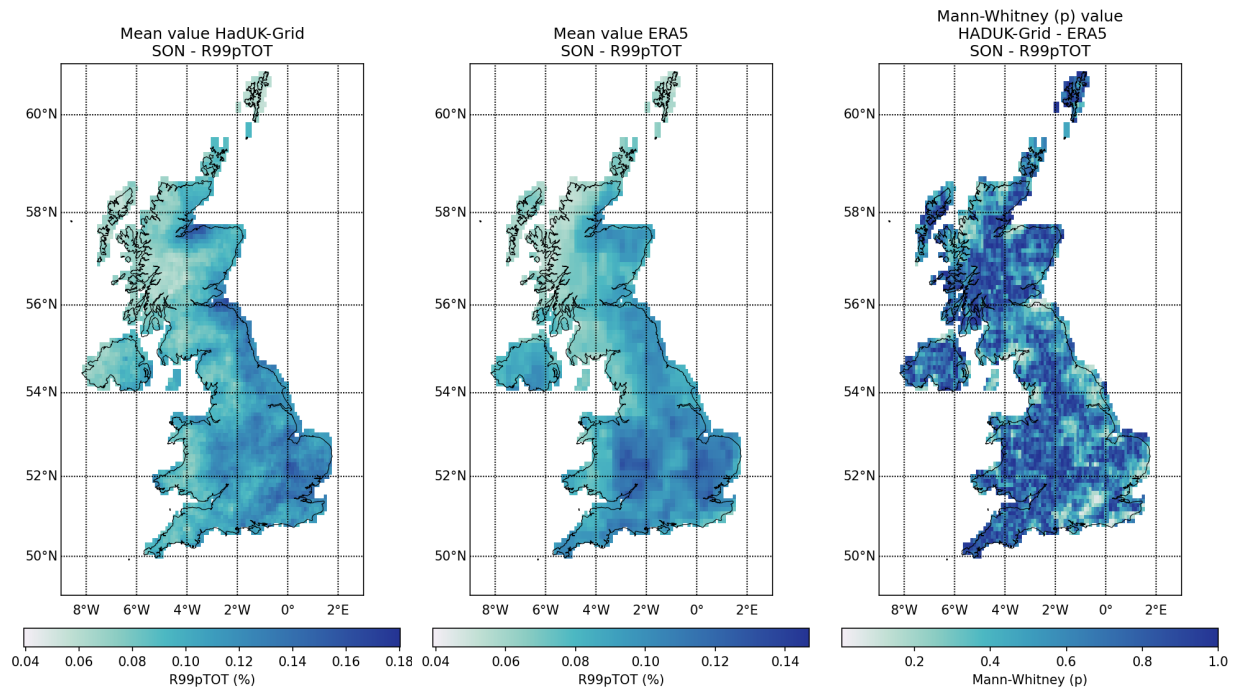


Figure 32: Spatial distribution of R99pTOT values obtained from HadUK-Grid and ERA5 with Mann-Whitney test p value, Levene -center in the median- p value, and Pearson and Spearman correlation coefficient (r), for autumn (SON) over the 2001-2019 climatological period (cont.).

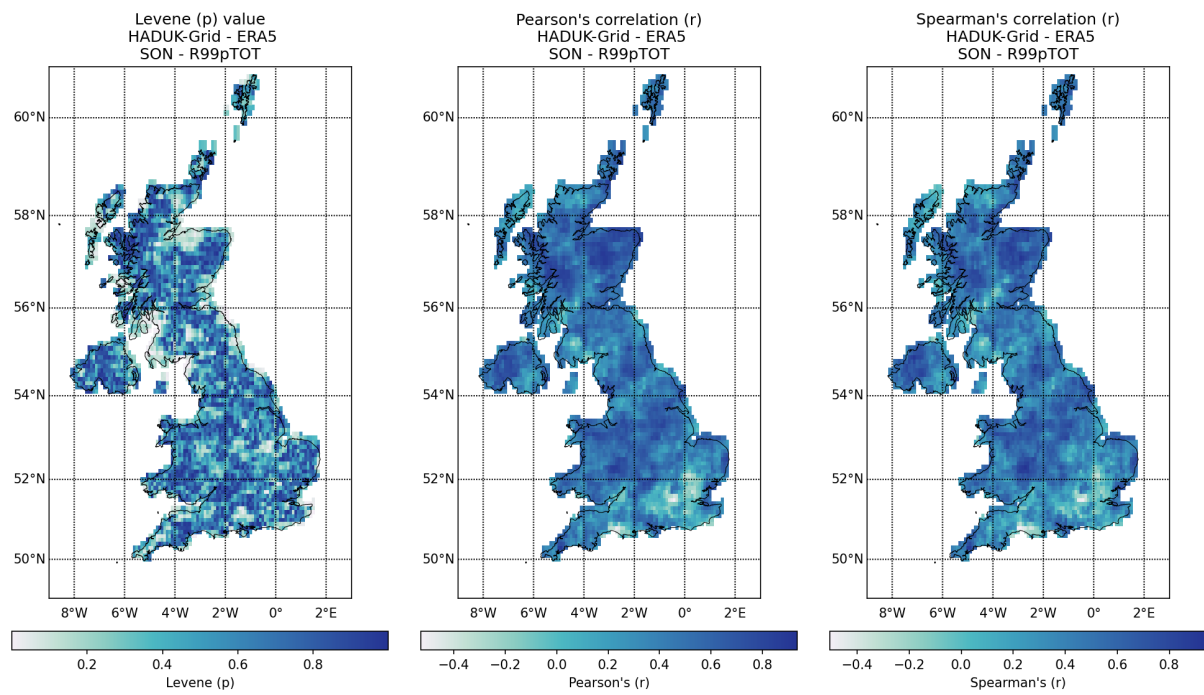


Figure 32: Spatial distribution of R99pTOT values obtained from HadUK-Grid and ERA5 with Mann-Whitney test p value, Levene -center in the median- p value, and Pearson and Spearman correlation coefficient (r), for autumn (SON) over the 2001-2019 climatological period.

2.3 Non-Threshold Indices - PRCPTOT, RX1day, RX5day, SDII

2.3.1 IMERG DATA

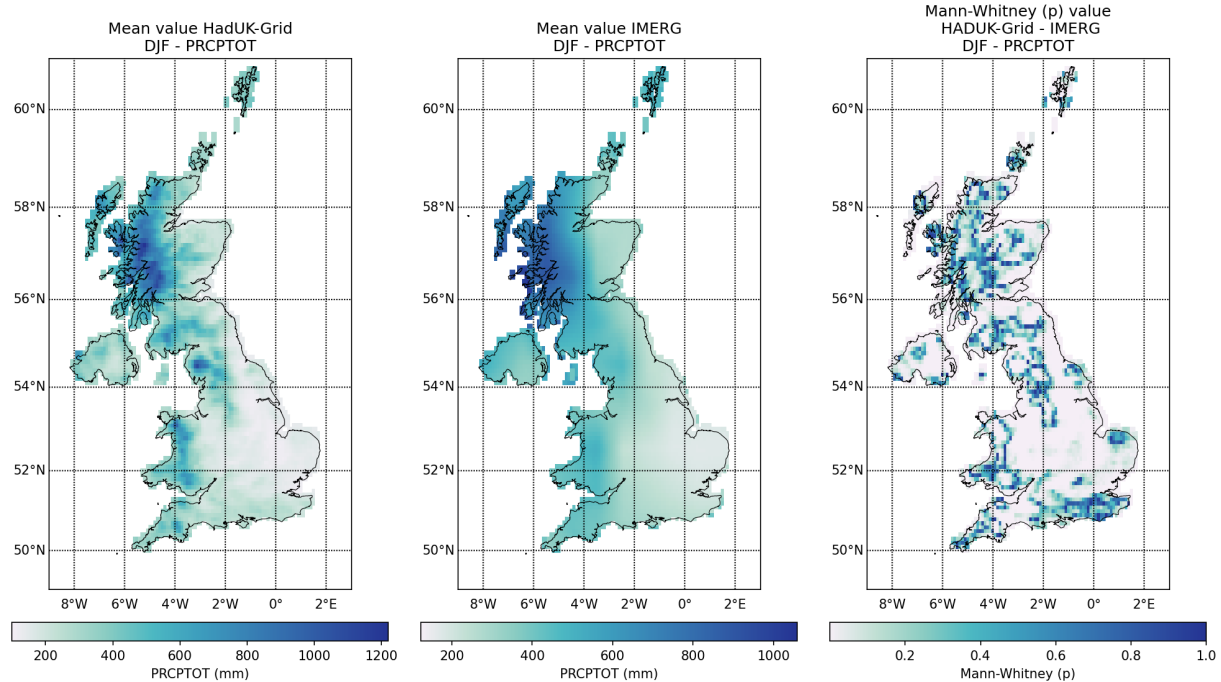


Figure 33: Spatial distribution of PRCPTOT values obtained from HadUK-Grid and IMERG with Mann-Whitney test p value, Levene -center in the median- p value, and Pearson and Spearman correlation coefficient (r), for winter (DJF) over the 2001-2019 climatological period.

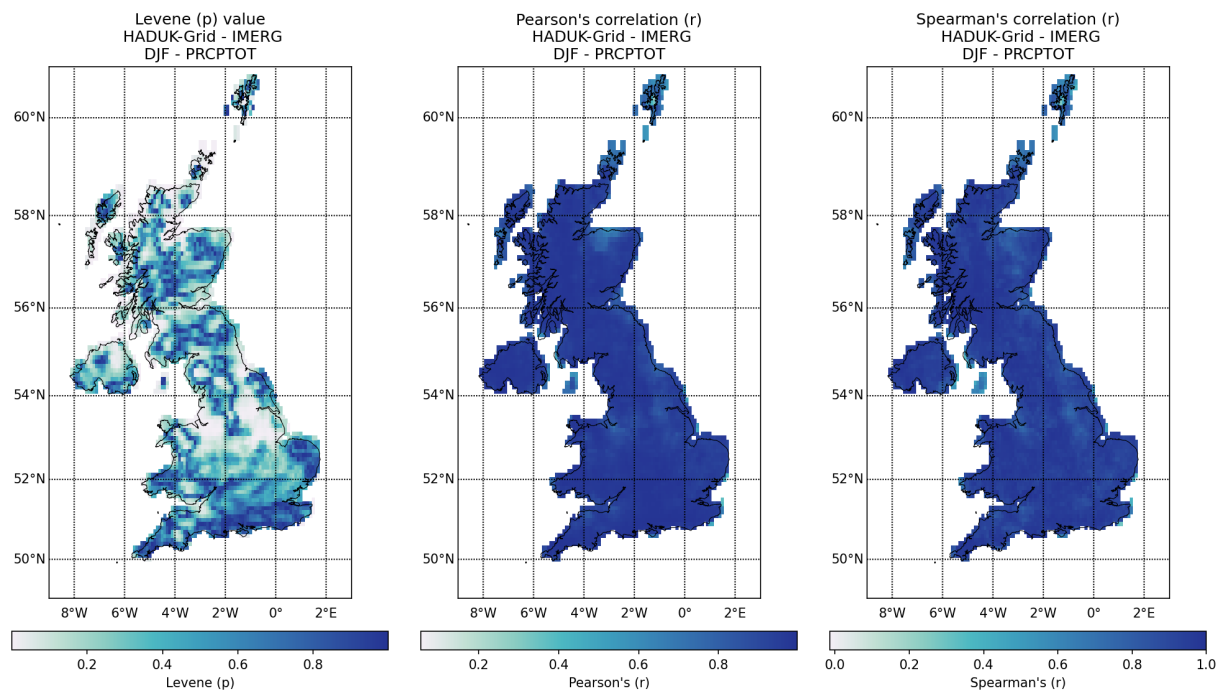


Figure 33: Spatial distribution of PRCPTOT values obtained from HadUK-Grid and IMERG with Mann-Whitney test p value, Levene -center in the median- p value, and Pearson and Spearman correlation coefficient (r), for spring (DJF) over the 2001-2019 climatological period (cont.).

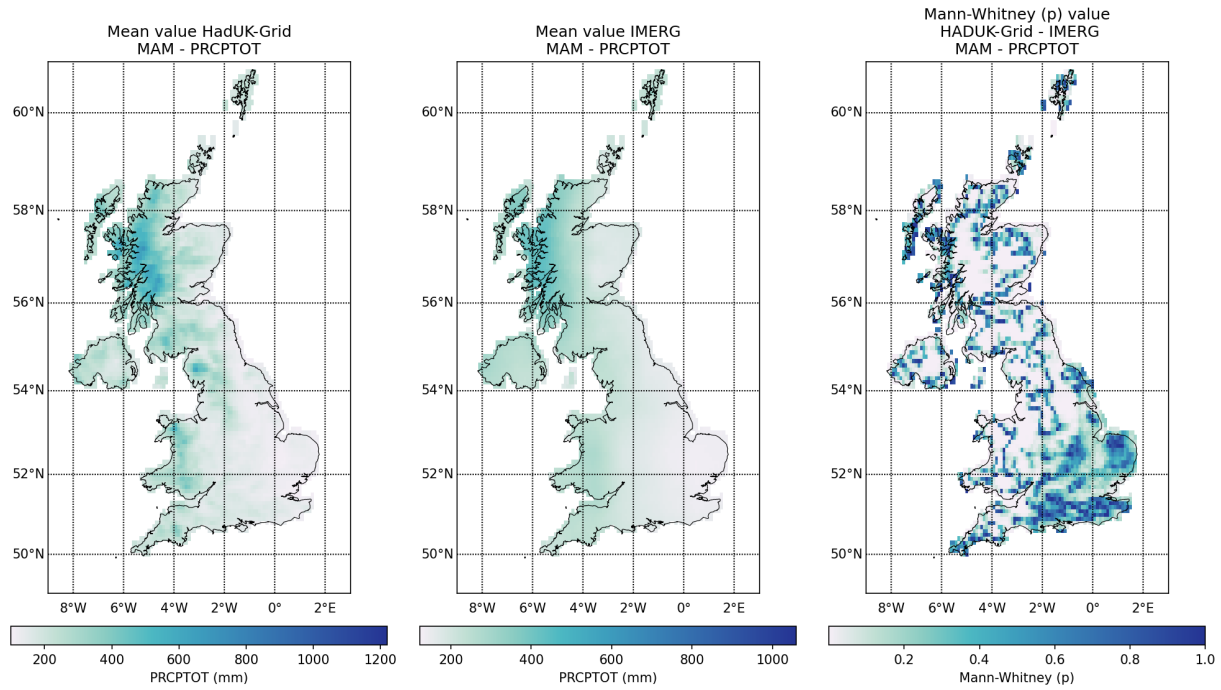


Figure 33: Spatial distribution of PRCPTOT values obtained from HadUK-Grid and IMERG with Mann-Whitney test p value, Levene -center in the median- p value, and Pearson and Spearman correlation coefficient (r), for spring (MAM) over the 2001-2019 climatological period (cont.).

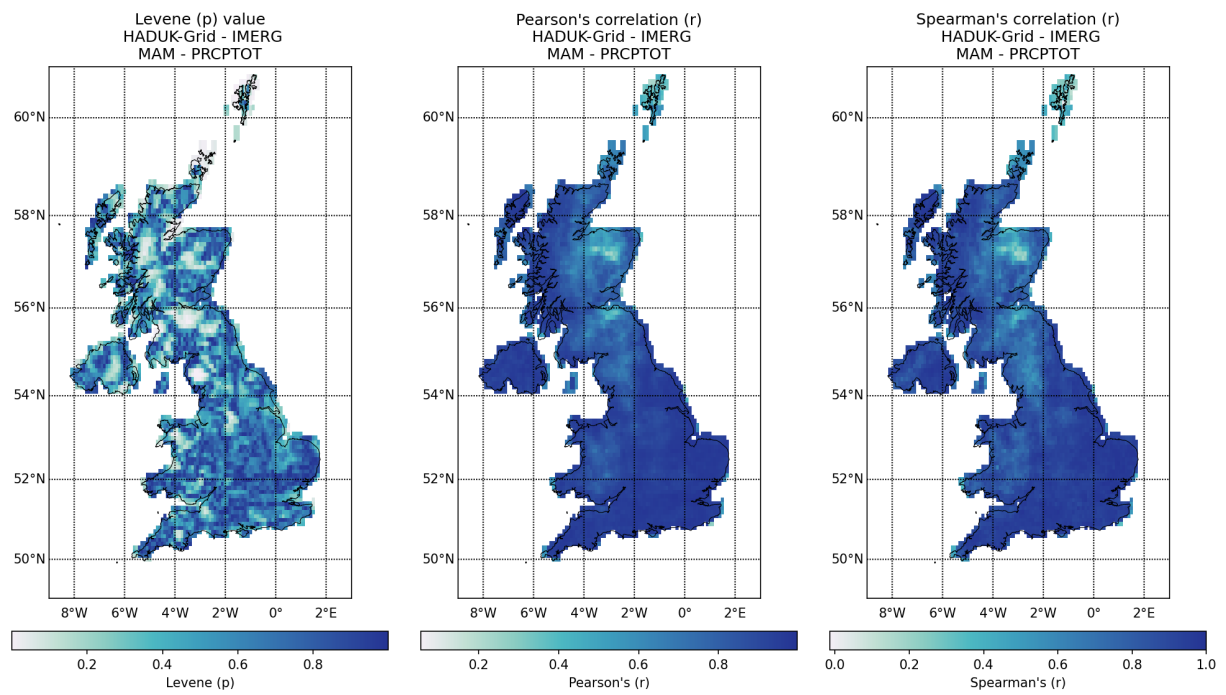


Figure 33: Spatial distribution of PRCPTOT values obtained from HadUK-Grid and IMERG with Mann-Whitney test p value, Levene -center in the median- p value, and Pearson and Spearman correlation coefficient (r), for spring (MAM) over the 2001-2019 climatological period (cont.).

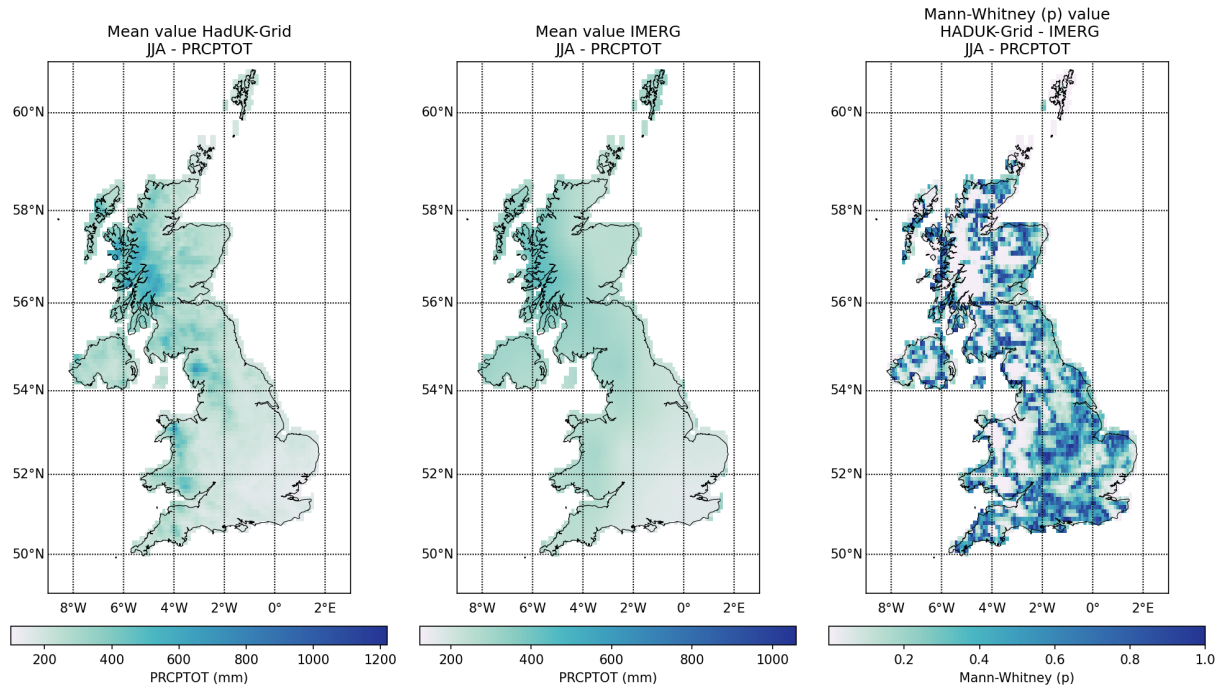


Figure 33: Spatial distribution of PRCPTOT values obtained from HadUK-Grid and IMERG with Mann-Whitney test p value, Levene -center in the median- p value, and Pearson and Spearman correlation coefficient (r), for summer (JJA) over the 2001-2019 climatological period (cont.).

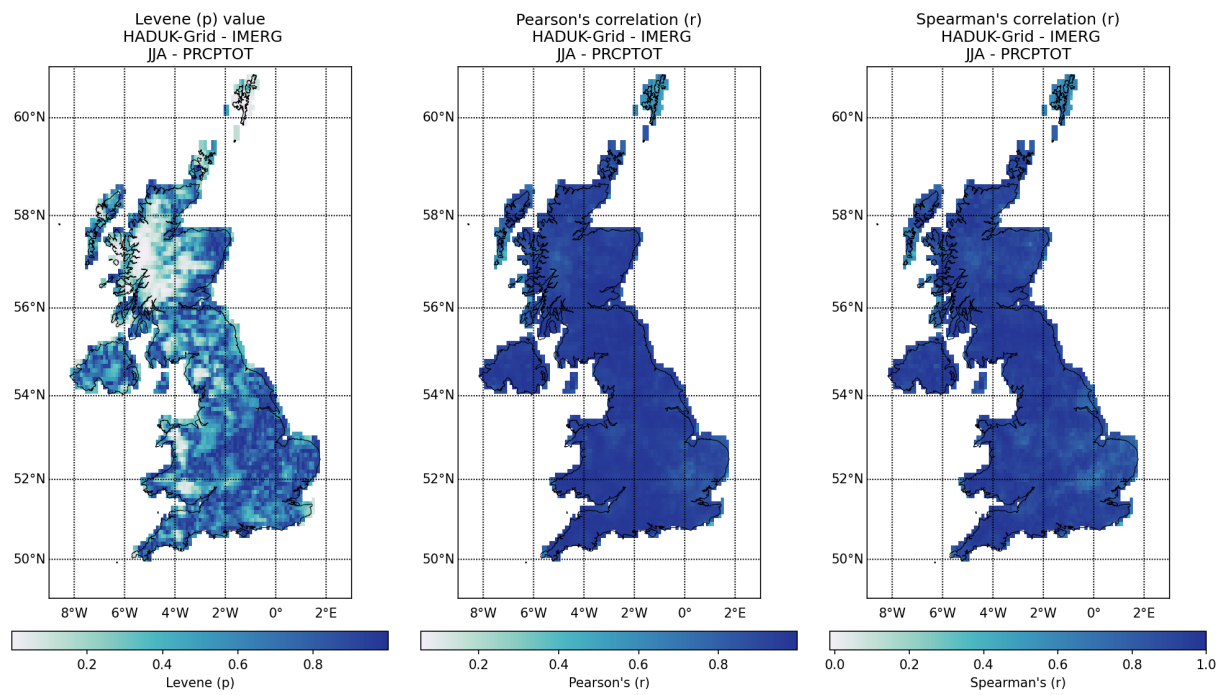


Figure 33: Spatial distribution of PRCPTOT values obtained from HadUK-Grid and IMERG with Mann-Whitney test p value, Levene -center in the median- p value, and Pearson and Spearman correlation coefficient (r), for summer (JJA) over the 2001-2019 climatological period (cont.).

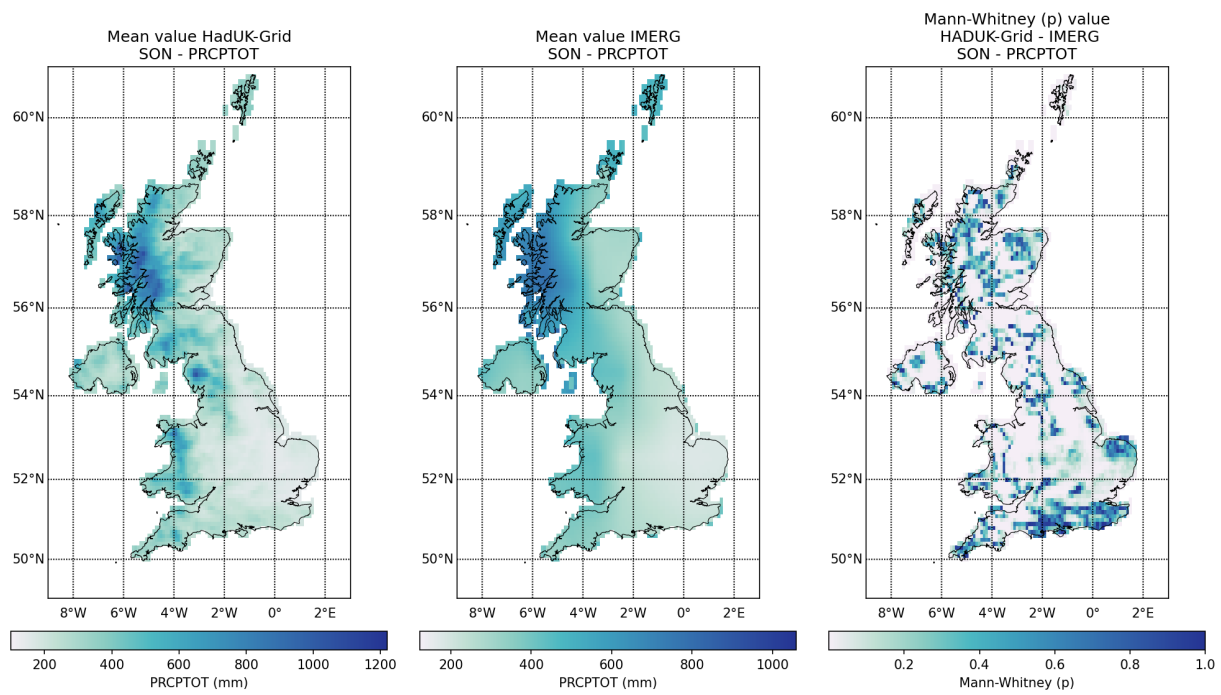


Figure 33: Spatial distribution of PRCPTOT values obtained from HadUK-Grid and IMERG with Mann-Whitney test p value, Levene -center in the median- p value, and Pearson and Spearman correlation coefficient (r), for autumn (SON) over the 2001-2019 climatological period (cont.).

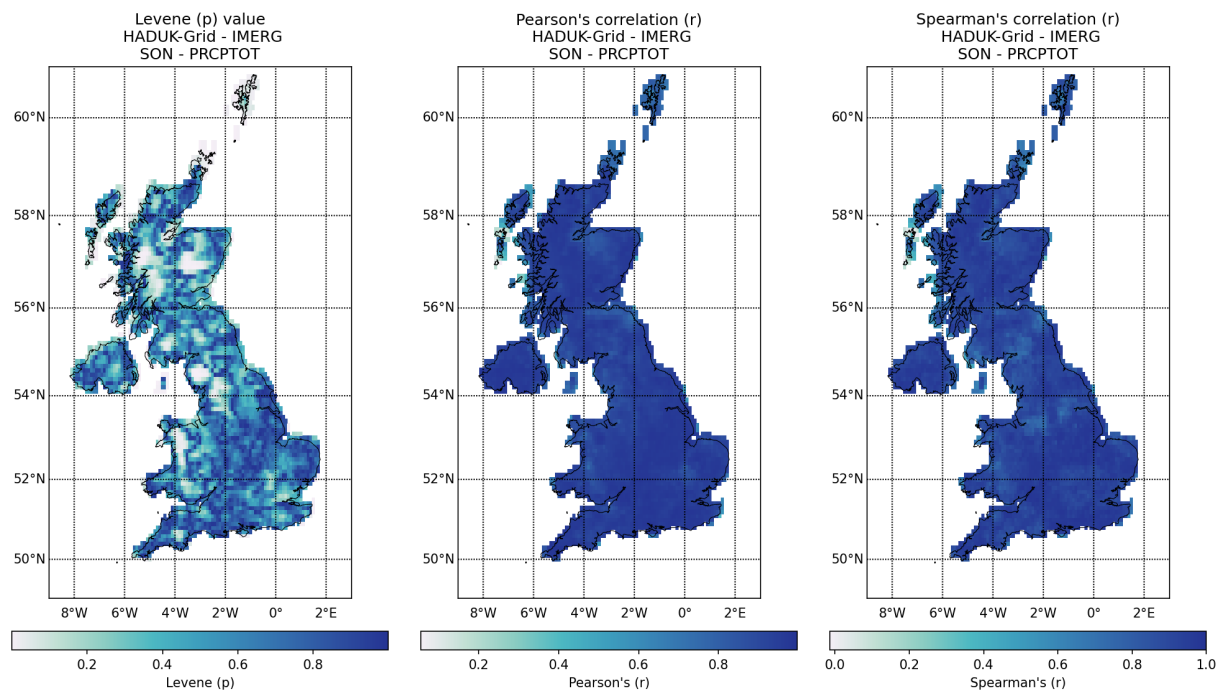


Figure 33: Spatial distribution of PRCPTOT values obtained from HadUK-Grid and IMERG with Mann-Whitney test p value, Levene -center in the median- p value, and Pearson and Spearman correlation coefficient (r), for autumn (SON) over the 2001-2019 climatological period.

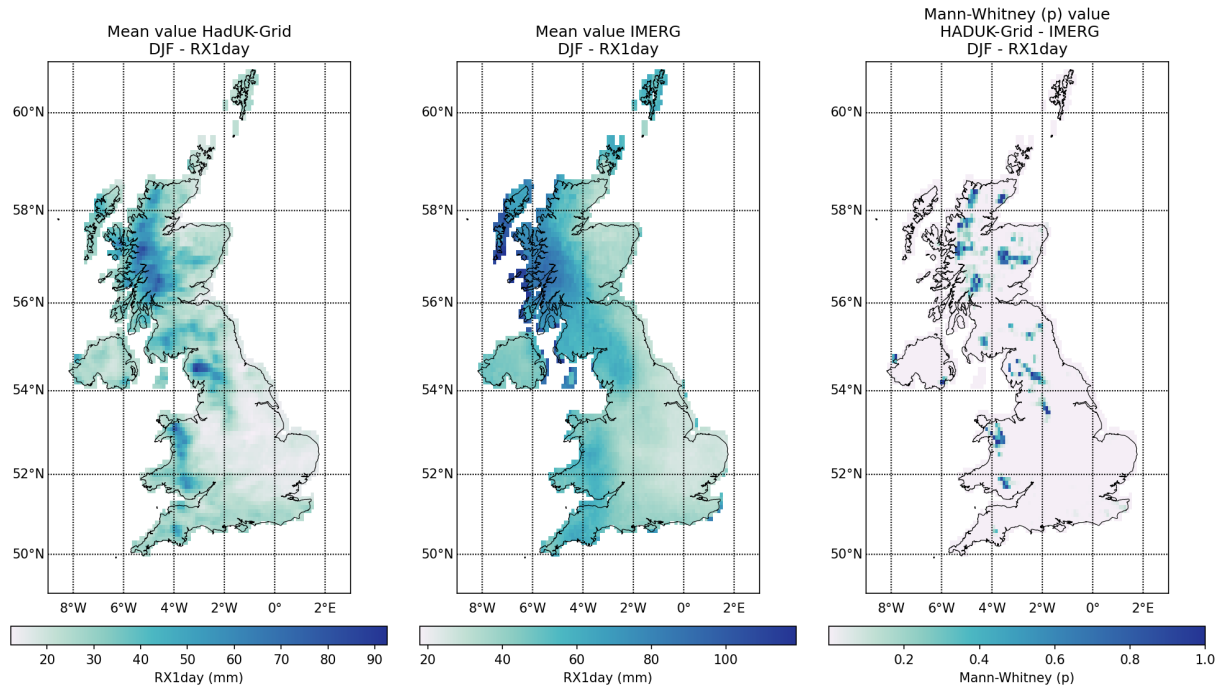


Figure 34: Spatial distribution of RX1day values obtained from HadUK-Grid and IMERG with Mann-Whitney test p value, Levene -center in the median- p value, and Pearson and Spearman correlation coefficient (r), for winter (DJF) over the 2001-2019 climatological period.

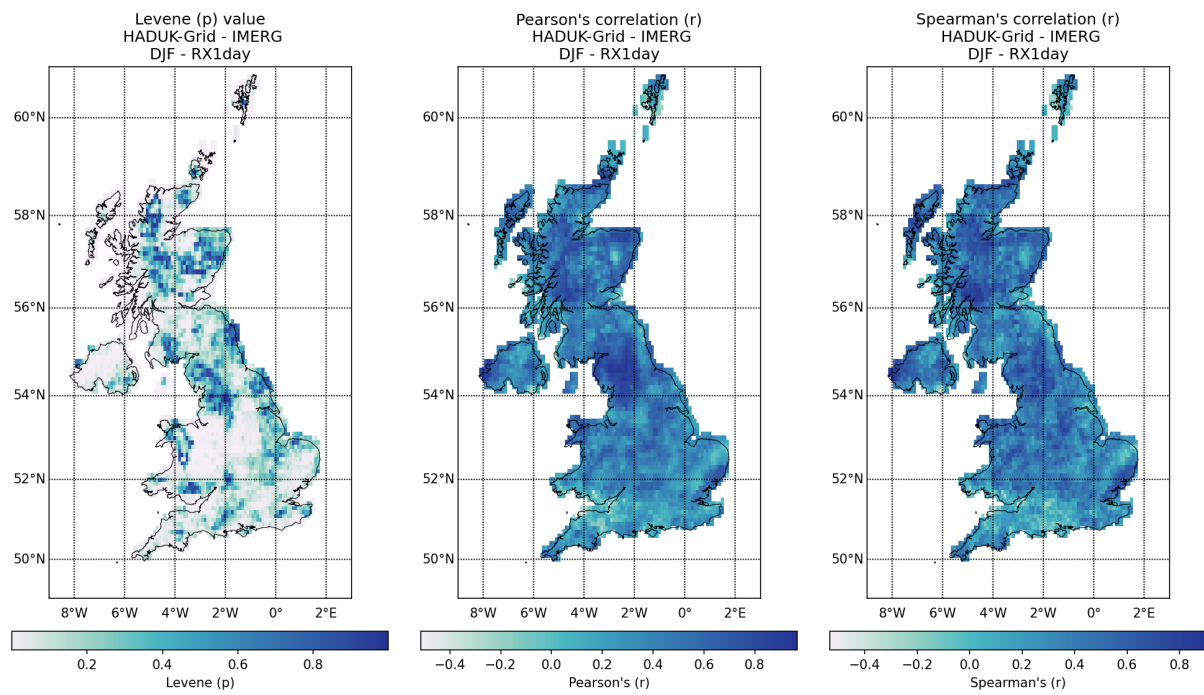


Figure 34: Spatial distribution of RX1day values obtained from HadUK-Grid and IMERG with Mann-Whitney test p value, Levene -center in the median- p value, and Pearson and Spearman correlation coefficient (r), for spring (DJF) over the 2001-2019 climatological period (cont.).

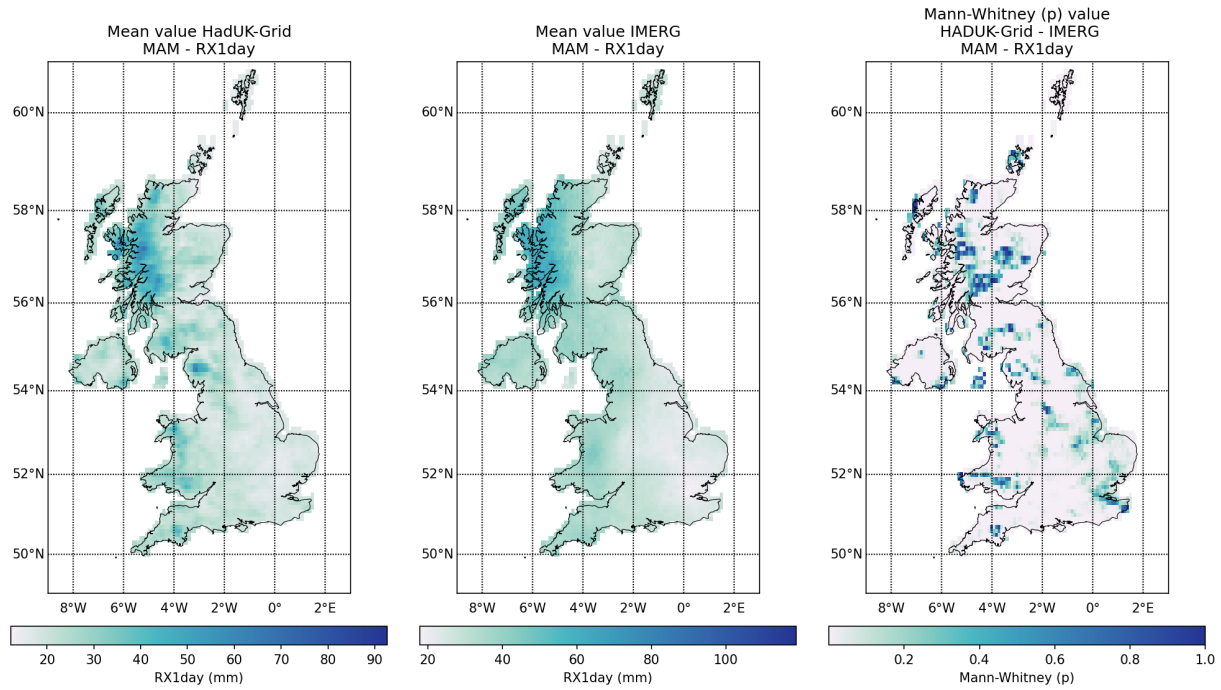


Figure 34: Spatial distribution of RX1day values obtained from HadUK-Grid and IMERG with Mann-Whitney test p value, Levene -center in the median- p value, and Pearson and Spearman correlation coefficient (r), for spring (MAM) over the 2001-2019 climatological period (cont.).

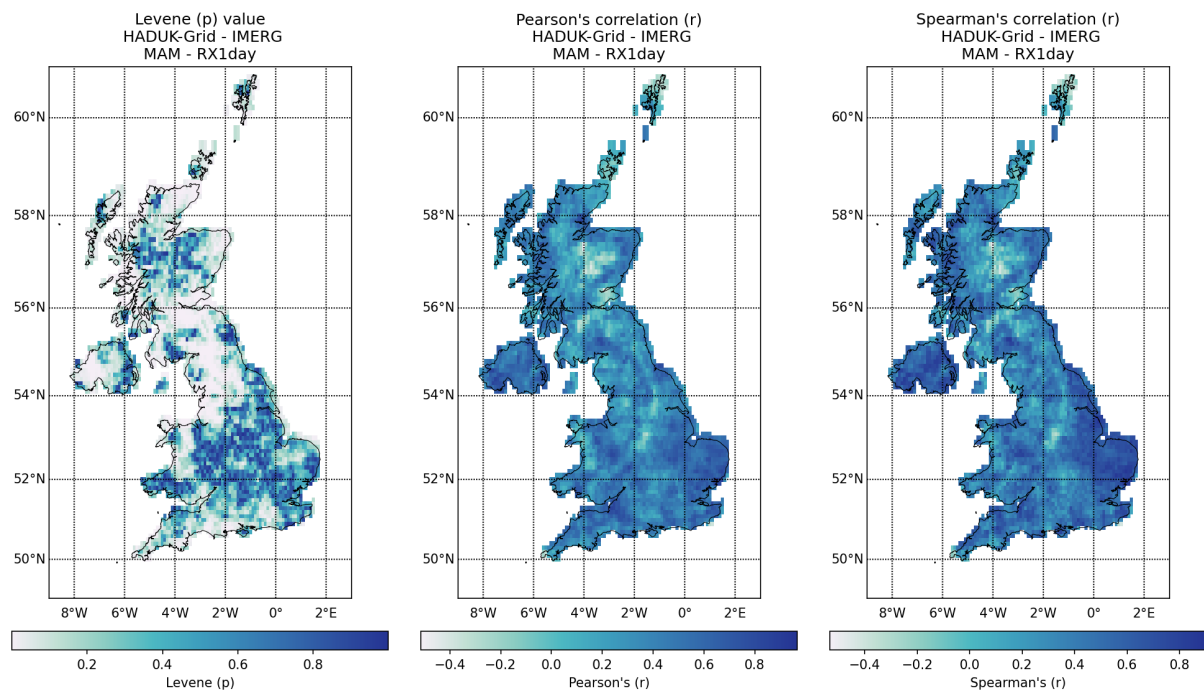


Figure 34: Spatial distribution of RX1day values obtained from HadUK-Grid and IMERG with Mann-Whitney test p value, Levene -center in the median- p value, and Pearson and Spearman correlation coefficient (r), for spring (MAM) over the 2001-2019 climatological period (cont.).

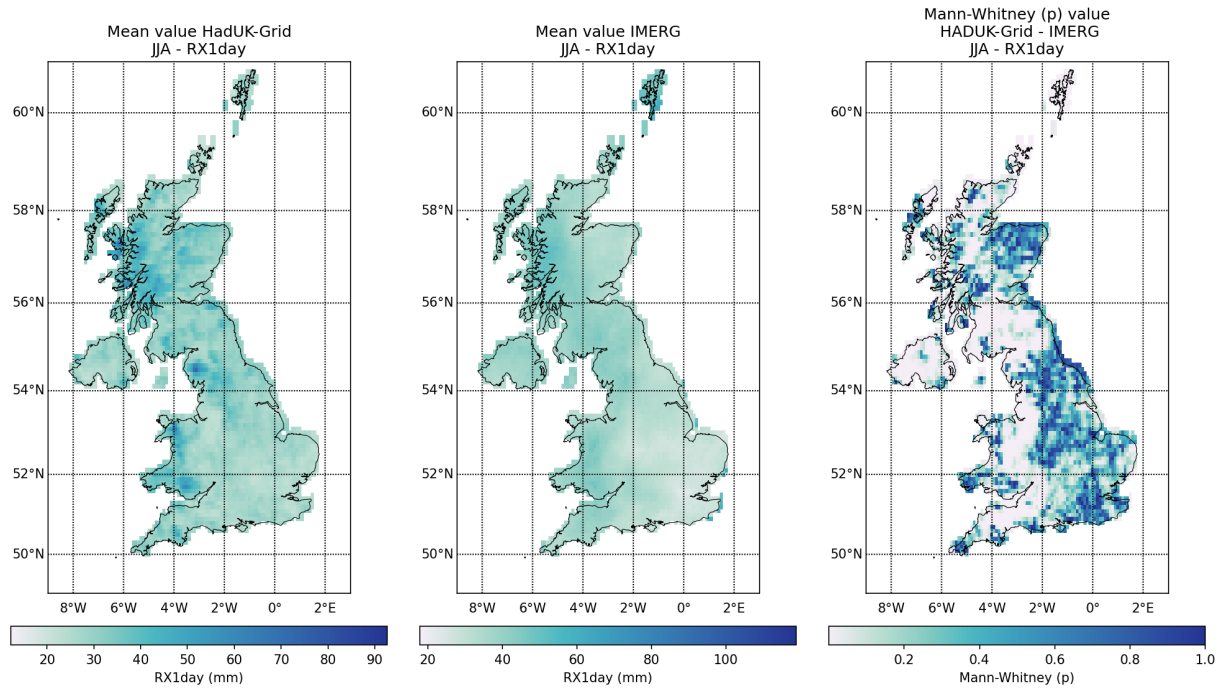


Figure 34: Spatial distribution of RX1day values obtained from HadUK-Grid and IMERG with Mann-Whitney test p value, Levene -center in the median- p value, and Pearson and Spearman correlation coefficient (r), for summer (JJA) over the 2001-2019 climatological period (cont.).

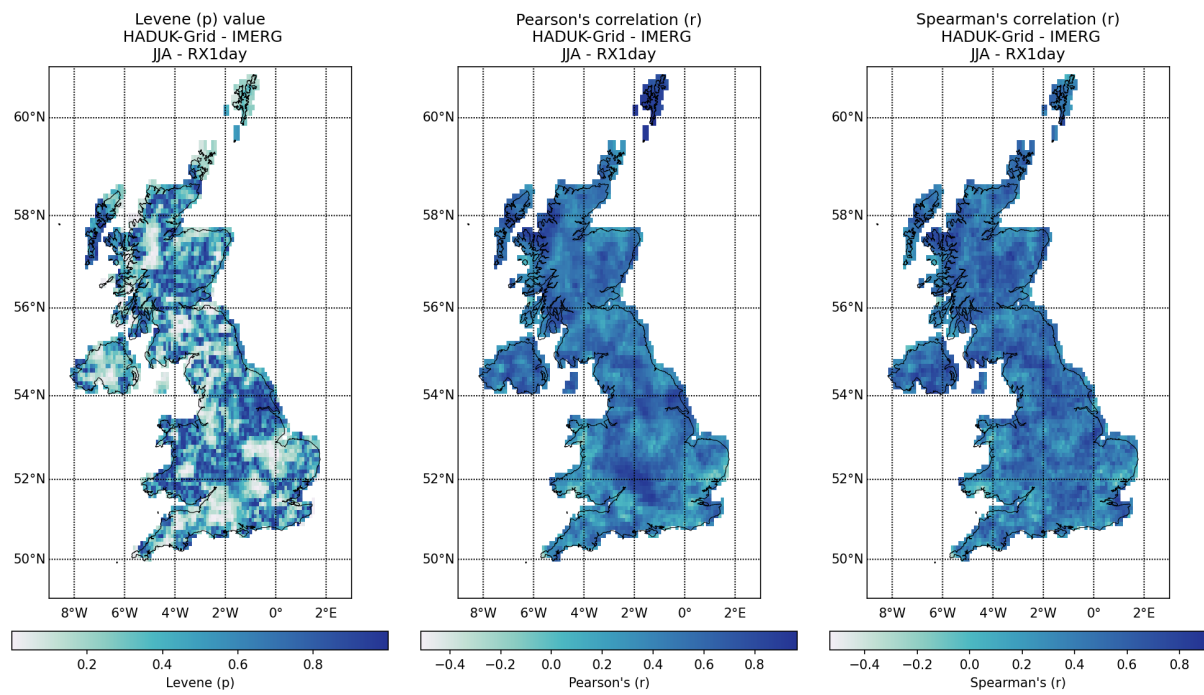


Figure 34: Spatial distribution of RX1day values obtained from HadUK-Grid and IMERG with Mann-Whitney test p value, Levene -center in the median- p value, and Pearson and Spearman correlation coefficient (r), for summer (JJA) over the 2001-2019 climatological period (cont.).

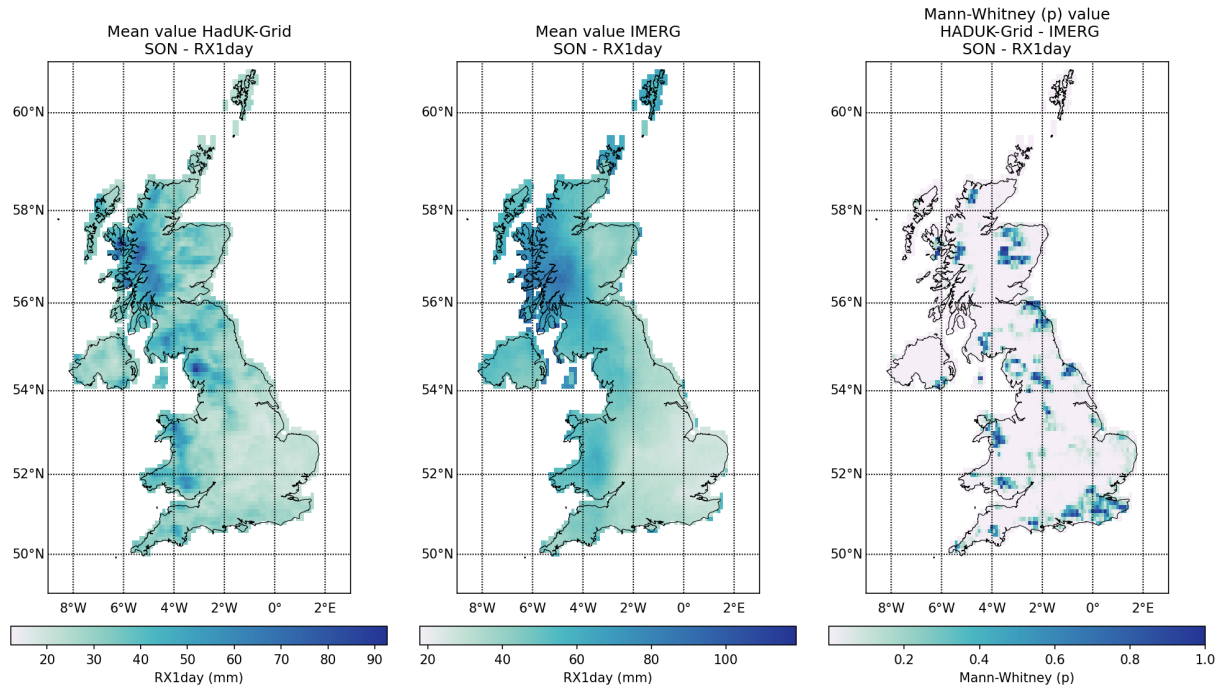


Figure 34: Spatial distribution of RX1day values obtained from HadUK-Grid and IMERG with Mann-Whitney test p value, Levene -center in the median- p value, and Pearson and Spearman correlation coefficient (r), for autumn (SON) over the 2001-2019 climatological period (cont.).

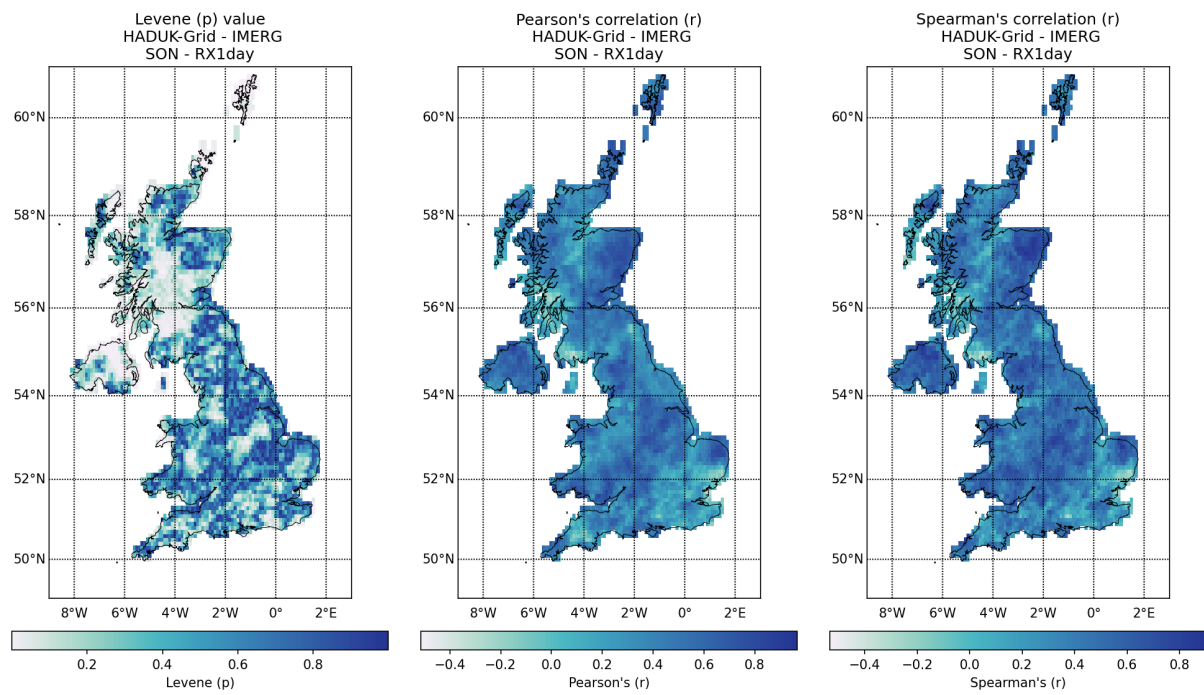


Figure 34: Spatial distribution of RX1day values obtained from HadUK-Grid and IMERG with Mann-Whitney test p value, Levene -center in the median- p value, and Pearson and Spearman correlation coefficient (r), for autumn (SON) over the 2001-2019 climatological period.

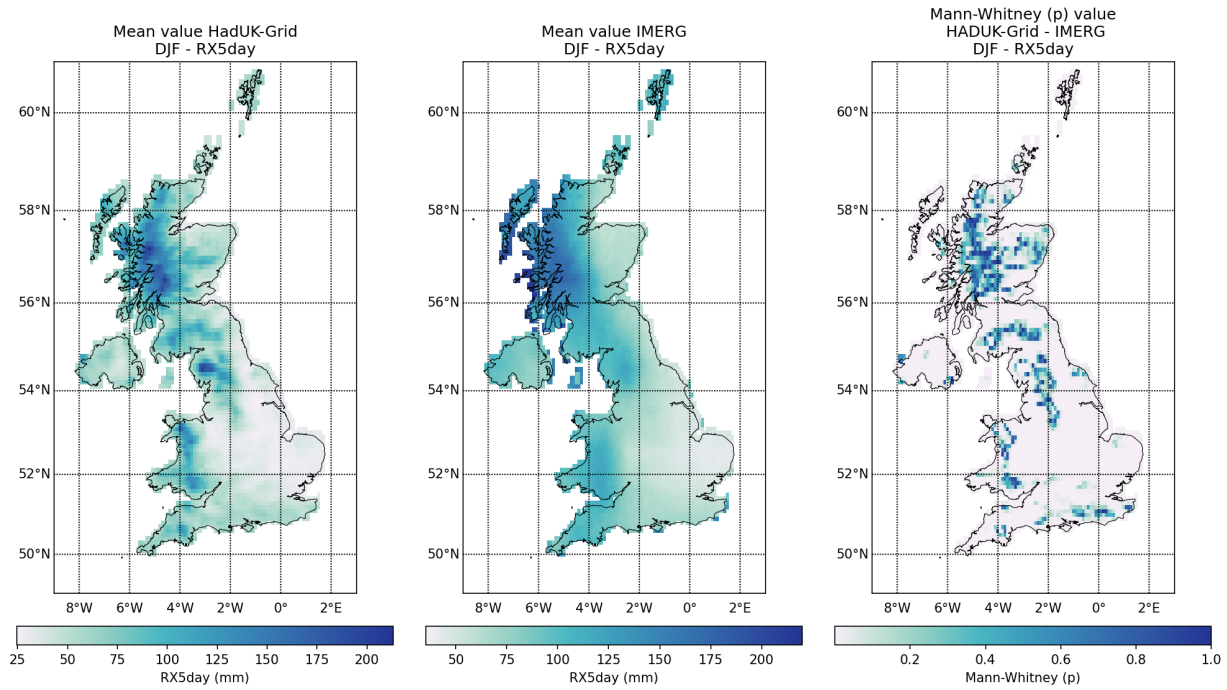


Figure 35: Spatial distribution of RX5day values obtained from HadUK-Grid and IMERG with Mann-Whitney test p value, Levene -center in the median- p value, and Pearson and Spearman correlation coefficient (r), for winter (DJF) over the 2001-2019 climatological period.

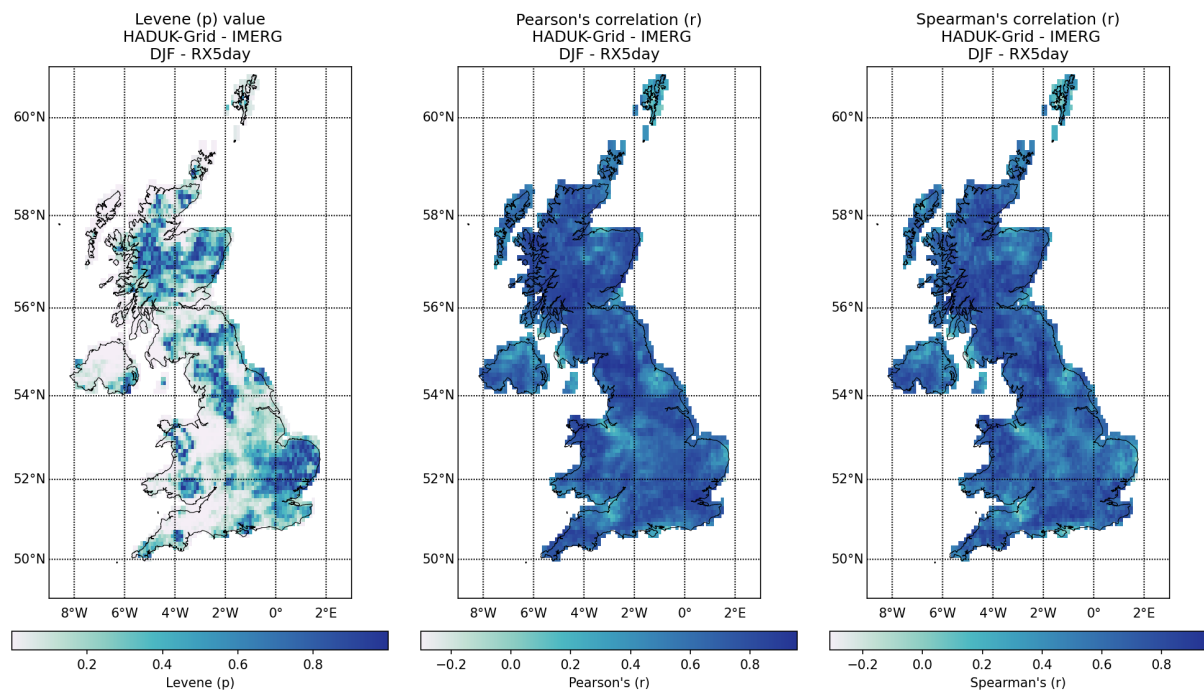


Figure 35: Spatial distribution of RX5day values obtained from HadUK-Grid and IMERG with Mann-Whitney test p value, Levene -center in the median- p value, and Pearson and Spearman correlation coefficient (r), for spring (DJF) over the 2001-2019 climatological period (cont.).

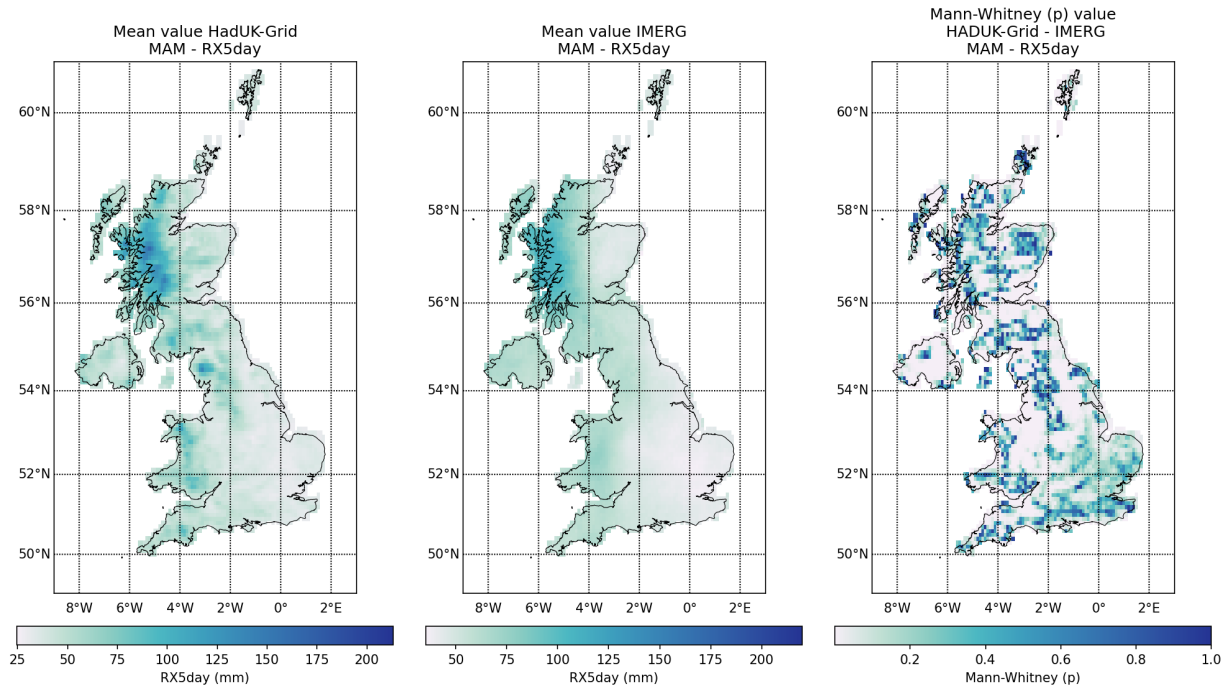


Figure 35: Spatial distribution of RX5day values obtained from HadUK-Grid and IMERG with Mann-Whitney test p value, Levene -center in the median- p value, and Pearson and Spearman correlation coefficient (r), for spring (MAM) over the 2001-2019 climatological period (cont.).

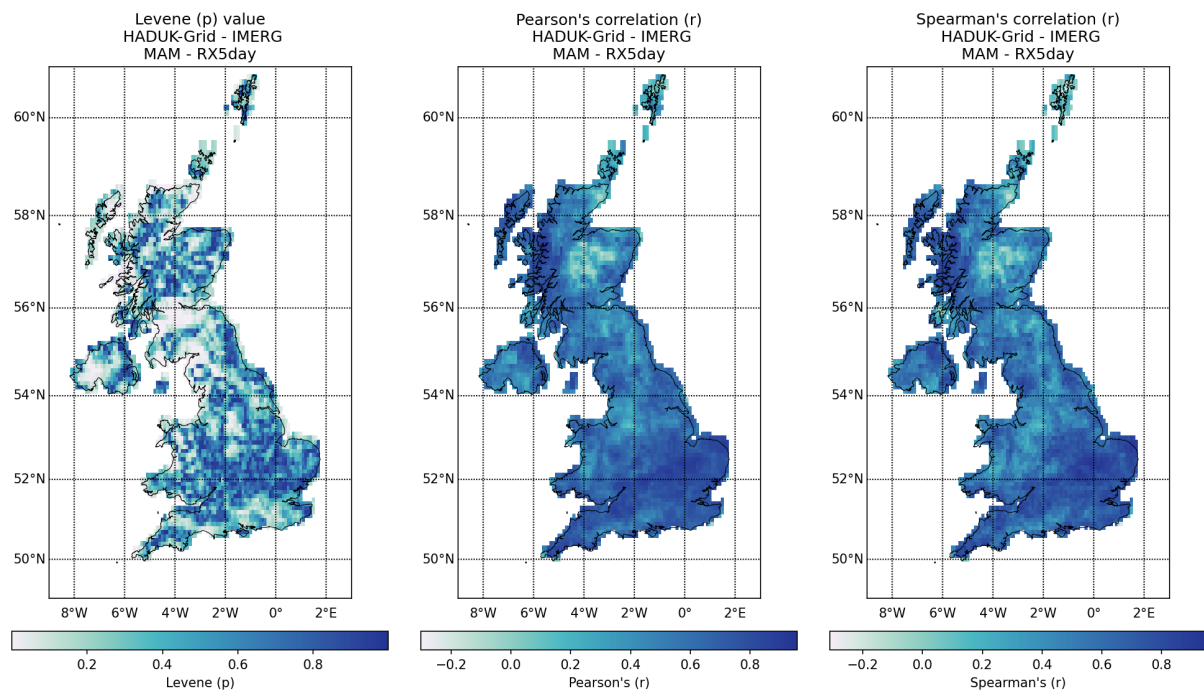


Figure 35: Spatial distribution of RX5day values obtained from HadUK-Grid and IMERG with Mann-Whitney test p value, Levene -center in the median- p value, and Pearson and Spearman correlation coefficient (r), for spring (MAM) over the 2001-2019 climatological period (cont.).

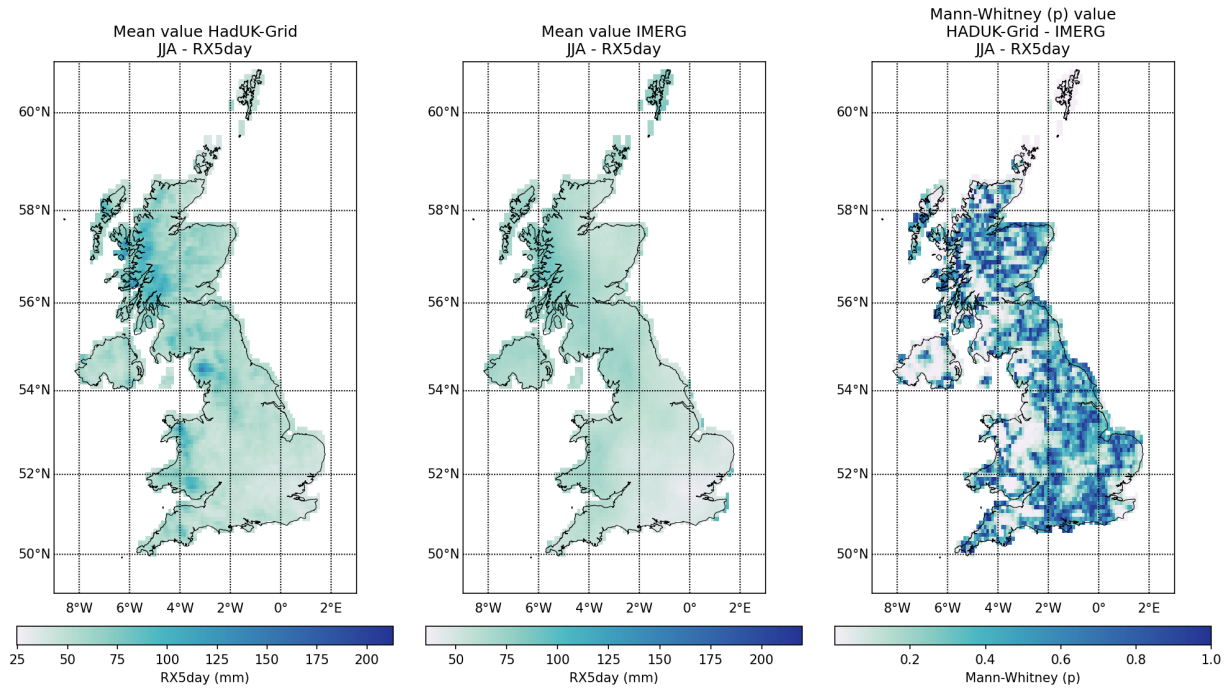


Figure 35: Spatial distribution of RX5day values obtained from HadUK-Grid and IMERG with Mann-Whitney test p value, Levene -center in the median- p value, and Pearson and Spearman correlation coefficient (r), for summer (JJA) over the 2001-2019 climatological period (cont.).

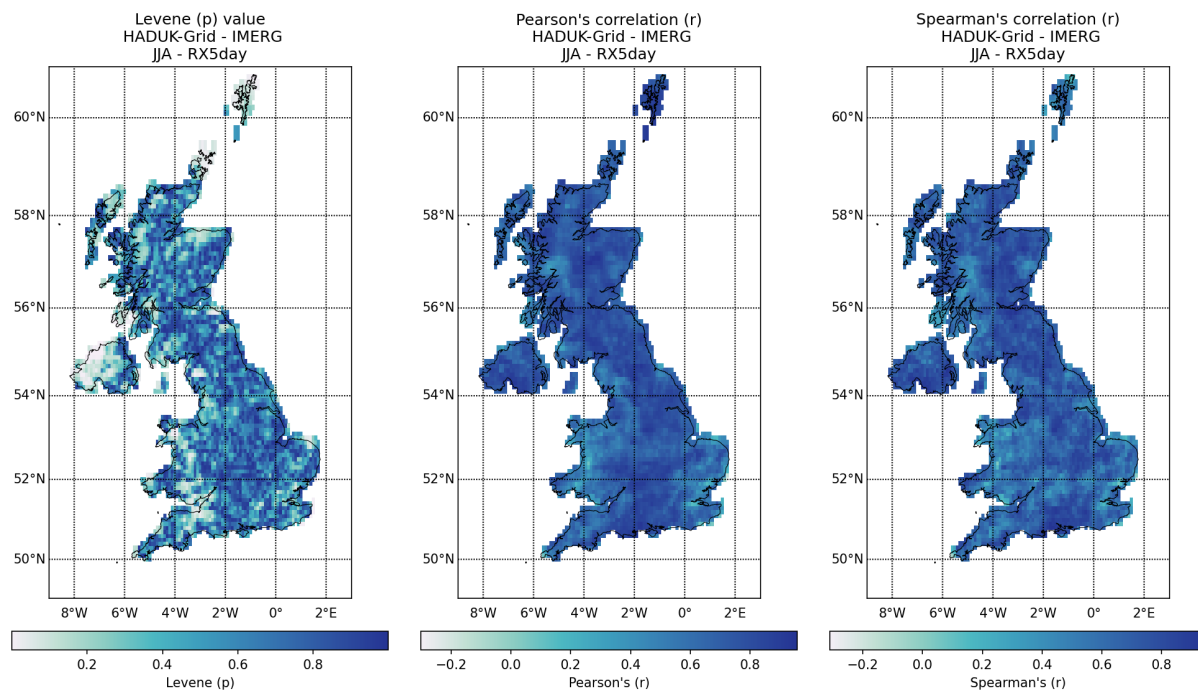


Figure 35: Spatial distribution of RX5day values obtained from HadUK-Grid and IMERG with Mann-Whitney test p value, Levene -center in the median- p value, and Pearson and Spearman correlation coefficient (r), for summer (JJA) over the 2001-2019 climatological period (cont.).

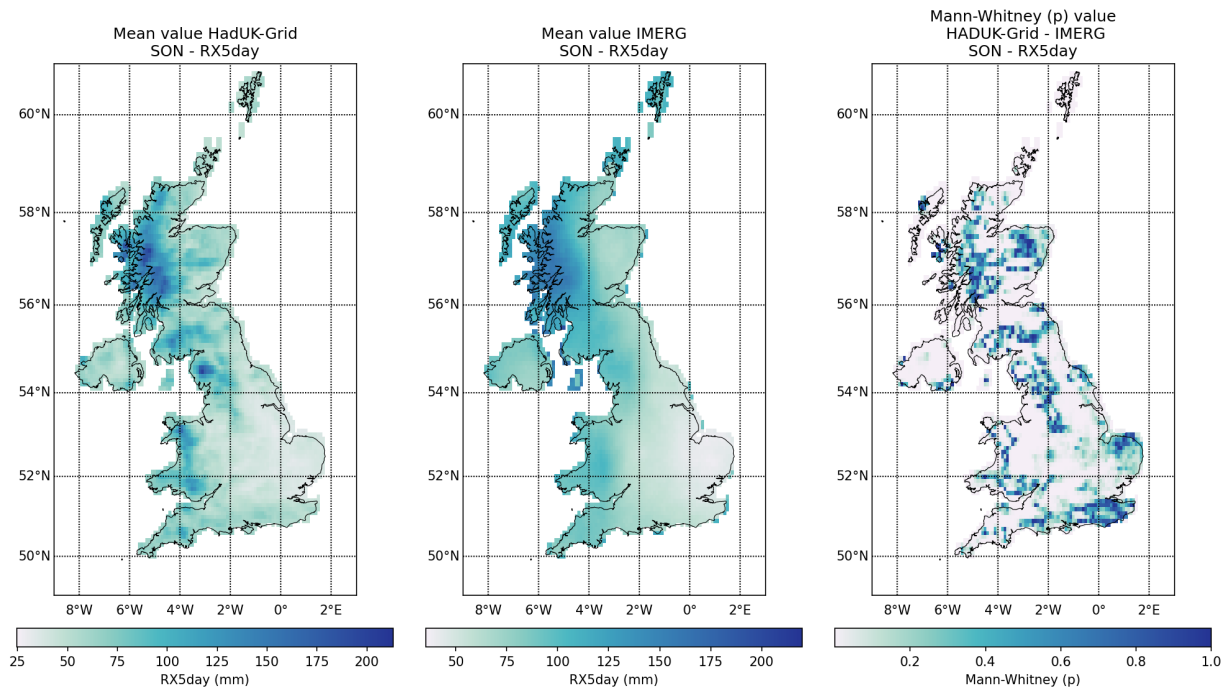


Figure 35: Spatial distribution of RX5day values obtained from HadUK-Grid and IMERG with Mann-Whitney test p value, Levene -center in the median- p value, and Pearson and Spearman correlation coefficient (r), for autumn (SON) over the 2001-2019 climatological period (cont.).

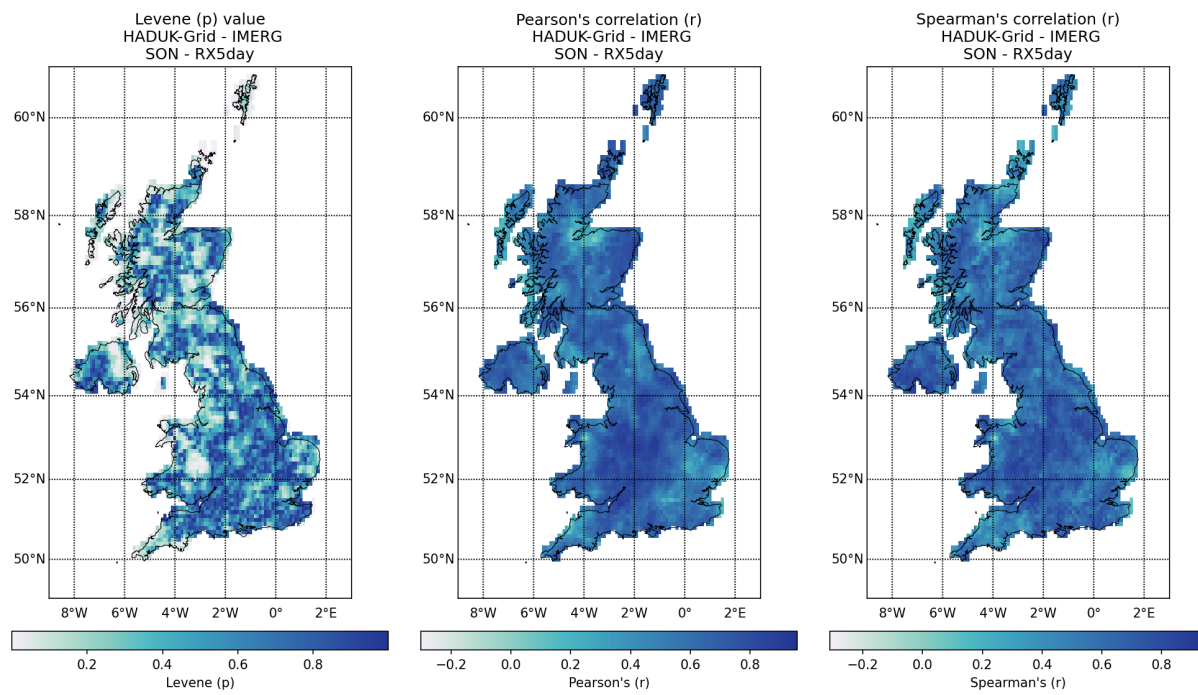


Figure 35: Spatial distribution of RX5day values obtained from HadUK-Grid and IMERG with Mann-Whitney test p value, Levene -center in the median- p value, and Pearson and Spearman correlation coefficient (r), for autumn (SON) over the 2001-2019 climatological period.

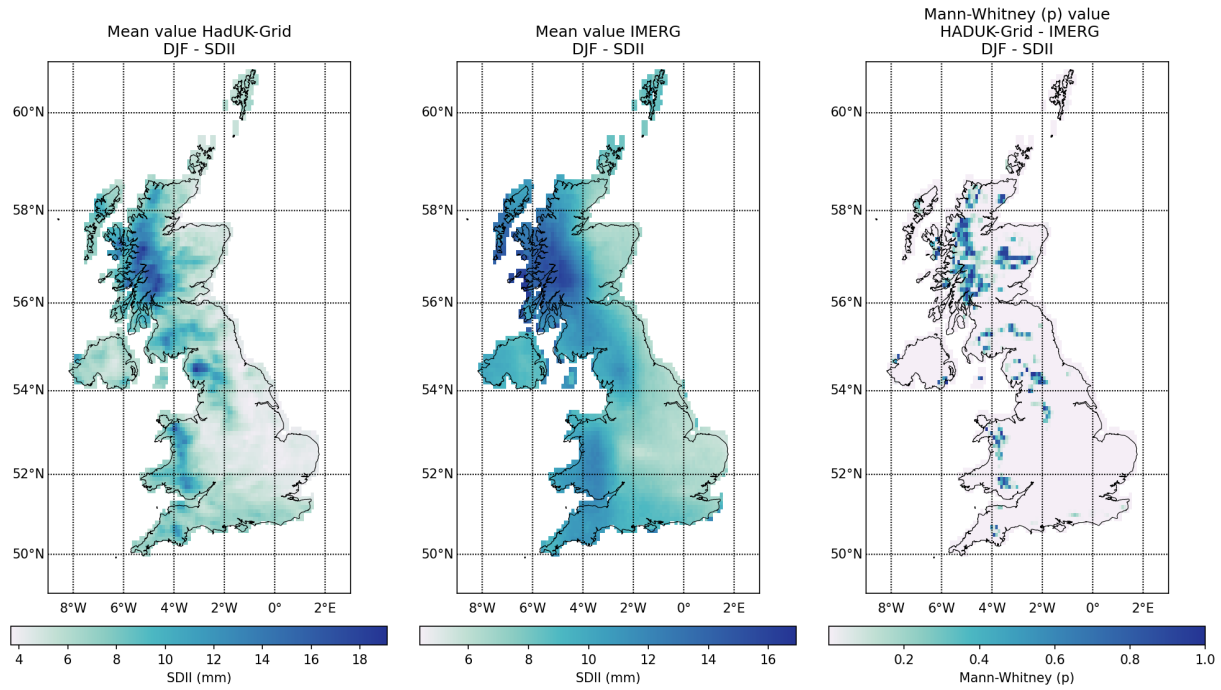


Figure 36: Spatial distribution of SDII values obtained from HadUK-Grid and IMERG with Mann-Whitney test p value, Levene -center in the median- p value, and Pearson and Spearman correlation coefficient (r), for winter (DJF) over the 2001-2019 climatological period.

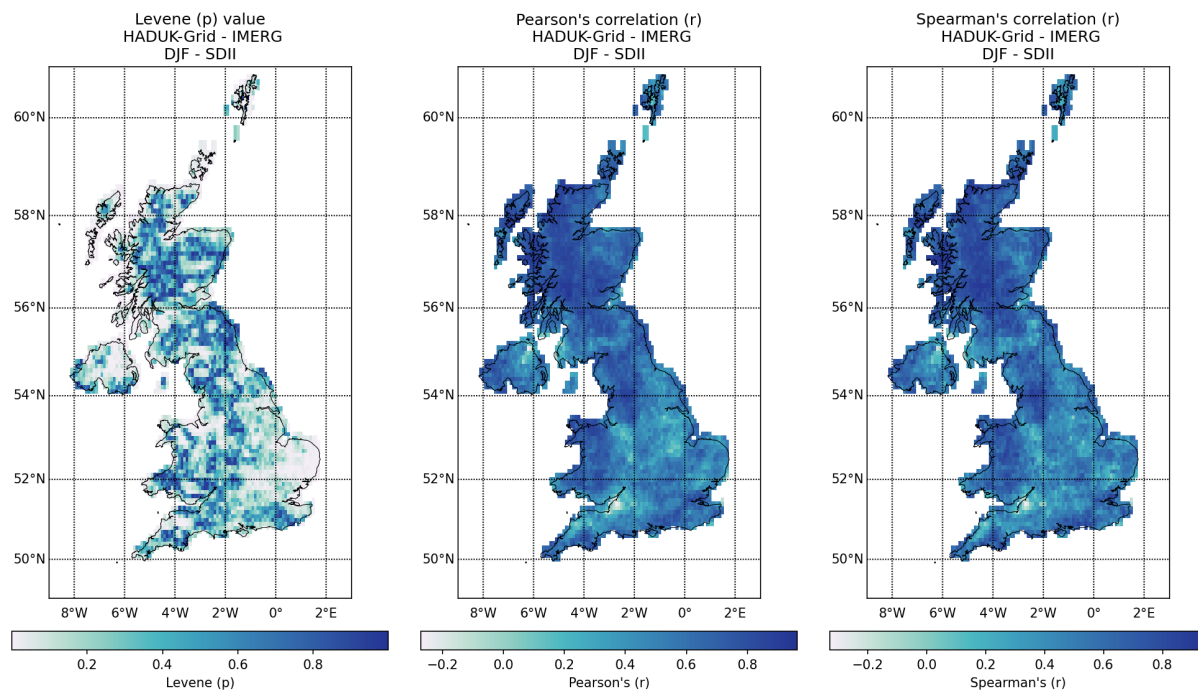


Figure 36: Spatial distribution of SDII values obtained from HadUK-Grid and IMERG with Mann-Whitney test p value, Levene -center in the median- p value, and Pearson and Spearman correlation coefficient (r), for spring (DJF) over the 2001-2019 climatological period (cont.).

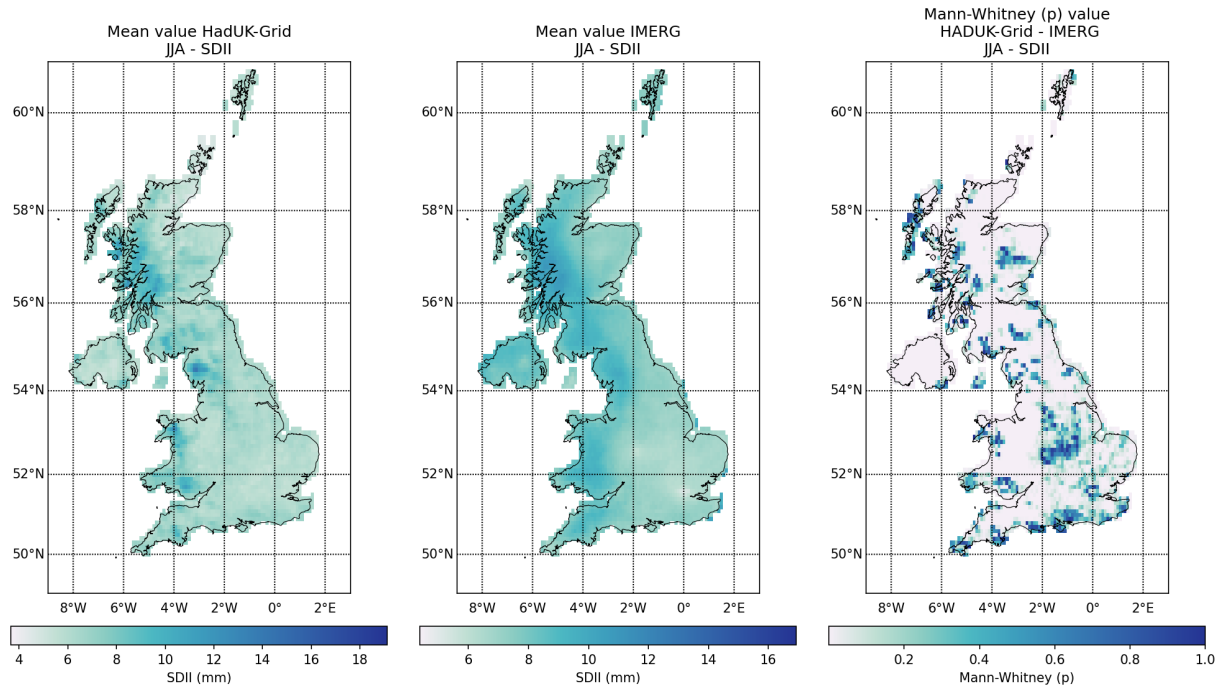


Figure 36: Spatial distribution of SDII values obtained from HadUK-Grid and IMERG with Mann-Whitney test p value, Levene -center in the median- p value, and Pearson and Spearman correlation coefficient (r), for summer (JJA) over the 2001-2019 climatological period (cont.).

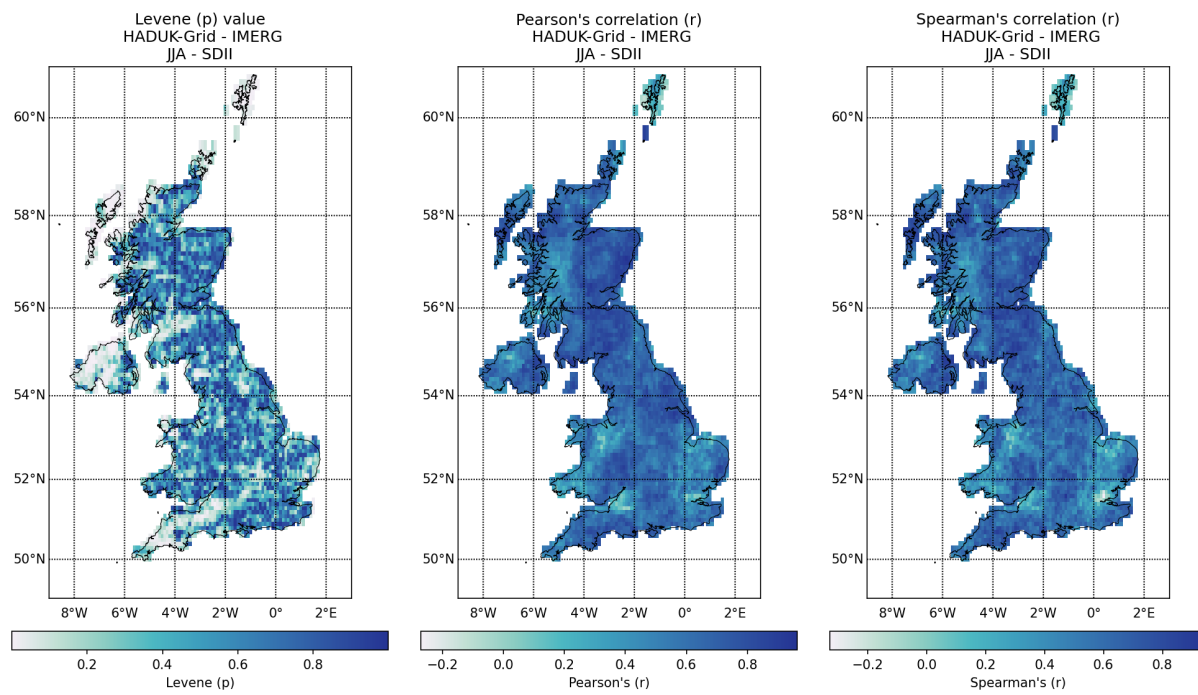


Figure 36: Spatial distribution of SDII values obtained from HadUK-Grid and IMERG with Mann-Whitney test p value, Levene -center in the median- p value, and Pearson and Spearman correlation coefficient (r), for summer (JJA) over the 2001-2019 climatological period (cont.).

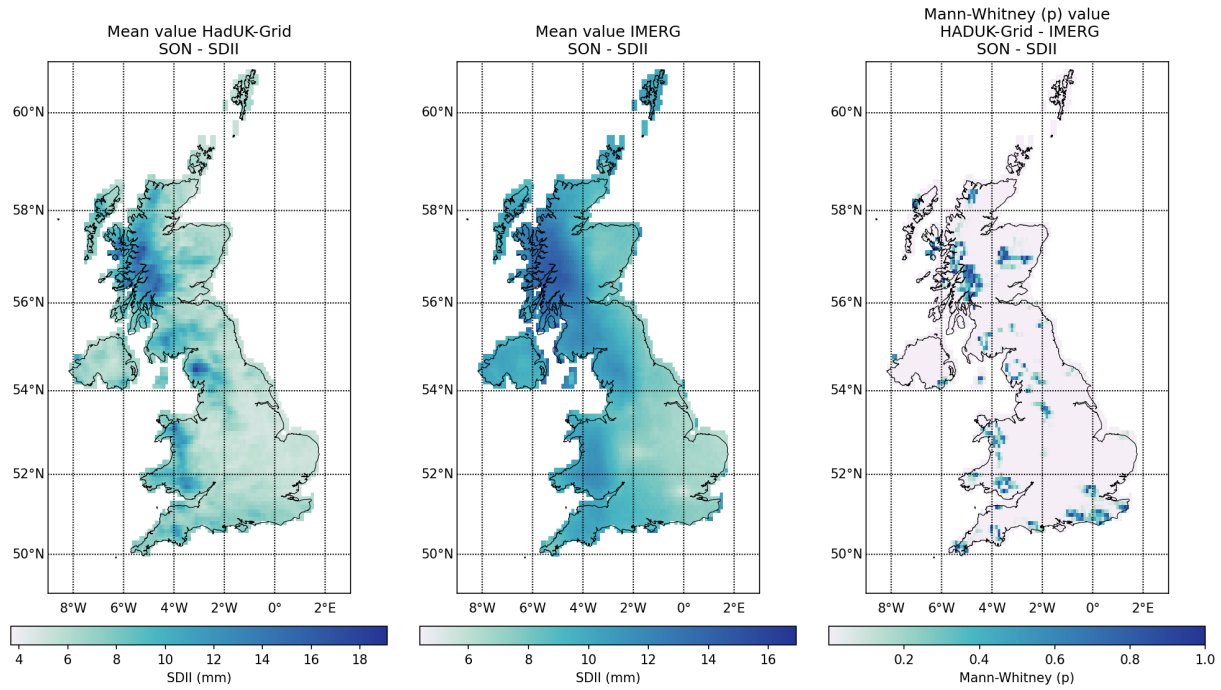


Figure 36: Spatial distribution of SDII values obtained from HadUK-Grid and IMERG with Mann-Whitney test p value, Levene -center in the median- p value, and Pearson and Spearman correlation coefficient (r), for autumn (SON) over the 2001-2019 climatological period (cont.).

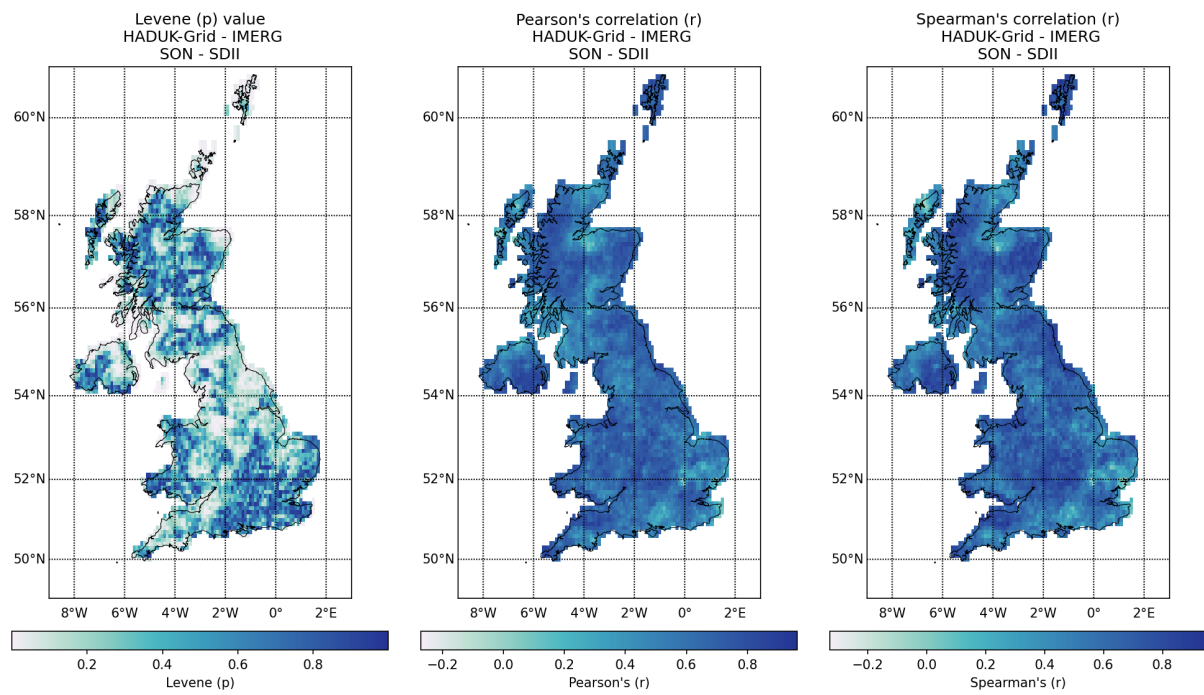


Figure 36: Spatial distribution of SDII values obtained from HadUK-Grid and IMERG with Mann-Whitney test p value, Levene -center in the median- p value, and Pearson and Spearman correlation coefficient (r), for autumn (SON) over the 2001-2019 climatological period.

2.3.2 ERA5 DATA

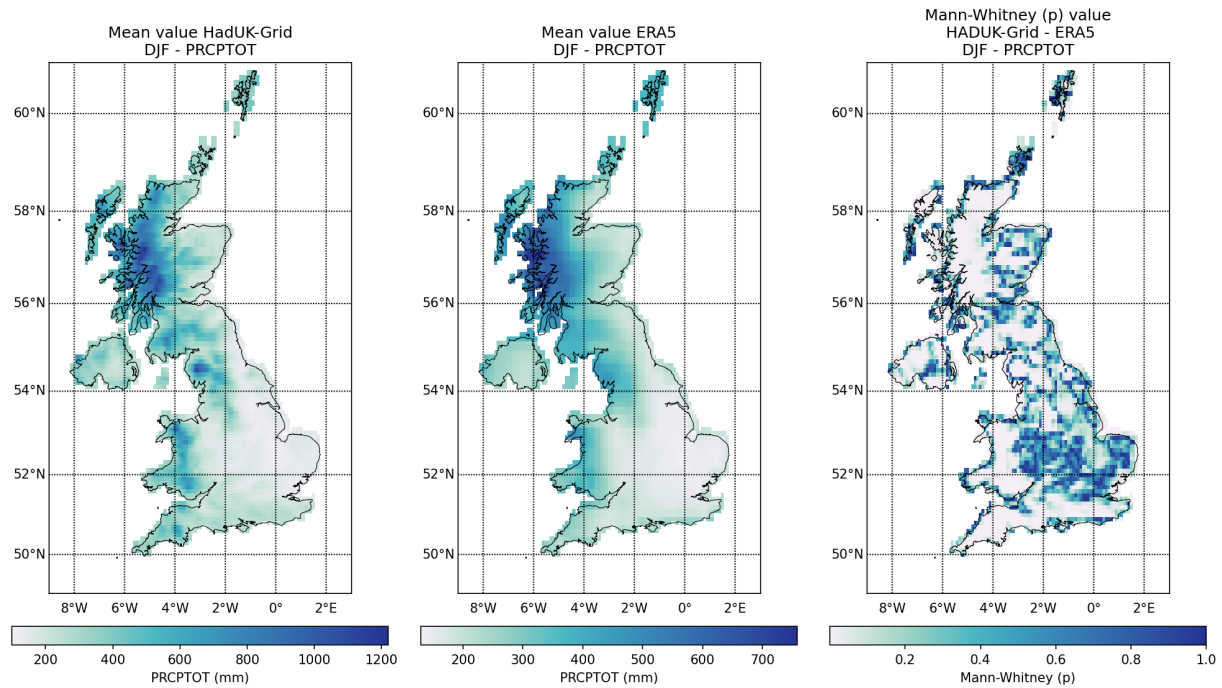


Figure 37: Spatial distribution of PRCPTOT values obtained from HadUK-Grid and ERA5 with Mann-Whitney test p value, Levene -center in the median- p value, and Pearson and Spearman correlation coefficient (r), for winter (DJF) over the 2001-2019 climatological period.

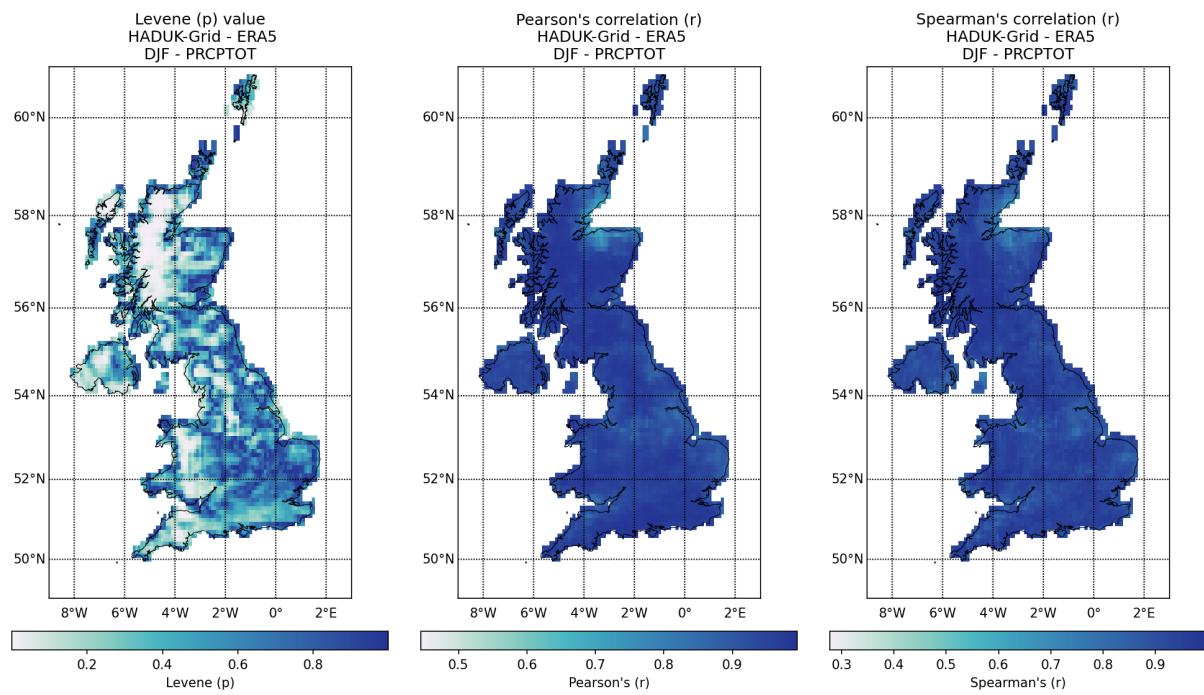


Figure 37: Spatial distribution of PRCPTOT values obtained from HadUK-Grid and ERA5 with Mann-Whitney test p value, Levene -center in the median- p value, and Pearson and Spearman correlation coefficient (r), for spring (DJF) over the 2001-2019 climatological period (cont.).

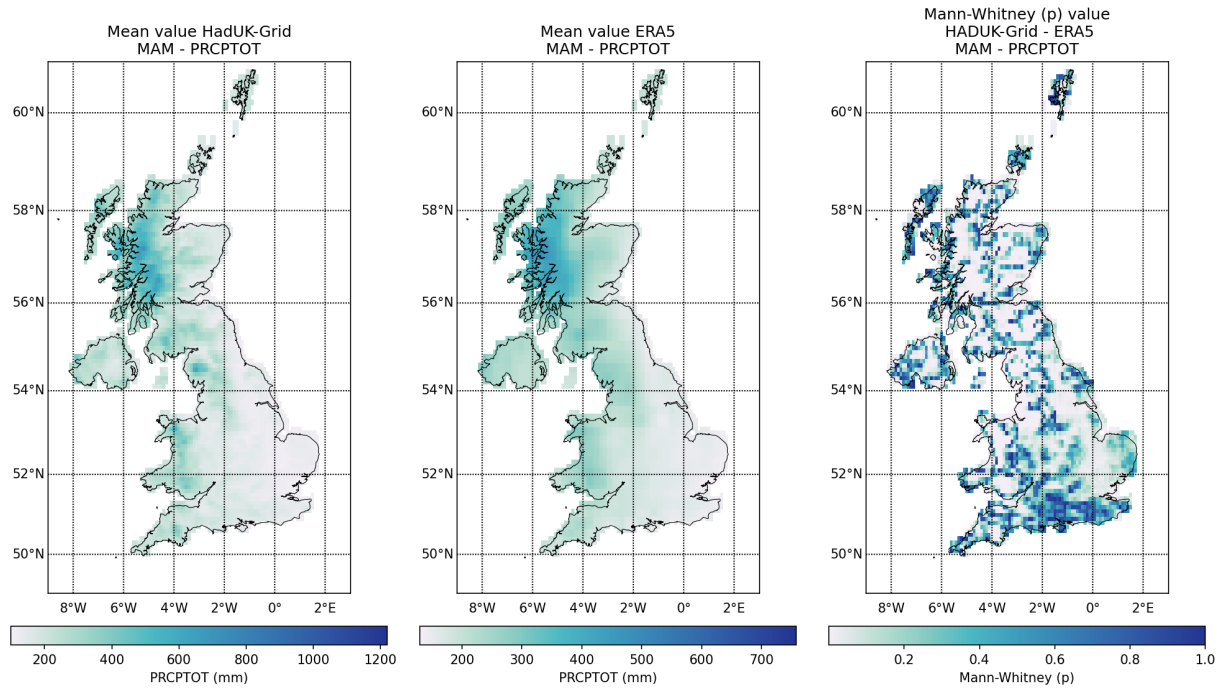


Figure 37: Spatial distribution of PRCPTOT values obtained from HadUK-Grid and ERA5 with Mann-Whitney test p value, Levene -center in the median- p value, and Pearson and Spearman correlation coefficient (r), for spring (MAM) over the 2001-2019 climatological period (cont.).

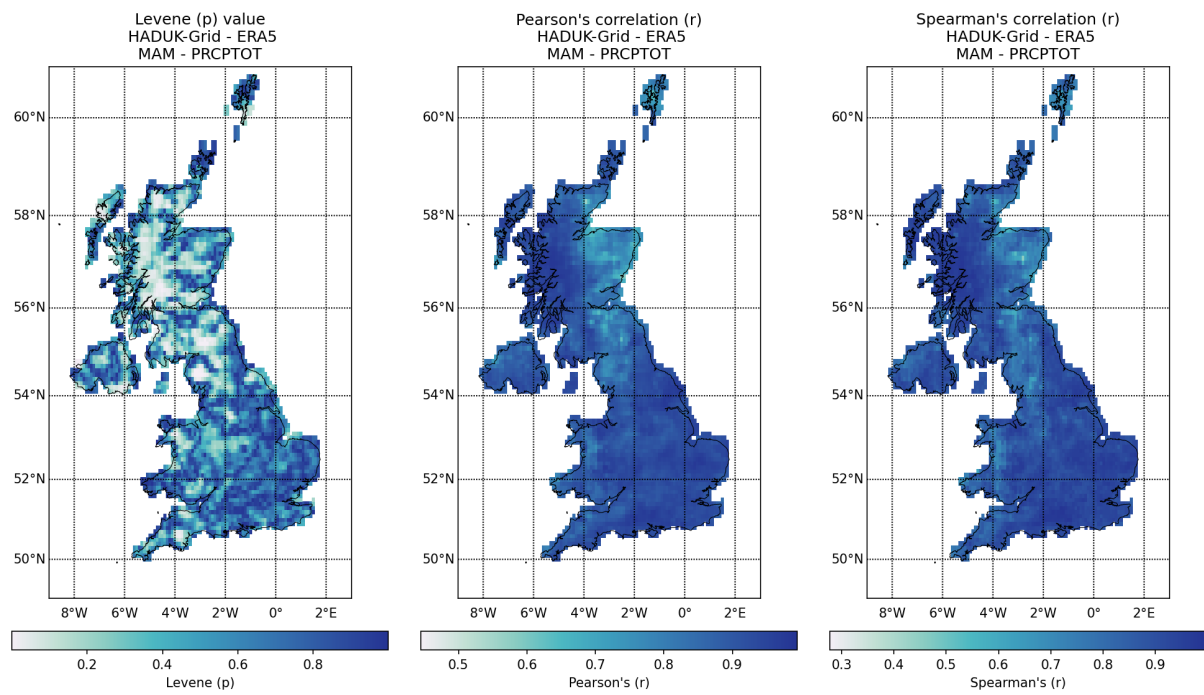


Figure 37: Spatial distribution of PRCPTOT values obtained from HadUK-Grid and ERA5 with Mann-Whitney test p value, Levene -center in the median- p value, and Pearson and Spearman correlation coefficient (r), for spring (MAM) over the 2001-2019 climatological period (cont.).

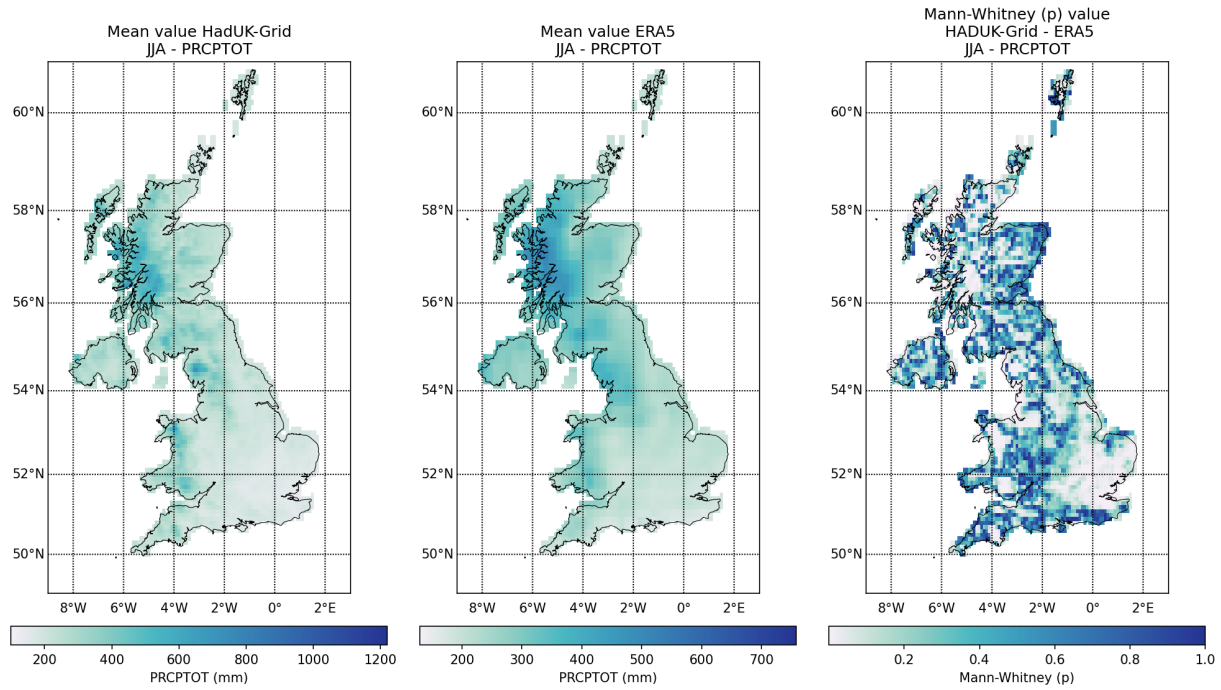


Figure 37: Spatial distribution of PRCPTOT values obtained from HadUK-Grid and ERA5 with Mann-Whitney test p value, Levene -center in the median- p value, and Pearson and Spearman correlation coefficient (r), for summer (JJA) over the 2001-2019 climatological period (cont.).

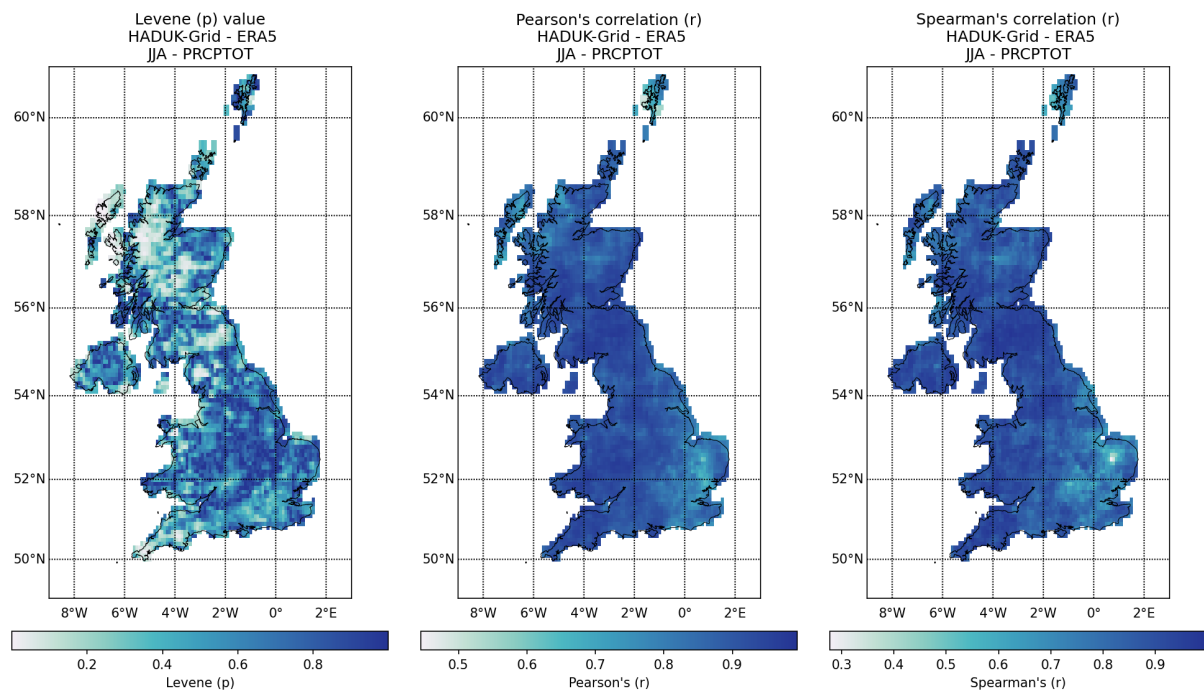


Figure 37: Spatial distribution of PRCPTOT values obtained from HadUK-Grid and ERA5 with Mann-Whitney test p value, Levene -center in the median- p value, and Pearson and Spearman correlation coefficient (r), for summer (JJA) over the 2001-2019 climatological period (cont.).

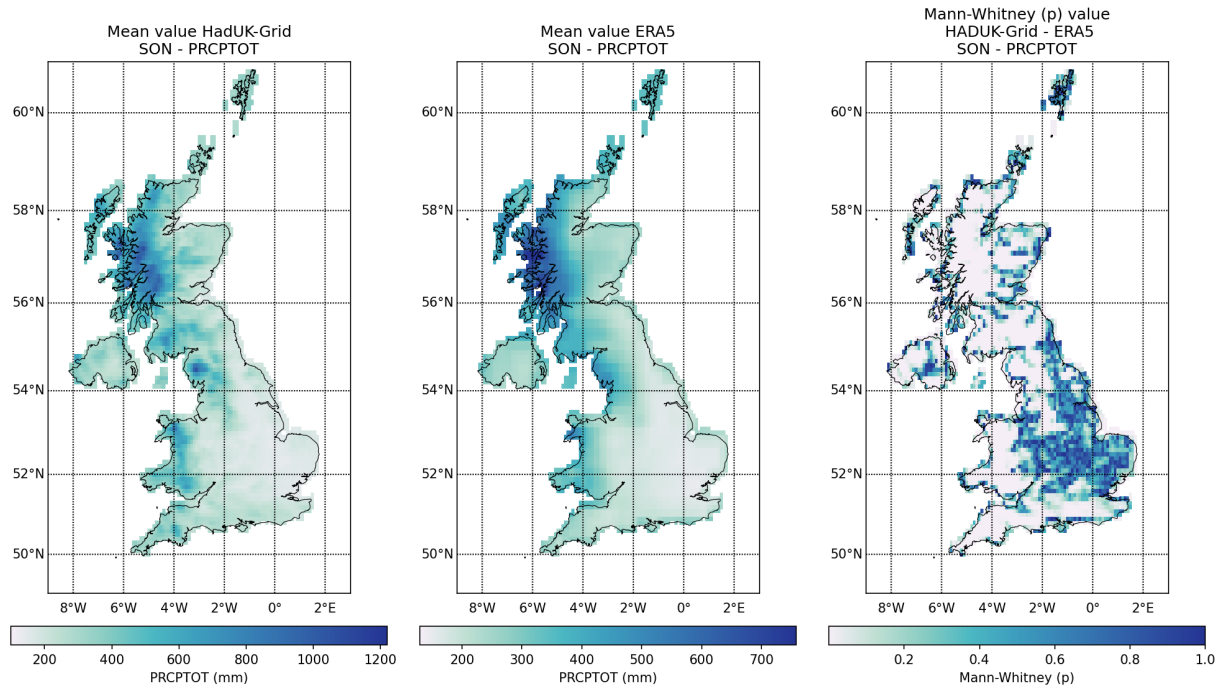


Figure 37: Spatial distribution of PRCPTOT values obtained from HadUK-Grid and ERA5 with Mann-Whitney test p value, Levene -center in the median- p value, and Pearson and Spearman correlation coefficient (r), for autumn (SON) over the 2001-2019 climatological period (cont.).

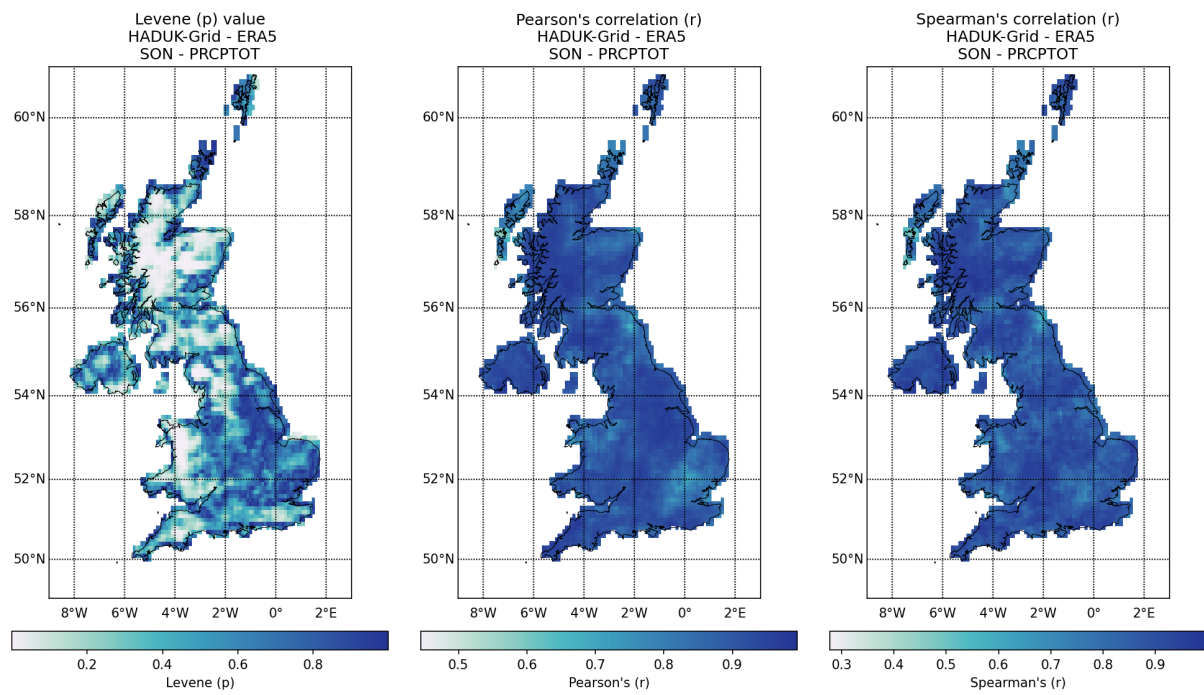


Figure 37: Spatial distribution of PRCPTOT values obtained from HadUK-Grid and ERA5 with Mann-Whitney test p value, Levene -center in the median- p value, and Pearson and Spearman correlation coefficient (r), for autumn (SON) over the 2001-2019 climatological period.

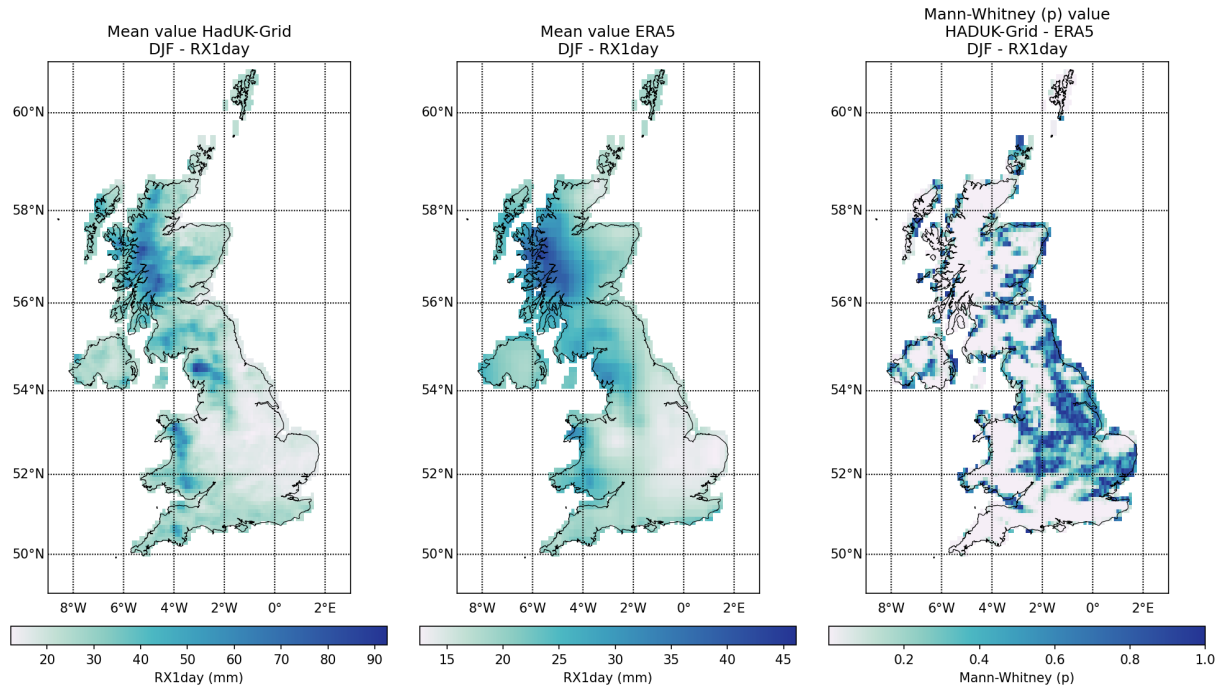


Figure 38: Spatial distribution of RX1day values obtained from HadUK-Grid and ERA5 with Mann-Whitney test p value, Levene -center in the median- p value, and Pearson and Spearman correlation coefficient (r), for winter (DJF) over the 2001-2019 climatological period.

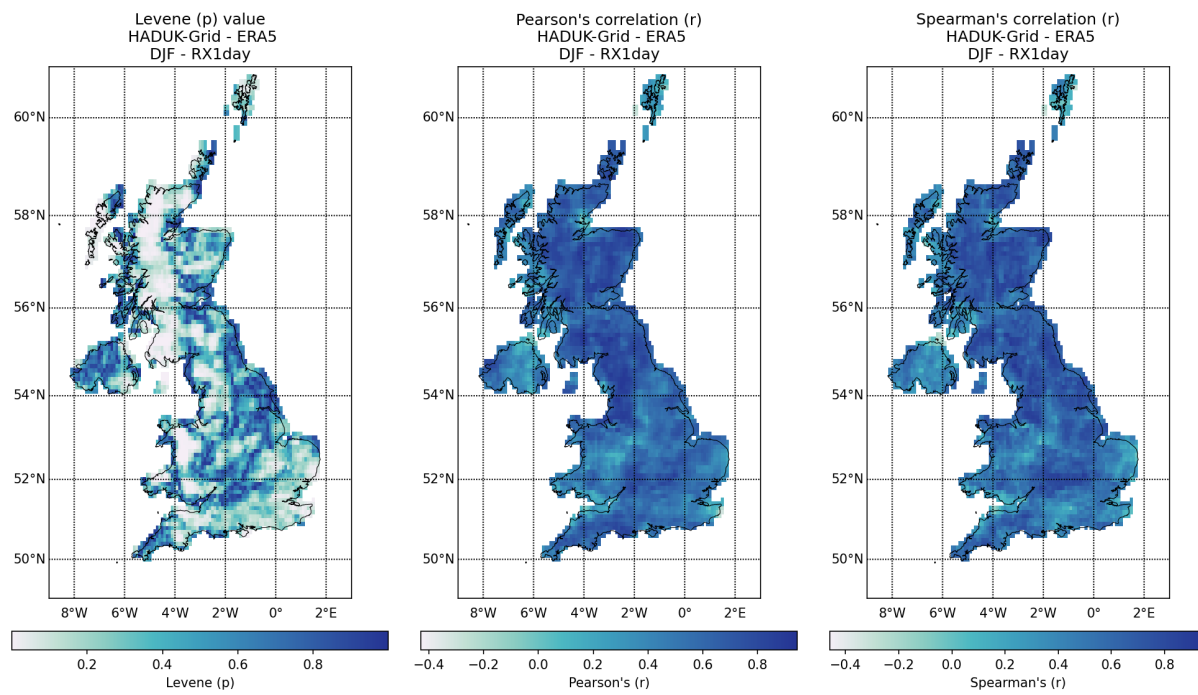


Figure 38: Spatial distribution of RX1day values obtained from HadUK-Grid and ERA5 with Mann-Whitney test p value, Levene -center in the median- p value, and Pearson and Spearman correlation coefficient (r), for spring (DJF) over the 2001-2019 climatological period (cont.).

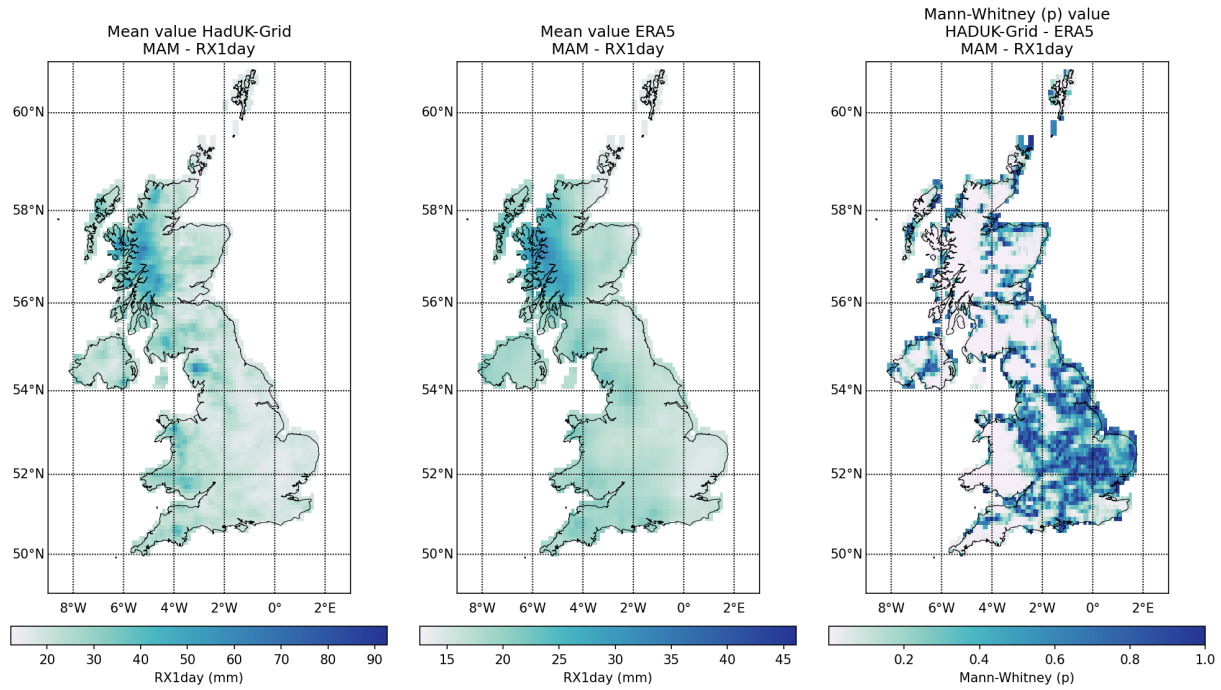


Figure 38: Spatial distribution of RX1day values obtained from HadUK-Grid and ERA5 with Mann-Whitney test p value, Levene -center in the median- p value, and Pearson and Spearman correlation coefficient (r), for spring (MAM) over the 2001-2019 climatological period (cont.).

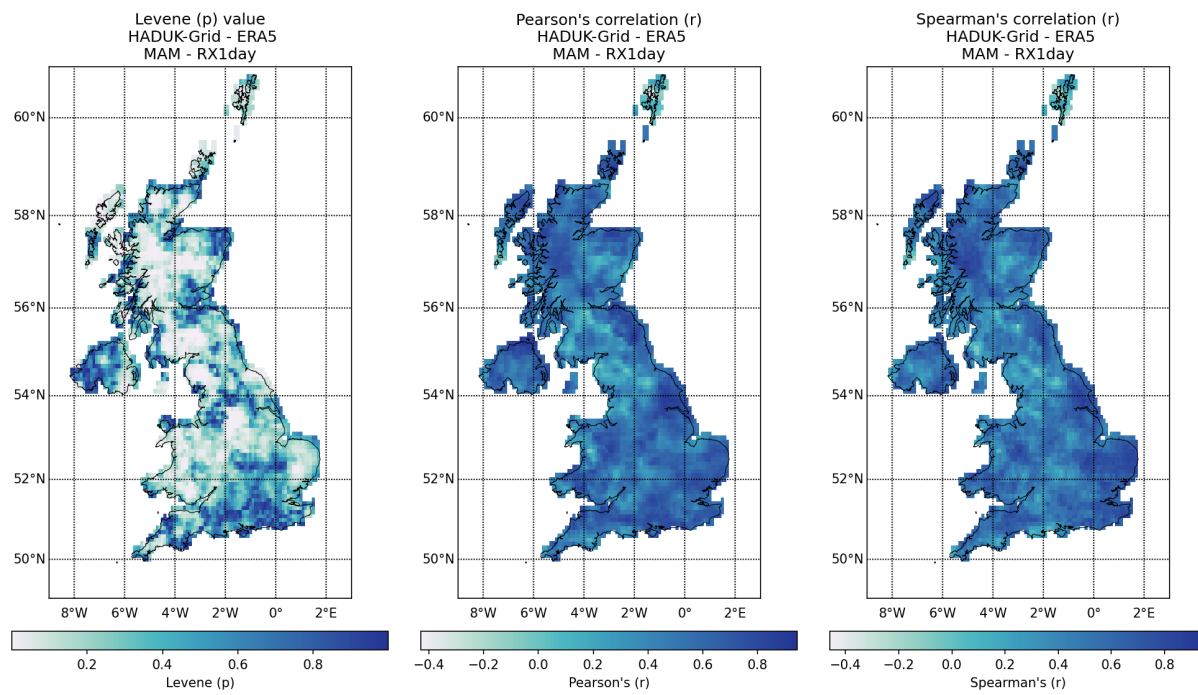


Figure 38: Spatial distribution of RX1day values obtained from HadUK-Grid and ERA5 with Mann-Whitney test p value, Levene -center in the median- p value, and Pearson and Spearman correlation coefficient (r), for spring (MAM) over the 2001-2019 climatological period (cont.).

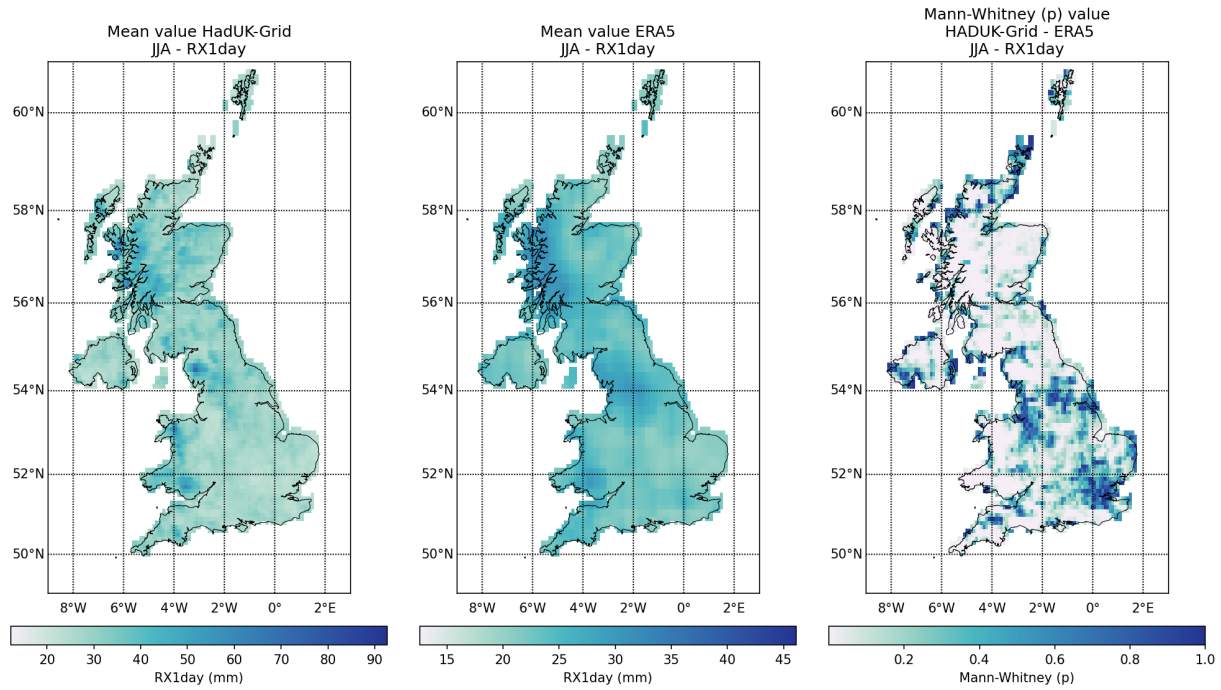


Figure 38: Spatial distribution of RX1day values obtained from HadUK-Grid and ERA5 with Mann-Whitney test p value, Levene -center in the median- p value, and Pearson and Spearman correlation coefficient (r), for summer (JJA) over the 2001-2019 climatological period (cont.).

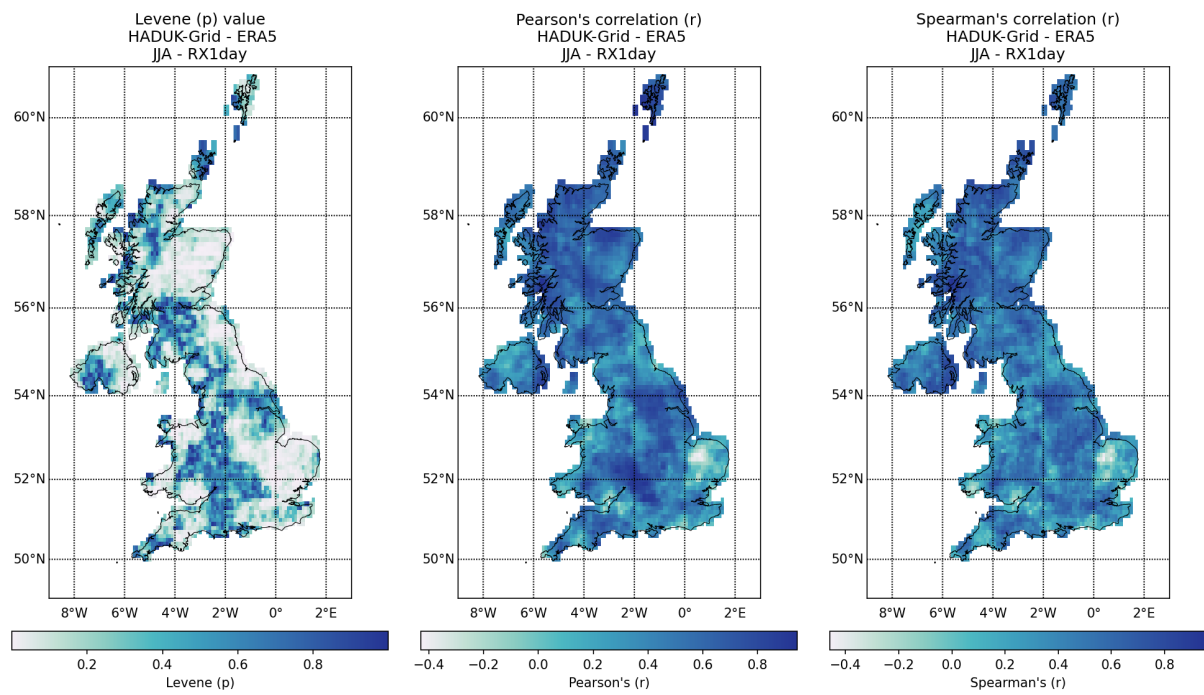


Figure 38: Spatial distribution of RX1day values obtained from HadUK-Grid and ERA5 with Mann-Whitney test p value, Levene -center in the median- p value, and Pearson and Spearman correlation coefficient (r), for summer (JJA) over the 2001-2019 climatological period (cont.).

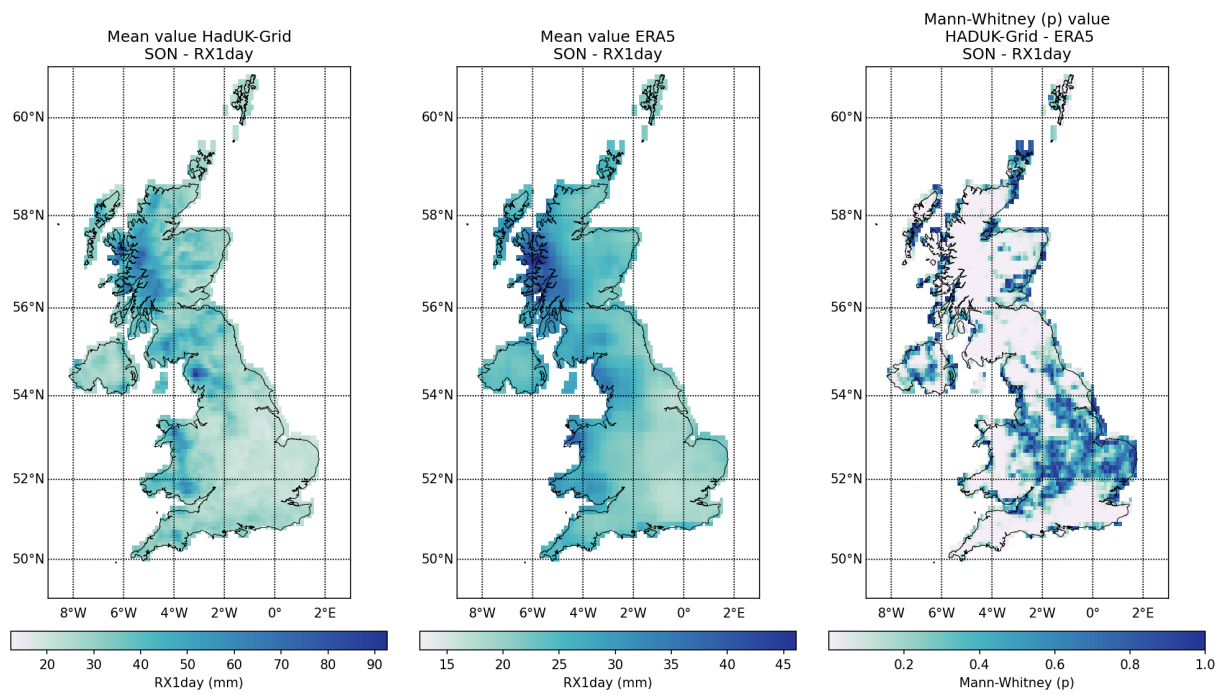


Figure 38: Spatial distribution of RX1day values obtained from HadUK-Grid and ERA5 with Mann-Whitney test p value, Levene -center in the median- p value, and Pearson and Spearman correlation coefficient (r), for autumn (SON) over the 2001-2019 climatological period (cont.).

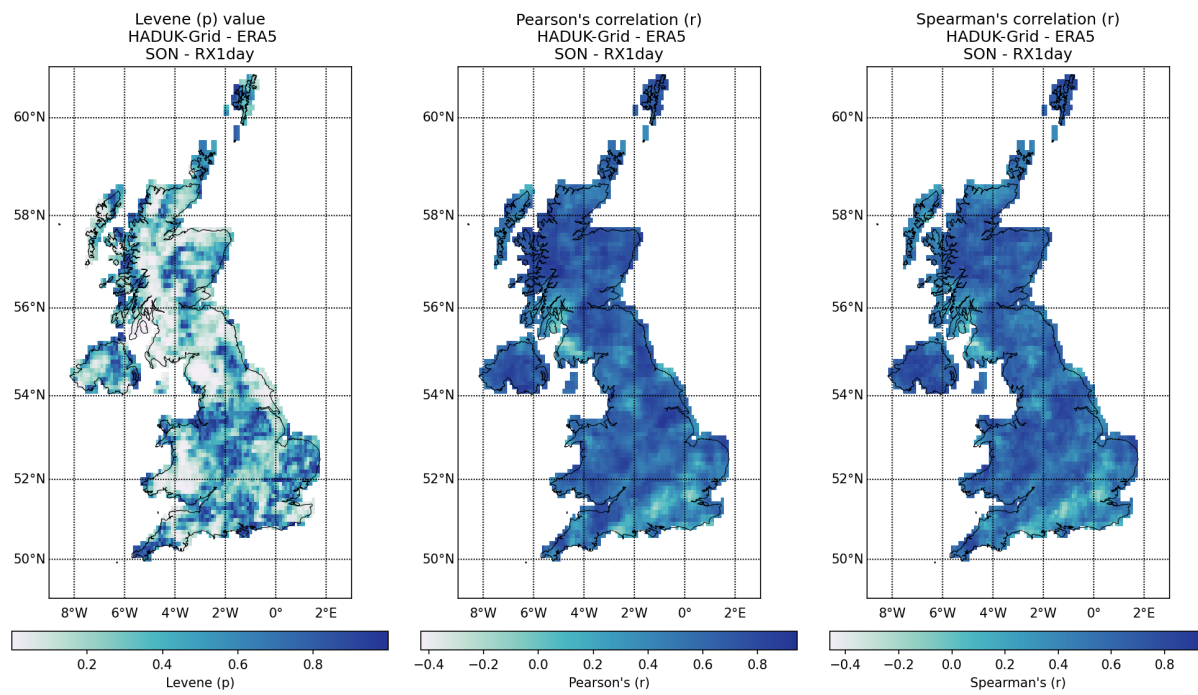


Figure 38: Spatial distribution of RX1day values obtained from HadUK-Grid and ERA5 with Mann-Whitney test p value, Levene -center in the median- p value, and Pearson and Spearman correlation coefficient (r), for autumn (SON) over the 2001-2019 climatological period.

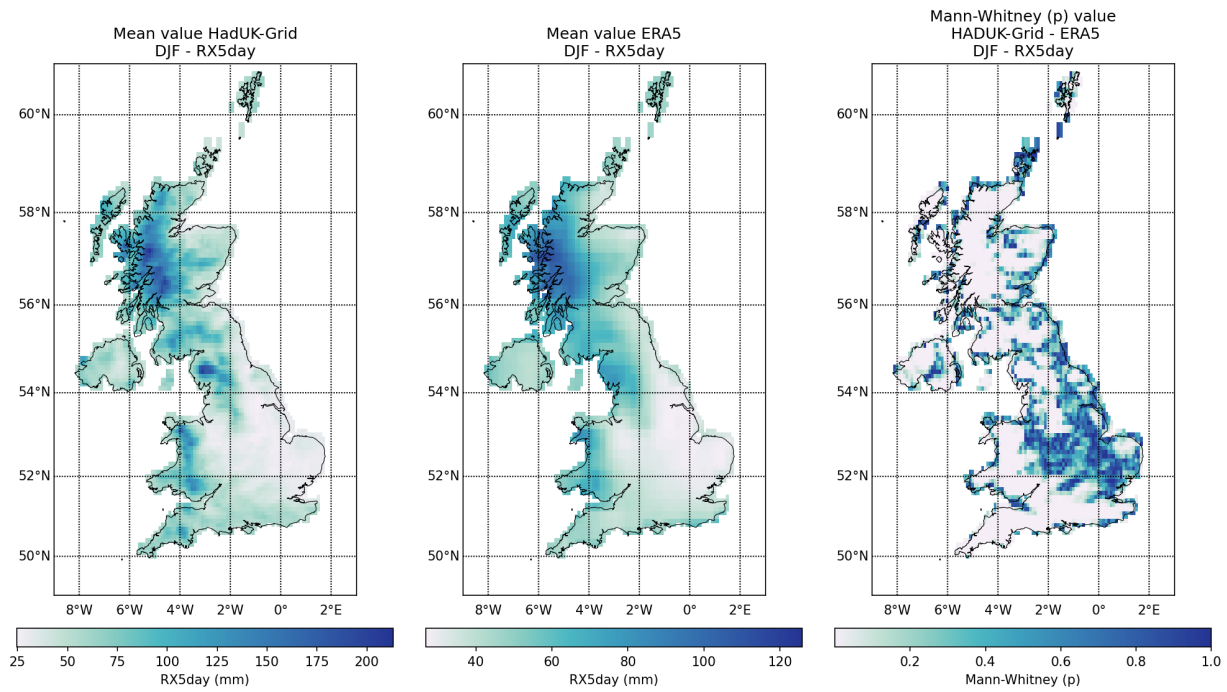


Figure 39: Spatial distribution of RX5day values obtained from HadUK-Grid and ERA5 with Mann-Whitney test p value, Levene -center in the median- p value, and Pearson and Spearman correlation coefficient (r), for winter (DJF) over the 2001-2019 climatological period.

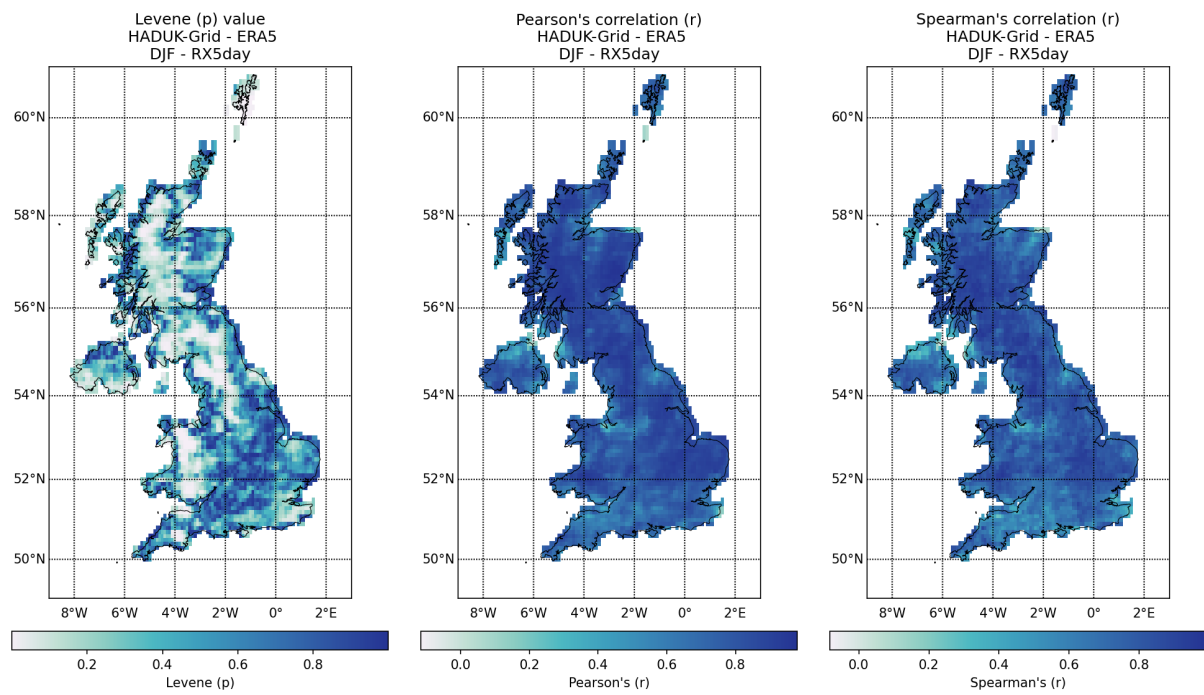


Figure 39: Spatial distribution of RX5day values obtained from HadUK-Grid and ERA5 with Mann-Whitney test p value, Levene -center in the median- p value, and Pearson and Spearman correlation coefficient (r), for spring (DJF) over the 2001-2019 climatological period (cont.).

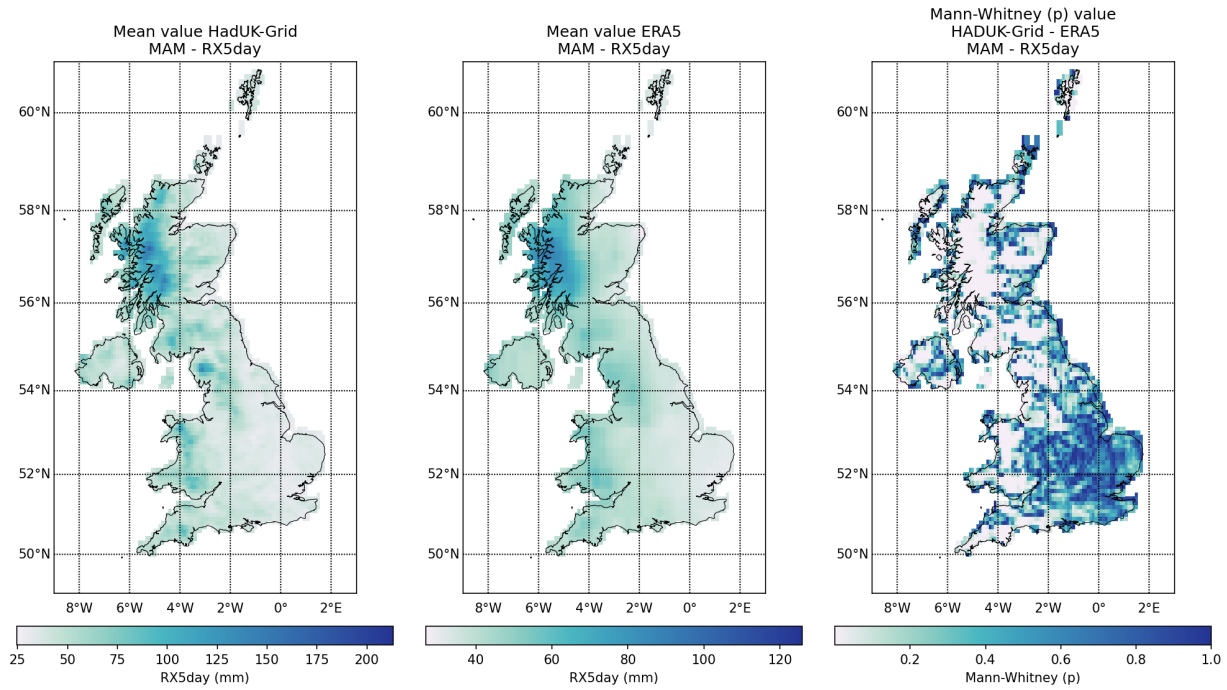


Figure 39: Spatial distribution of RX5day values obtained from HadUK-Grid and ERA5 with Mann-Whitney test p value, Levene -center in the median- p value, and Pearson and Spearman correlation coefficient (r), for spring (MAM) over the 2001-2019 climatological period (cont.).

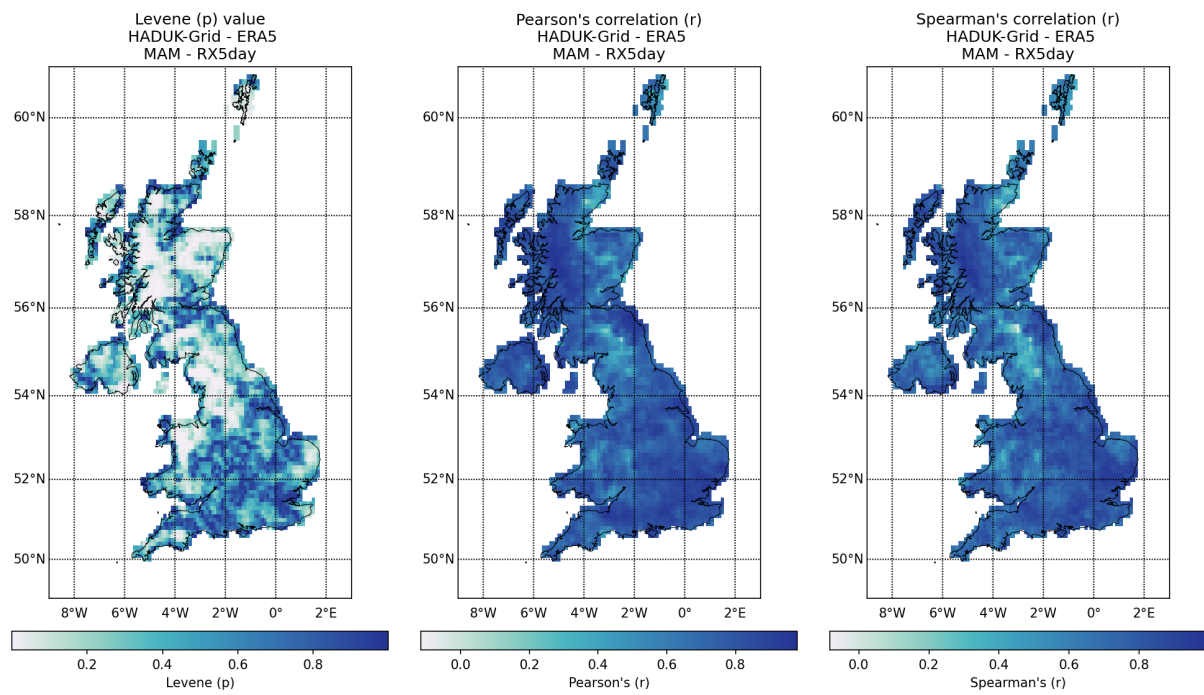


Figure 39: Spatial distribution of RX5day values obtained from HadUK-Grid and ERA5 with Mann-Whitney test p value, Levene -center in the median- p value, and Pearson and Spearman correlation coefficient (r), for spring (MAM) over the 2001-2019 climatological period (cont.).

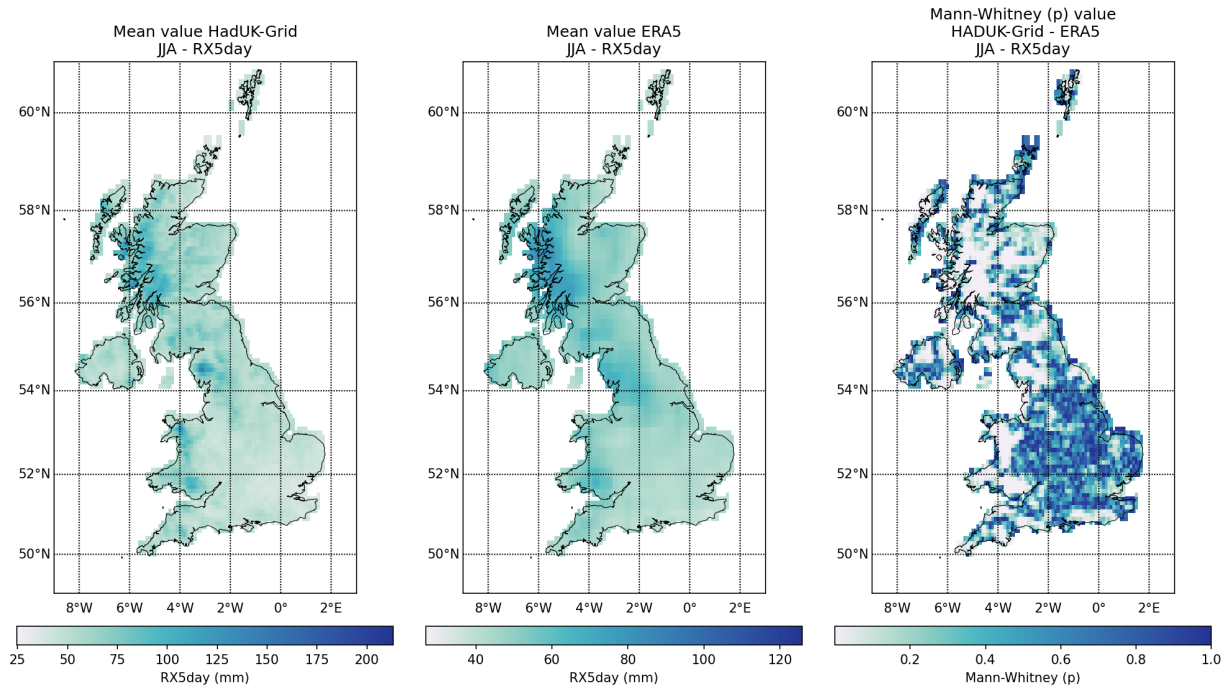


Figure 39: Spatial distribution of RX5day values obtained from HadUK-Grid and ERA5 with Mann-Whitney test p value, Levene -center in the median- p value, and Pearson and Spearman correlation coefficient (r), for summer (JJA) over the 2001-2019 climatological period (cont.).

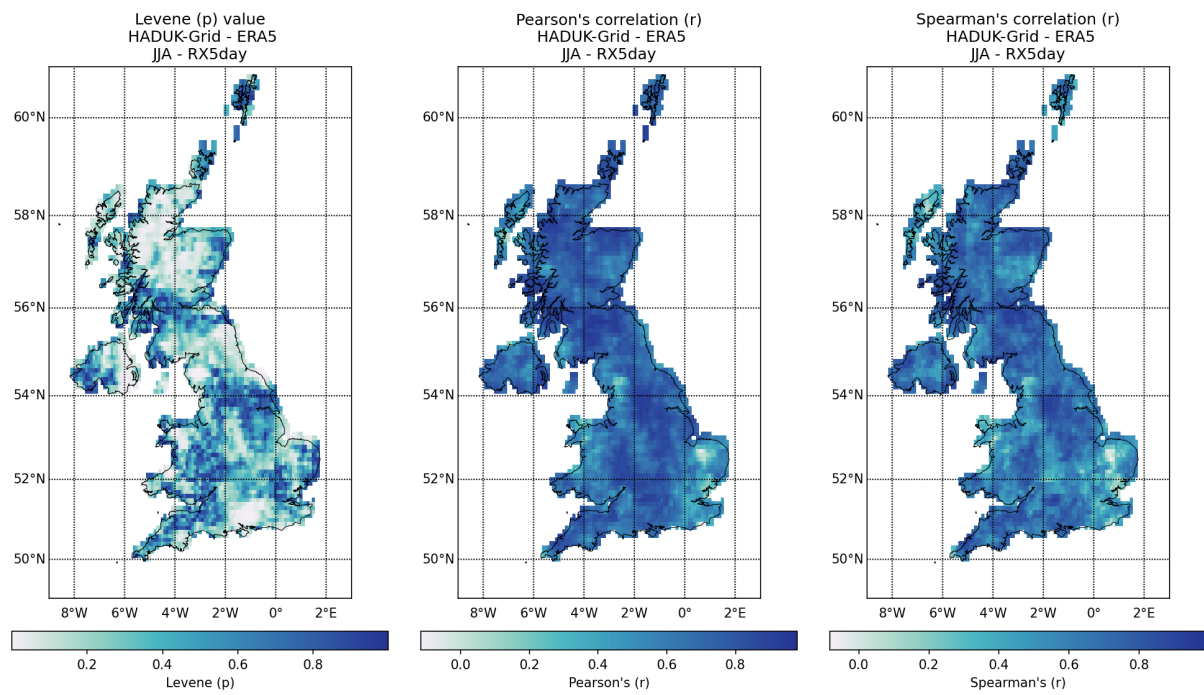


Figure 39: Spatial distribution of RX5day values obtained from HadUK-Grid and ERA5 with Mann-Whitney test p value, Levene -center in the median- p value, and Pearson and Spearman correlation coefficient (r), for summer (JJA) over the 2001-2019 climatological period (cont.).

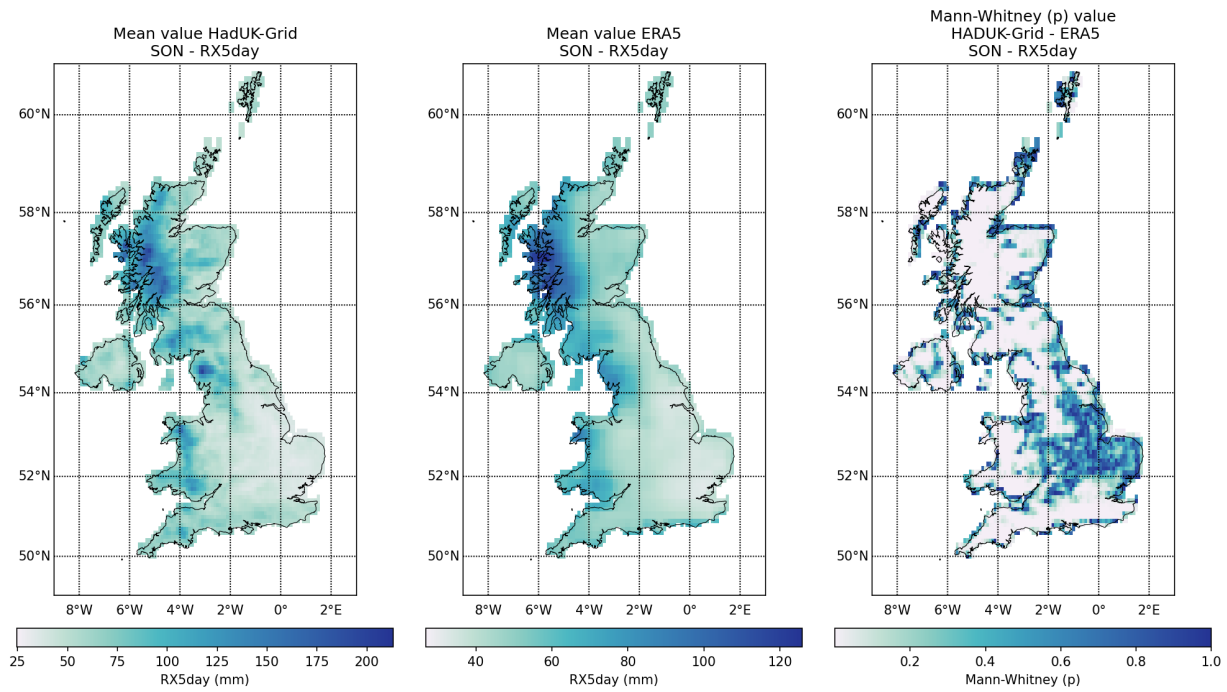


Figure 39: Spatial distribution of RX5day values obtained from HadUK-Grid and ERA5 with Mann-Whitney test p value, Levene -center in the median- p value, and Pearson and Spearman correlation coefficient (r), for autumn (SON) over the 2001-2019 climatological period (cont.).

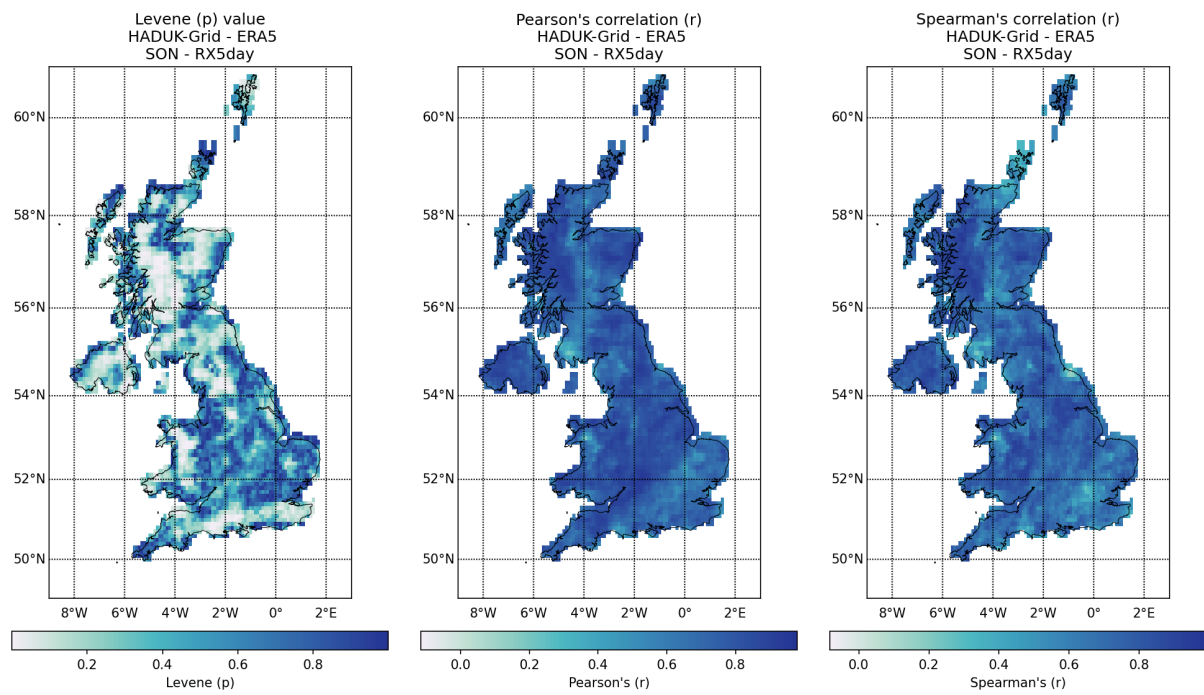


Figure 39: Spatial distribution of RX5day values obtained from HadUK-Grid and ERA5 with Mann-Whitney test p value, Levene -center in the median- p value, and Pearson and Spearman correlation coefficient (r), for autumn (SON) over the 2001-2019 climatological period.

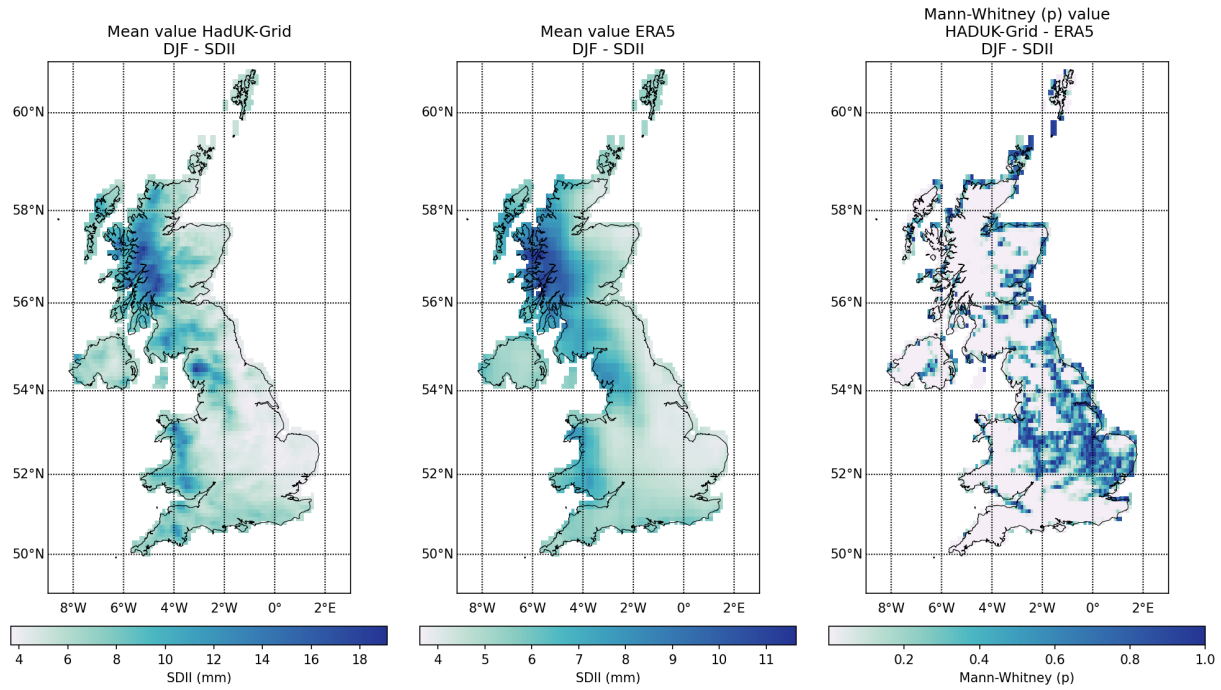


Figure 40: Spatial distribution of SDII values obtained from HadUK-Grid and ERA5 with Mann-Whitney test p value, Levene -center in the median- p value, and Pearson and Spearman correlation coefficient (r), for winter (DJF) over the 2001-2019 climatological period.

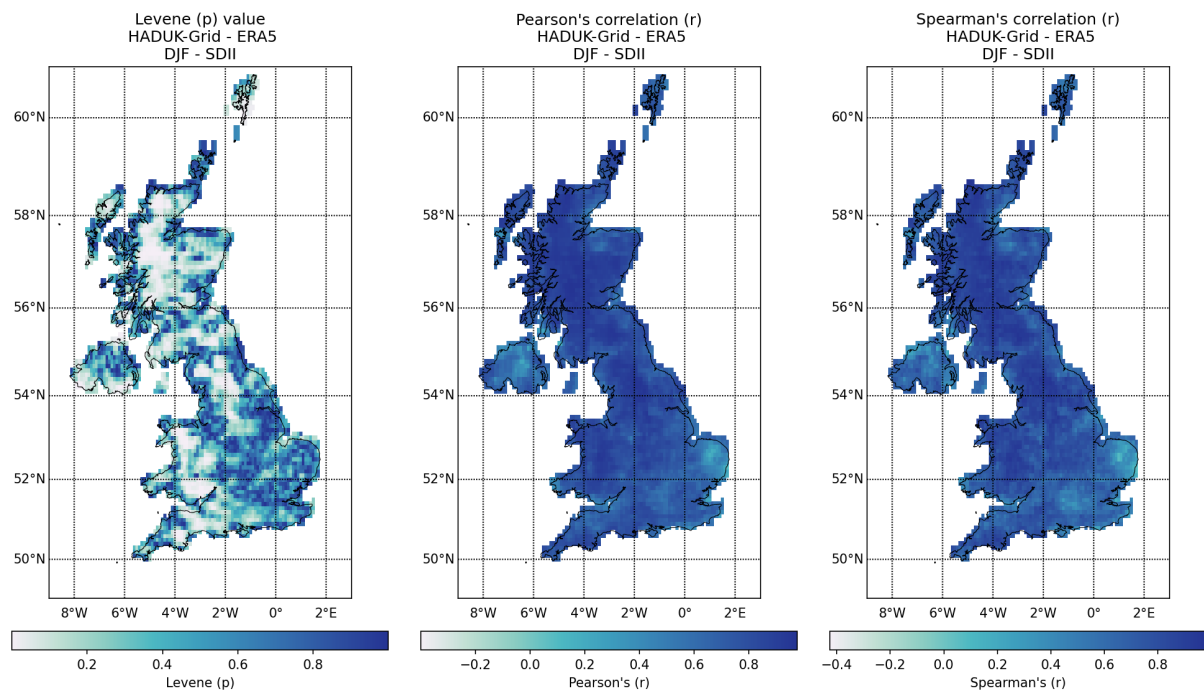


Figure 40: Spatial distribution of SDII values obtained from HadUK-Grid and ERA5 with Mann-Whitney test p value, Levene -center in the median- p value, and Pearson and Spearman correlation coefficient (r), for spring (DJF) over the 2001-2019 climatological period (cont.).

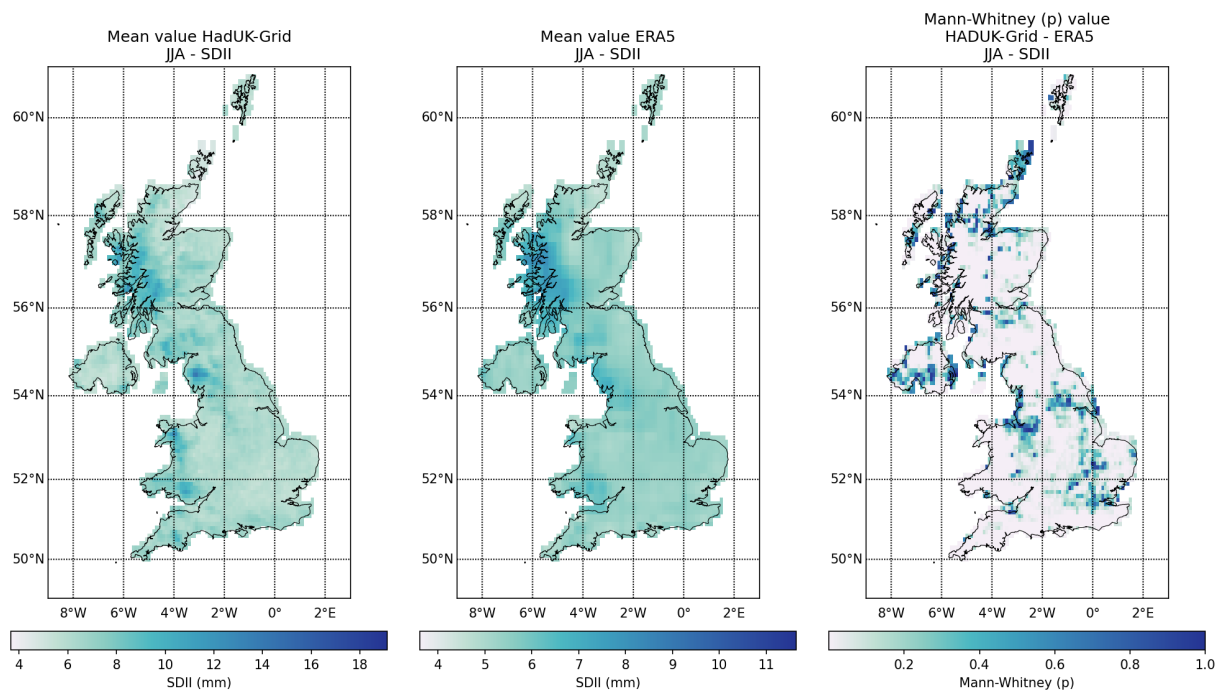


Figure 40: Spatial distribution of SDII values obtained from HadUK-Grid and ERA5 with Mann-Whitney test p value, Levene -center in the median- p value, and Pearson and Spearman correlation coefficient (r), for summer (JJA) over the 2001-2019 climatological period (cont.).

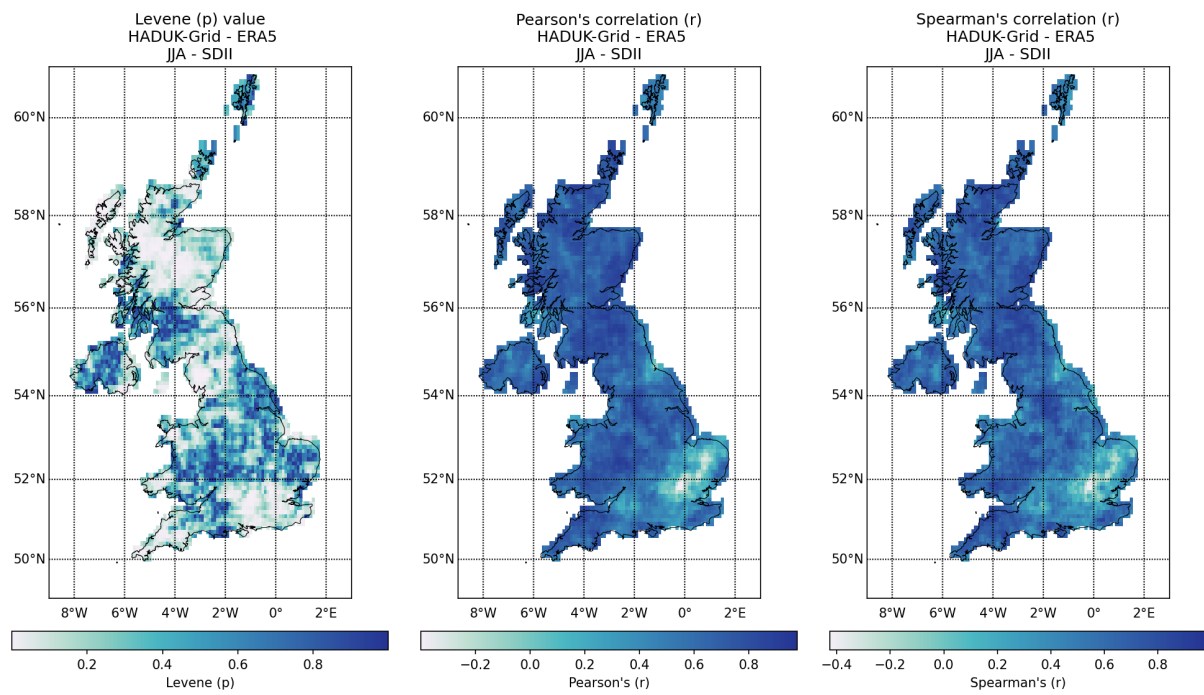


Figure 40: Spatial distribution of SDII values obtained from HadUK-Grid and ERA5 with Mann-Whitney test p value, Levene -center in the median- p value, and Pearson and Spearman correlation coefficient (r), for summer (JJA) over the 2001-2019 climatological period (cont.).

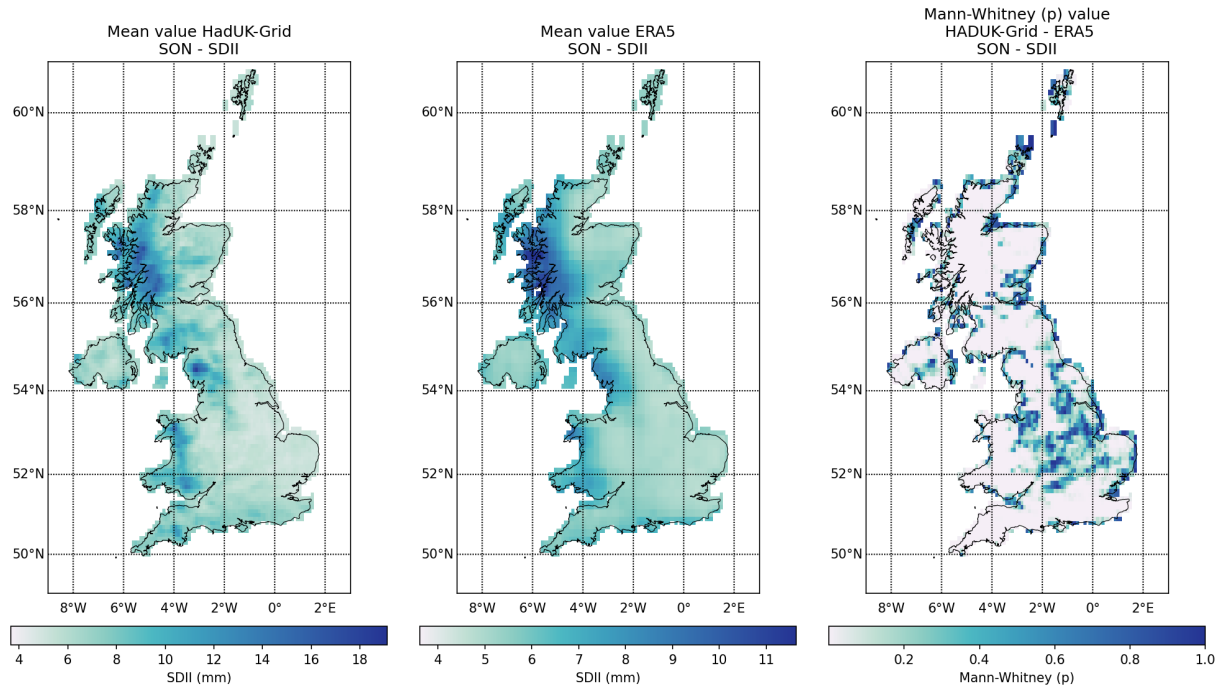


Figure 40: Spatial distribution of SDII values obtained from HadUK-Grid and ERA5 with Mann-Whitney test p value, Levene -center in the median- p value, and Pearson and Spearman correlation coefficient (r), for autumn (SON) over the 2001-2019 climatological period (cont.).

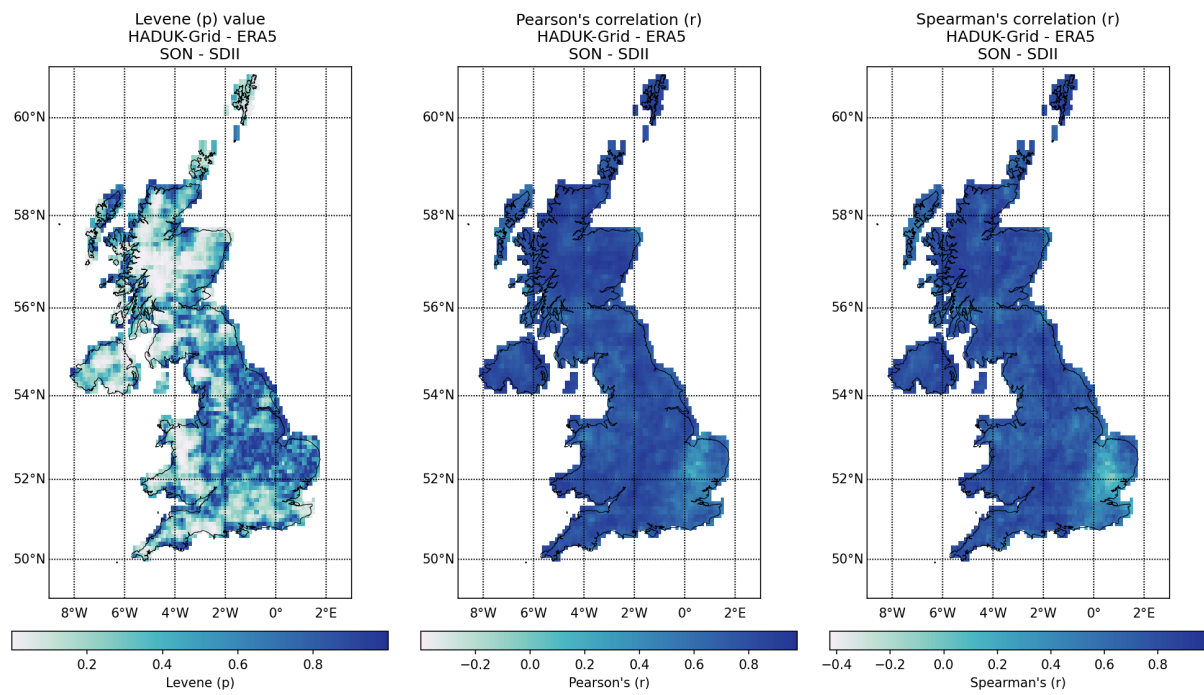


Figure 40: Spatial distribution of SDII values obtained from HadUK-Grid and ERA5 with Mann-Whitney test p value, Levene -center in the median- p value, and Pearson and Spearman correlation coefficient (r), for autumn (SON) over the 2001-2019 climatological period.